CANADIAN THESES ON MICROFICHE

THÈSES CANADIENNES SUR MICROFICHE

National Library of Canada
Collections Development Branch

Canadian Theses on
Microfiche Service

Ottawa, Canada
K1A 0N4

Bibliothèque nationale du Canada
Direction du développement des collections

Service des thèses canadiennes
sur microfiche

NOTICE

The quality of this microfiche is heavily dependent upon the quality of the original thesis submitted for microfilming. Every effort has been made to ensure the highest quality of reproduction possible.

If pages are missing, contact the university which granted the degree.

Some pages may have indistinct print especially if the original pages were typed with a poor typewriter ribbon or if the university sent us an inferior photocopy.

Previously copyrighted materials (journal articles, published tests, etc.) are not filmed.

Reproduction in full or in part of this film is governed by the Canadian Copyright Act, R.S.C. 1970, c. C-30. Please read the authorization forms which accompany this thesis.

AVIS

La qualité de cette microfiche dépend grandement de la qualité de la thèse soumise au microfilmage. Nous avons tout fait pour assurer une qualité supérieure de reproduction.

S'il manque des pages, veuillez communiquer avec l'université qui a conféré le grade.

La qualité d'impression de certaines pages peut laisser à désirer, surtout si les pages originales ont été dactylographiées à l'aide d'un ruban usé ou si l'université nous a fait parvenir une photocopie de qualité inférieure.

Les documents qui font déjà l'objet d'un droit d'auteur (articles de revue, examens publiés, etc.) ne sont pas microfilmés.

La reproduction, même partielle, de ce microfilm est soumise à la Loi canadienne sur le droit d'auteur, SRC 1970, c. C-30. Veuillez prendre connaissance des formules d'autorisation qui accompagnent cette thèse.

THIS DISSERTATION
HAS BEEN MICROFILMED
EXACTLY AS RECEIVED

LA THÈSE A ÉTÉ
MICROFILMÉE TELLE QUE
NOUS L'AVONS REÇUE

NL 339 (r. 86/09)

Canada

0-315-19562-2

220

National Library
of Canada

Canadian Theses Division

Ottawa, Canada
K1A 0N4

Bibliothèque nationale
du Canada

Division des thèses canadiennes

67470

PERMISSION TO MICROFILM — AUTORISATION DE MICROFILMER

- Please print or type — Écrire en lettres moulées ou dactylographier

Full Name of Author — Nom complet de l'auteur

BARBARA JOAN GOWR-SALIN

Date of Birth — Date de naissance

23/04/53

Country of Birth — Lieu de naissance

CANADA

Permanent Address — Résidence fixe

2083 MARLOWE AV
N.D.G. MONTREAL
H4A 3L4

Title of Thesis — Titre de la thèse

THIOL-IMIDAZOLE PAIRS AS MODELS OF PAPAIN

University — Université

UNIVERSITY OF ALBERTA

Degree for which thesis was presented — Grade pour lequel cette thèse fut présentée

Ph.D.

Year this degree conferred — Année d'obtention de ce grade

1984

Name of Supervisor — Nom du directeur de thèse

R.S. BROWN

Permission is hereby granted to the NATIONAL LIBRARY OF CANADA to microfilm this thesis and to lend or sell copies of the film.

The author reserves other publication rights, and neither the thesis nor extensive extracts from it may be printed or otherwise reproduced without the author's written permission.

L'autorisation est, par la présente, accordée à la BIBLIOTHÈQUE NATIONALE DU CANADA de microfilmer cette thèse et de prêter ou de vendre des exemplaires du film.

L'auteur se réserve les autres droits de publication; ni la thèse ni de longs extraits de celle-ci ne doivent être imprimés ou autrement reproduits sans l'autorisation écrite de l'auteur.

Date

Dec 03/83

Signature

Barbara J Gowr-Salin

NL-91 (4/77)

THE UNIVERSITY OF ALBERTA

THIOL-IMIDAZOLE PAIRS AS MODELS OF PAPAIN ACTION

By

© BARBARA JOAN GOUR-SALIN

A THESIS

SUBMITTED TO THE FACULTY OF GRADUATE STUDIES AND RESEARCH

IN PARTIAL FULFILMENT OF THE REQUIREMENTS FOR THE DEGREE

OF DOCTOR OF PHILOSOPHY.

DEPARTMENT OF CHEMISTRY

EDMONTON, ALBERTA

Spring, 1984

THE UNIVERSITY OF ALBERTA

RELEASE FORM

NAME OF AUTHOR Barbara Joan Gour-Salin

TITLE OF THESIS Thiol-Imidazole Pairs as Models of Papain Action.

DEGREE FOR WHICH THESIS WAS PRESENTED Ph.D.

YEAR THIS DEGREE WAS GRANTED 1984

Permission is hereby granted to THE UNIVERSITY OF ALBERTA LIBRARY to produce single copies of this thesis and to lend or sell such copies for private, scholarly or scientific research purposes only.

The author reserves other publication rights, and neither the thesis nor extensive extracts from it may be printed or otherwise reproduced without the author's written permission.

(Signed) Barbara J. Gour-Salin

PERMANENT ADDRESS:

2083 Marlowe Avenue
N.D.G., Quebec
Canada

DATED Oct. 6, 1983

THE UNIVERSITY OF ALBERTA

FACULTY OF GRADUATE STUDIES AND RESEARCH

The undersigned certify that they have read, and recommend to the Faculty of Graduate Studies and Research, for acceptance, a thesis entitled THIOL-IMIDAZOLE PAIRS OF MODELS OF PAPAIN ACTION submitted by BARBARA JOAN GOUR-SALIN in partial fulfilment of the requirements for the degree of Doctor of Philosophy.

Karl R. Kopecky

M J Robins

H B Dunford

Michael James

Mary Spencer

Date September 30, 1983

To my husband, Eric,
who helped the most.

ABSTRACT

The bifunctional thiols 4(7')-thiomethylbenzimidazole (8a) and 1-methyl-4-thiomethylbenzimidazole (8b) were synthesized to study the effect of the proximally positioned imidazole group on the nucleophilicity of the thiol group. The cysteine proteases contain a sulfhydryl group of a cysteine residue and an imidazole group of a histidine residue in their active site and it is of interest to know whether or not these two groups can exhibit cooperative catalysis.

Kinetic studies of the catalysis of the hydrolysis of *p*-nitrophenylacetate in 31.6% ethanol/H_2O (v/v) at 25°C by compounds (8a) and (8b), by two monofunctional thiols benzylmercaptan (6) and cyclohexylmethylthiol (7) and seven monofunctional imidazole compounds benzimidazole (10a), 1-methylbenzimidazole (10b), tetrahydrobenzimidazole (11a), 1-methyltetrahydrobenzimidazole (11b), 4(7')-hydroxymethylbenzimidazole (12a), 1-methyl-4-hydroxymethylbenzimidazole (12b) and 1-methyl-4-hydroxymethyltetrahydrobenzimidazole (13b) were carried out. In the neutral pH region it was found that the thiol-imidazole pairs (8a) and (8b) provided some type of additional catalysis over and above that due to the thiolate anion. The mechanism of this cooperative catalysis could be due to a general base assisted thiol attack on *p*-nitrophenylacetate, imidazolium ion providing catalysis via a general acid mechanism or the zwitterion could be taking an active part in the catalysis.

The rates of hydrolysis of the corresponding thiolacetate-imidazole compounds (65) and (27) were also studied to investigate

as to whether the proximal imidazole group could significantly enhance the rates of hydrolysis of thiolacetates. In this case the imidazole group was found to have little effect on the hydrolysis rates.

ACKNOWLEDGEMENTS

I would like to thank Dr. R.S. Brown for suggesting the project and for helping all the members of our group to become competent experimentalists.

I would like to thank the present members of my committee for the effort they expended reading my thesis and I would also like to express my appreciation to Drs. R.B. Jordan and W.A. Ayer in particular, for the many helpful discussions we had.

I would also like to thank John Wilson, Janet Laird and Peter Nagainis for their friendship and support during the last few months I spent in Edmonton.

Finally, I would like to express my appreciation to Dr. B. Belleau for giving me the opportunity to finish my thesis and also to Dr. A.G. Shaver for proofing the final draft of my thesis.

TABLE OF CONTENTS

PAGE

INTRODUCTION 1

Imidazole Catalysis 3

Papain: Structure and Mechanism 9

RESULTS AND DISCUSSION: ACYLATION STUDIES 23

Introduction to Research 23

Synthesis 25

Basicities 40

Catalytic Studies 43

RESULTS AND DISCUSSION: DEACYLATION STUDIES 110

Introduction to Research 110

Synthesis 116

Catalytic Studies 119

EXPERIMENTAL 146

Synthesis 146

Kinetic Measurements 193

pKa Determinations 197

REFERENCES 198

APPENDIX I: INSTRUMENTATION 207

APPENDIX II: NON-LINEAR LEAST SQUARES 218

LIST OF TABLES

TABLE	DESCRIPTION	PAGE
1.	pH Values Corresponding to Various [OH^-] in 31.6% Ethanol/H_2O, 0.25 M KCl Solutions.	42
2.	Titrimetrically Determined Ionization Constants of Some Monofunctional and Bifunctional Imidazole-Containing Compounds in Ethanol/H_2O Solutions.	44
3.	Pseudo-First Order and Second Order Rate Constants for the Hydrolysis of *p*-Nitrophenylacetate with Benzyl Mercaptan (*6*).	48
4.	Pseudo-First Order and Second Order Rate Constants for the Hydrolysis of *p*-Nitrophenylacetate with Cyclohexylmethylthiol (*7*).	50
5.	Pseudo-First Order and Second Order Rate Constants for the Hydrolysis of *p*-Nitrophenylacetate with Benzimidazole (*10a*).	55
6.	Pseudo-First Order and Second Order Rate Constants for the Hydrolysis of *p*-Nitrophenylacetate with Tetrahydrobenzimidazole (*11a*).	59
7.	Pseudo-First Order and Second Order Rate Constants for the Hydrolysis of *p*-Nitrophenylacetate with 1-Methyltetrahydrobenzimidazole (*11b*).	60
8.	Pseudo-First Order and Second Order Rate Constants for the Hydrolysis of *p*-Nitrophenylacetate with 1-Methyl-4,5[4'-Hydroxymethyltetramethylene]imidazole (*13b*).	70
9.	Ionization Constants and Second Order Rate Constants for Some Substituted Benzimidazole Compounds.	74

TABLE	DESCRIPTION	PAGE
10.	Ionization Constants and Second Order Rate Constants for Some Substituted Imidazole Compounds.	77
11.	Pseudo-First Order and Second Order Rate Constants for the Hydrolysis of p-Nitrophenylacetate with 4(7')-Thiomethylbenzimidazole (8a).	78
12.	Pseudo-First Order and Second Order Rate Constants for the Hydrolysis of p-Nitrophenylacetate with 1-Methyl-4-Thiomethylbenzimidazole (8b).	79
13.	Ionization Constants and Second Order Rate Constants for the Hydrolysis of p-Nitrophenylacetate with 2-Mercaptobenzimidazole (46), 2-Mercaptomethylbenzimidazole (47), 5-Methyl-2-mercaptomethylbenzimidazole (48), 5-Bromo-2-mercaptomethylbenzimidazole (49), 2-(2-Mercaptoethyl)benzimidazole (50), 2-(3-Mercaptopropyl)benzimidazole (51), 2-(1-Mercaptoethyl)benzimidazole (52), and 2-Methylthiomethylbenzimidazole (53).	82
14.	Ionization Constants and Second Order Rate Constants for the Hydrolysis of p-Nitrophenylacetate with 4-Mercaptoethylimidazole (54), 4-Mercaptomethylimidazole (55), and 1-Methyl-5-Mercaptoethylimidazole (56).	87
15.	Second Order Rate Constants Derived from the Nucleophilic Attack of the Thiolate Anion of Selected Imidazole-Thiol Pairs on p-Nitrophenylacetate.	102
16.	Chemical Shift Positions of the Protons of N-Acylated, O-Acylated and Diacylated 4(7')-Hydroxymethylbenzimidazole.	118
17.	Pseudo-First Order and Second Order Rate Constants for the Decompositon of Benzyl Thioacetate (70).	120

TABLE	DESCRIPTION	PAGE
18.	Pseudo-First Order and Second Order Rate Constants for the Decompositon of Benzyl Acetate (71).	124
19.	Pseudo-First Order and Second Order Rate Constants For the Decomposition of 4(7')-Thioacetoxybenzimidazole (65).	126
20.	Pseudo-First Order and Second Order Rate Constants For the Decomposition of 1-Methyl-4-Thioacetoxymethylbenzimidazole (27).	127
21.	Pseudo-First Order and Second Order Rate Constants For the Decomposition of 4(7')-Acetoxymethylbenzimidazole (69a).	129
22.	Pseudo-First Order and Second Order Rate Constants For the Decomposition of 1-Methyl-4-Acetoxymethylbenzimidazole (69b).	130
23.	Pseudo-First Order and Second Order Rate Constants For the Decomposition of 1-Acetylbenzimidazole (74).	136
24.	Pseudo-First Order and Second Order Rate, Constants For the Decomposition of 1-Acetyl-3-Methylbenzimidazolium Acetate (76).	140
25.	Pseudo-First Order and Second Order Rate Constants For the Decomposition of 1-Acetyl-3-Methyltetrahydrobenzimidazolium Acetate (77).	141
26.	Pseudo-First Order Rate Constants for the Hydrolysis of p-Nitrophenylacetate with Benzyl Mercaptan.	228
27.	Pseudo-First Order Rate Constants for the Hydrolysis of p-Nitrophenylacetate with Cyclohexylmethylthiol.	230
28.	Pseudo-First Order Rate Constants for the Hydrolysis of p-Nitrophenylacetate with Benzimidazole.	232

TABLE	DESCRIPTION	PAGE
29.	Pseudo-First Order Rate Constants for the Hydrolysis of *p*-Nitrophenylacetate with Tetrahydrobenzimidazole.	233
30.	Pseudo-First Order Rate Constants for the Hydrolysis of *p*-Nitrophenylacetate with 1-Methyltetrahydrobenzimidazole.	234
31.	Pseudo-First Order Rate Constants for the Hydrolysis of *p*-Nitrophenylacetate with 1-Methyl-4-Hydroxymethyltetrahydrobenzimidazole.	235
32.	Pseudo-First Order Rate Constants for the Hydrolysis of *p*-Nitrophenylacetate with 4(7')-Thiomethylbenzimidazole.	236
33.	Pseudo-First Order Rate Constants for the Hydrolysis of *p*-Nitrophenylacetate with 1-Methyl-4-Thiomethylbenzimidazole	238
34.	Pseudo-First Order Rate Constants for the Hydrolysis of *p*-Nitrophenylacetate with 4(7')-Hydroxymethylbenzimidazole	240
35.	Pseudo-First Order Rate Constants for the Hydrolysis of *p*-Nitrophenylacetate with 1-Methyl-4-Hydroxymethylbenzimidazole	241
36.	Pseudo-First Order Rate Constants for the Hydrolysis of *p*-Nitrophenylacetate with 1-Methylbenzimidazole	242

LIST OF FIGURES

FIGURE	DESCRIPTION	PAGE
1.	Rates of imidazole catalyzed ester hydrolysis as a function of the rate of alkaline hydrolysis: nucleophilic reactions of acetates, ● ; general-base catalysis of acetates, ■ ; general-base catalysis of methyl and ethyl esters, ▲ . Trifluoroethyl acetate rate measured with N-methylimidazole.	4
2.	The active site region of papain near the essential thiol group (reproduced from reference 17a).	11
3.	Nuclear Overhauser Effect from irradiation of the N-methyl (δ 3.9) of 4-carboxy-1-methylbenzimidazole (23) in $CDCl_3$.	30
4.	Nuclear Overhauser Effect from irradiation of the N-methyl (δ 3.8) of 1-methyl-ethyl-S-4-benzimidazolmethyl xanthate (25) in $CDCl_3$.	32
5.	Plot of pH vs $[OH^-]$ as determined from known concentrations of NaOH in ethanol/H_2O (31.6% ethanol).	43
6.	Plot of the second order rate constant (k_{cat}) vs pH for benzyl mercaptan (6), cyclohexylmethylthiol (7), 4(7')-thiomethylbenzimidazole (8a) and 1-methyl-4-thiomethylbenzimidazole (8b). For 4(7')-thiomethylbenzimidazole (8a) and 1-methyl-4-thiomethylbenzimidazole (8b) the values above 9.2 are extrapolated from the value at 9.2 and the known pKa's of these compounds.	52
7.	Plot of the second order rate constant k_{cat} vs pH for benzimidazole (10a), tetrahydrobenzimidazole (11a), 1-methyltetrahydrobenzimidazole (11b) and 1-methyl-4,5-[4'-hydroxymethyltetramethylene]-	

FIGURE DESCRIPTION PAGE

imidazole (13b). 1-Methylbenzimidazole (10b), 4(7')-hydroxymethylbenzimidazole (12a) and 4-hydroxymethyl-1-methylbenzimidazole (12b) exhibited no effective rate enhancement over the hydroxide and buffer terms. 58

8. The ^{1}H-NMR spectra of p-nitrophenylacetate in $CDCl_3$ (a), the hydrochloride salt of tetrahydrobenzimidazole (11a) in ethanol-d_6 (b) and the hydrochloride salt of 1-methyltetrahydrobenzimidazole (11b) in ethanol-d_6 (c). 64

9. The ^{1}H-NMR spectra of the reaction of p-nitrophenylacetate with tetrahydrobenzimidazole (11a) in ethanol-d_6, NaOD/D_2O as a function of time. 66

10. The ^{1}H-NMR spectra of the reaction of p-nitrophenylacetate with 1-methyltetrahydrobenzimidazole (11b) in ethanol-d_6, NaOD/D_2O as a function of time. 69

11. Plots of k_{cat} vs pH for 2-mercaptobenzimidazole (46), 2-mercaptomethylbenzimidazole (47), 5-methyl-2-mercaptomethylbenzimidazole (48), 5-bromo-2-mercaptomethylbenzimidazole (49), 2-(2-mercaptoethyl)benzimidazole (50), 2-(3-mercaptopropyl)benzimidazole (51), 2-(1-mercaptoethyl)benzimidazole (52) and 2-methylthiomethylbenzimidazole (53). 85

12. Plots of k_{cat} (M^{-1} min^{-1}) vs pH for 4-mercaptoethylimidazole (54), 4-mercaptomethylimidazole (55) and 1-methyl-5-mercaptoethylimidazole (56). 89

13. Plots of a_H vs $k_{cat}(a_H^2 + K_1a_H + K_1K_2)$ for 4(7')-thiomethylbenzimidazole (8a) and 1-methyl-4-thiomethylbenzimidazole (8b). 95

FIGURE DESCRIPTION PAGE

14. Plots of a_H vs $k_{cat}(a_H^2 + K_1a_H + K_1K_2)$ for 2-mercaptobenzimidazole (46), 2-(2-mercaptoethyl)benzimidazole (50), 2-(3-mercaptopropyl)benzimidazole (51) and 2-(1-mercaptoethyl)benzimidazole (52). 97

15. Plots of $k_{cat}(a_H^2 + K_1a_H + K_1K_2)$ vs a_H for 2-mercaptomethylbenzimidazole (47), 5-methyl-2-mercaptomethylbenzimidazole (48) and 5-bromo-2-mercaptomethylbenzimidazole (49). 99

16. Plots of $k_{cat}(a_H^2 + K_1Ka_H + K_1K_2)$ vs a_H for 4-mercaptoethylimidazole (54), 4-mercaptomethylimidazole (55) and 1-methyl-5- mercaptoethylimidazole (56). 101

17. Plot of k_{obs} vs pH for the decomposition of benzyl thioacetate (70), benzyl acetate (71), 4(7')-acetoxymethylbenzimidazole (69a), 1-methyl-4-acetoxymethylbenzimidazole (69b), 4(7')-thioacetoxymethylbenzimidazole (65) and 1-methyl-4-thioacetoxymethylbenzimidazole (27). 122

18. A plot of the continuous scans of the UV-VIS spectrum of N-acetylbenzimidazole (74) as it is hydrolyzed to benzimidazole (10a) in formic acid/sodium formate buffer at 25°C. 134

19. A plot of k_{obs} vs pH for N-acetylimidazole (66), 1-acetyl-3-methylimidazolium chloride (67), N-acetylbenzimidazole (74), 1-acetyl-3-methylbenzimidazolium acetate (76) and 1-acetyl-3-methyltetrahydrobenzimidazolium acetate (77). 139

20. Timing diagram for the interface between the Apple II+ Microprocessor and the Cary 210 UV-VIS Spectrometer. 209

Introduction

Imidazole and imidazole compounds have received special attention as catalysts of ester hydrolysis[1] because of the apparent involvement of the imidazole group of a histidine residue in the mechanism of action of numerous hydrolytic enzymes including chymotrypsin, trypsin, cholinesterase, ribonuclease and papain.

The most studied enzyme of the esterases is α-chymotrypsin which like trypsin, subtilism and elastase contains a serine hydroxyl group and a histidine imidazole group in its active site. It is believed that the attack of the hydroxyl of Ser-195 results in an acyl enzyme intermediate which then collapses to the final products. Consequently, a vast amount of effort has been expended on the study of the bimolecular and intramolecular catalysis of imidazoles on oxygen esters.[1]

However, there is an additional group of proteolytic enzymes which require the sulfhydryl group of cysteine, rather than the hydroxyl group of serine, as well as the imidazole group of the histidine residue for activity. In this class of enzymes papain is the best known and is obtained from the fully grown green fruits of the tropical pawpaw or melon tree (*Carica papaya*). Other enzymes belonging to this group are chymopapain which can also be isolated from papaya latex[2a], ficin from the fig tree,[2b] bromelain from pineapple,[2c] mexicain from the leaves or fruit of *Pileus mexicanus*[2d], ascelpain from the milkweed root[2e] and euphorbain from the latex of *Euphorbia lathyrus*[2f]. The enzymes from animal tissue called cathepsins[2g] belong to this group as well as clostipain from

Closrudium histolyticum[2h] and streptococcal proteinase from bacteria[2i]. The bacterially derived cysteine proteinases are used as exotoxins to break down the cellular proteins of the invaded host. In the case of plant-derived cysteine proteinases, the biological roles have not as yet been established. However, they could be defence-related enzymes which protect the plant from invasion by fungi and parasitic insects.

In contrast to the effort expended on the study of the catalysis of oxygen-imidazole pairs as models for α-chymotrypsin there has been little effort made to study the catalysis which results from an imidazole in close juxtaposition with a thiol group as found in the active site of papain. Our aim, therefore, was to study the reactivity of imidazole-thiol pairs to form thiol esters and then to investigate the subsequent catalysis of the thiol ester hydrolysis by a closely positioned imidazole or imidazolium ion. It was hoped that fundamental information concerning the catalysis of imidazole-thiol pairs in aqueous solution would be obtained and that perhaps plausible mechanisms of action for papain and other sulfhydryl enzymes could be postulated.

Before delving into the results of these catalytic studies, it is necessary both to review what is already known about imidazole catalysis of the hydrolysis of oxygen esters as well as the structure and the proposed mechanisms of action for papain. This will enable us to extrapolate the results of the small-molecule studies of imidazole-thiol pairs to the real enzyme.

Imidazole Catalysis

The hydrolysis and transfer of the acyl groups of esters is catalyzed by imidazole by two different mechanistic pathways: through nucleophilic catalysis with the intermediate formation of an acyl imidazole[3-8] and through general base catalysis in which imidazole acts solely as a catalyst for proton transfer.[6,9]

Nucleophilic attack on p-nitrophenylacetate (PNPA) can take place by attack of the anion in the case of weakly basic imidazoles, which are substituted with strongly electron-withdrawing groups.[10] More basic imidazoles can attack as the neutral imidazole species,[4,5] and lastly reactions of imidazole itself with certain substituted p-nitrobenzoates contain a term in the rate law which is second order with respect to imidazole and corresponds to a general base catalysis by imidazole of the nucleophilic attack of imidazole of these esters.[11]

Kirsch and Jencks[12] have examined the hydrolysis of acetyl esters with good leaving groups (i.e. acetic anhydride, phenyl esters), acetyl and n-alkylacyl esters with very poor leaving groups (i.e. methyl and ethyl esters) and an alcohol activated ester (i.e. trifluoroethyl acetate). Inspection of Figure 1 (reproduced from Reference 12) reveals the following points of interest.

With the exception of N,O-diacetyl-N-methylhydroxylamine, the points for the acetate compounds fall on a line which is straight for the better leaving groups but shows a downward curvature for the acetates of less acidic phenols. As the leaving groups become still more basic there is a sharp downward curvature, and the points for acetoxime acetate, trifluoroethyl acetate and ethyl acetate are

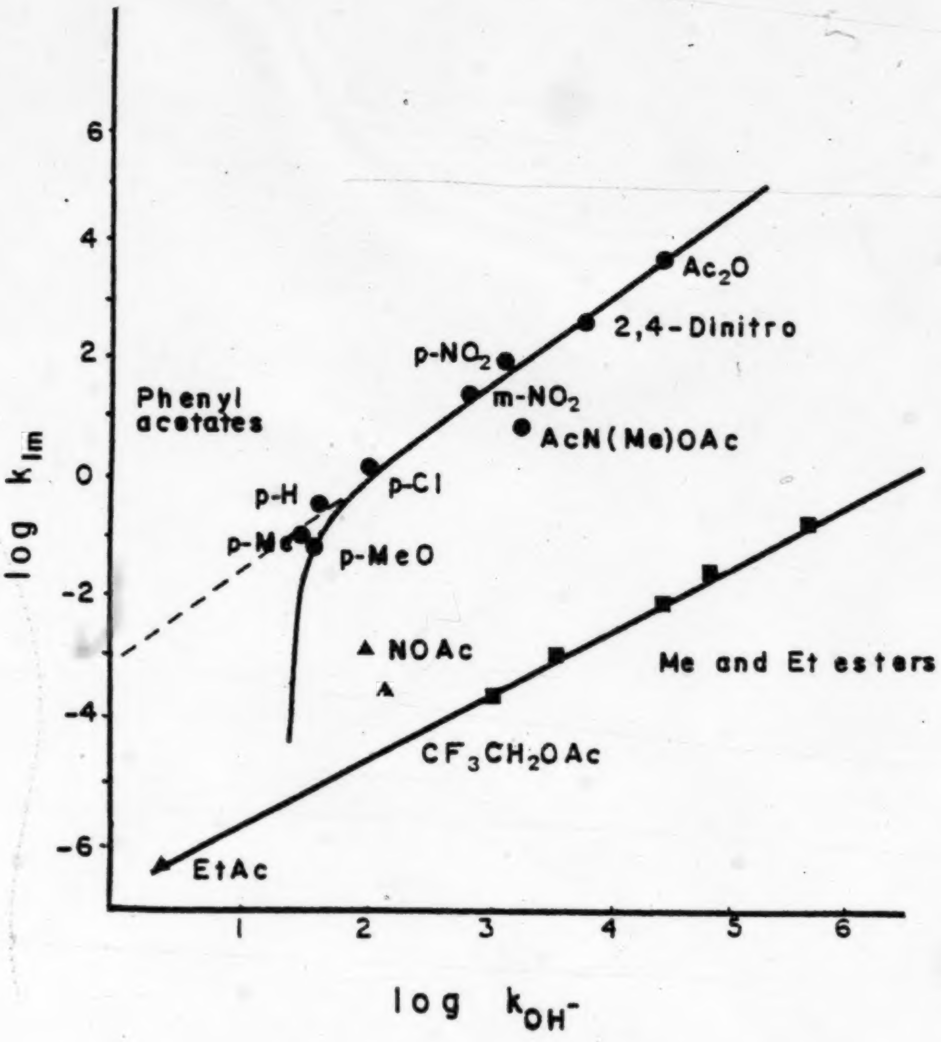

Figure 1: Rates of imidazole catalyzed ester hydrolysis as a function of the rate of alkaline hydrolysis: nucleophilic reactions of acetates, ● ; general-base catalysis of acetates, ■ ; general-base catalysis of methyl and ethyl esters, ▲ . Trifluoroethyl acetate rate measured with N-methylimidazole (reproduced from reference 12).

several orders of magnitude below those of the more reactive esters. The points for these compounds approach the line for the general-base catalyzed hydrolysis of methyl and ethyl esters. Therefore, the curve for hydrolysis of acetates with leaving groups having pKa values in the range 4-16 is sigmoid, with upper and lower portions corresponding to nucleophilic and general-base catalysis, respectively and a sharp break between, corresponding to a change in the mechanism of catalysis. The break in the curve must correspond to the position at which the basicity of the leaving group becomes such that it can no longer be displaced by imidazole, and nucleophilic displacement is no longer evident. If the mechanism involves a tetrahedral intermediate the imidazole is preferentially expelled with a poor leaving group leading to starting material rather than products.[5,12]

In summary[13], therefore, in intermolecular reactions involving phenyl acetates as substrates, bimolecular nucleophilic displacement of phenoxide (Equation 1) is the exclusive pathway until the pKa of the conjugate acid of the leaving group exceeds that of imidazolium

1.

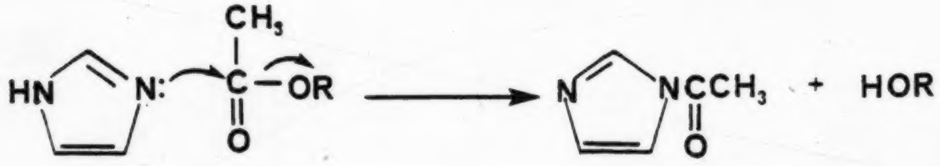

ion by (ΔpKa) ≈3.0. When ΔpKa > 3 (ie with phenyl esters) general base assistance of the attack of imidazole by imidazole

2.

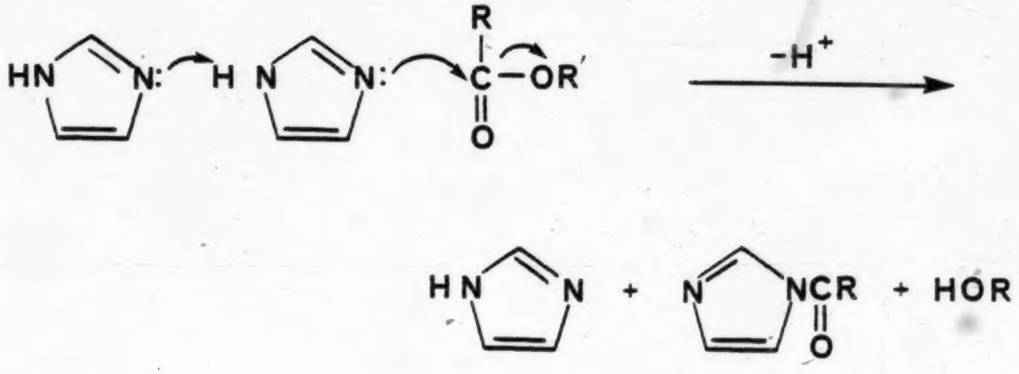
HN
N:
H
N
N:
R
C
OR′
O
-H⁺
HN
N
+
N
NCR
O
+ HOR′

3.

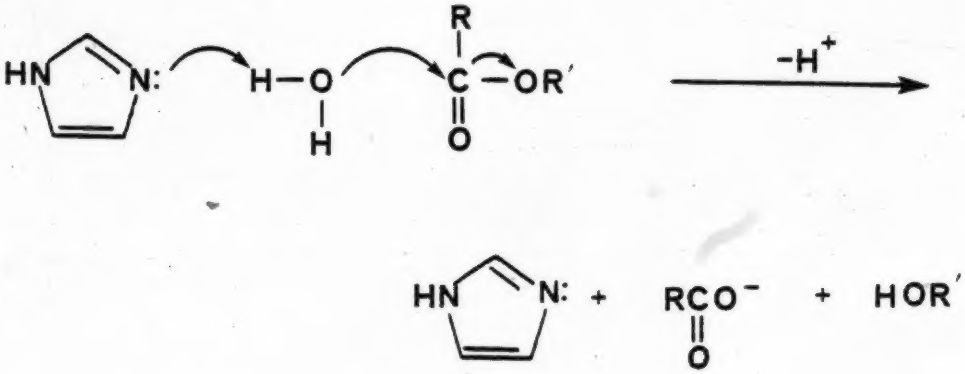
HN
N:
H
O
H
R
C
OR′
O
-H⁺
HN
N:
+
RCO⁻
O
+
HOR′

(Equation 2) becomes of importance. When pKa >>> 3 (ie aliphatic esters) general base assistance of the attack of water by imidazole (Equation 3) is the sole mechanism for catalysis of hydrolysis.

Although intramolecular imidazole catalysis of ester hydrolysis has received less attention, direct nucleophilic displacement is a very facile process for phenyl acetates of γ-(4-imidazolyl) butyrate (1) yielding the bicyclic lactam intermediate[14,15] (1a). (Equation 4).

4. 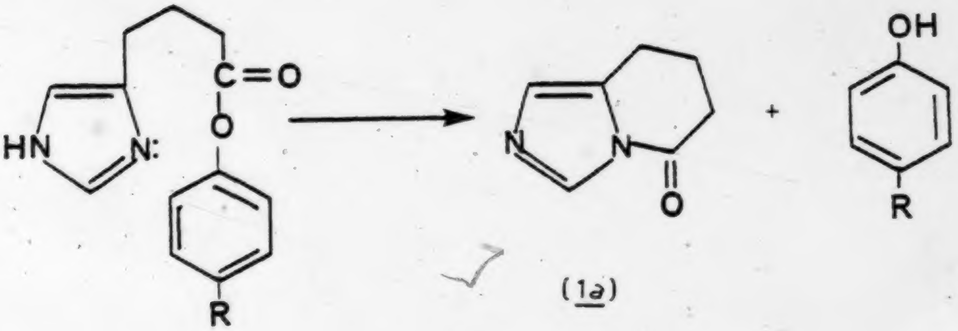

(1) (1a)

R= p-NO_2, m-NO_2, p-Cl, H

Fife[16] and co-workers also studied the intramolecular catalysis due to an imidazole in a series of esters of o-(2-imidazoyl)-benzoic

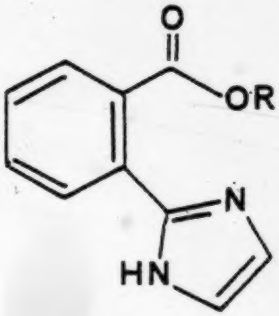

(2) R = Me
(3) R = CH_2CF_3
(4) R = Ph

acid. For the methyl ester (2), in the neutral pH region, imidazole reacts as a general base with an H_2O molecule to catalyze the hydrolysis of the ester. At high pH's the rate enhancement of the hydrolysis of the trifluoroethyl ester (3) is due to nucleophilic attack by the imidazole anion while at lower pH's imidazole itself is acting as a nucleophile.

Two discrete steps can be observed in the hydrolysis of the phenyl ester (4) at pH values > 5.5 which correspond to cyclization (phenol release) to the cyclic intermediate (5) and to slower hydrolysis of the intermediate.

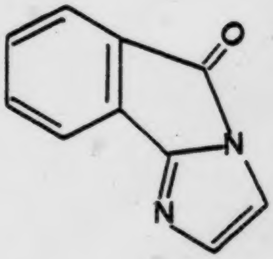

(5)

As in the case of the trifluoroethyl ester, nucleophilic attack by the neutral imidazole ring, and the imidazole anion or the kinetically equivalent attack of the neutral species catalyzed by hydroxide ion is responsible for the cyclization.

Papain: Structure and Mechanism

Perhaps the single most important evidence for the potential groups involved in papain-mediated hydrolysis is the X-ray crystal structure reported by Drenth and coworkers.[17] Because of the susceptibility of the Cys-25 group to air oxidation, papain has never been crystallized in its native form, but rather as an activatable enzyme with Cys-25 blocked as a mixed disulfide (papain S-SCH_3) or as a non-activatable form where the cysteine was oxidized probably to a sulfinic acid.[17a] Earlier structure determinations of papain were done with various mercuri derivatives.[17a] The conformation of the protein backbone remains surprisingly constant in the different derivatives, a finding which led Drenth to conclude[17a] that these structures must be quite similar to that of the native enzyme. The active site region is shown in Figure 2 (reproduced from reference 17a) in which one sees the active Cys-25 and His-159 which is hydrogen-bonded to the side chain of Asn-175. At a distance of 6.7 Angstroms from the imidazole ring and 7 Angstroms from Cys-25 is found the side chain carboxyl group of Asp-158.

Lowe[18] has proposed that papain operates through the mechanism shown in Scheme 1 where imidazole acts as a general base to aid the attack of the thiol on the carbonyl carbon to form a tetrahedral intermediate which subsequently decomposes to give the intermediate thioacyl enzyme. The existence of this intermediate thiol ester acyl enzyme has been confirmed spectrophotometrically.[19]

There seems to be little doubt that transient tetrahedral intermediates are involved in both the acylation and deacylation

Figure 2: The active site region of papain near the essential thiol group (reproduced from reference 17a).

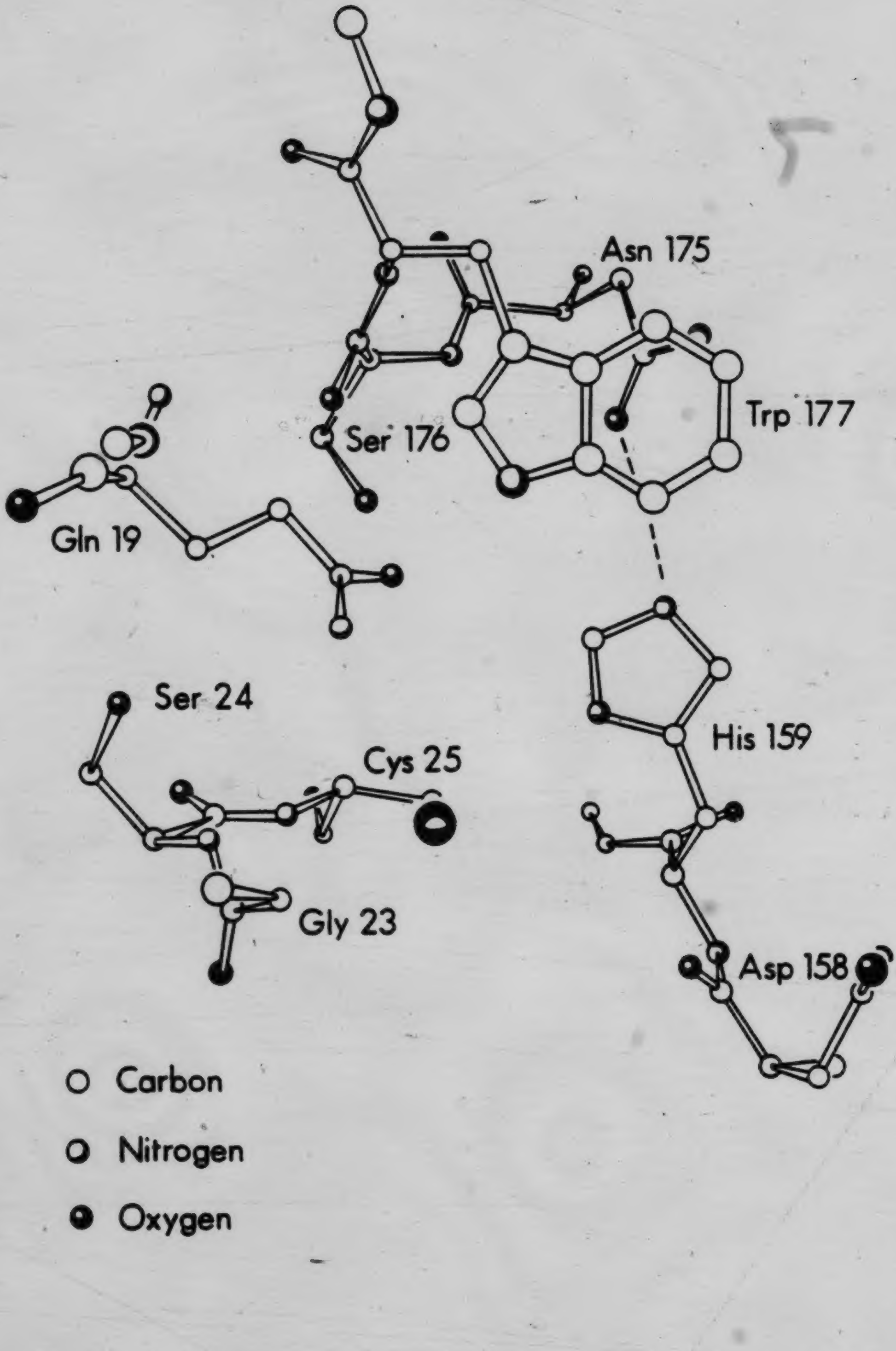
Asn 175
Trp 177
Ser 176
Gln 19
Ser 24
Cys 25
His 159
Gly 23
Asp 158
○ Carbon
○ Nitrogen
● Oxygen

PROPOSED MECHANISM OF ACTION OF PAPAIN

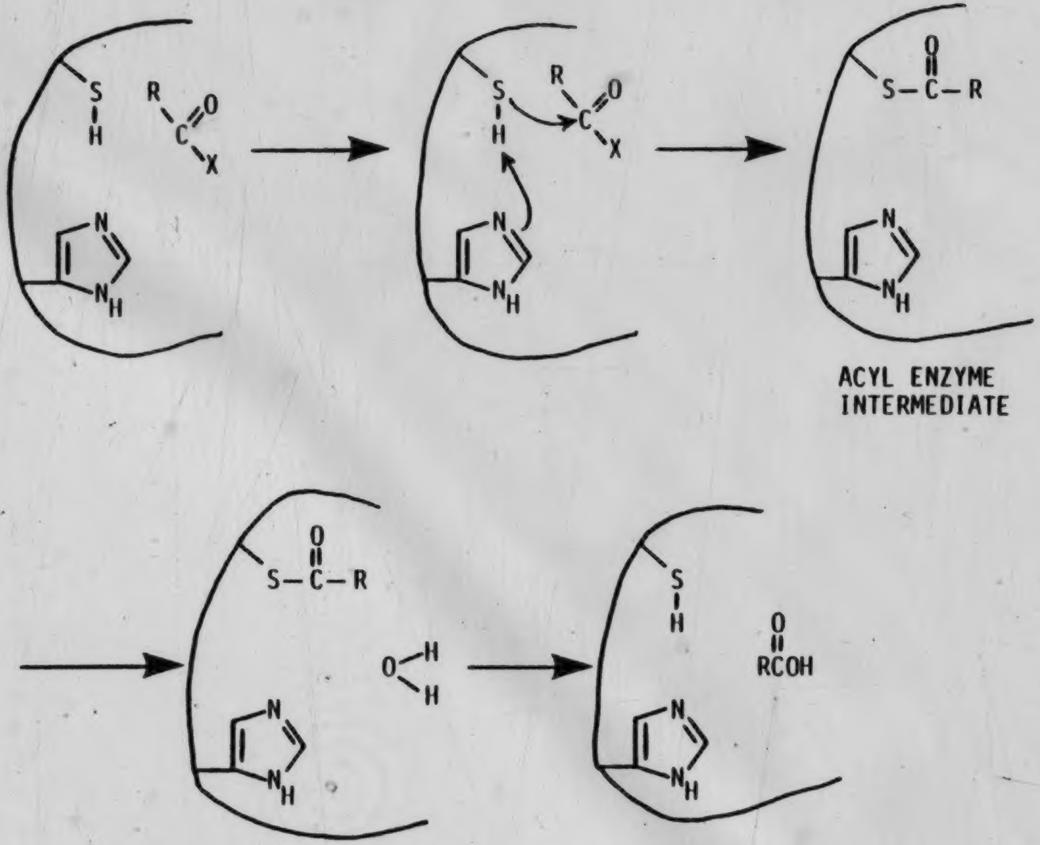
S
H
R
C
O
X
N
NH
ACYL ENZYME
INTERMEDIATE
S–C–R
O–H
H
RCOH

Scheme 1

steps. Thus, using a series of p-substituted phenyl esters of hippuric acid, a Hammett ρ-parameter value of 1.2 was observed for the overall acylation of the enzyme[20] whereas for p-substituted anilides of hippuric acid a $\rho = -1.04$ was obtained.[21] These values are most easily accounted for by assuming the involvement of a tetrahedral intermediate, with its formation being general-base catalyzed and its breakdown being general-acid catalyzed. The formation of the tetrahedral intermediate is assumed to be rate-determining for the acyl esters and the breakdown of the tetrahedral intermediate to be rate determining for the anilides. This latter conclusion has been confirmed by nitrogen kinetic isotope effect k^{14}/k^{15} studies on the papain catalyzed hydrolysis of N-benzoyl-L-arginimide,[22] where a value close to the theoretical limit was observed. This indicated the rate-limiting step involved the breaking of the carbon-nitrogen bond.

Also, associated with the deacylation step is a solvent isotope effect where $k_{H_2O}/k_{D_2O} = 2.75$ for α-N-benzyl-L-argininyl papain[23], 2.7 for benzoyl papain[24] and 3.35 for trans-cinnamoyl papain[19a] indicative of a general base mechanism.

However, there is little precedent[25] in the literature for general base catalysis of thiol attack in any reaction although the effect of enforced proximity of a general base on thiol reactivity remains to be established.

Whitaker[25f] and Fersht[25d], in a study of the reaction of a variety of mercaptans with different esters found that all had rates dependent upon the concentration of anion, RS^-, present. Likewise, Jencks and coworkers[25h] reacted methoxyethanethiol, benzenethiol, mercaptoethanol and ethylmercaptan with acetaldehyde to form the corresponding hemithioacetals and also found that it was the thiolate anion which was attacking the carbonyl group. It therefore appears that thiols react as their anions and apparently require no general-base assistance.

The proton liberation upon binding of zinc chloride and methylmercuric iodide to the thiol group of papain has been examined as a function of pH by Sluyterman and Wijdenes.[26] It was found that: in the neutral pH range the thiol group or the neighbouring imidazole group in the free enzyme carries a proton; at low pH both groups do so; whereas at high pH neither group carries a proton. These findings were confirmed by Nicholson and Shafer[27] who probed the pH dependence of the charge in the environment of the active site of papain by comparing the pK perturbations exhibited by nitrophenol reporter groups linked to the active site thiol group. Polgar[28] appears to be the first to suggest that in the neutral pH range the thiol and imidazole groups in the active site really exist as a thiolate-imidazolium ion pair and it was the thiolate anion which acted as a powerful nucleophile toward substrate. He observed a U.V. spectrum[28a] at pH's less than 8 which was assigned to the thiolate anion and attributed its stability to ion pair stabilization provided by the adjacent imidazolium ion. Later, Lewis et al.[29] attempted to characterize the ionization behaviour of the thiol group at the active site of papain by determining titrimetrically the pH dependence of the difference in proton content of papain and papain S-SCH_3, where Cys-25 is methylthiolated and cannot form a thiolate anion. These studies clearly showed that the ionization of the active site thiol group was linked to the ionization of another group which was presumed to be His-159. Lewis[29] postulated that it was the pK of the thiol group which was found to change from 3.3 to 7.6 upon deprotonation of His-159 and similarly it was the pK of His-159 which shifted from 4.3 to 8.5 when the active site thiol was deprotonated. In confirmation of these results it was found by a different technique that in papain-S-SCH_3,[30] the pK of His-159 is 3.9. Therefore, when the methylthio blocking group is removed and Cys-25 forms a thiolate anion the pK of His-159 should rise to about 8.5. Studies[31] on the pH dependence of NMR spectra of the catalytically active succinyl-papain and its methylthio derivative (succinyl-papain-S-SCH_3) showed that indeed the imidazole of His-159 has a pK of 8.6 in active papain. When the cysteinyl residue is methylthiolated the imidazole of His-159 is completely deprotonated between pH 6 and 10 indicating that the pK has dropped to about 4 in the inactive form of the enzyme. Fluorometric titrations[32] of papain, succinyl-papain and their corresponding Cys-25 methylthio derivatives also showed that removal of the methylthio group from Cys-25 resulted in an increase of approximately 4 pK units in the fluorometrically determined pK value. Thus, in the physiological pH range, 90% of papain contains a thiolate-imidazolium ion pair at the active site. Lewis and Shafer[33] also discovered that the reaction of a series of amides and esters with papain was modulated by two acid ionizations rather than a single ionization as previously believed. An ion pair reaction scheme, with predominantly charge-charge interactions in the ion pair predicts that the two acid ionizations correspond to deprotonation of the thiol of Cys-25 and the carboxyl group of Asp-158 respectively. The ion pair mechanism is attractive since it avoids the lack of precedent of general-base catalysis of thiol attack and it allows a large effective concentration of nucleophilic thiolate anion in the active site at pK values well below that of cysteine.

Recent support for the catalytically competent ion pair mechanism for papain acylation comes from the pioneering cryoenzymology studies on papain-catalyzed hydrolyses of both ester[34b] and amide[34c] substrates by Fink and Angelides[34]. It is generally accepted by enzymologists that after the initial productive binding of substrate to the active site of the enzyme (at an essentially diffusion controlled rate) a series of intermediates and transiton-state complexes occur, leading to the eventual release of products and free enzyme. Cryoenzymology is a method which utilizes the fact that different steps in the overall enzyme-catalyzed reaction usually have different free energies and enthalpies of activation. If the reaction is initiated by mixing enzyme and substrate at a suitably low temperature only the first step, the initial complexation to form the noncovalent Michaelis complex, ES, will occur as there is insufficient energy available to overcome the barrier to form the next intermediate. If the temperature is then gradually raised, a point will be reached where the complex ES transforms into the subsequent intermediate I_2. If the temperature is kept constant or lowered, I_2 may be trapped. This process may be repeated until a temperature is reached at which turnover occurs. Any intermediate for which $k_i >> k_{-i} + k_{(i+1)}$ can be accumulated in this manner (Equation 5).

$$5.\ \underset{k_{-1}}{\overset{k_i}{\rightleftharpoons}} I_i \xrightarrow{k(i+1)}$$

The major advantages of this technique stem from the potential to accumulate essentially all of the enzyme in the form of a particular intermediate and that the large rate reductions allow the most specific substrates to be used. The main limitation is the need to use an aqueous organic cryosolvent to avoid frozen solvents.

For the cleavage of N-carbobenzoxy-L-lysine methyl ester Fink[34b] has proposed the following simplest scheme (Equation 6).

$$6.\ E + S \underset{k_{-1}}{\overset{k_1}{\rightleftharpoons}} ES_1 \underset{k_{-2}}{\overset{k_2}{\rightleftharpoons}} I \underset{k_{-3}}{\overset{k_3}{\rightleftharpoons}} ES + P_1 \xrightarrow{k_4} E + P_2$$

Reaction 1 (k_1) is interpreted as very rapid substrate binding, where $k_1 > 1\ sec^{-1}$ at -65°C under pseudo-first order conditions. This ES complex undergoes a substrate-induced conformational change ($k_{obs} > 10^3\ sec^{-1}$ extrapolated to 25°C) in which His-159 moves from its crystallographically determined position[17a] (H-bonded to Asn-175) to one involving electrostatic interaction with Asp-158. Thus, the substrate-induced conformational change brings the enzyme into a catalytically competent thiolate-imidazolium ion pair, in which the imidazolium ion now gains additional electrostatic stabilization from the adjacent carboxylate ion. Reaction 3 involves the formation of the acyl enzyme ($k_3 \cong 10\ sec^{-1}$ extrapolated to 25°C).

Reaction 4 is, of course, the hydrolysis of the acyl enzyme which is known to be rate-limiting for esters[23] and therefore, under cryoenzymology conditions is so slow that the intermediate acyl enzyme concentration builds up.

For a specific amide substrate[34c] (i.e. N-carbobenzoyl-L-lysine-p-nitroanilide) the situation is similar with several intermediate stages in the catalysis being observed. After rapid substrate binding, substrate-induced conformational change and formation of the catalytically important ion pair, a slow step corresponding to the postulated formation of a tetrahedral intermediate is observed with an extrapolated first order rate constant $k_{obs} \cong 65 \pm 10\ \mathrm{sec}^{-1}$ (25°C). For the hydrolysis of amides breakdown of this tetrahedral intermediate to form the acyl enzyme intermediate is rate determining.[34f]

Fink's data are interpreted in the following manner (Scheme 2). Firstly, the substrate binds to the enzyme whose active site is similar to that determined crystallographically.[17a] The enzyme is then activated by repositioning of the imidazole group of His-159 next to Asp-158. The carboxylate group of Asp-158 then electrostatically stabilizes $H\text{-}Im^+$ which in turn stabilizes $Cys\text{-}S^-$ in the active species. In the case of this form of papain, the thiolate anion can attack the ester or amide "C=O" forming a tetrahedral intermediate which then collapses to the acyl enzyme intermediate.

It should be mentioned that recent crystallographic adduct studies indicate[17d] that the side chain carboxyl group of Asp 158 is too far away to take part in the hydrolysis mechanism.

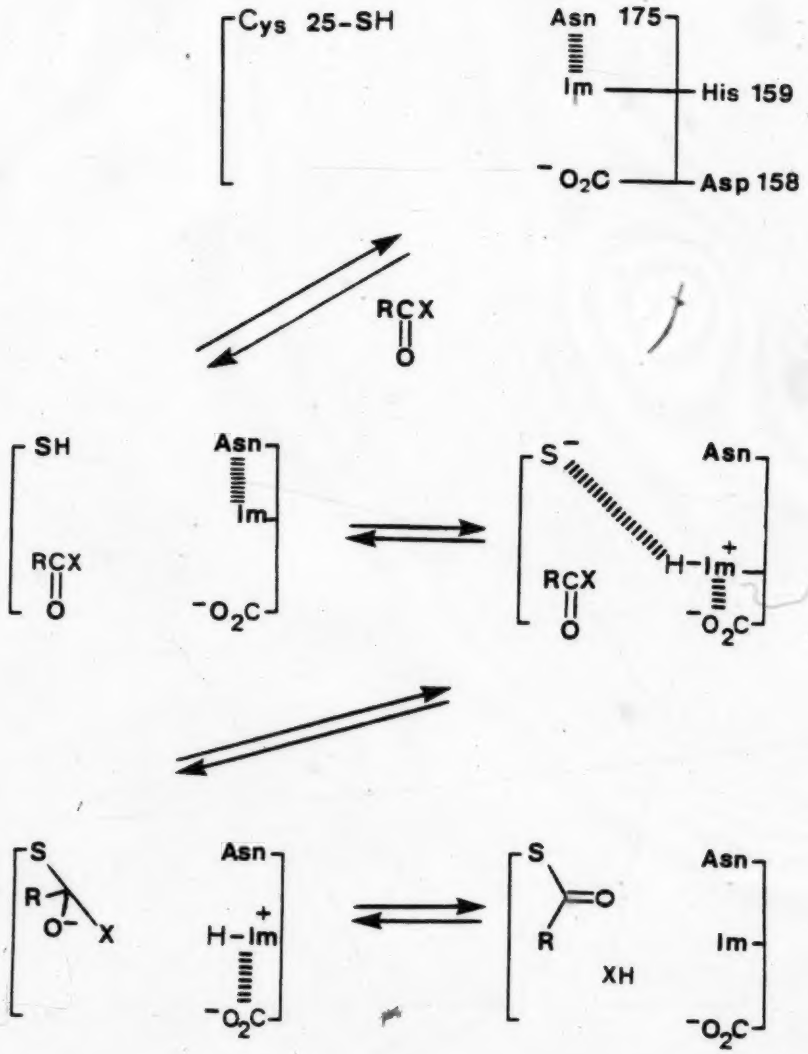
Cys 25-SH
Asn 175
Im
His 159
^-O_2C
Asp 158
RCX
O
SH
Asn
Im
RCX
O
^-O_2C
S^-
Asn
H-Im+
RCX
O
^-O_2C
S
R
O$^-$
X
Asn
H-Im+
^-O_2C
S
O
R
XH
Asn
Im
^-O_2C

Scheme 2

In view of the above evidence and the fact that the decomposition of the acyl enzyme appears to be subject to a general base catalysis by some group, the following mechanisms appear to be reasonable for the deacylation step. The imidazole group of His-159 could act as a general base removing a proton of water as it attacks, leading directly to the product (Scheme 3). As discussed earlier there are many precedents for this type of attack on oxygen esters in the study of small molecules.[35,36,37] However, general base catalysis by imidazole on unactivated thiol esters has not been observed.

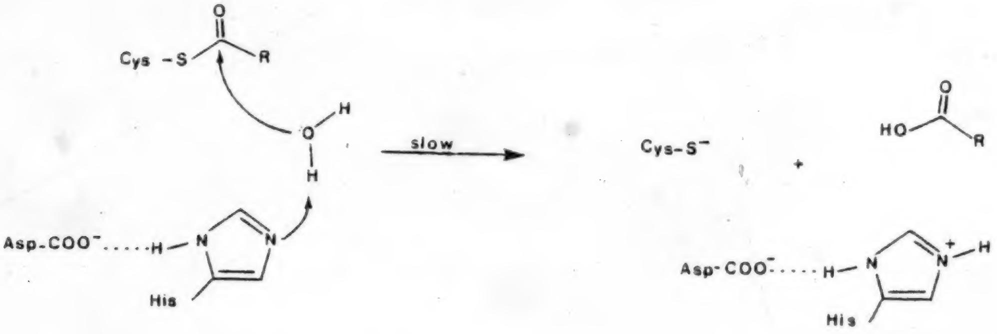

Scheme 3

In the enzyme the aspartate group can also act as a general base on the imidazole group which in turn nucleophilically displaces the thiolate. This leads to a new intermediate acyl enzyme whose breakdown could be rapid (Scheme 4).

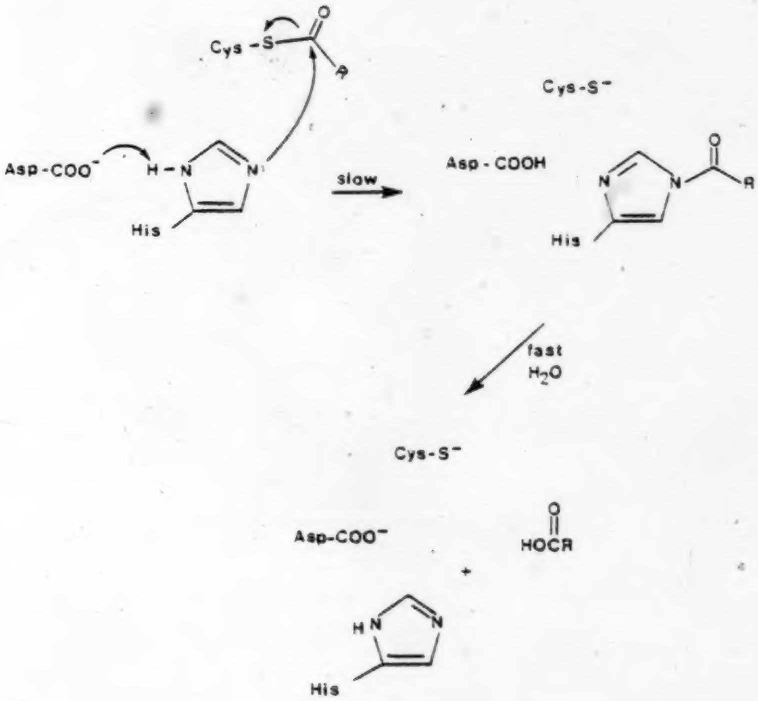
Cys -S
O
R
Asp-COO⁻
H - N
N
His
slow
Cys-S⁻
Asp - COOH
N
N
O
R
His
fast
H₂O
Cys-S⁻
Asp-COO⁻
O
HOCR
+
H N
N
His

Scheme 4

Finally there could be rapid formation of the imidazole-acyl intermediate whose decomposition is rate-limiting and subject to the observed solvent isotope effect[38] (Scheme 5).

In this case the carboxylate group stabilizes the N-acyl imidazolium species by electrostatic interactions. Schemes 4 and 5 are attractive since both intermolecular and intramolecular nucleophilic attack by imidazole on oxygen and sulphur esters is well known.

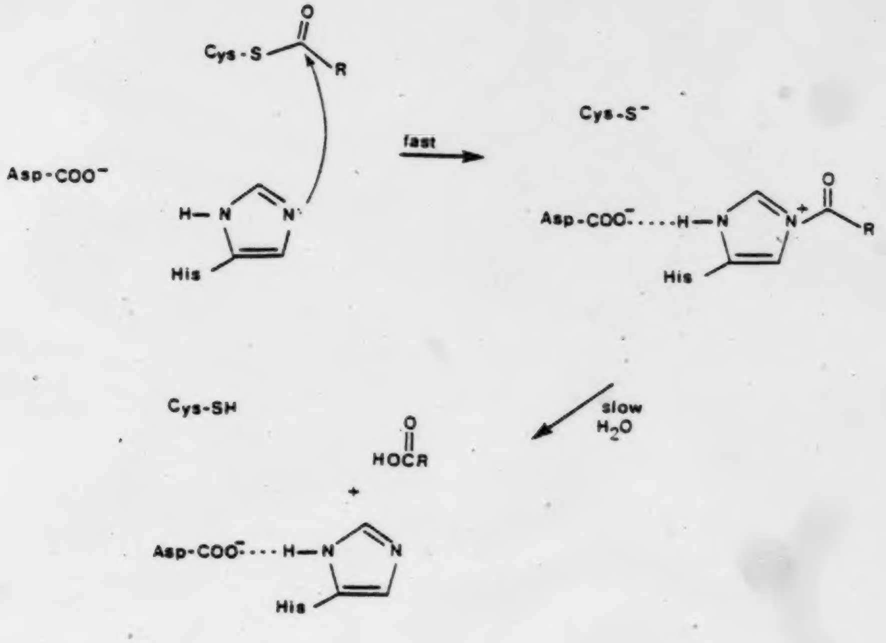
Cys-S
R
Asp-COO⁻
H—N
N
His
fast
Cys-S⁻
Asp-COO⁻·····H—N
N⁺
R
His
slow
H₂O
Cys-SH
HOCR
+
Asp-COO⁻····H—N
N
His

Scheme 5

Results and Discussion: Acylation Studies

The purpose of this project was to study the reactivity of imidazole-thiol pairs to form thiol esters and the subsequent catalysis of the thiol ester hydrolysis by a closely positioned imidazole or imidazolium ion. From these results it was hoped that plausible mechanisms of action for the enzyme could be proposed.

In order to investigate the role of the imidazole group on the acylation of a thiol, the reaction of the following compounds with p-nitrophenylacetate (PNPA) was studied. First, some free thiols, in this case benzyl mercaptan (6) and cyclohexylmethylthiol (7) were examined to see how rapidly an uncatalyzed thiol would attack PNPA. Second, it was intended that mercaptans with adjacent imidazoles as in compounds (8) and (9) be studied to see if a kinetically significant rate enhancement of acylation was provided by the imidazole. In these compounds the thiomethyl group is held close enough to the imidazole to favour a general base or an electrostatic interaction which would likely appear in the kinetic rate profiles. Also by changing from the benzimidazole system to the tetrahydrobenzimidazole system the pKa of the imidazole group changes from about 5.5 for (8a,b) to about 8 for (9a,b). It has been claimed that the pKa of the His-159 group in papain ranges between 4[18] and 8[30-32,34], the former value being attributable to a non-polar medium effect in the active site, and the latter to an electrostatic stabilization of the imidazolium ion by the carboxylate group of Asp-158[34]. On the basis of most of the current evidence it appears that the higher value is more likely. It is unlikely however, that we could mimic this type of

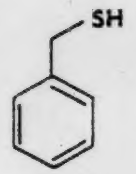

(6)

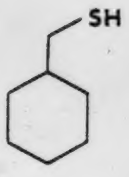

(7)

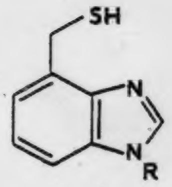

(8a) R = H
(8b) R = CH_3

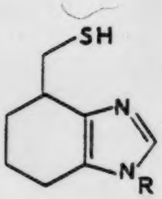

(9a) R = H
(9b) R = CH_3

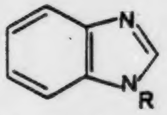

(10a) R = H
(10b) R = CH_3

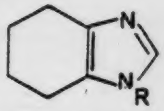

(11a) R = H
(11b) R = CH_3

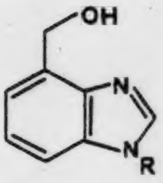

(12a) R = H
(12b) R = CH_3

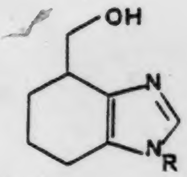

(13a) R = H
(13b) R = CH_3

intramolecular electrostatic interaction between the COO^- and HIm^+ ions in small molecules as solvent effects present in the active site cannot be approximated easily in aqueous solution. However, structurally adjusting the imidazole pKa should produce the same net effect if the catalysis relies on a high pKa for the imidazole.

Third, as control experiments, benzimidazole (10a), 1-methylbenzimidazole (10b), tetrahydrobenzimidazole (11a) and 1-methyltetrahydrobenzimidazole (11b), which have no free thiol, would be studied under the same conditions to ensure that nitrogen acylation or general base catalysis by the imidazole was not occurring to a significant extent.

Lastly, the cooperativity of the analogous alcohol-imidazole compounds (12) and (13) would be studied.

Synthesis: Acylation Studies

The synthesis of 4(7')-thiomethylbenzimidazole (8a) was based on the synthesis of benzimidazole systems reported by Jones et al.[39] The methyl group of (15), obtained by protective acylation of the amino group[40] of 2-amino-3-nitrotoluene (14) was oxidized to the carboxylic acid (16) by treatment with potassium permanganate.[40] Following removal of the protecting group[40] the nitro group was reduced with stannous chloride in hydrochloride acid[39] to give (18). The imidazole ring was introduced by condensation with formic acid and 4(7')-benzimidazole carboxylic acid (19) was converted to its methyl ester by Fischer esterification[41] to give (20). Reduction of (20) to the alcohol (12a) with lithium aluminum hydride followed by treatment with thionyl chloride gave the corresponding chloride, (21). This was treated with potassium ethyl xanthate to give (22) which was reduced to the free thiol (8a) with lithium aluminum hydride (Scheme 6).

The N-methyl derivatives were made in a similar manner. 4(7')-carboxymethylbenzimidazole (20) was treated with one equivalent each of methyl iodide and sodium hydride to give 1-methyl-4-carboxymethylbenzimidazole (23) (Scheme 7). It was important that the methyl group was in the position indicated (Figure 3). If the other nitrogen had been methylated any general base interaction with the thiol would be eliminated. Therefore, to determine the position of the methyl group Nuclear Overhauser experiments were conducted. Irradiation of the N-methyl group led to enhancement of the signals due to H_2 and H_7 (Figure 3). Irradiation of the O-methyl group led to no signal enhancement of any ring protons. Had the methyl group been positioned on the other nitrogen one would expect only enhancement of H_2. 1-Methyl-4-carboxymethylbenzimidazole (23) was treated with lithium aluminum hydride to give the alcohol (12b) which in turn was reacted with thionyl chloride to give the corresponding chloride (24) as before (Scheme 7). This was treated with potassium ethyl xanthate to give 1-methyl-ethyl-S-4-benzimidazolmethyl xanthate (25). Similar Nuclear Overhauser experiments were carried out which confirmed the results which were found for 1-methyl-4-carboxymethylbenzimidazole (23). Again one could see only enhancement of the signals representing H_2 and H_7 from irradiation of the N-methyl group (Figure 4). Lithium aluminum hydride reduction of the xanthate did not lead cleanly to the thiol so the chloro substituent of (24) was displaced with sodium

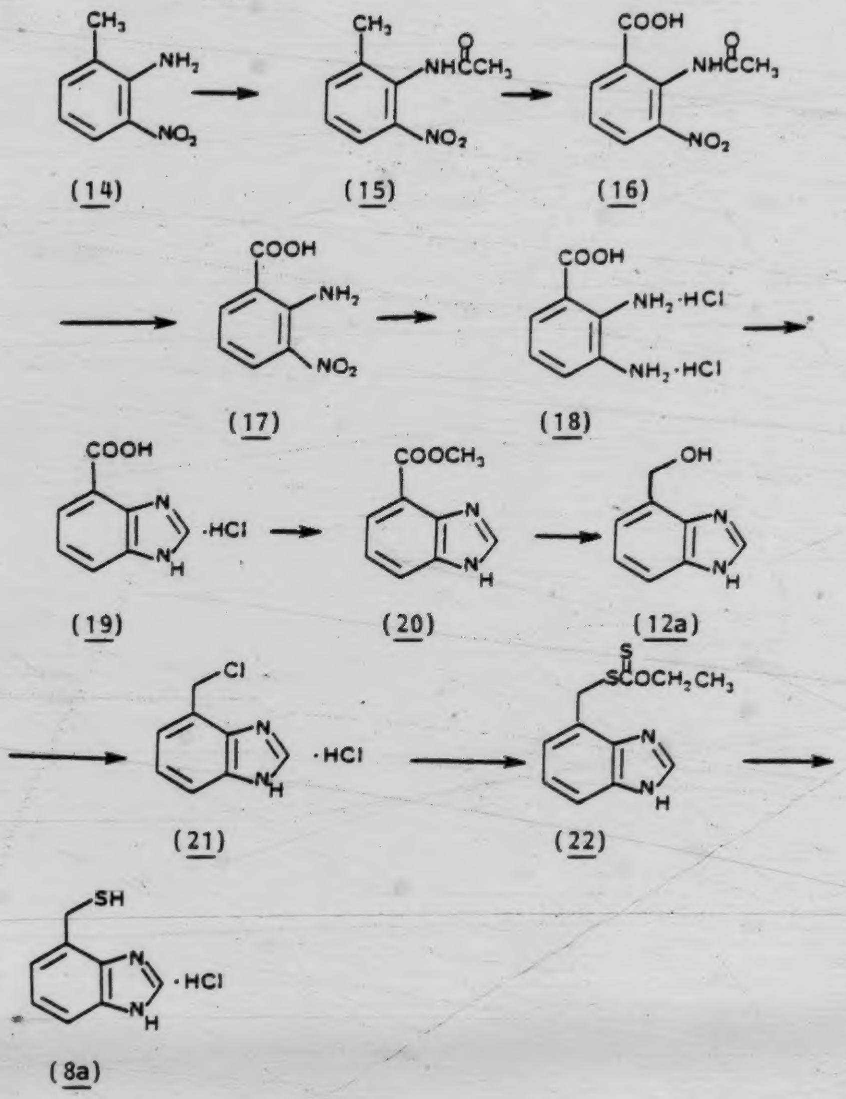
(14)
(15)
(16)
(17)
(18)
(19)
(20)
(12a)
(21)
(22)
(8a)

Scheme 6

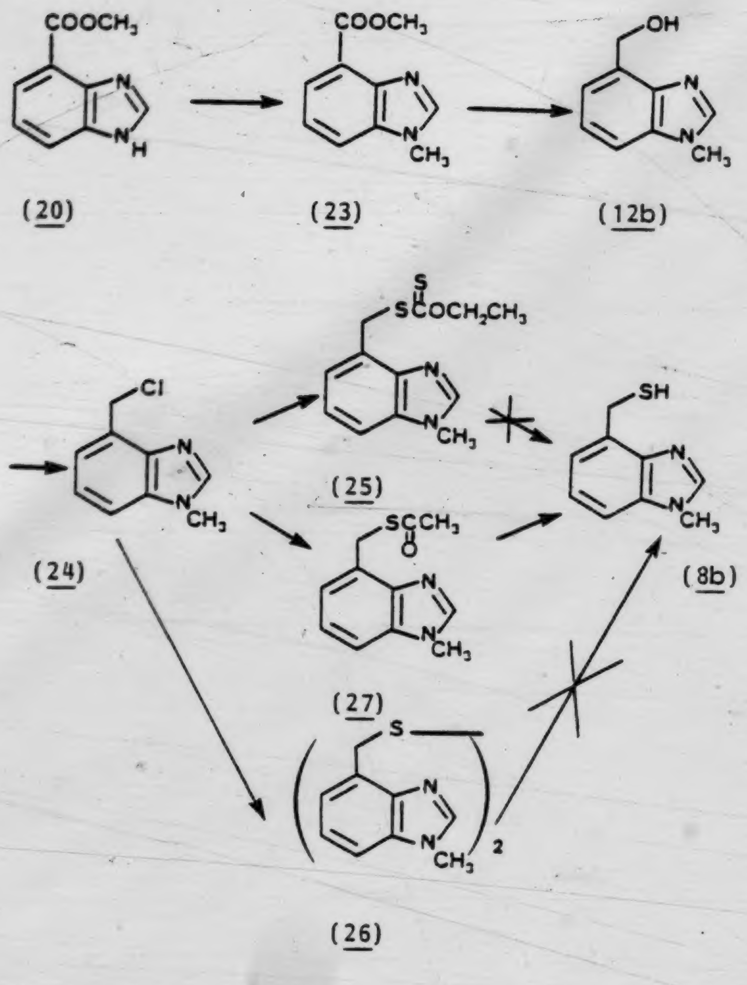
COOCH₃
N
H
(20)
COOCH₃
N
CH₃
(23)
OH
N
CH₃
(12b)
Cl
N
CH₃
(24)
S
SCOCH₂CH₃
N
CH₃
(25)
SH
N
CH₃
(8b)
SCCH₃
O
N
CH₃
(27)
S
N
CH₃
2
(26)

Scheme 7

Figure 3: Nuclear Overhauser Effect from irradiation of the N-methyl (δ 3.9) of 4-carboxy-1-methylbenzimidazole (23) in $CDCl_3$.

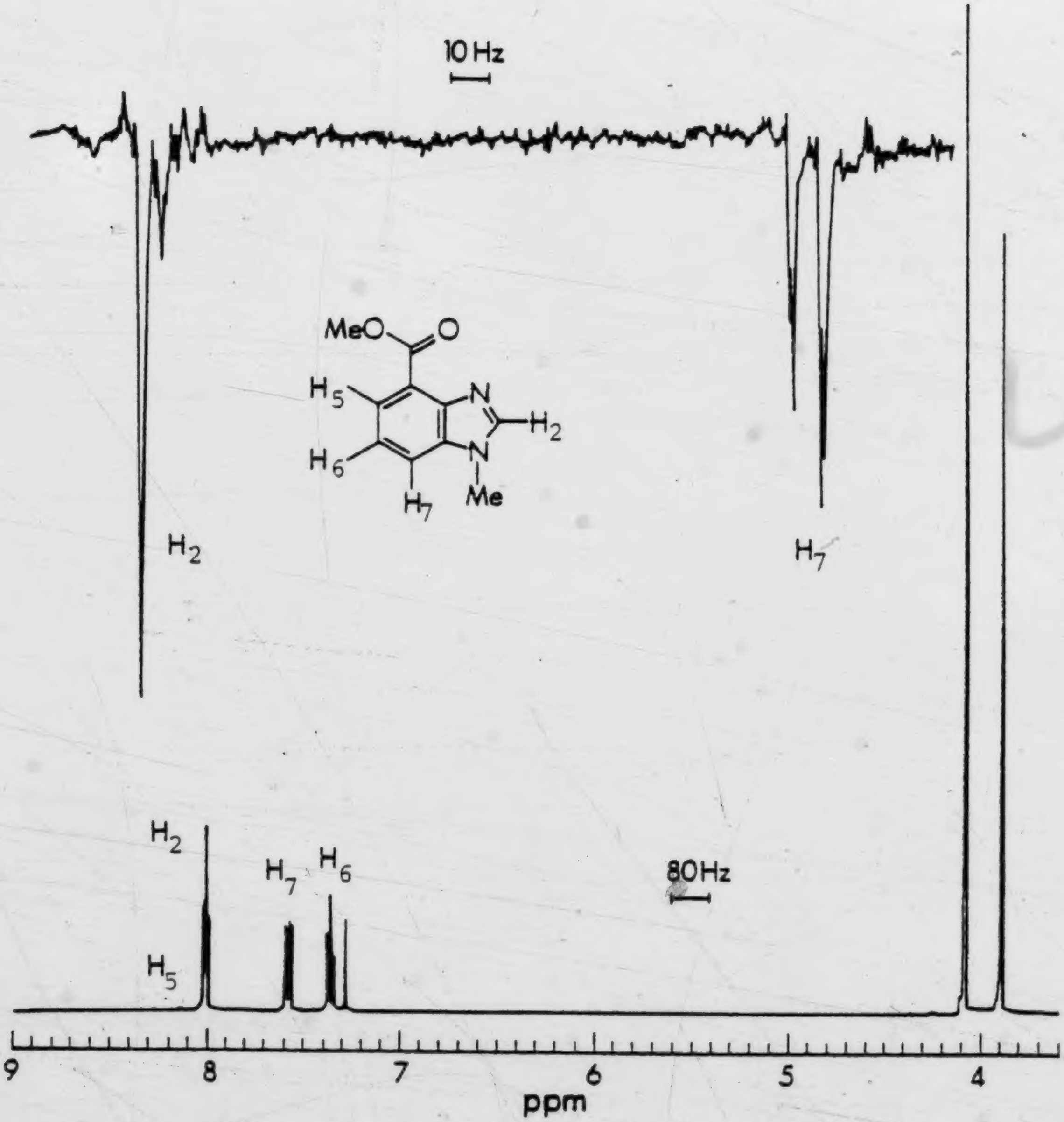
10 Hz
H$_2$
H$_7$
MeO
O
H$_5$
N
H$_2$
H$_6$
N
H$_7$
Me
H$_2$
H$_7$
H$_6$
H$_5$
80Hz
9
8
7
6
5
4
ppm

Figure 4: Nuclear Overhauser Effect from irradiation of the N-methyl (δ 3.8) of 1-methyl-ethyl-S-4-benzimidazolmethyl xanthate (25) in $CDCl_3$.

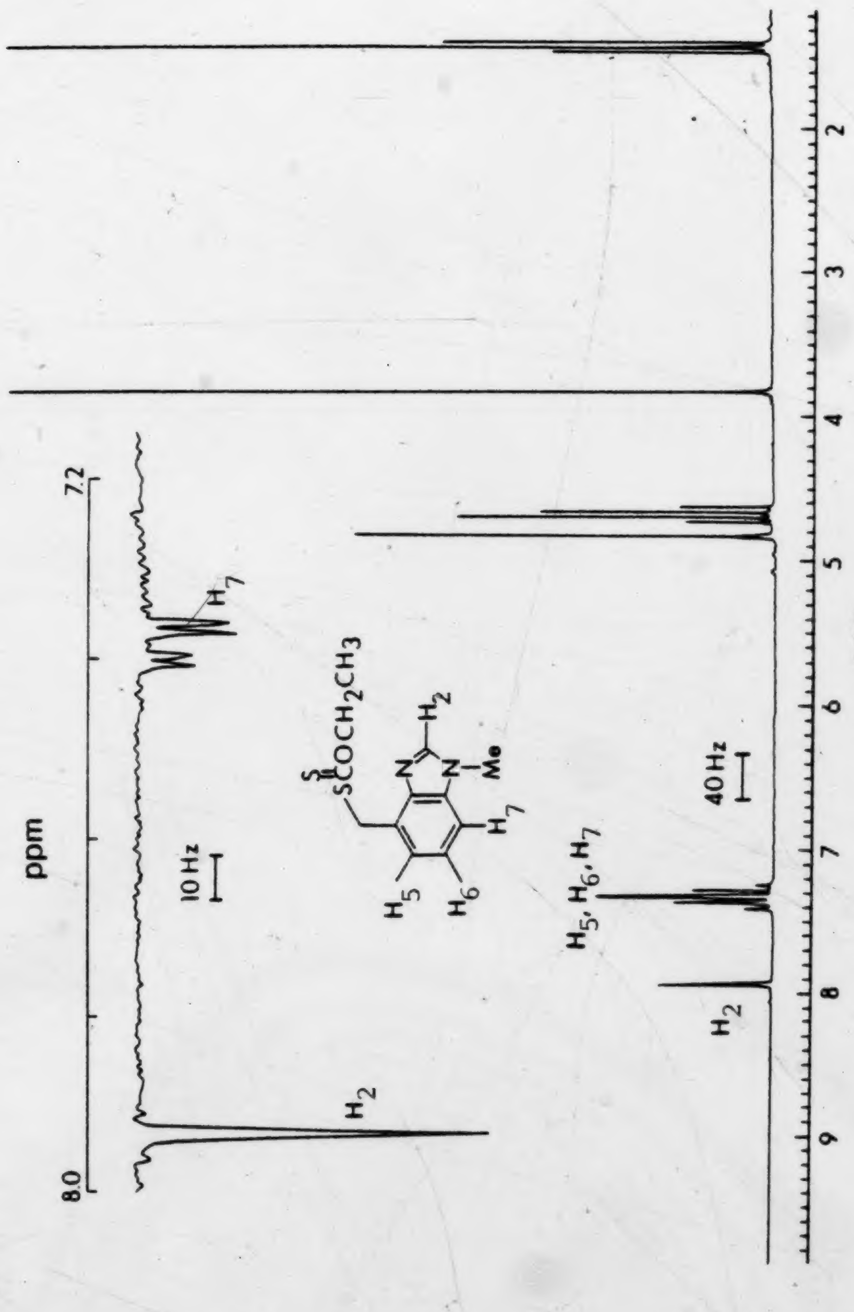
ppm
8.0
7.2
H₂
H₇
10 Hz
SCOCH₂CH₃
S
N
N
Me
H₂
H₅
H₆
H₇
H₅, H₆, H₇
H₂
40 Hz
9
8
7
6
5
4
3
2
ppm

sulfhydrate under nitrogen atmosphere. This gave the disulfide (26) which likewise could not be cleanly reduced with either $LiAlH_4$ or Zn/AcOH. However, displacement of the chloride with potassium thioacetate to give (27) followed by rapid hydrolysis did yield the desired thiol (8b) (Scheme 7).

Benzimidazole (10a) was produced from ring closure of the dihydrochloride salt of phenylenediamine (28) with formic acid.[42] 1-Methylbenzimidazole (10b) was synthesized by treating benzimidazole (10a) with one equivalent each of methyl iodide and sodium hydride (Scheme 8).

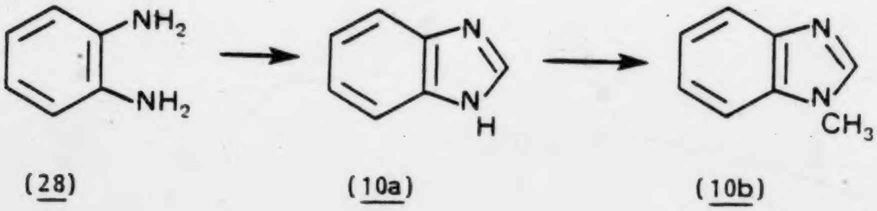

Scheme 8

Tetrahydrobenzimidazole (11a) and 1-methyltetrahydrobenzimidazole (11b) were obtained from the high pressure hydrogenation[43] of benzimidazole (10a) and 1-methylbenzimidazole (10b) respectively (Scheme 9).

Microanalytically pure benzyl mercaptan (6) was obtained from Aldrich and used without further purification in the reaction with PNP . The disulfide content was found to be negligible by titration with iodine.[44]

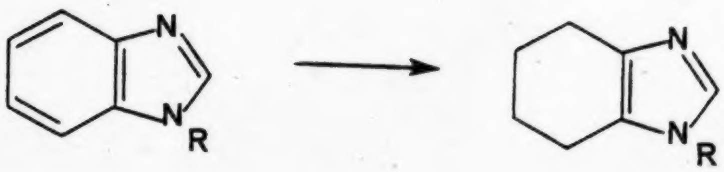

(10a) R=H
(10b) R=CH_3

(11a) R=H
(11b) R=CH_3

Scheme 9

Cyclohexylmethylthiol (7) was synthesized by displacement of

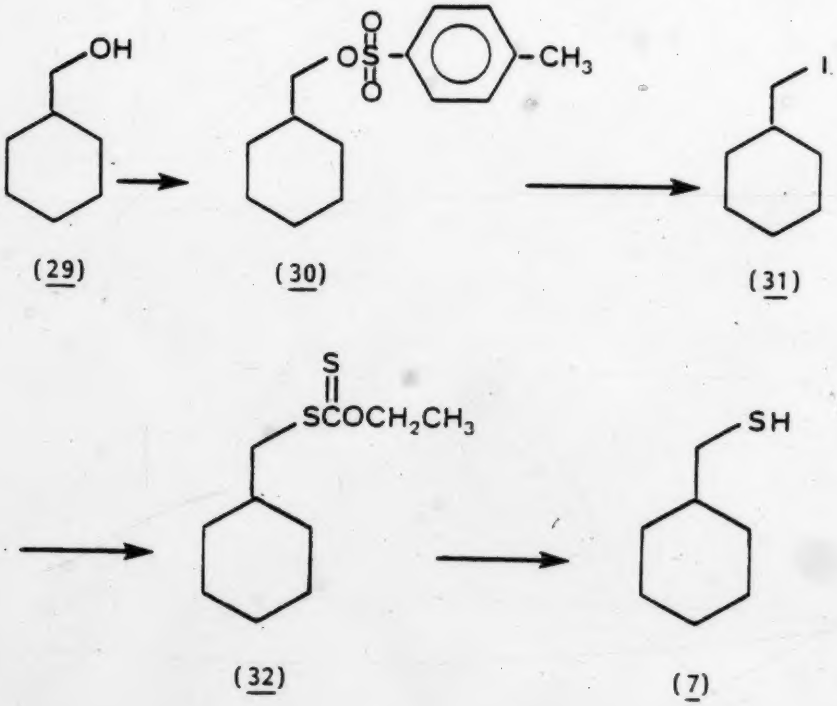
OH
O
OS
O
CH3
I
S
SCOCH2CH3
SH

(29) (30) (31)

(32) (7)

Scheme 10

the tosylate group of cyclohexylmethyltosylate (30)[45] by sodium iodide[46] followed by formation of the corresponding xanthate (32) which was reduced to the free thiol (7) with lithium aluminum hydride (Scheme 10).

Entry into the tetrahydrobenzimidazole systems in order to synthesize 4(7')-hydroxymethyltetrahydrobenzimidazole (13a) and 1-methyl-4-hydroxymethyltetrahydrobenzimidazole (13b) can be approached from at least two directions. The imidazole ring can be formed on an already existing cyclohexyl ring or a benzimidazole system containing the correct functionality can be reduced to the tetrahydrobenzimidazole analogue. Preliminary investigations centered on introducing the imidazole ring on the already reported compounds 6-bromo-2-ethoxycarbonylcyclohexanone (37b) or 6-bromo-2-methoxycarbonylcyclohexanone (37a).[47] Pimelic acid (33) was converted to its dimethyl ester (34) by Fischer esterification[41]. The ring was closed via a Diekmann condensation[48] to give 2-methoxycarbonylcyclohexanone (36a). The corresponding ethyl ester (36b) could also be made by reacting cyclohexanone (35) with diethyl carbonate[49] but in lower yield. Bromination[47] of (36) gave compound (37) which when refluxed with formamide[49] or reacted with formamidine acetate[50,51] in formic acid produced (38). The ester (38) was then reduced to the alcohol (13a) with lithium aluminum hydride (Scheme 11). Yields from the ring closure were so low (presumably due to condensations involving the carboalkoxy group) that the investigation of the alternative route in which a benzimidazole system is reduced to its corresponding tetrahydrobenzimidazole analogue was undertaken. High pressure

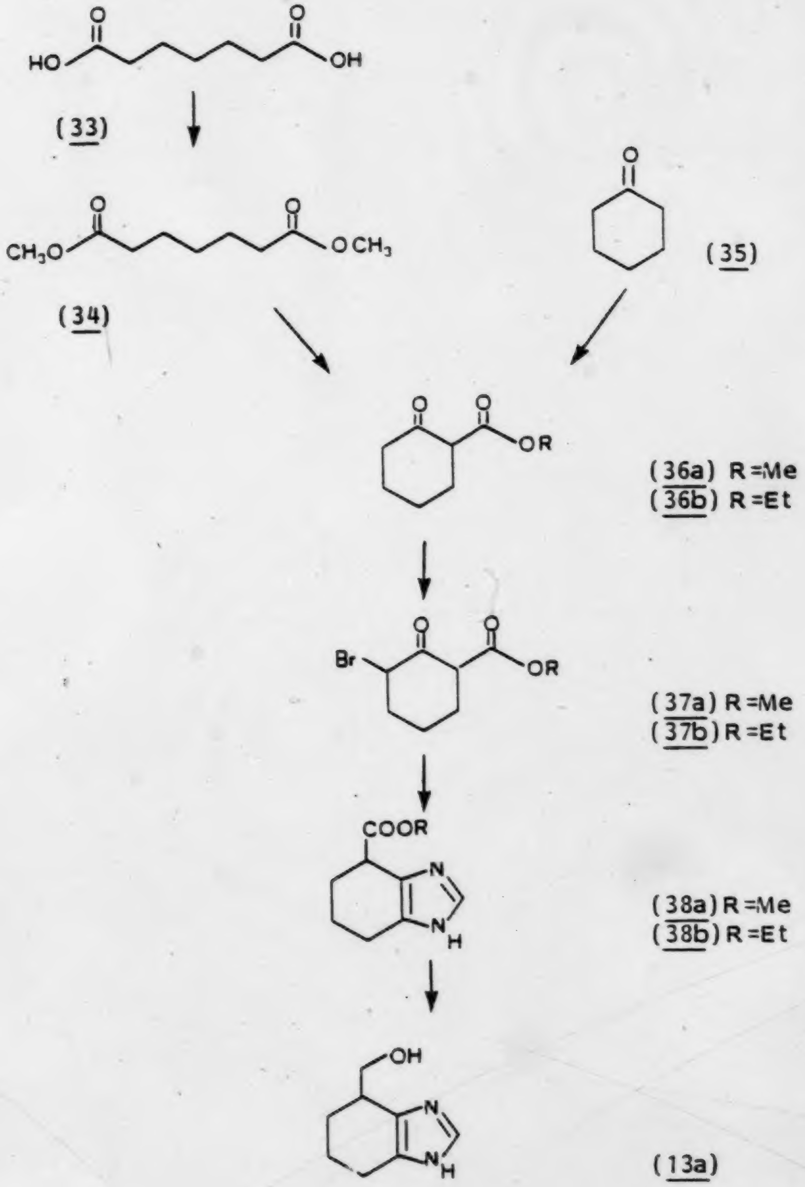
HO
OH
(33)
CH₃O
OCH₃
(34)
(35)
OR
(36a) R=Me
(36b) R=Et
Br
OR
(37a) R=Me
(37b) R=Et
COOR
N
N H
(38a) R=Me
(38b) R=Et
OH
N
N H
(13a)

Scheme 11

hydrogenations of several benzimidazole systems had been reported by Butula[43] in 1973 although none of them were substituted in the 4(7') position. Therefore, high pressure hydrogenation of 4(7')-carboxymethylbenzimidazole (20) was attempted over rhodium or palladium catalysts in a variety of solvents but total reduction to the tetrahydrobenzimidazole system could not be attained (Scheme 12).

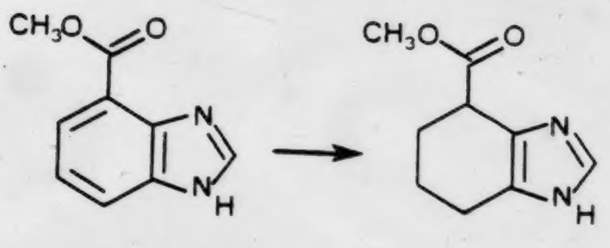

(20) (38a)

Scheme 12

However, it was found that the 4(7')-carboxymethylbenzimidazole system could be reduced to the corresponding dihydro derivative quite easily using a Birch reduction and the remaining double bond removed by low pressure hydrogenation (Scheme 13). The imidazole "NH" was protected by reacting 4(7')-carboxymethylbenzimidazole (20) with one equivalent each of methoxymethylchloride and sodium hydride to give (39a) which was reduced to (40a) with sodium in liquid ammonia and to the tetrahydro derivative (41a) by low pressure hydrogenation over platinum oxide. However, all attempts to remove the protecting group with concentrated acid, $TiCl_4$, or $ZnBr_2$ failed.[52] Methoxyethoxymethylchloride[52] and 1-chloro-1-methoxyethane[53] were also successfully used to protect the imidazole during the Birch reduction but again these could not be removed after reduction to their tetrahydro analogues. Attempts to protect 4(7')-carboxymethylbenzimidazole with trimethyl orthoformate[54], a protecting group which could have been easily removed after reduction failed. All examples[54] reported using this protecting group were of imidazoles of substantially higher basicity than the benzimidazole systems we were using. This was believed to be the reason for the difficulty in reacting our compounds with triethyl orthoformate.

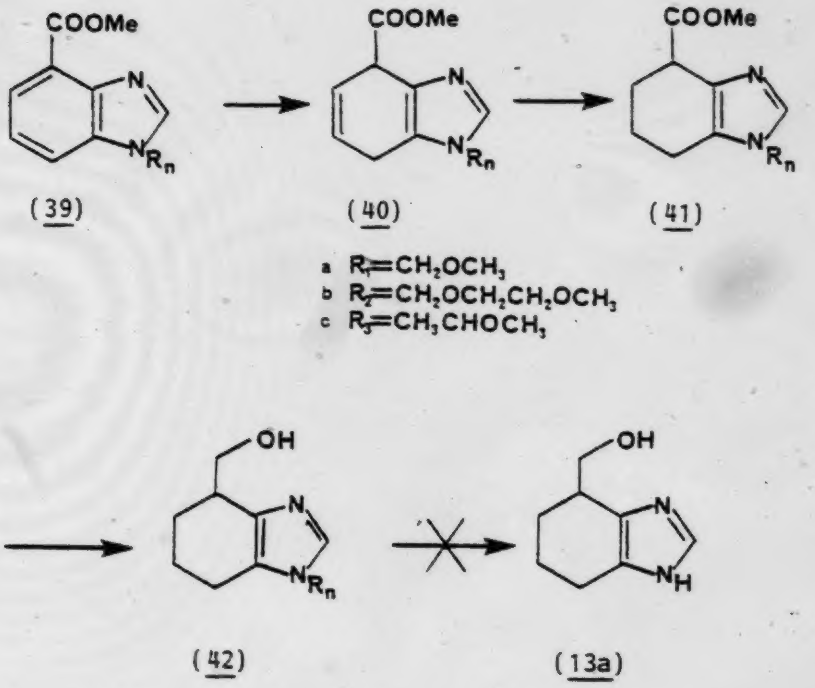

(39) (40) (41)

a R_1=CH_2OCH_3
b R_2=$CH_2OCH_2CH_2OCH_3$
c R_3=CH_3CHOCH_3

(42) (13a)

Scheme 13

However, the N-methyl analogue (23) could be obtained from the reaction of 4(7')-carboxymethylbenzimidazole with sodium hydride and iodomethane. Treatment of 1-methyl-4-carboxymethylbenzimidazole (23) with sodium and liquid ammonia led cleanly to the dihydro derivative

(43) which was easily hydrogenated to the corresponding tetrahydro compound (44). Reduction of the methyl ester with lithium aluminum hydride gave the desired alcohol (13b). The alcohol, which was very hydroscopic, was converted to the hydrochloride salt of the chloride (45) for microanalysis (Scheme 14).

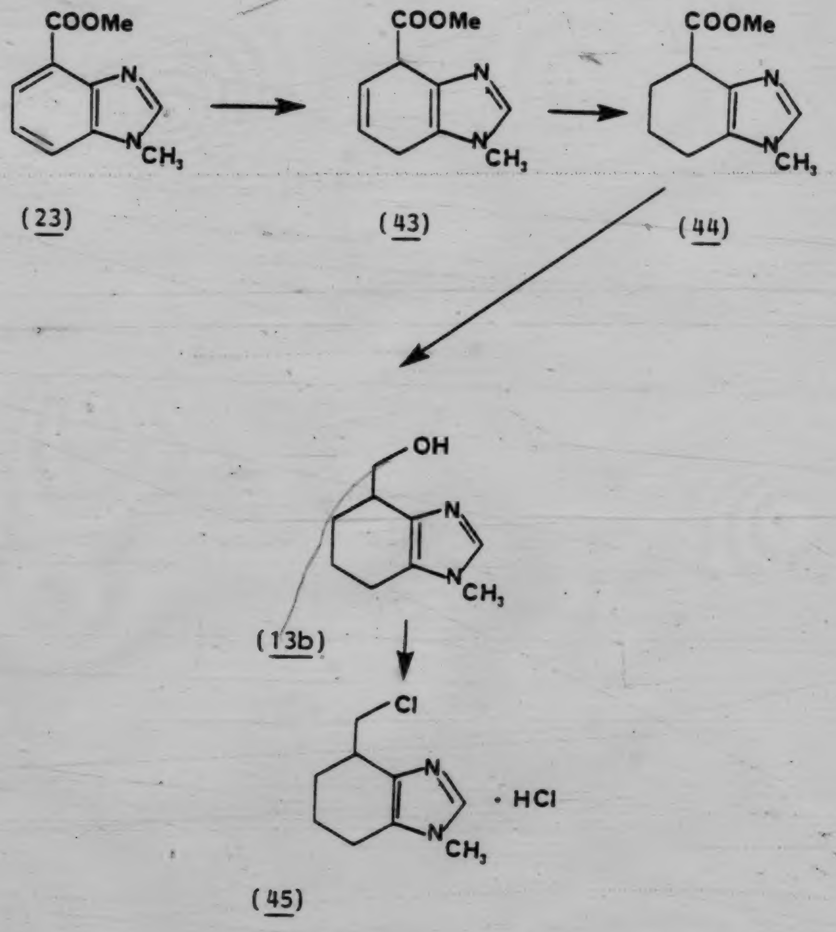
COOMe
N
N
CH₃
(23)
COOMe
N
N
CH₃
(43)
COOMe
N
N
CH₃
(44)
OH
N
N
CH₃
(13b)
Cl
N
N
CH₃
· HCl
(45)

Scheme 14

Basicities

Ionization constants of these compounds were determined by potentiometric titration methods modified from the method of Breslow[55] and assumes that the pKa's are well separated. Briefly, the protonated forms of the compounds were titrated with 0.1000 N NaOH in ethanol/water at 25°C and the data were analyzed according to the classical function $pK = H_O + \log[LH]/[L^-]$[56] where $H_0 = \log a_H \gamma_{L^-}/\gamma_{LH}$ and is approximately equal to pH in dilute aqueous solutions.

If L is an organic base which can accept three protons according to the following equations

$$L + H^+ = LH^+$$

$$LH^+ + H^+ = LH_2^{+}$$

$$LH_2^{++} + H^+ = LH_3^{+++}$$

then the equilibrium constants Ka_1, Ka_2 and Ka_3 can therefore be defined as shown below:

$$pKa_1 = pH + \log[LH^+]/[L]$$

$$pKa_2 = pH + \log[LH_2^{++}]/[LH^+]$$

$$pka_3 = pH + \log[LH_3^{+++}]/[LH_3^{++}]$$

Therefore $pKa_1 = pH$ when $\log[LH^+]/[L] = 0$ and $\log[LH^+]/[L] = 0$ when $[L] = [LH^+]$.

Let us define n_H as the average number of hydrogen ions bound per molecule of base.

$$n_H = ([LH^+] + 2[LH_2^{++}] + 3[LH_3^{+++}])/([L] + [LH^+] + [LH_2^{++}] + [LH_3^{+++}])$$

$$n_H = ([LH^+] + 2[LH_2^{++}] + 3[LH_3^{+++}])/[L_t]$$

Therefore $pKa_1 = pH$ when $n_H = 0.5 = [LH^+]/[L_t]$

Similarly

$$pKa_2 = pH \text{ when } n_H = 1.5 = ([LH^+] + 2[LH_2^{++}])/[L\ ]$$

$$pKa_3 = pH \text{ when } n_H = 2.5 = (2[LH_2^{++}] + 3[LH_3^{+++}])/[L_t]$$

It is then only necessary to express n_H as a function of experimentally determined variables:

7. $n_H = ([H]_t - [H^+] - [OH^-]_{added} + [OH^-])/[L_t]$

where:

$[H^+]_t$ = total concentration of strong acid added at the beginning.

$[H^+]$ is derived from the pH reading. The mean activity coefficient of HCl in 0.3 M salt solutions[57] or in 20% ethanol[58] does not vary significantly from that of dilute solutions of HCl in pure water. Therefore, the assumption that $[H^+] \approx pH$ can be made and used in equation 7. To check that this assumption was indeed valid dilute solutions of HCl in water were made up in the low pH range and the pH meter was adjusted for linearity from pH 1.16 to 5.16. The same concentrations of HCl were dissolved in 0.25 M KCl solutions and there was no significant difference in the pH readings. Finally, the same concentrations of HCl were made up in 31.6% ethanol/water, 0.25 M KCl solutions and again there was no significant difference in the readings obtained from those obtained for the HCl solutions in pure water. Therefore, in equation 7 $-\log[H^+] \equiv pH$ for pH's 1 to 5 and above pH 5 this term becomes negligible.

$[OH^-]_{added}$ is the concentration of $[OH^-]$ added during the titration.

$[OH^-]$ is obtained from the calibration curve in Figure 5. Known concentrations of NaOH were dissolved in the ethanol/water mixture used for the titration measurements and above a [OH$^-$] of 1×10^{-4} M the pH readings no longer remained linearly dependent on [OH$^-$] (Table 1, Figure 5). Therefore, a plot of n_H vs pH allowed us to obtain the pH value when n_H = 0.5, 1.5, 2.5. Each pKa was the average of at least three reproducible runs. The results are given in Table 2.

Table 1

pH	p[OH$^-$]
12.56	1.68
11.47	2.68
10.36	3.68
9.32	4.68
8.32	5.68

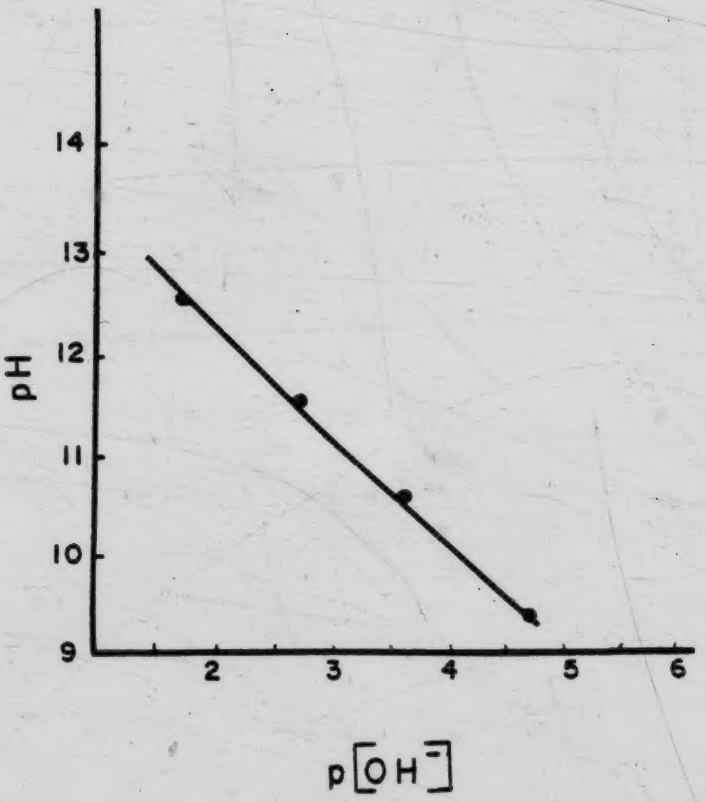

Figure 5: Plot of pH vs p[OH⁻] as determined from known concentrations of NaOH in ethanol/H_2O (31.6% ethanol).

Catalytic Studies

The rates of acylation were followed spectrophotometrically using a Cary 210 UV-VIS spectrometer. To aid in data collection the Cary 210 was interfaced to a Rockwell Aim 65 microprocessor (Appendix 1).

The catalysis of the decomposition of PNPA with these compounds was followed under pseudo-first order conditions where [catalyst] = 10, 20, 30 [PNPA] by monitoring the appearance of p-nitrophenoxide (PNP) at 400 nm. The pH was kept constant by using buffers: HEPES (6.8-7.2), TRICINE (7.6-8.8), CHES (9.2-10.0) and CAPS (10.4-10.8).

Table 2

	pK_{a_1}	pK_{a_2}
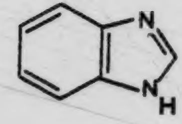	5.54±0.02	
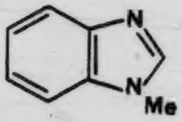	5.44±0.05	
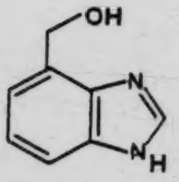	5.41±0.09	
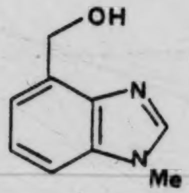	5.25±0.05	
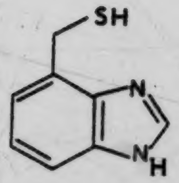	5.45±0.05	9.75±0.1
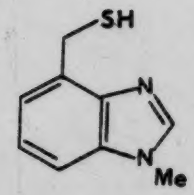	5.2±0.1	9.8±0.1

	pK_{a_1}
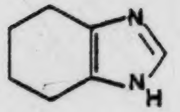	8.05±0.05
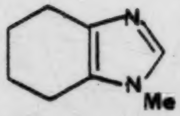	8.20±0.05
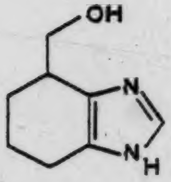	8.00±0.05
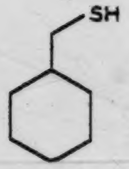	10.8±0.1
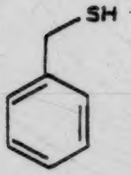	10.0±0.1

A typical run was performed by adding 3.0 mL of 0.5 N KCl, 1 mL 0.1051 N HNO_3, 1 mL 95% ethanol and 0.025 mmol of the substance to be titrated in 1 mL ethanol to the thermostatted cell (25°C) and titrating with 0.1000 N NaOH.

All reaction rates except for the reaction of cyclohexylmethylthiol (7) with PNPA were monitored in 31.6% ethanol/H_2O (v/v) with an ionic strength equal to 0.345 M by addition of a calculated amount of KCl (after correction for the amount of ionized buffer) and [buffer] = 0.21 M in large excess over [catalyst]. The measurements involving acylation of cyclohexylmethylthiol (7) with PNPA were monitored in H_2O /EtOH(95%)/THF (64.4/29/6.6) (v/v) with an ionic strength of 0.33 M and [buffer] = 0.19 M. Tetrahydrofuran was used here due to the insolubility of (7) in the aqueous ethanol mixture. The rate of decomposition of PNPA in the absence of catalyst was determined at pH 8.4 in this solvent mixture and was found to be equal within experimental error, to the value determined for the decomposition in aqueous ethanol alone. Therefore it was assumed that the THF would make little difference in the values determined for (7) + PNPA.

All solutions used for the acylation of 4(7')-thiomethylbenzimidazole (8a) and 1-methyl-4-thiomethylbenzimidazole (8b) were deoxygenated bubbling argon through them to prevent air oxidation of the thiol to the corresponding disulfide. Even with this precaution values for the second order rate constants above 9.2 had to be obtained by extrapolation from the value at pH 9.2 and the known pKa (Table 2) of the compound. All experiments were followed to completion and the pseudo-first order rate constants were obtained from a non-linear least squares analysis of the data (Appendix 2). In order to determine that the reactions were indeed pseudo-first plots of $\ln(A_\infty - A)$ vs time were checked for linearity over at least three half lives.

The rate equation for the decomposition of p-nitrophenylacetate is:

8. $$\text{rate} = (k_{H^+}[H^+] + k_{OH^-}[OH^-] + k_{H_2O}[H_2O] + k_{buff}[Buff] + k_{cat}[Cat])[PNPA]$$

where [Buff] is the buffer concentration and [Cat] is the concentration of the catalyst.

By doing each of the reactions both with and without catalyst we were able to combine all the water terms plus the buffer term as one constant so the rate expression was reduced to:

$$\text{rate} = (k' + k_{cat}[Cat])[PNPA]$$

$$k_{obs} = k' + k_{cat}[Cat]$$

The second order rate constants could be obtained by dividing by [Cat].

The results from the reaction of benzyl mercaptan (6) and cyclohexylmethylthiol (7) with p-nitrophenylacetate are given in Tables 3 and 4 respectively and illustrated in Figure 6. For (6) the reaction was studied from pH 10.8 to 7.6 and for each pH at least three different [Cat] to [PNPA] ratios were used, the catalyst always being in large excess so that pseudo-first order conditions are met. The pseudo-first order rate constant k'_{obs} was obtained by subtracting the buffer and water terms from k_{obs}. The second order rate constant k_{cat} was obtained by dividing k'_{obs} by the total concentration of mercaptan added to the solution and k_{RS^-} by dividing k'_{obs} by the concentration of thiolate anion present in

TABLE 3

PSEUDO-FIRST ORDER AND SECOND ORDER RATE CONSTANTS FOR THE HYDROLOYSIS OF *p*-NITROPHENYLACETATE WITH BENZYL MERCAPTAN[a].

pH±0.02	[RSH][b] 10^3 M.	$[RS^-]$[c] 10^3 M.	$k_{obs.} - (k_{hydrol.} + k_{buff.})$ $min.^{-1}$	$k_{cat.}$ $M.^{-1}$ $min.^{-1}$[d]	k_{RS^-} $M.^{-1}$ $min.^{-1}$[e]
10.8	1.34	1.16	1.291 ± 0.035	967	1113
10.8	2.68	2.31	2.760 ± 0.006	1030	1194
10.8	4.02	3.47	3.52 ± 0.02	877	1173
				Av̄. = 958 ± 75	Av̄. = 1160 ± 47
10.4	1.34	0.959	$9.91 \pm 0.055 \times 10^{-1}$	740	1033
10.4	2.68	1.92	1.967 ± 0.025	734	1033
10.4	4.02	2.88	2.837 ± 0.075	708	1024
				Av̄. = 727 ± 19	Av̄. = 1030 ± 6
10.0	0.667	3.33×10^{-1}	$3.08 \pm 0.1 \times 10^{-1}$	462	924
10.0	1.34	6.70×10^{-1}	$5.66 \pm 0.06 \times 10^{-1}$	423	845
10.0	2.02	1.01	$9.86 \pm 0.3 \times 10^{-1}$	488	976
10.0	1.26	6.30×10^{-1}	$5.64 \pm 0.01 \times 10^{-1}$	447	895
				Av̄. = 455 ± 32	Av̄. = 910 ± 65
9.6	0.667	1.91×10^{-1}	$1.59 \pm 0.2 \times 10^{-1}$	236	832
9.6	1.34	3.83×10^{-1}	$3.16 \pm 0.05 \times 10^{-1}$	234	825
9.6	2.02	5.77×10^{-1}	$4.67 \pm 0.07 \times 10^{-1}$	230	809
9.6	4.02	1.15	$9.75 \pm 0.25 \times 10^{-1}$	246	848
9.6	2.52	7.2×10^{-1}	$6.25 \pm 0.1 \times 10^{-1}$	247	868
9.6	1.26	3.6×10^{-1}	$2.90 \pm 0.03 \times 10^{-1}$	230	805
9.6	3.78	1.08	$9.13 \pm 0.03 \times 10^{-1}$	241	845
				Av̄. = 238 ± 9	Av̄. = 833 ± 35
9.2	2.26	3.10×10^{-1}	$2.40 \pm 0.06 \times 10^{-1}$	106	774
9.2	3.39	4.65×10^{-1}	$3.84 \pm 0.02 \times 10^{-1}$	113	830
9.2	1.34	1.84×10^{-1}	$1.56 \pm 0.03 \times 10^{-1}$	115	816
9.2	1.34	1.84×10^{-1}	$1.50 \pm 0.02 \times 10^{-1}$	112	848
9.2	1.26	1.73×10^{-1}	$1.63 \pm 0.02 \times 10^{-1}$	120	942
				Av̄. = 113 ± 7	Av̄. = 842 ± 100
8.8	1.13	6.73×10^{-2}	$7.18 \pm 0.06 \times 10^{-2}$	63.5	1067
8.8	2.26	1.35×10^{-1}	$1.34 \pm 0.02 \times 10^{-1}$	59.5	992
8.8	3.39	2.02×10^{-1}	$1.98 \pm 0.03 \times 10^{-1}$	58.5	980
8.8	1.26	7.51×10^{-2}	$6.78 \pm 0.07 \times 10^{-2}$	53.8	903
				Av̄. = 58.8 ± 5	Av̄. = 985 ± 83
8.4	1.13	2.78×10^{-2}	$2.53 \pm 0.03 \times 10^{-2}$	22.4	910
8.4	2.26	5.56×10^{-2}	$5.19 \pm 0.05 \times 10^{-2}$	22.9	934
8.4	3.39	8.33×10^{-2}	$6.78 \pm 0.05 \times 10^{-2}$	25.7	833
				Av̄. = 23.7 ± 2	Av̄. = 892 ± 59
8.0	1.13	1.11×10^{-2}	$1.25 \pm 0.075 \times 10^{-2}$	10.5	1126
8.0	2.26	2.22×10^{-2}	$2.45 \pm 0.055 \times 10^{-2}$	10.6	1105
8.0	3.39	3.32×10^{-2}	$3.64 \pm 0.075 \times 10^{-2}$	10.5	1095
				Av̄. = 10.5 ± 0.1	Av̄. = 1109 ± 17
7.6	1.13	4.50×10^{-3}	$4.88 \pm 0.20 \times 10^{-3}$	4.2	1084
7.6	2.26	9.00×10^{-3}	$9.73 \pm 0.15 \times 10^{-3}$	4.3	1081
7.6	3.39	1.35×10^{-2}	$1.17 \pm 0.04 \times 10^{-2}$	3.4	866
				Av̄. = 4.0 ± 0.6	Av̄. = 1010 ± 144

a. Determined in 31.6% EtOH/H_2O (v/v). [Buffer] = 0.21 M. μ = 0.345 M. [PNPA] = 1.52×10^{-4} M to 2.03×10^{-4} M.

b. [RSH] = total concentration of thiol added.

c. [RS] = total concentration of thiolate anion present as determined from the known pK_a (10.0 ± 0.10).

d. $k_{cal.} = k_{obs.} - k_{hydrol.} + k_{buff.})/[RSH]$.

e. $k_{RS} = k_{obs.} - (k_{hydrol.} + k_{buff.})/[RS]$.

TABLE 4

PSEUDO-FIRST ORDER AND SECOND ORDER RATE CONSTANTS FOR THE HYDROLYSIS OF *p*-NITROPHENYLACETATE WITH CYCLOHEXYLMETHYLTHIOL[a].

pH±0.02	[RSH][b] 10^3 M.	$[RS^-]$[c] 10^3 M.	$k_{obs.} - (k_{hydrol.} + k_{buff.})$ $min.^{-1}$	$k_{cat.}$ $M.^{-1}$ $min.^{-1}$[d]	k_{RS^-} $M.^{-1}$ $min.^{-1}$[e]
10.8	3.14	1.57	$8.83 \pm 0.03 \times 10^{-1}$	281	562
10.8	4.04	2.02	1.15 ± 0.01	285	569
10.8	4.93	2.47	1.42 ± 0.10	289	612
				Av̄. = 285 ± 5	Av̄. = 568 ± 6
10.4	3.14	8.94	$5.32 \pm 0.03 \times 10^{-1}$	169	594
10.4	3.59	1.02	$5.59 \pm 0.02 \times 10^{-1}$	156	546
10.4	3.19	9.08×10^{-1}	$5.23 \pm 0.06 \times 10^{-1}$	164	575
				Av̄. = 163 ± 7	Av̄. = 572 ± 26
10.0	3.19	4.36×10^{-1}	$1.88 \pm 0.04 \times 10^{-1}$	58.9	431
10.0	4.40	6.00×10^{-1}	$2.54 \pm 0.06 \times 10^{-1}$	57.7	423
10.0	5.50	7.50×10^{-1}	$3.48 \pm 0.03 \times 10^{-1}$	63.2	464
				Av̄.= 59.9 ± 3.3	Av̄. = 439 ± 25
9.6	3.19	1.89×10^{-1}	$1.01 \pm 0.03 \times 10^{-1}$	31.7	533
9.6	4.40	2.61×10^{-1}	$1.31 \pm 0.03 \times 10^{-1}$	29.7	502
9.6	4.40	2.61×10^{-1}	$1.22 \pm 0.05 \times 10^{-1}$	27.6	467
				Av̄. = 29.7 ± 1.2	Av̄. = 500 ± 33
9.2	3.19	7.82×10^{-2}	$4.10 \pm 0.09 \times 10^{-2}$	12.9	524
9.2	3.52	8.62×10^{-2}	$4.18 \pm 0.03 \times 10^{-2}$	11.9	485
9.2	2.86	7.00×10^{-2}	$3.51 \pm 0.09 \times 10^{-2}$	12.3	501
				Av̄. = 12.3 ± 0.45	Av̄. = 503 ± 21
8.8	3.19	3.15×10^{-2}	$1.54 \pm 0.04 \times 10^{-2}$	4.83	487
8.8	3.63	3.59×10^{-2}	$1.87 \pm 0.09 \times 10^{-2}$	5.15	520
8.8	3.62	3.58×10^{-2}	$1.35 \pm 0.04 \times 10^{-2}$	3.72	376
				Av̄. = 4.57 ± 0.85	Av̄. = 461 ± 85
8.4	3.63	1.44×10^{-2}	$7.18 \pm 0.03 \times 10^{-3}$	1.96	498
8.4	3.19	1.26×10^{-2}	$7.22 \pm 0.06 \times 10^{-3}$	2.26	570
8.4	2.86	1.13×10^{-2}	$6.52 \pm 0.09 \times 10^{-3}$	2.28	575
				Av̄. = 2.17 ± 0.21	Av̄. = 548 ± 50

a. Determined in H_2O/EtOH (95%)/THF (64.4/29/6.6) (v/v). [Buffer] = 0.19. μ = 0.33 M. [PNPA] = 1.52×10^{-4} M.

b. [RSH] = total concentration of thiol added.

c. $[RS^-]$ = total concentration of thiolate anion present as determined from the known pK_a (10.8 ± 0.1).

d. $k_{cat.} = k_{obs.} - (k_{hydrol.} + k_{buff.})/[RSH]$.

e. $k_{RS^-} = k_{obs.} - (k_{hydrol.} + k_{buff.})/[RS^-]$.

Figure 6: Plot of the second order rate constant k_{cat} vs pH for benzyl mercaptan (6), cyclohexylmethylthiol (7), 4(7')-thiomethylbenzimidazole (8a) and 1-methyl-4-thiomethylbenzimidazole (8b). For 4(7')-thiomethylbenzimidazole (8a) and 1-methyl-4-thiomethylbenzimidazole (8b) the values above 9.2 are extrapolated from the value at 9.2 and the known pKa's of these compounds.

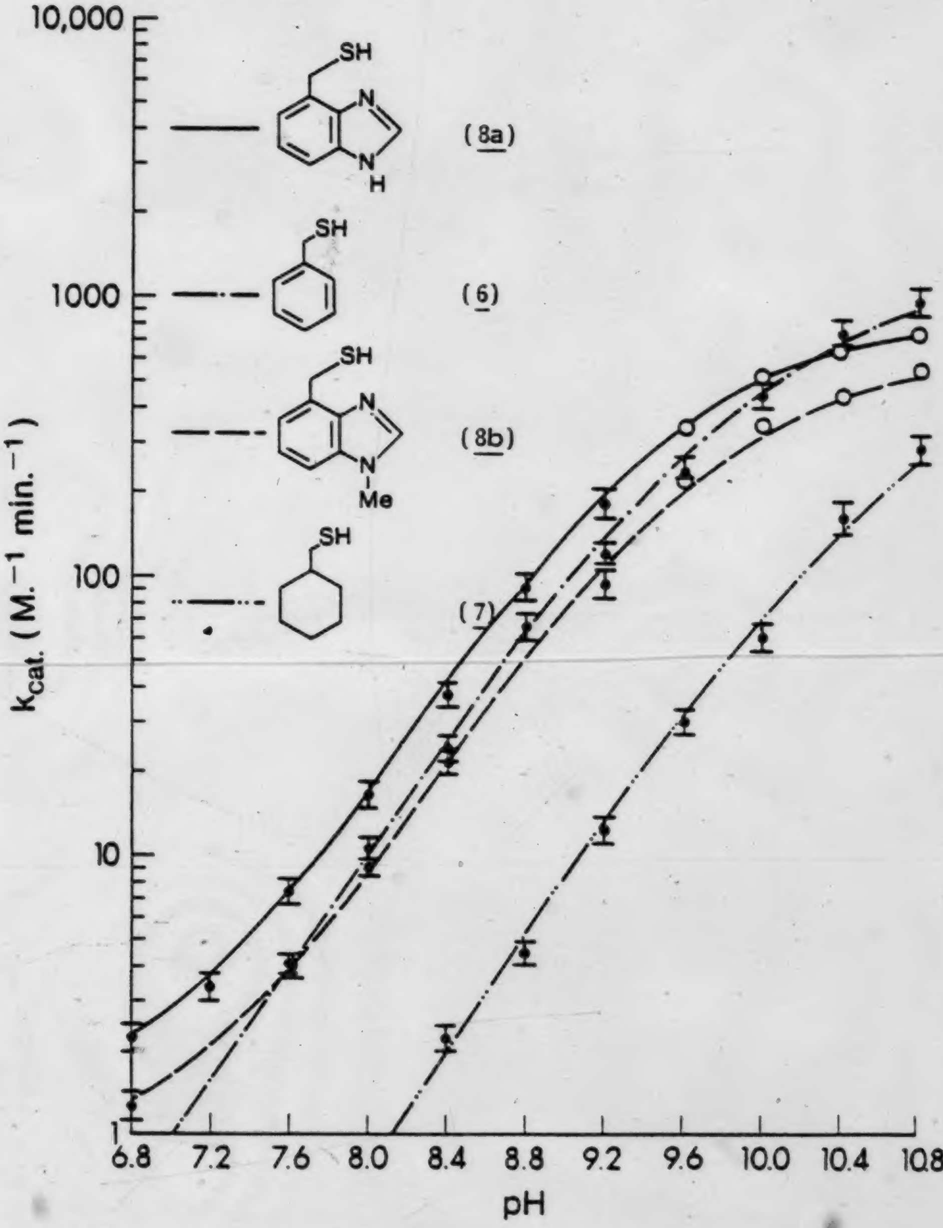
10,000
1000
100
10
1
$k_{cat.}$ (M.$^{-1}$ min.$^{-1}$)
SH
N
N
H
(8a)
SH
(6)
SH
N
N
Me
(8b)
SH
(7)
6.8
7.2
7.6
8.0
8.4
8.8
9.2
9.6
10.0
10.4
10.8
pH

solution. Benzyl mercaptan (6) may attack PNPA either as the thiol or the thiolate anion. The plot of the observed rate constant against pH shows a linear dependence on pH below the pKa of the thiol. The plot of k'_{obs} /[RS^-] vs pH gave a straight line of zero slope indicating that for benzyl mercaptan (6) the thiolate anion is the most active species (Scheme 15).

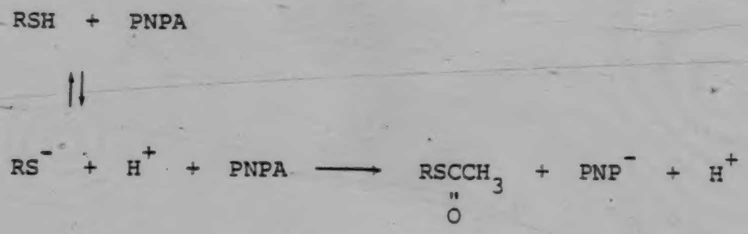

$$\begin{array}{l} \mathrm{RSH} + \mathrm{PNPA} \\ \quad\upharpoonleft\downharpoonright \\ \mathrm{RS}^- + \mathrm{H}^+ + \mathrm{PNPA} \longrightarrow \mathrm{RS}\underset{\underset{\mathrm{O}}{\|}}{\mathrm{C}}\mathrm{CH_3} + \mathrm{PNP}^- + \mathrm{H}^+ \end{array}$$

Scheme 15

A completely analogous situation exists for cyclohexymethylthiol (7) indicating again that it is the thiolate anion which is the active species.

These results concur with those previously found in the literature. Whitaker's[25f] studies with 2-mercaptoethanol, n-propylmercaptan, sodium mercaptoacetate and sodium β-mercaptopropionate (29.6°C, 5% ethanol/H_2O) and Lochon's[59] with furfurylmercaptan, *p*-chlorobenzylmercaptan, *p*-methoxybenzylmercaptan, thioglycerol and phenyl-3-propane thiol (30°C, 9.5% ethanol/H_2O) also indicated that it was the thiolate anion alone which was the active species in the catalysis. Fersht[25d] came to the important conclusion from his studies that even at 10 pH units below its pKa, ethanethiol is less nucleophilic than the thiolate anion, despite the latter presence in only one part in 10^{10}.

Product analysis of benzyl mercaptan (6) and cyclohexylmethylthiol (7) with PNPA was carried out by NMR. Benzyl mercaptan (6) and PNPA were dissolved in ethanol-d_6 and D_2O/NaOD was added to initiate the reaction. A new singlet due to the methylene hydrogens of benzyl thioacetate appeared at δ 4.04 at the expense of the singlet due to the methylene group of benzyl mercaptan (δ 3.66). Also, the peak due to the acetate methyl group of p-nitrophenylacetate at δ 2.26 was replaced by a singlet at δ 1.88 representing acetate anion. The final spectrum was identical to that of a mixture of p-nitrophenol and authentically synthesized benzyl thioacetate in the same solvent. Similar product analysis of the reaction of cyclohexylmethlythiol and p-nitrophenylacetate gave cyclohexylmethylthiol acetate and p-nitrophenoxide.

1-Methylbenzimidazole (10b), 4(7')-hydroxymethylbenzimidazole (12a), and 4-hydroxymethyl-1-methylbenzimidazole (12b) showed no catalysis over and above the buffer and hydroxide terms. The catalysis of the decomposition of PNPA with benzimidazole (10a) (Table 5) is independent of $[OH^-]$. The plot of k_{cat} (where $k_{cat} = k'_{obs}/[RIm]$) vs pH (Figure 7) gave a straight line of zero slope indicating that it is the non-protonated form of benzimidazole which is the active species. At the pH's studied, virtually all of the added benzimidazole (10a) is in its deprotonated form (pKa = 5.54). Both tetrahydrobenzimidazole (11a) and 1-methyltetrahydrobenzimidazole (11b) appear to have a similar dependence on $[OH^-]$ (Tables 6 and 7). Both show a first order dependence in base until the pKa of their respective imidazoles is approached (Figure 7). Again a plot of k_{Im}, where $k_{Im} = k'_{obs}/[RIm]$ ($[RIm]$ = concentration of imidazole present in its deprotonated form) vs pH gives a straight line of zero slope indicating that the deprotonated form of the

TABLE 5

PSEUDO-FIRST ORDER AND SECOND ORDER RATE CONSTANTS FOR THE HYDROLYSIS OF p-NITROPHENYLACETATE WITH BENZIMIDAZOLE[a]

pH±0.02	[RIm][b] 10^3 M.	$k_{obs.} - (k_{hydrol.} + k_{buff.})$ min.$^{-1}$	$k_{cat.}$ M.$^{-1}$ min.$^{-1}$[c]
7.6	2.68	$1.23 \pm 0.06 \times 10^{-3}$	0.46
7.6	2.52	$8.3 \pm 0.8 \times 10^{-4}$	0.33
7.6	1.26	$5.7 \pm 0.6 \times 10^{-4}$	0.45
			Av. = 0.41 ± 0.08
8.0	1.34	$5.4 \pm 1.0 \times 10^{-4}$	0.40
8.0	2.68	$9.0 \pm 0.7 \times 10^{-4}$	0.33
8.0	4.02	$1.5 \pm 0.1 \times 10^{-3}$	0.36
			Av. = 0.36 ± 0.04
8.4	4.02	$1.9 \pm 0.4 \times 10^{-3}$	0.47
8.4	2.52	$1.05 \pm 0.15 \times 10^{-3}$	0.42
8.4	2.68	$7.12 \pm 0.2 \times 10^{-4}$	0.27
			Av. = 0.40 ± 0.13

Table 5 (continued)

a. Determined in 31.6% $EtOH/H_2O$ (v/v). [Buffer] = 0.21 M. μ = 0.345 M. [PNPA] = 1.52×10^{-4} M.

b. [RIm] = total concentration of benzimidazole added.

c. $k_{cat.} = k_{obs.} - (k_{hydrol.} + k_{buff.})/[RIm]$.

Figure 7: Plot of the second order rate constant k_{cat} vs pH for benzimidazole (10a), tetrahydrobenzimidazole (11a), 1-methyltetrahydrobenzimidazole (11b) and 1-methyl-4,5-[4'-hydroxymethyltetramethylene]imidazole (13b). 1-Methylbenzimidazole (10b), 4(7')-hydroxymethylbenzimidazole (12a) and 4-hydroxymethyl-1-methylbenzimidazole (12b) showed no effective rate enhancement over the hydroxide and buffer terms.

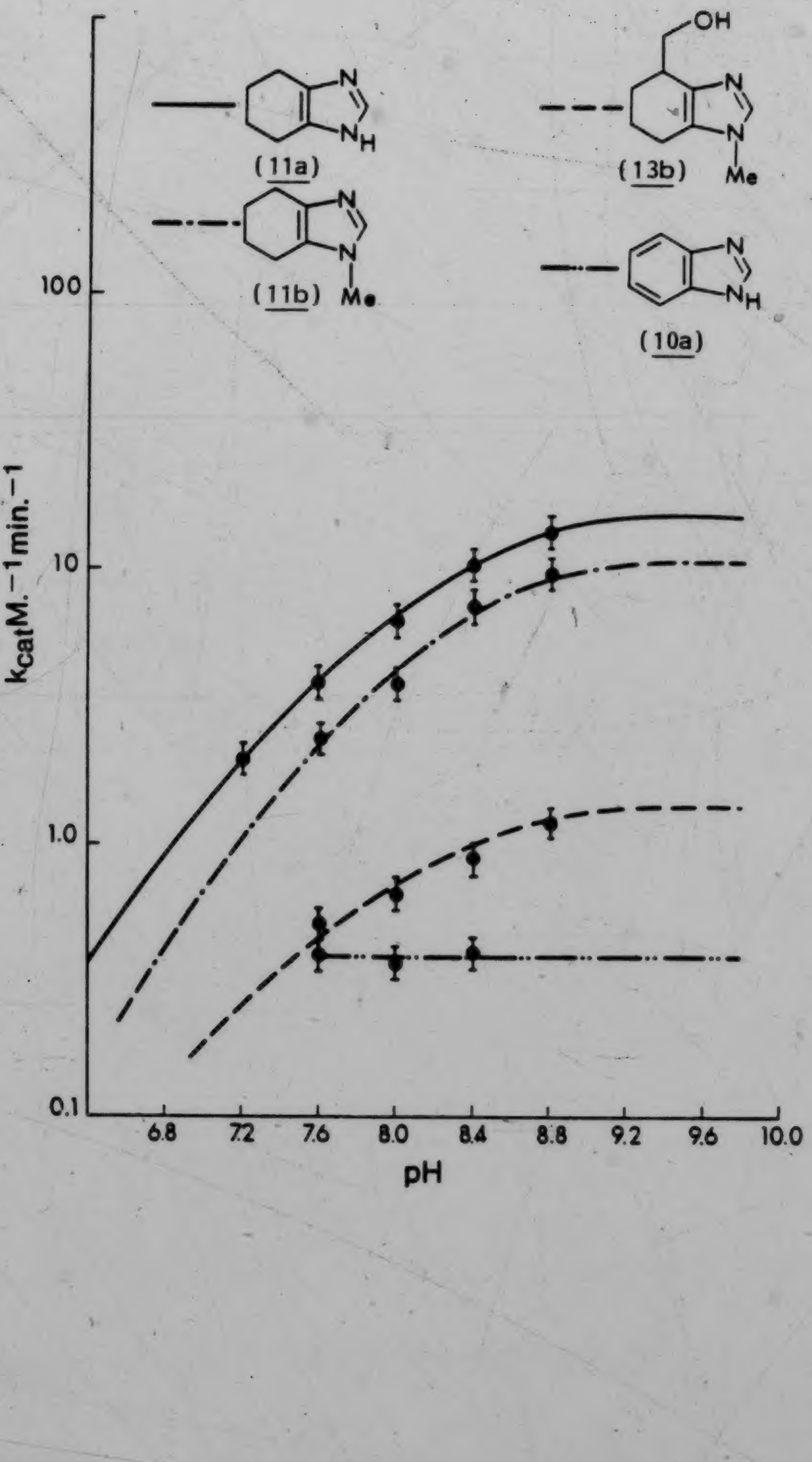
(11a)
(11b)
(13b)
(10a)
OH
N
NH
N Me
100
10
1.0
0.1
k_cat M.^-1 min.^-1
6.8
7.2
7.6
8.0
8.4
8.8
9.2
9.6
10.0
pH

TABLE 6

PSEUDO-FIRST ORDER AND SECOND ORDER RATE CONSTANTS FOR THE HYDROLYSIS OF *p*-NITROPHENYLACETATE WITH TETRAHYDROBENZIMIDAZOLE[a].

pH±0.02	$[RIm_T]$[b] x 10^3	$[RIm]$[c] x 10^3	$k_{obs.} - (k_{hydrol.} + k_{buff.})$ $min.^{-1}$	$k_{cat.}$ $M.^{-1}$ $min.^{-1}$[d]	$k_{Im.}$ $M.^{-1}$ $min.^{-1}$[e]
8.8	1.14	9.68×10^{-1}	$1.50 \pm 0.01 \times 10^{-2}$	13.16	15.5
8.8	1.43	1.21	$1.92 \pm 0.04 \times 10^{-2}$	13.42	15.86
8.8	2.23	1.89	$2.99 \pm 0.05 \times 10^{-2}$	13.41	15.82
				$A\bar{v}. = 13.33 \pm 0.17$	$A\bar{v}. = 15.73 \pm 0.23$
8.4	1.14	7.88×10^{-1}	$1.18 \pm 0.01 \times 10^{-2}$	10.42	14.97
8.4	2.23	1.54	$2.27 \pm 0.06 \times 10^{-2}$	10.14	14.74
8.4	1.55	1.07	$1.60 \pm 0.02 \times 10^{-2}$	10.33	14.95
				$A\bar{v}. = 10.30 \pm 0.16$	$A\bar{v}. = 14.89 \pm 0.15$
8.0	1.01	4.75×10^{-1}	$6.31 \pm 0.04 \times 10^{-2}$	6.25	13.28
8.0	1.14	5.37×10^{-1}	$7.41 \pm 0.01 \times 10^{-3}$	6.50	13.79
8.0	1.43	6.37×10^{-1}	$9.71 \pm 0.01 \times 10^{-3}$	6.79	14.42
				$A\bar{v}. = 6.51 \pm 0.28$	$A\bar{v}. = 13.83 \pm 0.55$
7.6	1.14	2.98×10^{-1}	$4.44 \pm 0.01 \times 10^{-3}$	3.89	14.89
7.6	1.43	3.74×10^{-1}	$5.62 \pm 0.04 \times 10^{-3}$	3.93	15.02
7.6	1.01	2.64×10^{-1}	$3.76 \pm 0.06 \times 10^{-3}$	3.71	14.24
				$A\bar{v}. = 3.84 \pm 0.13$	$A\bar{v}. = 14.72 \pm 0.48$
7.2	1.55	1.91×10^{-1}	$3.16 \pm 0.05 \times 10^{-3}$	2.04	16.54
7.2	2.23	2.76×10^{-1}	$4.60 \pm 0.02 \times 10^{-3}$	2.06	16.66
7.2	1.01	1.25×10^{-1}	$2.05 \pm 0.04 \times 10^{-3}$	2.02	16.40
				$A\bar{v}. = 2.04 \pm 0.02$	$A\bar{v}. = 16.53 \pm 0.13$

a. Determined in 31.6% EtOH/H_2O (v/v). [Buffer] = 0.21 M. μ = 0.345 M. [PNPA] = 1.52×10^{-4} M to 2.03×10^{-4} M.

b. $[RIm_T]$ = total concentration of tetrahydrobenzimidazole added.

c. [RIm] = concentration of non-protonated terrahydrobenzimidazole present as determined from the known pK_a (8.05 ± 0.05).

d. $k_{cat.} = k_{obs.} - (k_{hydrol.} + k_{buff.})/[RIm_T]$.

e. $k_{Im.} = k_{obs.} - (k_{hydrol.} + k_{buff.})/[RIm]$.

TABLE 7

PSEUDO-FIRST ORDER AND SECOND ORDER RATE CONSTANTS FOR THE HYDROLYSIS OF p-NITROPHENYLACETATE WITH 1-METHYLTETRAHYDROBENZIMIDAZOLE.[a]

pH±0.02	$[RIm_T]$[b] x 10^3	$[RIm]$[c] x 10^3	$k_{obs.} - (k_{hydrol.} + k_{buff.})$ $min.^{-1}$	$k_{cat.}$ $M.^{-1}$ $min.^{-1}$[d]	$k_{Im.}$ $M.^{-1}$ $min.^{-1}$[e]
8.8	1,16	9.28×10^{-1}	$1.06 \pm 0.05 \times 10^{-2}$	9.14	11.4
8.8	2.33	1.86	$2.27 \pm 0.05 \times 10^{-2}$	9.74	12.2
8.8	1.75	1.40	$1.80 \pm 0.03 \times 10^{-2}$	10.28	12.9
				Av. = 9.72 ± 0.56	Av. = 12.2 ± 0.7
8.1	1.16	7.11×10^{-1}	$8.18 \pm 0.05 \times 10^{-3}$	7.05	11.5
8.4	2.33	1.42	$1.75 \pm 0.06 \times 10^{-2}$	7.50	12.2
8.4	1.75	1.07	$1.38 \pm 0.04 \times 10^{-2}$	7.87	12.9
				Av. = 7.47 ± 0.42	Av. = 12.2 ± 0.7
8.0	1.16	4.49×10^{-1}	$4.42 \pm 0.06 \times 10^{-3}$	3.81	9.9
8.0	2.33	9.01×10^{-1}	$8.51 \pm 0.09 \times 10^{-3}$	3.65	9.4
8.0	1.75	6.77×10^{-1}	$7.31 \pm 0.05 \times 10^{-3}$	4.18	10.8
				Av. = 3.89 ± 0.29	Av. = 10.0 ± 0.8
7.6	1.16	2.32×10^{-1}	$3.04 \pm 0.04 \times 10^{-3}$	2.62	13.0
7.6	1.75	3.51×10^{-1}	$4.21 \pm 0.05 \times 10^{-3}$	2.40	12.0
7.6	1.47	2.94×10^{-1}	$3.42 \pm 0.06 \times 10^{-3}$	2.33	11.6
				Av. = 2.45 ± 0.17	Av. = 12.2 ± 0.8

a. Determined in 31.6% EtOH/H_2O (v/v). [Buffer] = 0.21 M. μ = 0.345 M. [PNPA] = 1.17×10^{-4} M.

b. $[RIm_T]$ = total concentration of 1-methyltetrahydrobenzimidazole added.

c. [RIm] = concentration of non-protonated 1-methyltetrahydrobenzimidazole present as determined from the known pK_a (8.20 ± 0.05).

d. $k_{cat.} = k_{obs.} - (k_{hydrol.} + k_{buff.})/[RIm_T]$.

e. $k_{Im.} = k_{obs.} - (k_{hydrol.} + k_{buff.})/[RIm]$.

imidazole is the active species. Benzimidazole (10a), tetrahydrobenzimidazole (11a) and 1-methyltetrahydrobenzimidazole (11b) can react with p-nitrophenylacetate either as a general base or as a nucleophile. The possibilities are illustrated for benzimidazole (10a) in Scheme 16. The general-base mechanism in which imidazole acts as a general base on a second imidazole can be eliminated as the rate studies show no second order dependence on the concentration of the imidazole species for compounds (10) and (11). NMR studies were performed in an attempt to distinguish between a nucleophilic and a general-base mechanism. In ethanol-d_6 the methyl group of the acetate of PNPA appeared as a singlet at δ 2.32 in the NMR spectrum (Figure 8). Upon addition of (10a) and NaOD/D_2O a singlet due to the N-acetyl methyl group of N-acetylbenzimidazole appeared at δ 2.76 and new peaks at δ 2.00 and δ 1.88 due to ethyl acetate and acetate anion respectively, were observed. Gradually the signal due to the N-acetyl methyl group of N-acetylbenzimidazole diminished as this compound was hydrolyzed and a spectrum due to p-nitrophenoxide and benzimidazole (10a) remained. The spectra obtained by following the reaction of PNPA with tetrahydrobenzimidazole (11a) are illustrated in Figures 8 and 9. In Figure 9a the four sets of doublets of doublets due to the aromatic protons of p-nitrophenylacetate and p-nitrophenoxide as well as the peak at δ 8.2 due to the C_2-H of (10a) in the low field region were observed. The singlet due to the acetyl methyl group of PNPA was found at δ 2.30 and that of the methyl group of N-acetyltetrahydrobenzimidazole at δ 2.58. The first traces of the peaks due to ethyl acetate (δ 2.0) and acetate anion (δ 1.88) were also

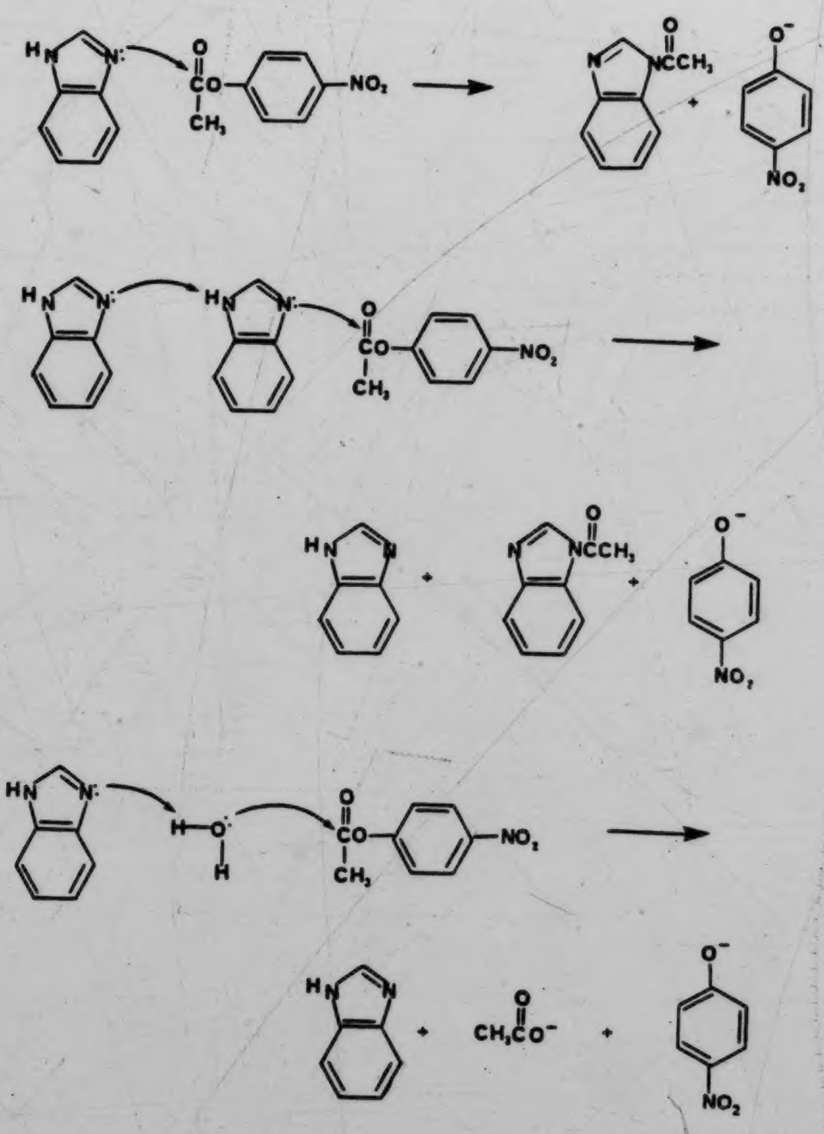

Scheme 16

Figure 8: The ^{1}H-NMR spectra of _p_-nitrophenylacetate in $CDCl_3$ (a), the hydrochloride salt of tetrahydrobenzimidazole (11a) in ethanol-d_6 (b) and the hydrochloride salt of 1-methyltetrahydrobenzimidazole (11b) in ethanol-d_6 (c).

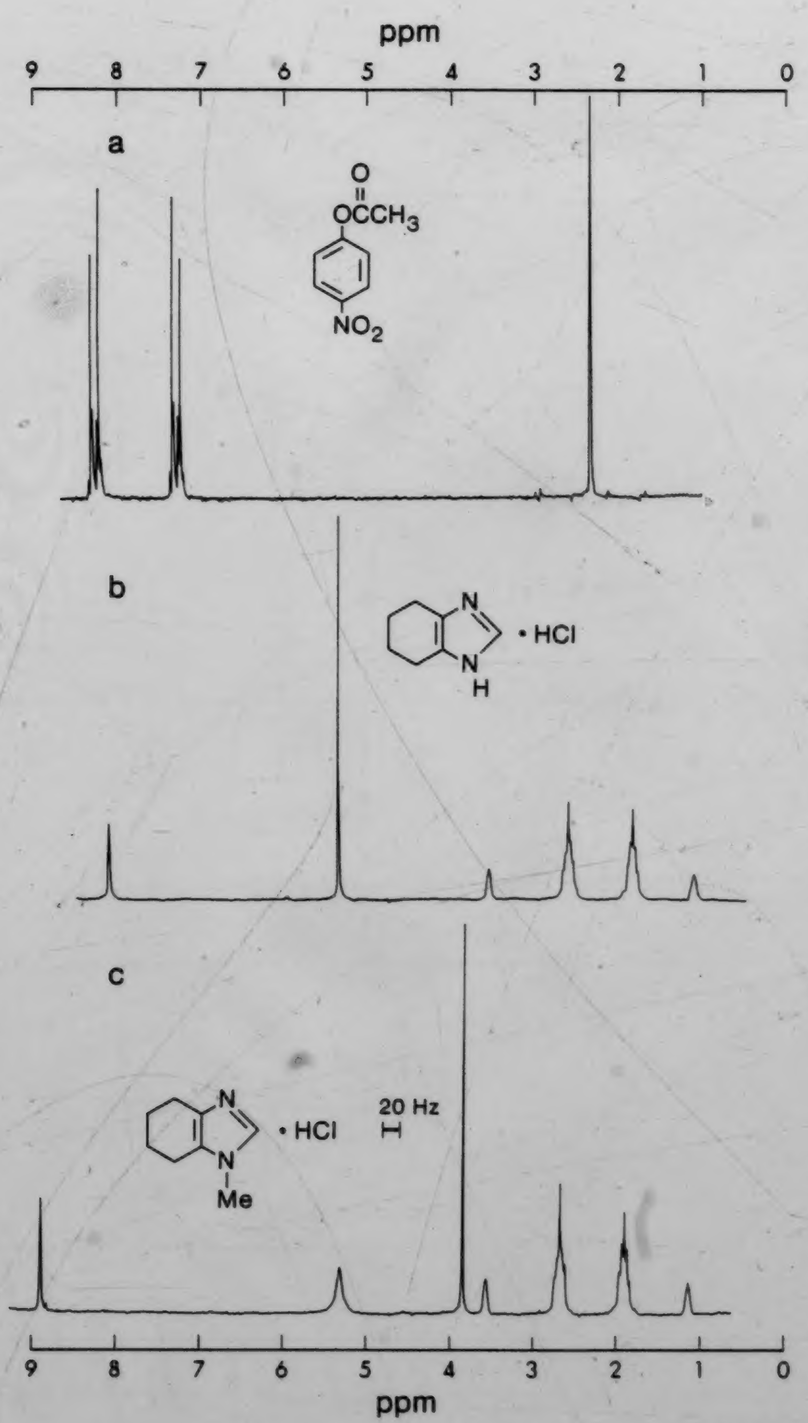
ppm
9
8
7
6
5
4
3
2
1
0
a
O
OCCH3
NO2
b
N
N
H
• HCl
c
N
N
Me
• HCl
20 Hz
9
8
7
6
5
4
3
2
1
0
ppm

Figure 9: The ^{1}H-NMR spectra of the reaction of p-nitrophenylacetate with tetrahydrobenzimidazole (11a) in ethanol-d_6, NaOD/D_2O as a function of time.

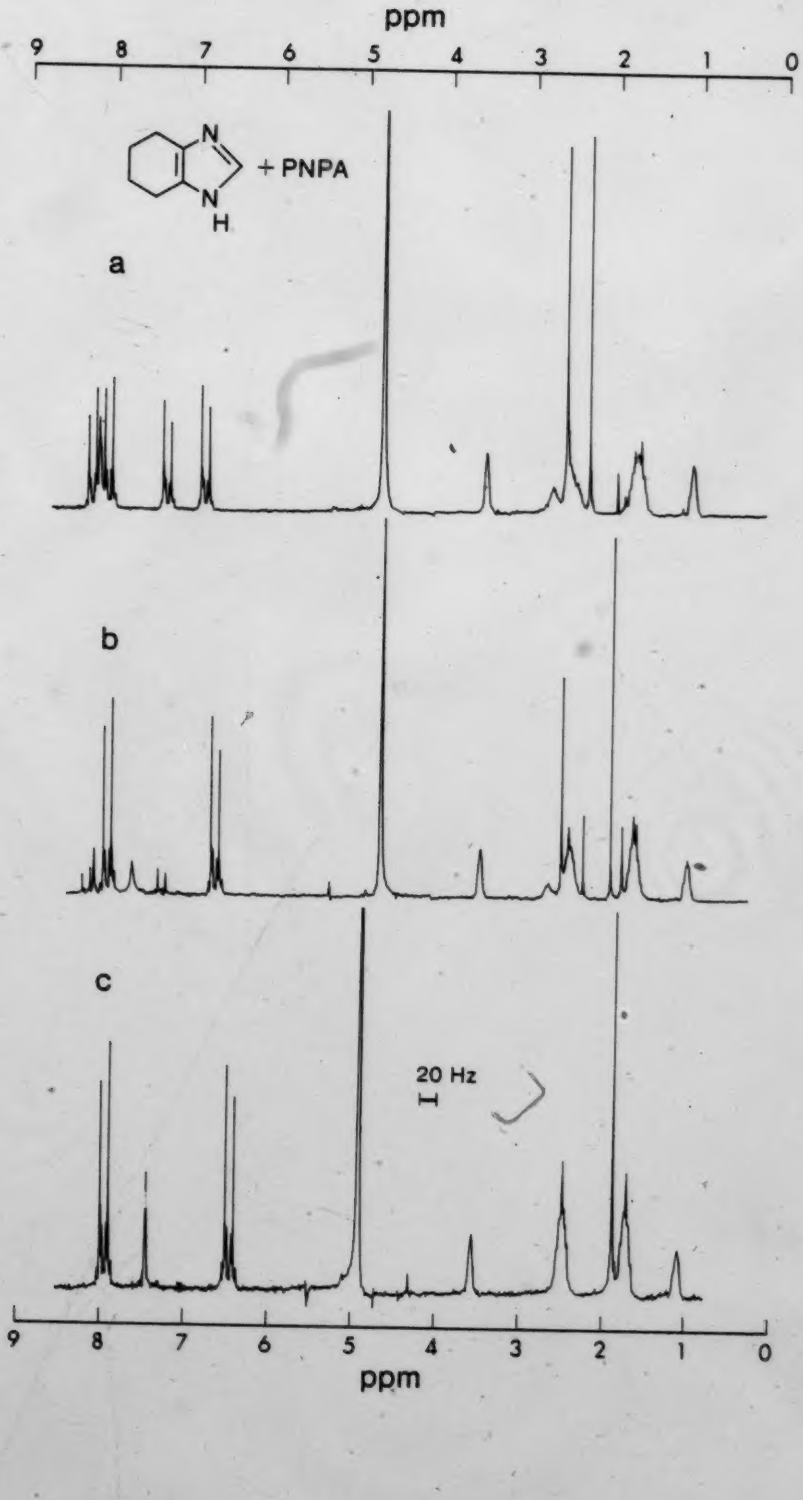
ppm
9
8
7
6
5
4
3
2
1
0
N
N
H
+ PNPA
a
b
c
20 Hz
9
8
7
6
5
4
3
2
1
0
ppm

observed in this spectrum. In Figure 9b there was almost no trace of PNPA while N-acetylbenzimidazole itself is partially hydrolyzed to give a large peak at δ 2.0 due to ethyl acetate. In the final spectrum shown in Figure 9c only the peaks due to p-nitro-phenoxide, tetrahydrobenzimidazole (11a) and acetate anion at δ 1.88 were observed. When the NMR studies of the reaction of PNPA with 1-methylbenzimidazole (10b) and 1-methyltetrahydrobenzimidazole (11b) were carried out no evidence for the formation of the N-acetyl compound were found. With both compounds, as shown for 1-methyltetrahydrobenzimidazole (11b) with PNPA in Figure 10 the singlet due to the acetate group of PNPA at δ 2.30 diminished and peaks due to ethyl acetate and acetate anion at δ 2.00 and δ 1.88, respectively, apppeared. However, as will be discussed later, the hydrolysis of 1-acetyl-3-methyltetrahydrobenzimidazolium and 1-acetyl-3-methylbenzimidazolium occurs very rapidly and the N-acetyl compounds would not be detectable in the NMR spectrum.

As mentioned earlier the hydroxy compounds (12a) and (12b) showed no rate enhancement over and above that provided by the water and buffer terms. As with (11) a plot of k_{cat}, where $k_{cat} = k'_{obs} / [RIm_t]$ ($[RIm_t]$ = total concentration of imidazole compound added), vs pH for 1-methyl-4-hydroxymethyltetrahydrobenzimidazole (13b) begins to level off as its pKa (8.00) is approached (Table 8, Figure 7). Again a plot of k_{Im} vs pH gives a straight line of zero slope indicating that the nonprotonated form of (13b) is the active species in the catalysis. In the case of the oxygen compounds, as depicted for (12a) in Scheme 17, either the oxygen or one of the nitrogens can attack PNPA nucleophilically to catalyze

Figure 10: The ^{1}H-NMR spectra of the reaction of p-nitrophenylacetate with 1-methyltetrahydrobenzimidazole (11b) in ethanol-d_6, $NaOD/D_2O$ as a function of time.

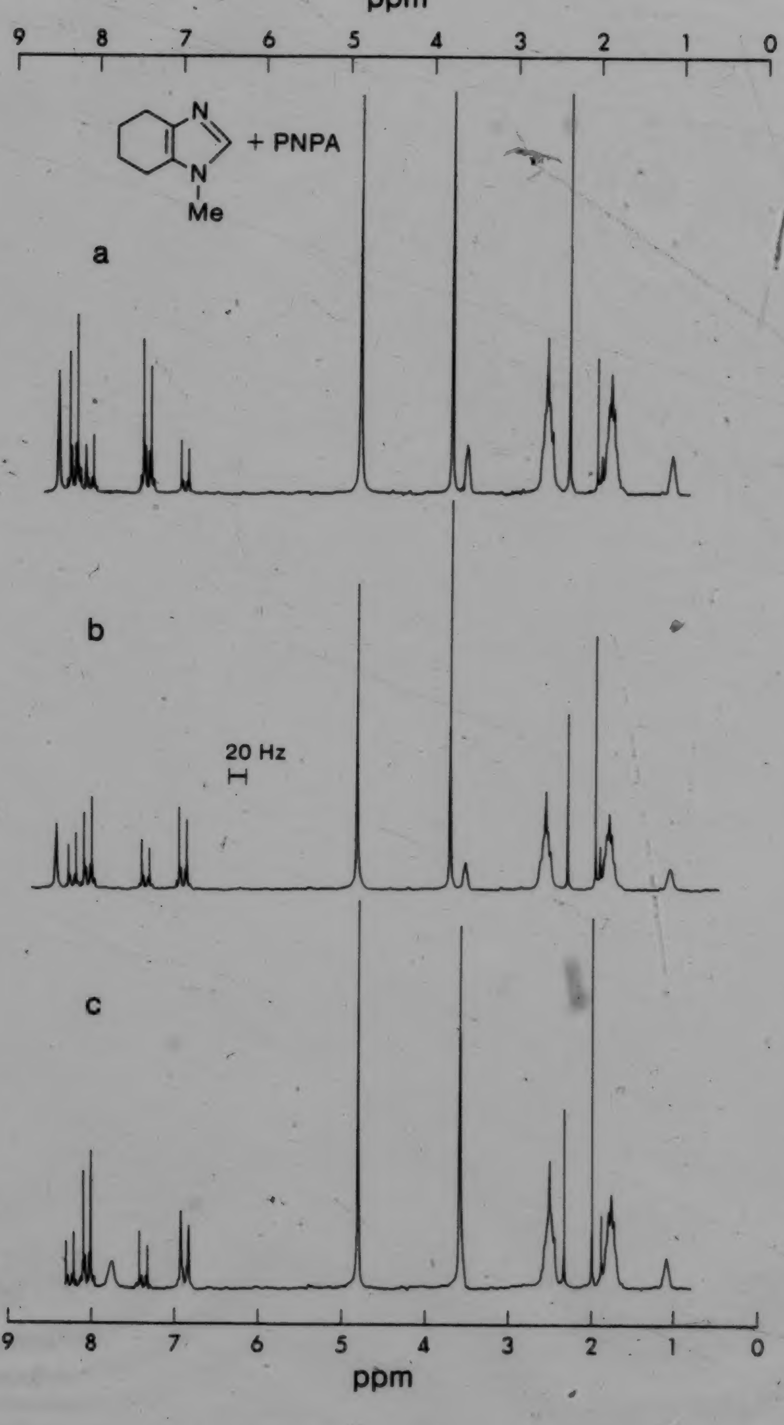
ppm
9
8
7
6
5
4
3
2
1
0
N
N
Me
+ PNPA
a
b
20 Hz
c
9
8
7
6
5
4
3
2
1
0
ppm

TABLE 8

PSEUDO-FIRST ORDER AND SECOND ORDER RATE CONSTANTS FOR THE DECOMPOSITION OF p-NITROPHENYLACETATE WITH 1-METHYL-4-HYDROXYMETHYLTETRAHYDROBENZIMIDAZOLE

pH±0.02	$[RIm_T]$[b] x 10^3	$[RIm]$[c] x 10^3	$k_{obs.} - (k_{hydrol.} + k_{buff.})$ min.$^{-1}$	$k_{cat.}$ M.$^{-1}$ min.$^{-1}$[d]	$k_{Im.}$ M.$^{-1}$ min.$^{-1}$[e]
8.8	2.34	2.02	$2.8 \pm 0.1 \times 10^{-3}$	1.20	1.4
8.8	1.17	1.01	$1.4 \pm 0.1 \times 10^{-3}$	1.20	1.4
8.8	2.34	2.02	$2.9 \pm 0.1 \times 10^{-3}$	1.24	1.4
				Av. = 1.21 ± 0.03	Av. = 1.4
8.4	1.17	8.36×10^{-1}	$1.0 \pm 0.1 \times 10^{-3}$	.87	1.2
8.4	2.34	1.67	$2.0 \pm 0.1 \times 10^{-3}$	.86	1.2
8.4	3.51	2.51	$3.1 \pm 0.1 \times 10^{-3}$	.88	1.2
				Av. = 0.87 ± 0.01	Av. = 1.2
8.0	3.51	1.76	$2.2 \pm 0.1 \times 10^{-3}$	.62	1.3
8.0	2.34	1.17	$1.5 \pm 0.1 \times 10^{-3}$	.65	1.3
8.0	1.17	5.85×10^{-1}	$7.9 \pm 0.2 \times 10^{-4}$	.68	1.4
				Av. = 0.65 ± 0.03	Av. = 1.33 ± 0.67

Table 8 (continued)

a. Determined in 31.6% EtOH/H_2O (v/v). [Buffer] = 0.21 M. $\mu = 0.345$. [PNPA] = 1.17×10^{-4} M.

b. $[RIm_T]$ = total concentration of 1-methyl-4-hydroxymethyltetrahydrobenzimidazole.

c. [RIm] = concentration of non-protonated 1-methyl-4-hydroxymethyltetrahydrobenzimidazole. present as determined from the known pK_a (8.00 ± 0.05).

d. $k_{cat.} = k_{obs.} - (k_{hydrol.} + k_{buff.})/[RIm_T]$.

e. $k_{Im.} = k_{obs.} - (k_{hydrol.} + k_{buff.})/[RIm]$.

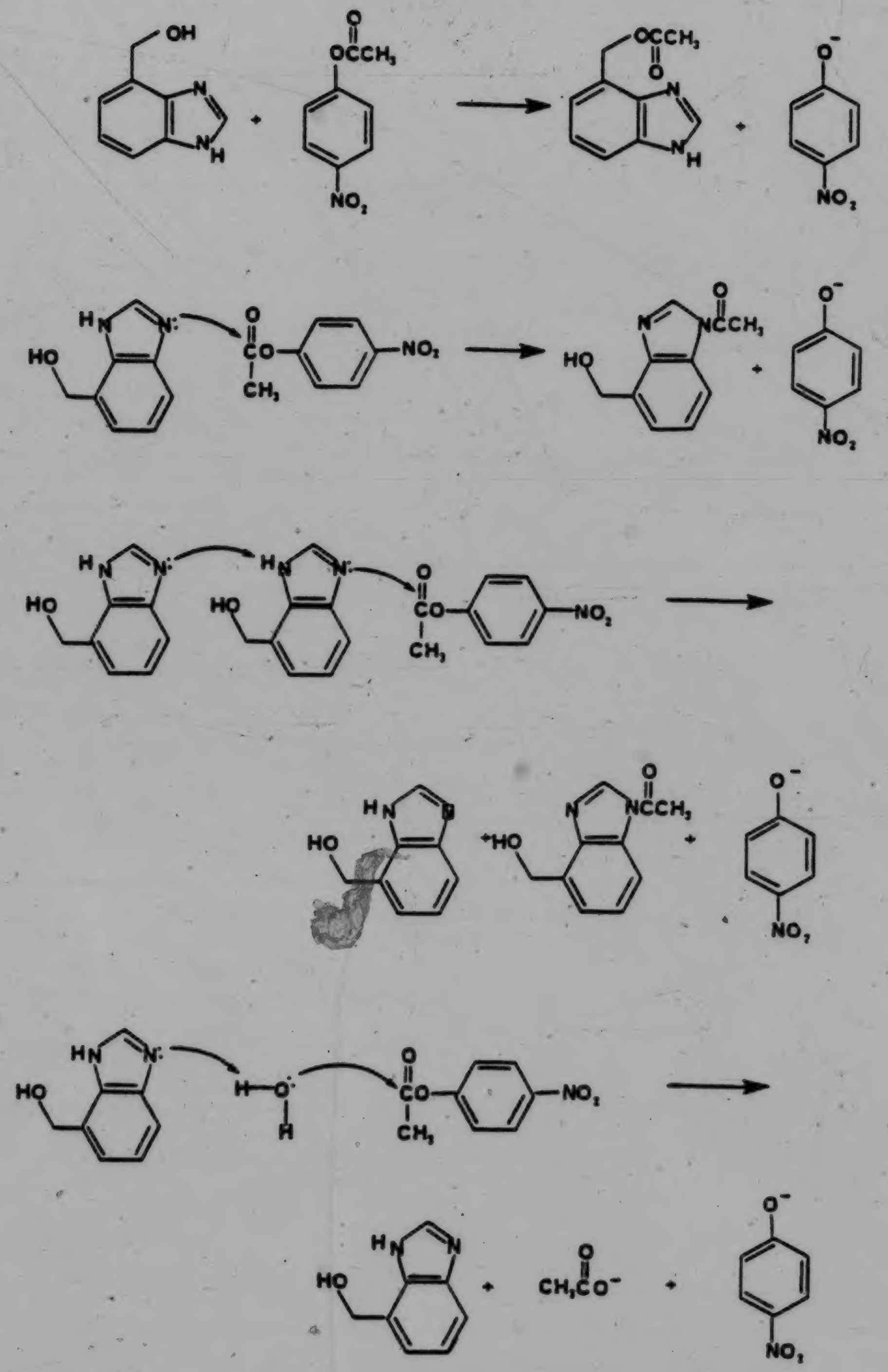

Scheme 17

a. Either of the two nitrogens of the imidazole ring can take part in the nucleophilic attack..

the hydrolysis. Alternatively the alcohol-imidazole compound can act as a general-base on another imidazole or on H_2O. Again, as there was not a second order dependence on [imidazole] in the rate equation the general-base mechanism in which imidazole acts as a general-base on a second molecule of imidazole can be eliminated. NMR studies showed the growth of singlets at δ 2.77 (N-acetyl methyl) and δ 5.04 (CH_2) due to the formation of the N-acetyl compound in the reaction of PNPA with 4(7')-hydroxymethylbenzimidazole (12a). The N-acetyl intermediate slowly hydrolyzed leaving peaks due to 4(7')-hydroxymethylbenzimidazole (12a), acetate anion and p-nitrophenoxide. There was no evidence for any acylation occurring on the oxygen atom. To try to induce the latter in a more hydrophobic medium, 4(7')-hydroxymethylbenzimidazole (12a) and PNPA were dissolved in deuterated acetonitrile. A few drops of deuterated DMSO were added to dissolve the alcohol. Again only the N-acetyl compound was detected. For the N-methyl-hydroxy compound (13b) neither the N-acetyl nor O-acetyl compounds were detected. As stated before, the decomposition of the N-methyl-N'-acetyl compounds would be expected to be so fast that the intermediate would not be detected in the NMR spectrum. Therefore, (13b) probably catalyzes the decomposition of the PNPA by nucleophilic attack by nitrogen.

Our studies on the catalysis of the hydrolysis of PNPA with benzimidazole analogues are in agreement with those found in the literature.[10,59,60] Cyclic benzimidazoles in general are found to have very weak catalytic activity (k_{cat}=0-6 M^{-1} min^{-1}) as summarized in Table 9 and have also been shown to attack PNPA nucleophilical-

Table 9[5b,59]

Compound	pK_{Im}	$k_{Im}(M^{-1}min^{-1})^{a}$
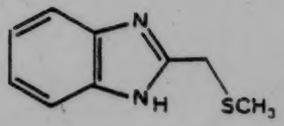	5.00	4.9[b]
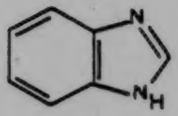	5.40	0.96
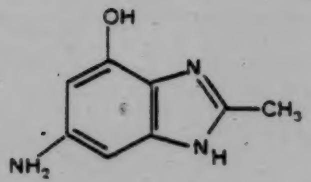	6.65	1.50
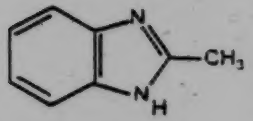	6.10	0.04
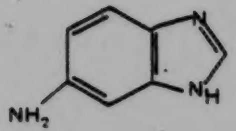	6.00	2.95
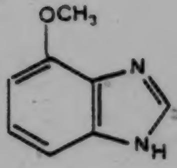	5.10	0.31
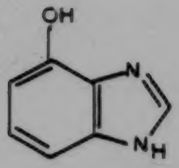	5.30	2.80

Compound	pK_{Im}	$k_{Im}(M^{-1}min^{-1})$
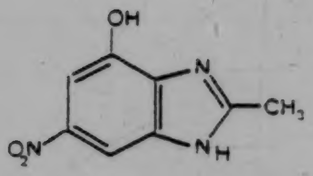	3.90	1.1
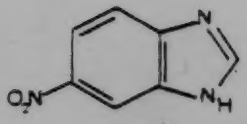	3.05	4.8
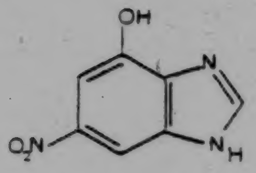	3.05	3.75
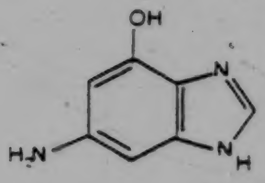	5.90	6.15

a. Kinetic experiments and pKa determinations were performed at 30±0.1°C in 28.5% ethanol/water.

b. Kinetic experiments and pKa determinations were performed at 30±0.1°C in 9.5% ethanol/water.

ly.[10] Those benzimidazole analogues containing an additional functional group exhibited no indications of cooperative catalysis.

Similarly a survey of the literature indicates that imidazoles which are not annulated to a benzene ring exhibit catalytic rate constant values of 0-25 $M^{-1}min^{-1}$ (Table 10) in reactions with PNPA in complete agreement with our results. These imidazole derivatives were also found to attack PNPA nucleophilically.

The catalysis of the hydrolysis of PNPA provided by compounds (8a) and (8b) (Tables 11 and 12) is similar to that exhibited by benzyl mercaptan (6) and cyclohexylmethylthiol (7) in the high pH range. This would indicate that in this region the catalysis is probably due to the thiolate anion. However in the pH range from 7.6 to 6.8 there is a positive deviation from a first order dependence in base (Figure 6). A plot of k'_{obs} /[RImS$^-$] vs pH where [RImS$^-$] is the concentration of thiolate anion present, does not give a straight line of zero slope. Like the alcohol systems, 4(7')-thiomethylbenzimidazole can attack PNPA nucleophilically in either of two ways (Scheme 18). Sulphur or nitrogen (N or N' atom) acylation can take place or again the imidazole can act as a general-base on another imidazole ring or on H_2O. NMR studies showed clearly that acylation was occurring on the sulphur atom. The spectra of the compounds obtained from the reaction of PNPA with (8a) and (8b) were identical to those of authentic samples of the S-acylated compounds. Therefore, it seems clear that it is the thiolate anion which is attacking PNPA at high pH's. However, what is happening to enhance the rates around neutrality? The imidazole can be acting as a general base to aid the thiol in its attack on

Table 10[5b]

Compound	pK_{Im}	k_{Im} ($M^{-1} min^{-1}$)[a]
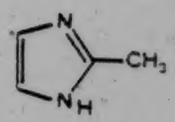	7.75	2.7
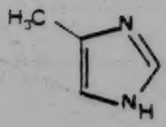	7.45	25
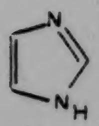	6.95	20.2
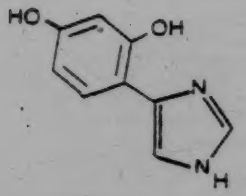	6.45	9.4
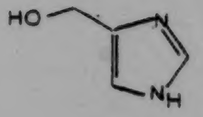	6.45	5.6
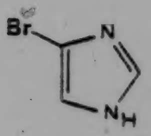	3.70	0.28

a. Kinetic experiments and pKa determinations were performed at 30±0.1°C in 28.5% etanol/water.

TABLE 11

PSEUDO-FIRST ORDER AND SECOND ORDER RATE CONSTANTS FOR THE DECOMPOSITION OF *p*-NITROPHENYLACETATE WITH 4(7')-THIOMETHYLBENZIMIDAZOLE[a].

pH±0.02	[RImSH][b] 10^3 M.	$[\text{RImS}^-]$[c] 10^3 M.	$k_{obs.} - (k_{hydrol.} + k_{buff.})$ min.^{-1}	$k_{cat.}$ $\text{M.}^{-1}\text{min.}^{-1}$[d]	k_{RImS^-} $\text{M.}^{-1}\ \text{min.}^{-1}$[e]
9.2	0.52	1.14×10^{-1}	$9.8 \pm 0.3 \times 10^{-2}$	188	859
9.2	0.45	9.91×10^{-2}	$7.23 \pm 0.06 \times 10^{-2}$	161	730
9.2	1.90	4.18×10^{-1}	$3.38 \pm 0.5 \times 10^{-1}$	178	809
				Av̄. = 176 ± 15	Av̄. = 799 ± 69
8.8	1.26	1.27×10^{-1}	$1.11 \pm 0.55 \times 10^{-1}$	88.6	873
8.8	1.26	1.27×10^{-1}	$1.17 \pm 0.50 \times 10^{-1}$	92.5	922
8.8	0.94	9.43×10^{-2}	$8.34 \pm 0.40 \times 10^{-2}$	89.1	885
				Av̄. = 90 ± 3	Av̄. = 893 ± 30
8.4	0.63	2.70×10^{-2}	$2.64 \pm 0.20 \times 10^{-2}$	41.7	975
8.4	1.26	5.39×10^{-2}	$4.21 \pm 0.05 \times 10^{-2}$	33.4	781
8.4	0.94	3.99×10^{-2}	$3.50 \pm 0.20 \times 10^{-2}$	37.4	874
				Av̄. = 37.5 ± 4.1	Av̄. = 877 ± 96
8.0	1.23	2.15×10^{-2}	$1.99 \pm 0.03 \times 10^{-2}$	16.2	926
8.0	1.40	2.44×10^{-2}	$2.49 \pm 0.03 \times 10^{-2}$	17.8	997
8.0	0.57	9.95×10^{-3}	$8.31 \pm 0.25 \times 10^{-3}$	14.5	832
				Av̄. = 16.2 ± 1.6	Av̄. = 918 ± 86
7.6	1.25	8.78×10^{-3}	$9.38 \pm 0.24 \times 10^{-3}$	7.5	1068
7.6	1.81	1.27×10^{-2}	$1.50 \pm 0.03 \times 10^{-2}$	8.25	1179
7.6	1.25	8.78×10^{-3}	$7.79 \pm 0.08 \times 10^{-3}$	6.23	887
				Av̄. = 7.3 ± 1.1	Av̄. = 1044 ± 157
7.2	0.73	2.06×10^{-3}	$2.94 \pm 0.06 \times 10^{-3}$	4.03	1427
7.2	0.56	1.57×10^{-3}	$2.29 \pm 0.04 \times 10^{-3}$	4.09	1455
7.2	0.59	1.66×10^{-3}	$2.42 \pm 0.10 \times 10^{-3}$	4.11	1457
				Av̄. = 4.11 ± 0.62	Av̄. = 1446 ± 19
6.8	0.50	5.53×10^{-4}	$1.23 \pm 0.03 \times 10^{-3}$	2.46	2224
6.8	0.59	6.62×10^{-4}	$1.42 \pm 0.10 \times 10^{-3}$	2.39	2144
6.8	0.78	8.77×10^{-4}	$1.91 \pm 0.07 \times 10^{-3}$	2.43	2177
				Av̄. = 2.43 ± 0.04	Av̄. = 2181 ± 42

a. Determined in 31.6% EtOH/H_2O (v/v). [Buffer] = 0.21 M. $\mu = 0.345$ M. [PNPA] = 1.52×10^{-4} M to 2.03×10^{-4} M.

b. [RImSH] = total concentration of 4(7')-thiomethylbenzimidazole added.

c. $[\text{RImS}^-]$ = concentration of the thiolate anion present as determined from the known macroscopic pK_a (9.75 ± 0.1).

d. $k_{cat.} = k_{obs.} - (k_{hydrol.} + k_{buff.})/[\text{RImSH}]$.

e. $k_{\text{RImS}^-} = k_{obs.} - (k_{hydrol.} + k_{buff.})/[\text{RImS}^-]$.

TABLE 12

PSEUDO-FIRST ORDER AND SECOND ORDER RATE CONSTANTS FOR THE DECOMPOSITION OF *p*-NITROPHENYLACETATE WITH 1-METHYL-4-THIOMETHYLBENZIMIDAZOLE[a].

pH±0.02	[RImSH][b] 10^3M.	[RImS$^-$][c] 10^3M.	$k_{obs.} - (k_{hydrol.} + k_{buff.})$ min.$^{-1}$	$k_{cat.}$ M.$^{-1}$ min.$^{-1}$[d]	k_{RImS^-} M.$^{-1}$ min.$^{-1}$[e]
9.2	1.87	3.75×10^{-1}	$1.68 \pm 0.1 \times 10^{-1}$	90	448
9.2	1.25	2.50×10^{-1}	$1.16 \pm 0.1 \times 10^{-1}$	93	462
9.2	1.25	2.50×10^{-1}	$1.16 \pm 0.08 \times 10^{-1}$	93	462
				Av̄. 92 ± 3	Av̄. = 457 ± 9
8.4	1.25	4.77×10^{-2}	$2.66 \pm 0.06 \times 10^{-2}$	21	557
8.4	1.25	4.77×10^{-2}	$2.11 \pm 0.04 \times 10^{-2}$	17	442
8.4	1.87	7.14×10^{-2}	$3.08 \pm 0.07 \times 10^{-2}$	16.5	431
				Av̄. = 18 ± 3	Av̄. = 477 ± 80
8.0	1.87	2.92×10^{-2}	$1.66 \pm 0.03 \times 10^{-2}$	8.9	567
8.0	1.11	1.72×10^{-2}	$1.03 \pm 0.05 \times 10^{-2}$	9.3	596
8.0	1.97	3.07×10^{-2}	$1.70 \pm 0.02 \times 10^{-2}$	8.6	553
				Av̄. = 8.9 ± 0.4	Av̄. = 572 ± 24
7.6	1.25	7.81×10^{-3}	$5.43 \pm 0.1 \times 10^{-3}$	4.3	695
7.6	1.87	1.17×10^{-2}	$6.99 \pm 0.07 \times 10^{-3}$	3.7	596
7.6	1.25	7.81×10^{-3}	$5.81 \pm 0.06 \times 10^{-3}$	4.7	744
				Av̄. = 4.2 ± 0.5	Av̄. = 678 ± 82
6.8	9.38×10^{-1}	9.38×10^{-4}	$1.18 \pm 0.07 \times 10^{-3}$	1.25	1259
6.8	1.87	1.87×10^{-3}	$2.80 \pm 0.1 \times 10^{-3}$	1.49	1493
6.8	2.48	2.48×10^{-3}	$3.18 \pm 0.1 \times 10^{-3}$	1.28	1282
				Av̄. = 1.34 ± 0.15	Av̄. = 1347 ± 148

a. Determined in 31.6% EtOH/H_2O (v/v). [Buffer] = 0.21 M. $\mu = 0.345$ M. [PNPA] = 1.26×10^{-4} M.

b. [RImSH] = total concentration of 1-methyl-4-thiomethylbenzimidazole added.

c. [RImS$^-$] = concentration of the thiolate anion present as determined from the known macroscopic pK_a (9.8 ± 0.1).

d. $k_{cat.} = k_{obs.} - (k_{hydrol.} + k_{buff.})/[RImSH]$.

e. $k_{RImS^-} = k_{obs.} - (k_{hydrol.} + k_{buff.})/[RImS^-]$.

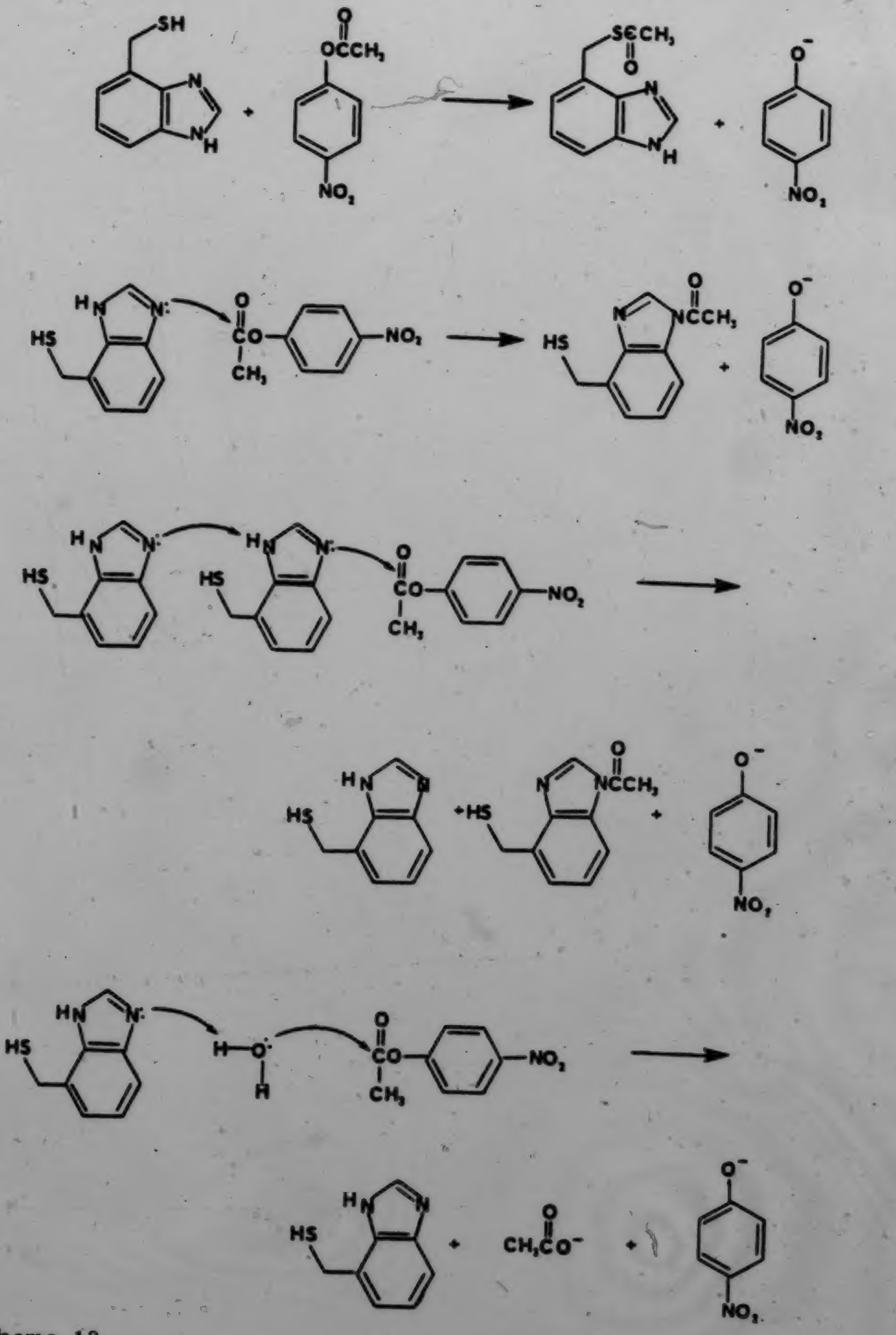
SH
OCCH₃
NO₂
SCCH₃
NO₂
O⁻
HS
NO₂
NCCH₃
HS
HS
CH₃
NO₂
NCCH₃
HS
NO₂
H-O
H
CH₃CO⁻

Scheme 18

a. Either of the two nitrogens of the imidazole ring can take part in the nucleophilic attack.

2

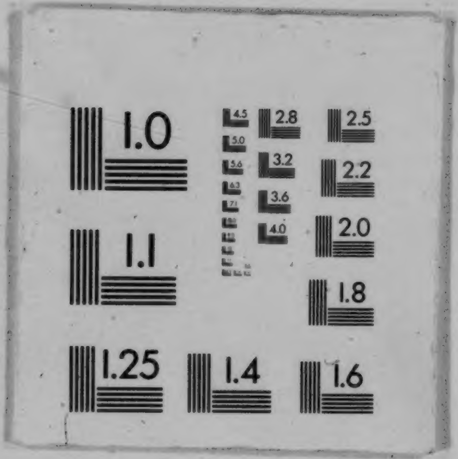
1.0
4.5
5.0
5.6
6.3
7.1
2.8
3.2
3.6
4.0
2.5
2.2
2.0
1.1
1.8
1.25
1.4
1.6

PNPA or, alternatively, a significant amount of the zwitterions (8c and 8d) may be present around neutral pH's. This would effectively

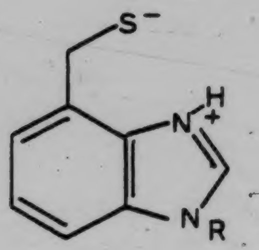

(8c) R=H
(8d) R=Me

increase the concentration of thiolate anion able to attack PNPA at these pH's. In theory, distinguishing between these two mechanisms is possible by studying the kinetic solvent deuterium isotope effect to probe a general base involvement. However, in this case there are problems as there will be an equilibrium isotope effect as well which would alter the relative concentrations of active thiolate species in D_2O as compared to H_2O.[61] Two other groups of researchers have also studied imidazole-thiol pairs as models of papain action and have also found that the plots of k_{cat} vs pH, for some of their compounds exhibit a positive deviation from a first order dependence in base indicating something in addition to the thiolate anion is providing catalytic activity. Lochon and Schoenleber[59] synthesized a series of benzimidazole-thiol pairs (Table 13, Figure 11) for reaction with PNPA and came to the conclusion that, for those compounds which did not show a first order dependence in base, there must be a substantial amount of catalysis due to the free thiol as

Table 13

Compound	pH	k_{Im} ($M^{-1} min^{-1}$)^a	
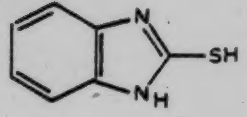 (46)	7.6	2.8	pK_1=4.28
	7.8	4.3	pK_2=9.12
	8.0	6.5	
	8.2	10.0	
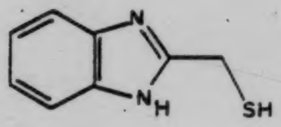 (47)	7.2	92	pK_1=4.95
	7.4	112	pK_2=8.50
	7.6	140	
	7.8	182	
	8.0	238	
	8.2	295	
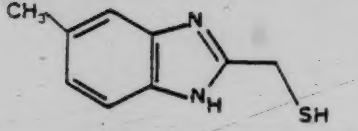 (48)	7.6	151	pK_1=5.10
	7.8	195	pK_2=8.50
	8.0	254	
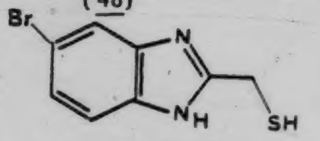 (49)	7.6	169	pK_1=4.30
	7.8	215	pK_2=8.50
	8.0	279	
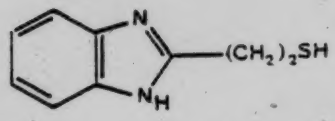 (50)	7.6	9	pK_1=5.45
	7.8	14	pK_2=9.77
	8.0	22	
	8.2	36	
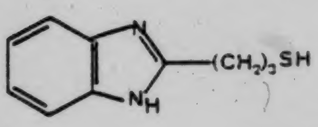 (51)	7.6	9.3	pK_1=5.60
	7.8	14.5	pK_2=9.90
	8.0	22	
	8.2	36	

Compound	pH	k_{Im} (M^{-1} min^{-1})	
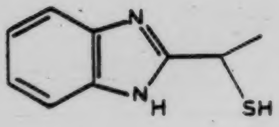 (52)	7.6	11.5	pK_1=5.10
	7.8	16.5	pK_2=8.65
	8.0	25	
	8.2	36	
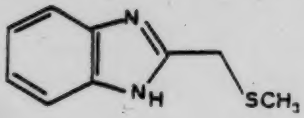 (53)	7.6	5	pK_1=5.00
	7.8	4.5	
	8.0	5	
	8.2	4.8	

a. Kinetic experiments and pKa determinations were performed at 30 0.1°C in 9.5% ethanol/water.

Figure 11: Plots of k_{cat} vs pH for 2-mercaptobenzimidazole (46), 2-mercaptomethylbenzimidazole (47), 5-methyl-2-mercaptomethylbenzimidazole (48), 5-bromo-2-mercaptomethylbenzimidazole (49), 2-(2-mercaptoethyl)-benzimidazole (50), 2-(3-mercaptopropyl)-benzimidazole (51), 2-(1-mercaptoethyl)-benzimidazole (52) and 2-methylthiomethylbenzimidazole (53).

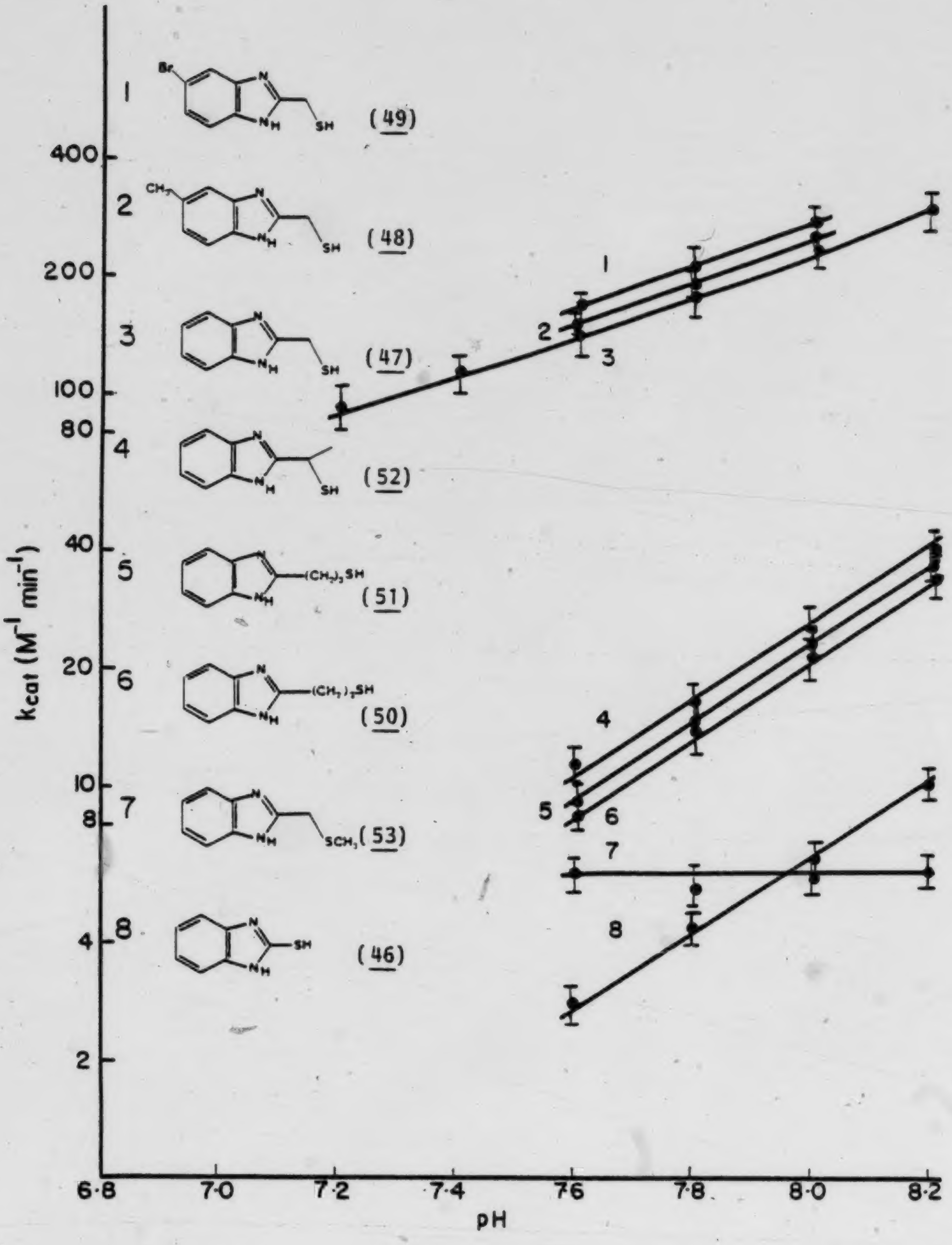
1
Br
N
NH
SH
(49)
2
CH3
N
NH
SH
(48)
3
N
NH
SH
(47)
4
N
NH
SH
(52)
5
N
NH
(CH2)3SH
(51)
6
N
NH
(CH2)2SH
(50)
7
N
NH
SCH3
(53)
8
N
NH
SH
(46)
400
200
100
80
40
20
10
8
4
2
kcat (M-1 min-1)
6·8
7·0
7·2
7·4
7·6
7·8
8·0
8·2
pH
1
2
3
4
5
6
7
8

the zwitterion is present in only negligible quantities.

Schneider and Wenck[62] studied the catalysis of the hydrolysis of PNPA by compounds (54), (55) and (56) (Table 14, Figure 12) and

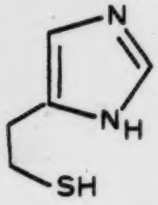

(54)

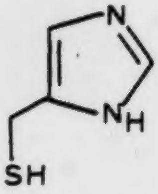

(55)

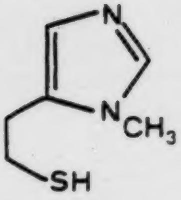

(56)

could not distinguish between a zwitterion and general-base mechanism for the catalytic activity in excess of that provided by the thiolate anion.

In order to determine if the zwitterion form of these imidazole-thiol pairs is indeed a viable catalytic species we must look at the equilibria governing its formation. Macroscopic pKa's can have several components arising from the detailed ionization processes. For example a dibasic acid, HAH, has two independent ionization processes yielding the anions AH^- and HA^- with equilibrium constants k_1 and k_2, where subscripts 1 and 2 denote the first and second protons in HAH as written. These in turn ionize to yield the same anion A^{-2} with equilibrium constants k_{12} and k_{21}, where the subscript 12 denotes loss of proton 2 following loss of proton 1 and subscript 21 denotes loss of proton 1 following loss of proton 2[63] (Scheme 19).

Table 14

Compound		pH	k_{Im} ($M^{-1}sec^{-1}$)[a]
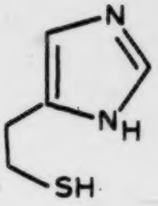	pK_1=7.2	6.5	.094
	pK_2=9.8	7.0	.194
		7.5	.386
		8.0	.665
		8.5	1.01
(54)		9.0	2.18
		9.5	4.31
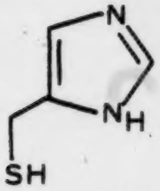	pK_1=6.6	6.5	.194
	pK_2=9.5	7.0	.324
		7.5	.454
		8.0	.876
		8.5	1.87
		9.0	4.38
(55)		9.5	8.42
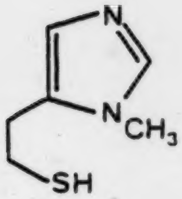	pK_1=7.4	6.5	.142
	pK_2=9.5	7.0	.338
		7.5	.744
		8.0	1.30
		8.5	2.00
		9.0	3.94
(56)		9.5	7.24

a. Kinetic experiments and pKa determinations were performed at 25 0.1°C in water.

Figure 12: Plots of k_{cat} (M^{-1} min^{-1}) vs pH for 4-mercaptoethylimidazole (54), 4-mercaptomethylimidazole (55) and 1-methyl-5-mercaptoethylimidazole (56).

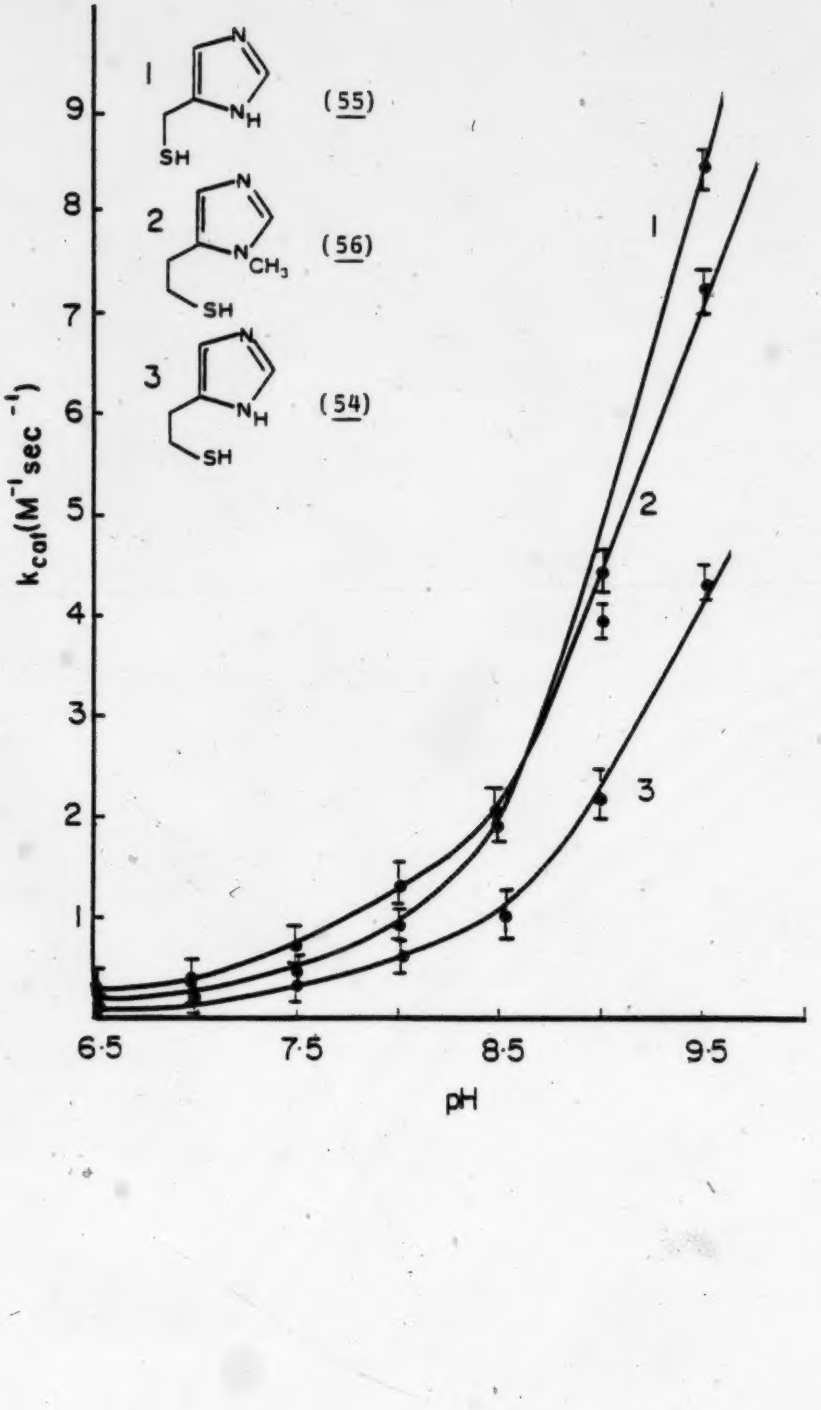
1
(55)
SH
N
NH
2
(56)
N
N CH3
SH
3
(54)
N
NH
SH
k_cat (M^-1 sec^-1)
9
8
7
6
5
4
3
2
1
6·5
7·5
8·5
9·5
pH
1
2
3

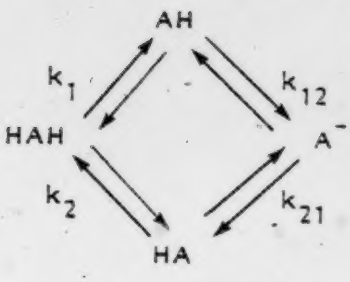
AH
HAH
A⁻
HA
k1
k12
k2
k21

Scheme 19

The ordinarily defined K_1 and K_2 are written in terms of the total concentration of $[HA^-]$ and $[AH^-]$.

9. $K_1 = k_1 + k_2$

10. $K_2 = k_{12}k_{21}/(k_{12} + k_{21})$

The constants k_1, k_2, k_{12} and k_{21} are known as microscopic ionization constants. Scheme 20 depicts the equilibria existing for any of the thiol-imidazole pairs discussed above.

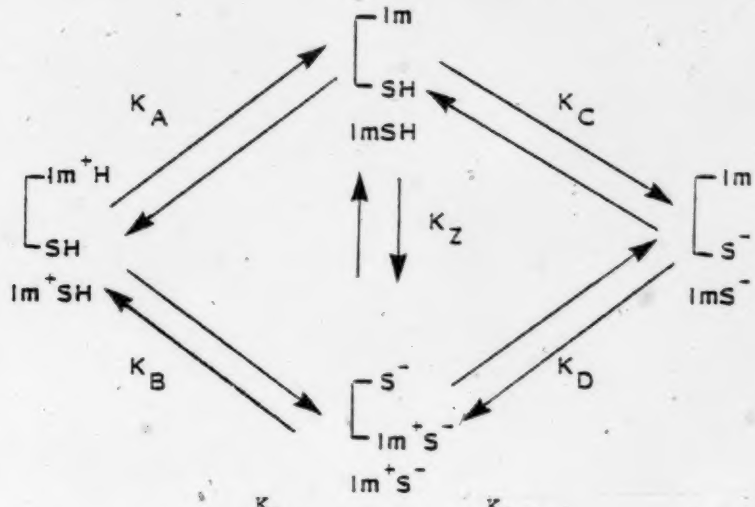
Im
SH
ImSH
Im⁺H
SH
Im⁺SH
Im
S⁻
ImS⁻
S⁻
Im⁺S⁻
Im⁺S⁻
KA
KC
KZ
KB
KD

$$Im^+SH \overset{K_1}{\rightleftharpoons} ImSH + Im^+S^- \overset{K_2}{\rightleftharpoons} ImS^-$$

Scheme 20

The rate expression may be defined in the following way:

11. Rate = $k_{cat}[ImSH]_t[PNPA]$ where $[ImSH]_t$ is the total concentration of thiol-imidazole present.

12. Rate = $(k_{ImS^-}[ImS^-]+k_{Im}[ImSH] + k_{Im'}[ImS^-] + k_{Im^+S^-}[Im^+S^-]$
$+ k_{ImSH}[ImSH])[PNPA]$ where ImS^- represents the anionic form which can provide catalysis through the thiolate anion or through the neutral imidazole ring with specific rate constants k_{ImS^-} and $k_{Im'}$, respectively. The neutral form of the thiolimidazole, ImSH, can provide catalysis either through the imidazole or the thiol functionalities. The catalysis due to each of these can be described by the specific rate constants k_{Im} and k_{ImSH} respectively. The protonated form of the thiol-imidazole represented by Im^+SH is most likely catalytically inactive and is present in very small amounts above pH 7. This species can be neglected in the rate equation. Finally, Im^+S^- represents the zwitterion and the catalysis due to the zwitterion can be represented by the specific rate constant $k_{Im^+S^-}$.

Therefore:

13. $[ImSH]_t = [ImSH] + [Im^+SH] + [Im^+S^-] + [ImS^-]$

and

14. $[Im^+SH] = [ImSH]a_H/K_A$

15. $[ImS^-] = K_C[ImSH]/a_H$

16. $[Im^+S^-] = K_Z[ImSH]$

Substituting equations 14,15, and 16 into equation 13 one obtains:

17. $[ImSH]_t = [ImSH] + [ImSH]a_H/K_A + K_C[ImSH]/a_H + K_Z[ImSH]$

and therefore

18. $[ImSH]_t = [ImSH](1 + a_H/K_A + K_C/a_H + K_Z)$

Let $X = (1 + a_H/K_A + K_C/a_H + K_Z)$

Then

19. $[\text{ImSH}] = [\text{ImSH}]_t/X$

20. $[\text{Im}^+\text{SH}] = [\text{ImSH}]_t a_H/XK_A$

21. $[\text{Im}^+\text{S}^-] = [\text{ImSH}]_t K_Z/X$

22. $[\text{ImS}^-] = [\text{ImSH}]_t K_C/Xa_H$

Substituting equations 19 through 22 into equation 12 results in:

23. $$\text{Rate} = \Big(\frac{(k_{\text{ImS}^-}[\text{ImSH}]_t K_C}{Xa_H} + \frac{k_{\text{Im}^+\text{S}^-}[\text{ImSH}]_t K_Z}{X} + \frac{k_{\text{Im}}[\text{ImSH}]_t}{X} + \frac{k_{\text{Im}'}[\text{ImSH}]_t K_C}{a_H X} + \frac{k_{\text{ImSH}}[\text{ImSH}]_t}{X}\Big)[\text{PNPA}]$$

24. $$\text{Rate} = \Big((k_{\text{ImS}^-}K_C/a_H + k_{\text{Im}^+\text{S}^-}K_Z + k_{\text{Im}} + k_{\text{Im}'}K_C/a_H + k_{\text{ImSH}})[\text{ImSH}]_t[\text{PNPA}]\Big)/X$$

Comparison of Equation 11 and Equation 24 shows:

25. $k_{cat} = (k_{\text{ImS}^-}K_C/a_H + k_{\text{Im}^+\text{S}^-}K_Z + k_{\text{Im}} + k_{\text{Im}'}K_C/a_H + k_{\text{ImSH}})/X$

Therefore

26. $k_{cat}X = k_{\text{ImS}^-}K_C/a_H + k_{\text{Im}^+\text{S}^-}K_Z + k_{\text{Im}} + k_{\text{Im}'}K_C/a_H + k_{\text{ImSH}}$

27. $$k_{cat}(1 + a_H/K_A + K_C/a_H + K_Z) = k_{\text{ImS}^-}K_C/a_H + k_{\text{Im}^+\text{S}^-}K_Z + k_{\text{Im}} + k_{\text{Im}'}K_C/a_H + k_{\text{ImSH}}$$

Knowing that $K_1K_2 = K_AK_C = K_BK_D$ and $K_Z = K_B/K_A$ we can multiply both sides of the equation by K_Aa_H to simplify:

28. $$k_{cat}(K_Aa_H + a_H^2 + K_AK_C + K_ZK_Aa_H) = K_CK_A(k_{\text{ImS}^-} + k_{\text{Im}'}) + (K_Ak_{\text{Im}^+\text{S}^-}K_Z + K_A(K_{\text{Im}} + k_{\text{ImSH}}))a_H$$

29. $$k_{cat} = ((K_Aa_H + a_H^2 + K_CK_A + K_Ba_H) = K_1K_2(k_{\text{ImS}^-} + k_{\text{Im}'}) + (K_Bk_{\text{Im}^+\text{S}^-} + K_A(k_{\text{Im}} + k_{\text{ImSH}}))a_H$$

30. $$k_{cat} = ((K_A + K_B)a_H + a_H^2 + K_1K_2) = K_1K_2\,(k_{ImS^-} + k_{Im'}) + (K_B k_{Im^+S^-} + K_A(k_{Im} + k_{ImSH}))a_H$$

31. $$k_{cat}(K_1a_H + a_H^2 + K_1K_2) = K_1K_2\,(k_{ImS^-} + k_{Im'}) + (K_B k_{Im^+S^-} + K_A(k_{Im} + k_{ImSH}))a_H.$$

Plots of $k_{cat}(a_H^2 + K_1a_H + K_1K_2)$ vs a_H for compounds (8), (46-52) and (54-56) (Figures 13, 14, 15 and 16) gave straight lines for which the slope is equal to $(K_B k_{ImS^-} + K_A(k_{Im} + k_{ImSH}))$ and the y intercept is equal to $K_1K_2(k_{ImS^-} + k_{Im'})$. There is some deviation from linearity as a_H approaches K_2. This is probably due to some error in the determined values for the macroscopic ionization constants.

Benzimidazoles are known to have very weak catalytic activity ($k_{cat} \equiv$ 0-6 M^{-1} min^{-1}).[10,59,60] Therefore, for compounds (8) and (46-52), the y intercept is approximately equal to $K_1K_2k_{ImS^-}$. For compounds (54-56), however, the catalysis due to the imidazole ring is no longer negligible but ranges from 0-25 M^{-1} min^{-1}. If we assume $k_{Im} \approx 25$ M^{-1} min^{-1} then k_{ImS^-} for compounds (54 (55) and (56) can be estimated. A summary of (intercept/K_1K_2), and slope values for these compounds is given in Table 15.

From Table 15 it can be seen that for 4(7')-thiomethylbenzimidazole (8a), $k_{ImS^-} = 824$ M^{-1} min^{-1} and for 1-methyl-4-thiomethylbenzimidazole (8b), $k_{ImS^-} = 490$ M^{-1} min^{-1}. These values agree quite well with the values obtained for k_{RS^-} (Tables 11 and 12) for these compounds in the high pH range where only the anion and not the zwitterion form is expected to be active (k_{RS^-} for (8a) = 850 M^{-1} min^{-1}, k_{RS^-} for (8b) = 477 $M^{-1}min^{-1}$.

Figure 13: Plots of a_H vs $k_{cat}(a_H^2 + K_1a_H + K_1K_2)$ for 4(7')-thiomethylbenzimidazole (8a) and 1-methyl-4-thiomethylbenzimidazole (8b).

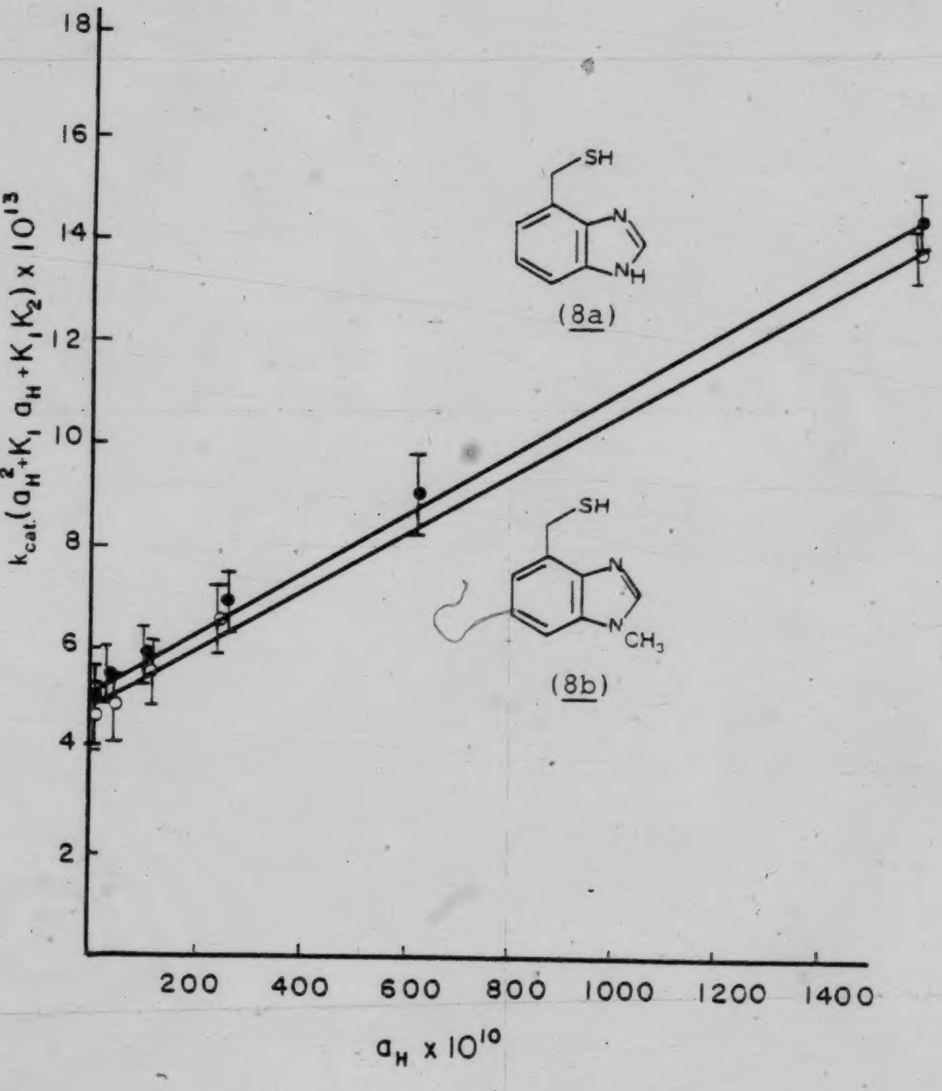
$k_{cat.}(a_H^2+K_1a_H+K_1K_2) \times 10^{13}$
18
16
14
12
10
8
6
4
2
200
400
600
800
1000
1200
1400
$a_H \times 10^{10}$
SH
N
NH
(8a)
SH
N
N
CH3
(8b)

Figure 14: Plots of a_H vs $k_{cat}(a_H^2 + K_1a_H + K_1K_2)$ for 2-mercaptobenzimidazole (46), 2-(1-mercaptoethyl)-benzimidazole (52), 2-(2-mercaptoethyl)-benzimidazole (50) and 2-(3-mercaptopropyl)-benzimidazole (51).

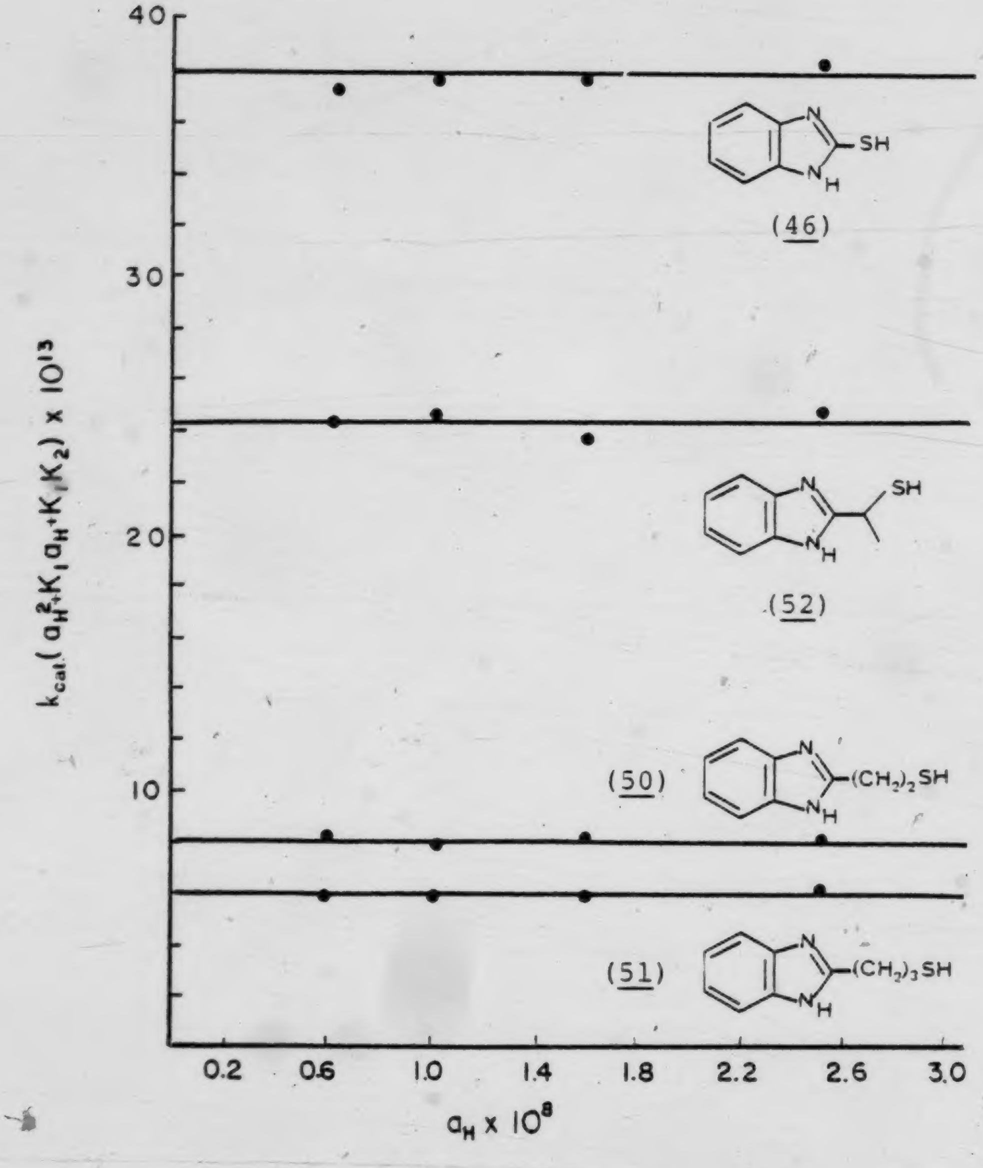
40
30
20
10
0.2
0.6
1.0
1.4
1.8
2.2
2.6
3.0
$a_H \times 10^8$
$k_{cat.}(a_H^2 + K_1 a_H + K_1 K_2) \times 10^{13}$
N
SH
NH
(46)
N
SH
NH
(52)
(50)
N
$(CH_2)_2SH$
NH
(51)
N
$(CH_2)_3SH$
NH

Figure 15: Plots of $k_{cat}(a_H^2 + K_1a_H + K_1K_2)$ vs a_H for 2-mercaptomethylbenzimidazole (47), 5-methyl-2-mercaptomethylbenzimidazole (48) and 5-bromo-2-mercaptomethylbenzimidazole (49).

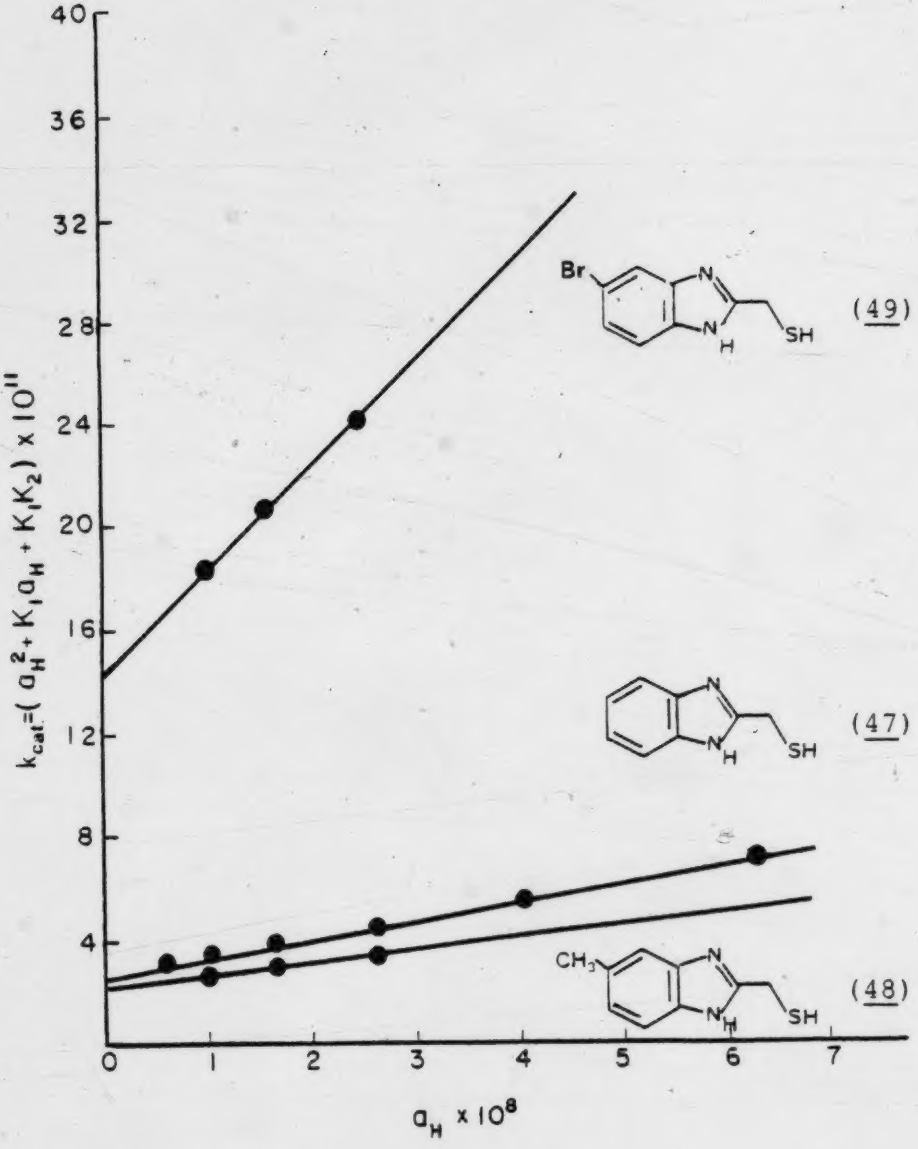
$k_{cat}(a_H^2 + K_1a_H + K_1K_2) \times 10^{11}$
40
36
32
28
24
20
16
12
8
4
0
1
2
3
4
5
6
7
$a_H \times 10^8$
Br
N
H
SH
(49)
N
H
SH
(47)
CH_3
N
H
SH
(48)

Figure 16: Plots of $k_{cat}(a_H^2 + K_1a_H + K_1K_2)$ vs a_H for 4-mercaptoethylimidazole (54), 4-mercaptoethylimidazole (55) and 1-methyl-5-mercaptomethylimidazole (56).

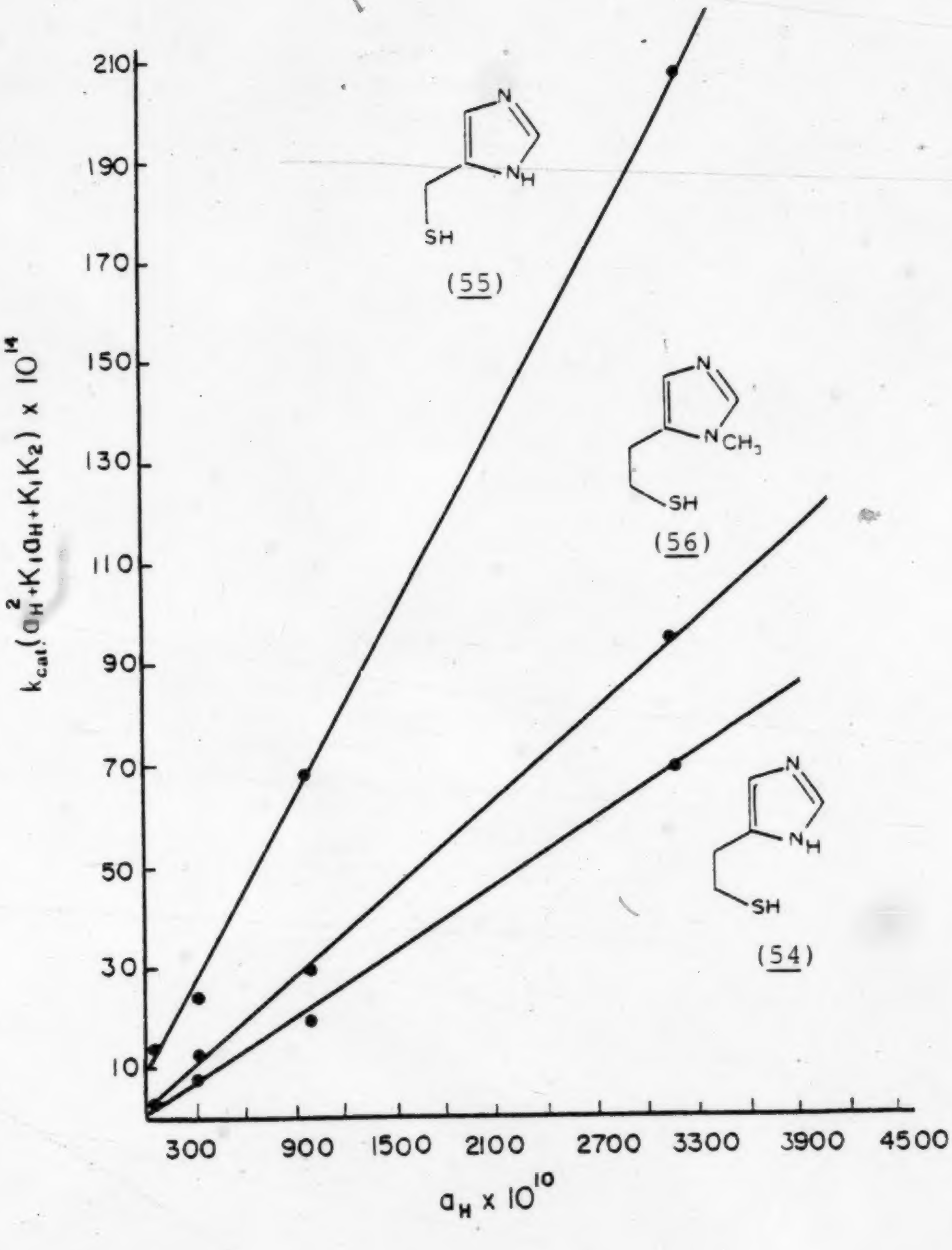
210
190
170
150
130
110
90
70
50
30
10
$k_{cat}(a_H^2 + K_1 a_H + K_1 K_2) \times 10^{14}$
300
900
1500
2100
2700
3300
3900
4500
$a_H \times 10^{10}$
N
NH
SH
(55)
N
NCH₃
SH
(56)
N
NH
SH
(54)

It is known that for benzimidazole compounds k_{Im}=0-6 M^{-1} min^{-1} [10,59,60] and $k_{Im} > k_{ImSH}$. Therefore, if the zwitterion activity is similar to that of a thiolate anion then perhaps $k_{Im^+S^-} \approx 10^3$. These values imply that the zwitterion term can contribute if $K_B/K_A > 10^{-2}$,

Table 15

Compound	Intercept/K_1K_2 $M^{-1}min^{-1}$	Slope	$(k_{ImSH} + k_{Im})$app M^{-1} min^{-1}
(8a)[a]	824	5.8×10^{-6}	1.66
(8b)[a]	490	6.3×10^{-6}	0.9
(46)[b]	95	0	0
(47)[b]	734	7.0×10^{-4}	62
(48)[b]	876	4.7×10^{-4}	60
(49)[b]	909	4.0×10^{-3}	80
(50)[b]	1327	0	0
(51)[b]	1899	0	0
(52)[b]	136	0	0
(54)[c]	980	2.2×10^{-6}	34.5
(55)[c]	1104	6.2×10^{-6}	25
(56)[c]	773	3.0×10^{-6}	75

(a) Determined in 31.6% EtOH/H_2O(v/v), 25±0.1°C.
(b) Determined in 9.5% EtOH/H_2O (v/v), 30±0.1°C.
(c) Determined in H_2O, 25±0.1°C.

not an unreasonable possibility if one looks at available values found in the literature[64c] for thiol-amine pairs. If one omits the zwitterion as a viable catalytic species then $k_{Im^+S^-} = 0$. Assuming that $K_A = K_1$, the slope then equals $K_1(k_{ImSH} + k_{Im})$. If we divide the slope by K_1 we obtain the apparent values of $(k_{ImSH} + k_{Im})$ for these compounds. If these are larger than expected from monofunctional systems, this also would be an indication of zwitterion activity. The values obtained are summarized in Table 15.

In our studies $k_{Im} = 0$ for 1-methylbenzimidazole (10b), 1-methyl-4-hydroxymethylbenzimidazole (12b), and 4(7')-hydroxymethylbenzimidazole (12a). Benzimidazole (10a), itself, exhibited a a small amount of catalytic activity ($k_{Im} = 0.39$ M^{-1} min^{-1}) and since there are no known examples of general base assisted catalysis by thiols on PNPA it would seem that the values of 1.66 and 0.9 M^{-1} min^{-1} are slightly high to represent only the catalysis due to the imidazole ring in compounds (8a) and (8b). Therefore, the zwitterion is probably taking an active part in the catalysis of the breakdown of PNPA even though it is present only in small amounts. To obtain a true estimate of k_{Im+S^-}, determination of the microconstants K_B and K_A would be necessary.

For compounds (46), (50), (51), and (52) values of 734, 1327, 1899, and 136 M^{-1} min^{-1} respectively are obtained for k_{ImS^-}. Plots of $k_{cat}(a_H^2 + K_1a_H + K_1K_2)$ vs a_H for these compounds give straight lines of zero slope indicating that there is no catalysis due to the zwitterion, free thiol or the imidazole ring. On the other hand, plots of $k_{cat}(a_H^2 + K_1a_H + K_1K_2)$ vs a_H for compounds (47), (48) an (49) yield straight lines of non-zero slope. Values of 734, 876, and 909 $M^{-1}min^{-1}$ respectively are obtained for k_{ImS^-}. If one ignores the zwitterion, values for $(k_{Im} + k_{ImSH})_{apparent}$ for these compounds of 62, 60 and 80 $M^{-1}min^{-1}$ respectively are obtained. These values are much higher than would be expected from monofunctional systems and therefore indicate zwitterion activity in the catalysis. For compounds (54), (55) and (56) values of 980, 1104, and 773 M^{-1} min^{-1} are obtained for k_{ImS^-} and values of 34.5, 25 and 75 $M^{-1}min^{-1}$ are obtained for $(k_{Im} + k_{ImSH})_{app}$. The values for $(k_{Im} + k_{ImSH})_{app}$ once again are larger than would be expected from the study of monofunctional systems; an indication of zwitterion activity.

The microconstants for both Lochon's[59] and Schneider's[62] compounds are unavailable. However, in order to obtain valid estimates for the specific rate constants for the zwitterion activity for compounds (8a) and (8b) attempts were made to obtain the microscopic equilibrium constants for these compounds.

There are a number of methods available for calculating microscopic pKa's in a system such as this.[64] It can be done analytically by NMR methods worked out by Rabenstein et al.[64a] which observe the chemical shift positions of the various C-H resonances as a function of pH. For example, downfield shifts of the C_2-H of imidazole are observed at low pH's, the peak position being indicative of the equilibrium position between Im and HIm^+.[64c]

A similar plot of pH vs chemical shift for the thiol methylene group gives the relative concentration of RCH_2SH and RCH_2S^- at a given pH. If one observes more RCH_2S^- at a given pH than can be accounted for on the basis of the thermodynamic pKa of RCH_2SH, then this provides evidence for the existence of the zwitterion. However, the NMR technique is only able to detect species which make up 5% of the solution or more and therefore could be used only under circumstances where there is a significant interaction of the thiol with the imidazole. Due to the large difference in the thermodynamic pKa's, our system did not lend itself to this type of analysis.

Raman spectroscopy could also be used to measure, quantitatively, the concentration of the protonated thiol, [RSH], at different pH's. If one observes a lower [RSH] at a given pH than can be accounted for on the basis of the thermodynamic pKa of RCH_2SH, then this provides evidence for the existence of the zwitterion. Attempts to get quantitative results using Raman spectroscopy to obtain the microconstants for (8a) and (8b) failed due to the interference of the fluorescence spectrum.

Finally, the microscopic pKa's can be determined using UV-VIS spectrophotometric techniques. Benesch and Benesch[64e] pioneered this approach in their 1955 paper and a slight modification of their methods were applied in an attempt to determine the microscopic equilibrium constants for compound (8b) as outlined below.

From Scheme 20, the equilibrium and mass balance relationships outlined previously and Beer's Law we can define the following equations where A=absorbance, b=cell length and ε is the molar extinction coefficient.

$$32.\quad A_{\lambda_1} = (\varepsilon_{1\lambda_1}[Im^+SH] + \varepsilon_{2\lambda_1}[ImSH] + \varepsilon_{3\lambda_1}[Im^+S^-] + \varepsilon_{4\lambda_1}[ImS^-])b$$

$$33.\quad A_{\lambda_1} = (\varepsilon_{1\lambda_1}a_H[ImSH]_t/K_AX + \varepsilon_{2\lambda_1}[ImSH]_t/X + \varepsilon_{3\lambda_1}K_Z[ImSH]_t/X + \varepsilon_{4\lambda_1}K_C[ImSH]_t/a_HX)b$$

where $X = (1 + K_C/a_H + a_H/K_A + K_Z)$

$$34.\quad A_{\lambda_1}/b = \frac{\varepsilon_{1\lambda_1}a_H/K_A + \varepsilon_{2\lambda_1} + \varepsilon_{3\lambda_1}K_Z + \varepsilon_{4\lambda_1}K_C/a_H)[ImSH]}{(1 + K_C/a_H + a_H/K_A + K_Z)}$$

35. $$A_{\lambda_1}/b[\mathrm{ImSH}]_t = \frac{\dfrac{\varepsilon_{1\lambda_1}a_H^2 + \varepsilon_{2\lambda_1}K_Aa_H + \varepsilon_{3\lambda_1}K_ZK_Aa_H + \varepsilon_{4\lambda_1}K_CK_A}{K_Aa_H}}{\dfrac{K_Aa_H + K_CK_A + a_H^2 + K_ZK_Aa_H}{K_Aa_H}}$$

36. $$\frac{A_{\lambda_1}}{[\mathrm{ImSH}]_t b} = \frac{\varepsilon_{1\lambda_1}a_H^2 + (\varepsilon_{2\lambda_1} + \varepsilon_{3\lambda_1}K_Z)\, K_Aa_H + \varepsilon_{4\lambda_1}K_CK_A}{K_Aa_H\ (1 + K_Z) + K_CK_A + a_H^2}$$

but $K_AK_C = K_1K_2$; and $K_Z = K_B/K_A$ therefore

$$K_Z + 1 = (K_B + K_A)/K_A = K_1/K_A$$

with these substitutions

37. $$\frac{A_{\lambda_1}}{b[\mathrm{ImSH}]_t} = \frac{\varepsilon_{1\lambda_1}a_H^2 + (\varepsilon_{2\lambda_1} + \varepsilon_{3\lambda_1}K_B/K_A)K_Aa_H + \varepsilon_{4\lambda_1}K_1K_2}{K_1a_H + K_1K_2 + a_H^2}$$

38. $$\frac{A_{\lambda_1}}{b[\mathrm{mSH}]_t} + \frac{\varepsilon_{1\lambda_1}a_H^2 + (\varepsilon_{2\lambda_1}K_A + \varepsilon_{3\lambda_1}(K_1-K_A))a_H + \varepsilon_{4\lambda_1}K_1K_2}{K_1a_H + K_1K_2 + a_H^2}$$

The molar extinction coefficients for $[\mathrm{Im^+SH}]$ and $[\mathrm{ImS^-}]$ can be determined independently at pH 1 and pH 12 respectively. Rearrangement of 38 allows us to isolate the term $\varepsilon_2K_A + \varepsilon_3(K_1-K_2)$. This term contains the microconstant K_A but not in a form that can be determined because ε_2 and ε_3 are also unknowns. Studies of the pH dependence of the absorbance maxima for benzimidazole (10a), 1-methylbenzimidazole (10b) and their protonated analogues show that there is a rapid increase in absorbance at 270, 275 and 280 nm as we pass through the pH range corresponding to $\mathrm{p}K_{\mathrm{Im}} \rightarrow \mathrm{p}K_{\mathrm{Im}^+}$ indicating that the protonated species have a higher molar extinction coefficient than the neutral species in these ranges. However, there is little change in the spectrum in the 260 nm region. Therefore, by collecting the absorbance vs pH values for (8b) at 260 nm one can make the approximation that $\varepsilon_1 = \varepsilon_2$ and $\varepsilon_3 = \varepsilon_4$ where $\varepsilon_1 = 6.96 \times 10^2$ and $\varepsilon_4 = 8.04 \times 10^2\ M^{-1}\ cm^{-1}$.

Equation 3^a was evaluated to give $\varepsilon_2 K_A + \varepsilon_3(K_1 - K_A)$ at pH's 5.80, 6.96 and 7.91. The results are given in the following three equations:

39. $5.747 \times 10^{-3} = \varepsilon_2 K_A + \varepsilon_3(K_1 - K_A)$ pH = 5.80
40. $5.712 \times 10^{-3} = \varepsilon_2 K_A + \varepsilon_3(K_1 - K_A)$ pH = 6.96
41. $5.728 \times 10^{-3} = \varepsilon_2\ {}_A + \varepsilon_3(K_1 - K_A)$ pH = 7.91

By substituting the approximate values for ε_2 and ε_3 one obtains values of 5.20, 5.23 and 5.22 for pK_A. However, the macroscopic pKa's are known only to 2% precision and the values for ε_2 and ε_3 are only approximations. It can be concluded on the basis of the above that $pK_A = 5.2 \pm 0.1$ and as $K_B = K_1 - K_A$ and $pK_1 = 5.2 \pm 0.1$ a meaningful value for K_B cannot be obtained other than it is probably at least one order of magnitude smaller than K_A. The same types of problems arise when one tries to evaluate K_B directly by substituting $K_1 - K_B$ for K_A.

Although a value for the rate constant expressing the catalysis due to the zwitterion cannot be obtained, the analysis of the kinetic data would seem to indicate that the observed pH rate profile for the decomposition of PNPA with all the thiol-imidazole pairs discussed, can be explained without postulating an unprecedented general base role for the imidazole. As previously stated, the histidine and cysteine in the active site of papain are believed to exist 90% in their ion pair form[30] and therefore the zwitterion explanation does indeed appear to be a viable alternative to the traditional but unproven general base mechanism for the acylation step in the enzyme.

It will be recalled that our original intention, before completion of the studies on (8) was to study the catalysis of the hydrolysis of PNPA also with (9). However, after completing the kinetic analysis on compounds (8) and on Lochon's[59] and Schneider's[62] compounds it became clear that if papain is acting via the zwitterion, a good model should have the highest zwitterion concentration possible at physiological pH's. This implies that the thermodynamic pKa's should be as close together as possible and as well, the thiol to thiolate anion equilibrium constant should be as low as possible. A survey of the pKa's of various monofunctional imidazole and thiol compounds, in addition to a survey of the thermodynamic pKa's described for thiol-imidazole pairs discussed earlier suggest that it is not obvious how one would obtain an adequately small ΔpKa for imidazoles carrying a thiomethyl group on an annulated six member ring. Therefore, we conclude that hydrolysis studies with compound (9) would in fact not provide a significant rate enhancement over that achieved by compounds (8). However, we believe that imidazoles containing a sulfhydryl groups with suitable pKa's can exist. For example, Lochon[59] found that $pK_{Im} = 4.95$ and $pK_{SH} = 8.5$ for compound (57).

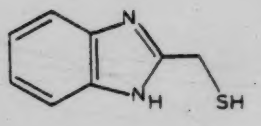

(57)

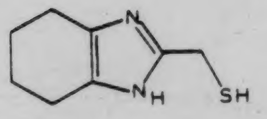

(58)

These values and some trends established in the present work suggest that the unreported compound (58) would have $pK_{Im} \approx 7.5$ and $pK_{SH} \approx 8.5$, values which would lead to high concentrations of the "S^- species" at neutral pH's. The study of the catalytic properties of compound (58) therefore, might prove to be an interesting future study. In addition its synthesis should be relatively straight forward as the key step, the high pressure hydrogenation of 2-benzimidazolecarboxylic acid (59) to the corresponding tetrahydrobenzimidazole compound (60) is reported to

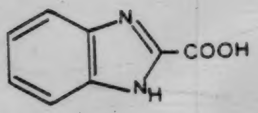

(59)

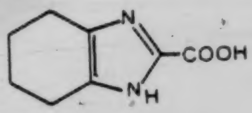

(60)

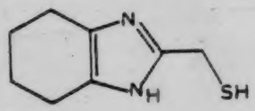

(58)

proceed in 80% yield.[43] Transformation of the resulting acid to the thiol should be readily accomplished. With this compound rate constants for the hydrolysis of PNPA might approach those found for papain.

Results and Discussion: Deacylation Step

Introduction to Research

Contrary to Lochon's report[59], simple thiol esters are not readily hydrolyzed except under highly alkaline or acidic conditions.[25a,18a]

Activated thiol esters having electron withdrawing groups such as CF_3, CCl_3 and CF_2CF_3 on the acyl group have been extensively studied by Schmir,[65,66] and Jencks[67] with respect to the unusual rate depression observed at low pH. Metal ions have been observed to catalyze hydrolysis.[68] Recent proton inventory studies by Hogg[69] have confirmed Bruice and Fedor's[66] observations that imidazole can act as a general-base to promote the hydrolysis of ethyl trifluorothiol acetate ($k_{H_2O}/k_{D_2O} = 2.84$[69]). However, in contrast to the situation with activated thiol esters, nitrogen-containing species have a strong propensity to attack non-activated thiol esters nucleophilically.[15,70,71,4,72,25e] Bruice and Fedor have observed that hydroxylamine,[72e] morpholine and hydrazine nucleophilically attack unactivated thiol esters and δ-thiolvalerolactone. The rate expressions also include terms which are second order in nitrogen species indicating that general-base and/or general-acid catalysis is also present. Imidazole is also an effective nucleophile towards thiol esters and exhibits observed second order rate constants of $k_n = 0.01\ M^{-1}min^{-1}$ (pH 7.13) and 0.04 $M^{-1}min^{-1}$ (pH 7.7) for attack on ethyl thioacetate[4] and n-butyl thioacetate,[72e] respectively.

Bruice[15] observed that the thiol ester n-propyl-γ-(4-imidazoyl)thiobutyrate (61) readily decomposed to the corresponding lactam (62) with a first order rate constant of $k = 1.5\ \mathrm{min}^{-1}$ at pH 7. However, lactam (62) decomposes only slowly around neutrality (Scheme 21).

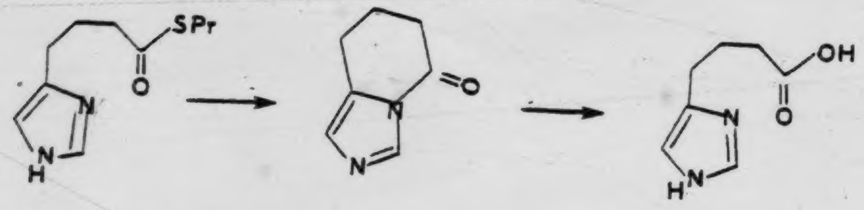

(61) (62)

Scheme 21

Similarly, Fife[70] observed that the thiol ester (63) cyclized to the lactam (64) with a first order rate constant of $k = 1.2\ \mathrm{min}^{-1}$ at pH 7. Again the intermediate N-acyl compound decomposed slowly around neutrality (Scheme 22).

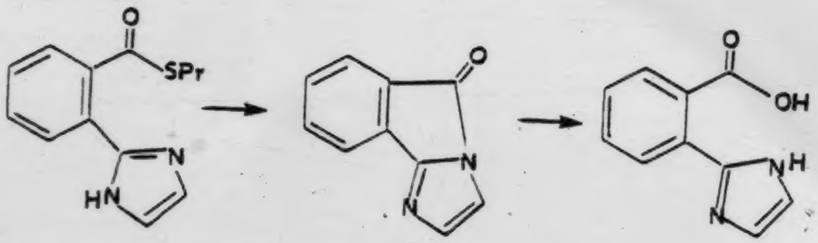

(63) (64)

Scheme 22

On the basis of the above it might be tempting to postulate a nucleophilic role for the imidazole in the enzyme although such postulations have been criticized by Bender and Brubacher[19a,b] on the basis of solvent isotope effects between 2.75[23] and 3.35 observed for the enzyme deacylation. Additionally, should a nucleophilic role for the His-159 imidazole actually be operative, the N-acyl imidazole intermediate decomposition itself must be catalyzed since both Bruice[15] and Fife[70] found these to decompose slowly around neutrality. The problem of solvent isotope effect has been ruled out by work done by Jencks et al.[38] They have shown that N-acetylimidazole hydrolyses exhibit a deuterium isotope effect of 2.5[38c] which is similar to that found for hydrolysis reactions using papain. These same studies also showed that N-acetyl imidazole, when protonated, can rapidly decompose at rates which approach those observed for the deacylation step in the enzyme. Recently, Lowe and Bendall[73] have demonstrated that papain action shows a pH dependence on two groups which exhibit cooperative ionization when irreversibly inhibited. These two groups were considered to be Asp-158 and His-159. An Asp-158-His-159 ion pair would allow the His-159 to become an effective nucleophile or general-base in enzyme deacylation. Diminuation of the rate observed at low pH could then be accounted for by protonation of Asp-158 which would reduce both the nucleophilicity and basicity of the imidazole thus inhibiting deacylation; or by protonation of His-159 which quenches its activity.

It is difficult to envision how nucleophilic attack by nitrogen could be inhibited since neutral imidazole is known to be a powerful nucleophile toward thiol esters. It seems possible to us that imidazole attack might be quite fast and that it is the hydrolysis of the N-acylimidazole which is rate-determining. To clarify the catalytic role of the imidazole the catalysis of the decomposition of compounds (65) and (27) was studied.

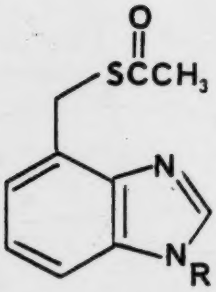

(65) R=H
(27) R=CH$_3$

Jencks and Carruiolo[38a] have shown that N-acetylimidazole (66) hydrolyzes by acid, neutral and base pathways according to equation (Scheme 23).

42. $-d(\underline{66})/dt = 2.8[(\underline{66})H^{+}] + 0.005\,[(\underline{66})] + 19000\,[(\underline{66})][OH^{-}]$

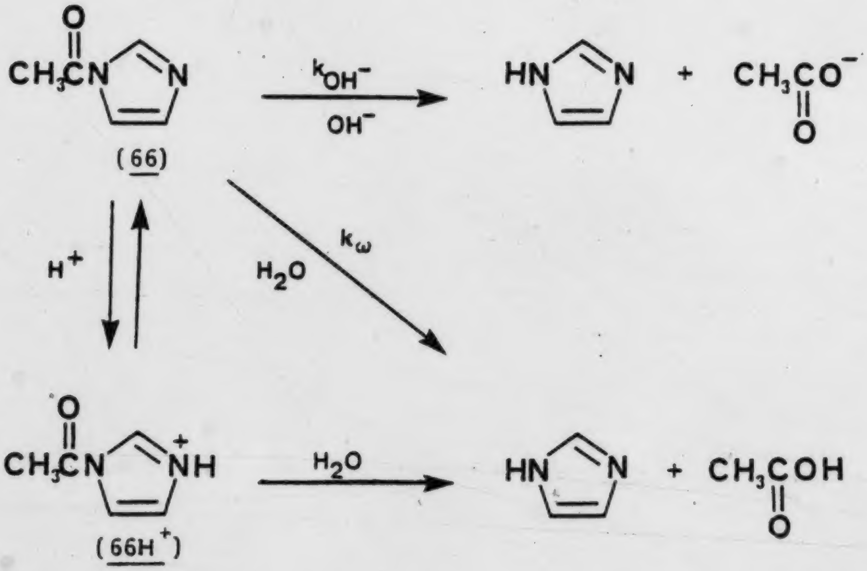
CH$_3$CN
O
N
(66)
k_{OH^-}
OH$^-$
HN
N
+
CH$_3$CO$^-$
O
H$^+$
H$_2$O
k_ω
CH$_3$CN
O
NH
+
(66H$^+$)
H$_2$O
HN
N
+
CH$_3$COH
O

Scheme 23

At low pH, the rate is controlled by reaction of (66)H$^+$ (pKa = 3.6)[38a] and the pH rate profile is level at pH's where the imidazole is completely protonated (k_{obs} = 2.8 min^{-1}).[38a] In a later study Jencks and Marburg[38c] showed that (66)H$^+$ and its N-methyl analogue (67) decomposed rapidly in water and exhibited solvent isotope effects greater than 2.0. Thus protonated N-acyl imidazole can decompose at rates which approach those found for the deacylation step in the enzyme.

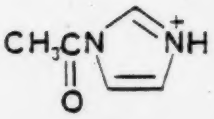

(66)

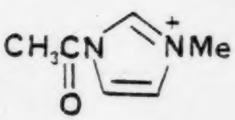

(67)

Therefore, in the case of compounds (65) and (27) if the N-acetylimidazole intermediate is being formed (Scheme 24) we would likely be able to observe (68a) spectrophotometrically at some pH as it would be expected to hydrolyze only slowly at neutral pH's. The hydrolysis of (65) itself, however, is not likely to be a good model for the proposed N-acyl intermediate in the enzyme since we have proposed that the intermediate exists in its protonated form stabilized by the adjacent Asp-COO$^-$ anion. Thus, overall the study of the methyl thiol ester (27) might be a better model for the enzyme since it leads to the N-methyl-N'-acetylimidazolium species (68b) which approximates more closely the proposed charged enzymic analogue. It was hoped that comparison of the rates of hydrolysis of (65) and (27) would give some concrete evidence as to whether this nucleophilic mechanism can lead to hydrolysis rates that are close

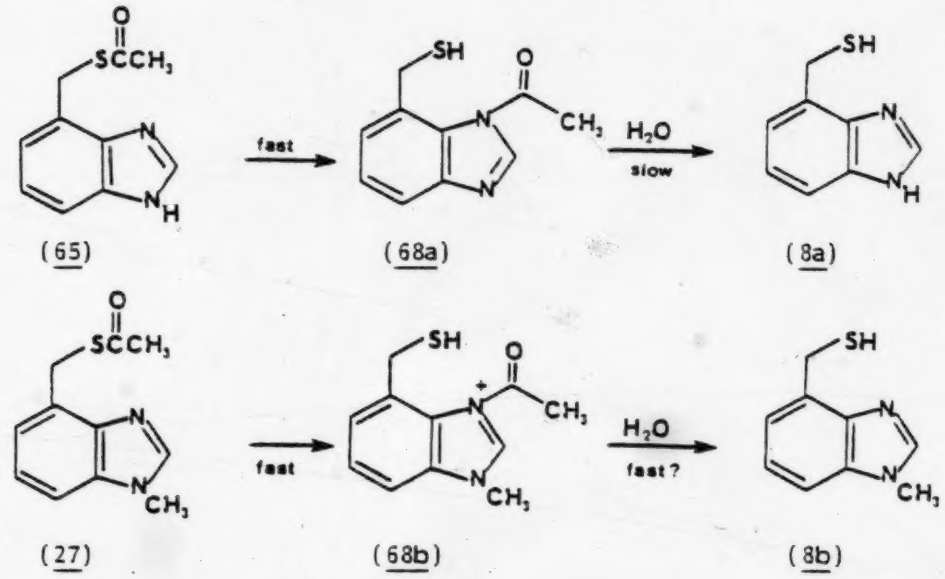
(65)
fast
(68a)
H_2O
slow
(8a)
(27)
fast
(68b)
H_2O
fast?
(8b)

Scheme 24

to those found for the enzyme.

The analogous oxygen systems (69) were also studied for comparison purposes. The decomposition of benzyl thioacetate (70) and benzyl acetate (71) had to be studied under the same conditions

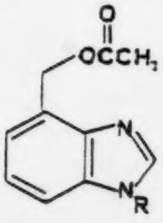

(69a) R=H
(69b) R=CH_3

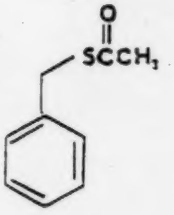

(70)

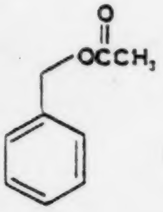

(71)

to determine the deacylation rates without a proximally positioned imidazole ring.

Synthesis

Benzyl alcohol (72) and benzyl thiol (6) were acylated with acetic anhydride as were 1-methyl-4-hydroxymethylbenzimidazole (12b) and 4(7')-hydroxymethylbenzimidazole (12a) (Scheme 25). It is interesting to note that the treatment of the latter two with benzoyl or acetyl chloride gave the corresponding chlorides as the only products.

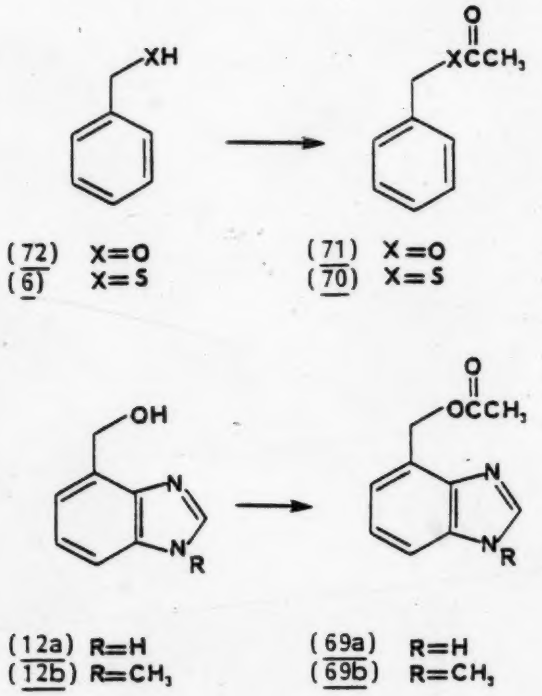
XH
O
XCCH$_3$
(72) X=O
(6) X=S
(71) X=O
(70) X=S
OH
O
OCCH$_3$
N
N
R
(12a) R=H
(12b) R=CH$_3$
(69a) R=H
(69b) R=CH$_3$

Scheme 25

In the case of (12a), acylation could occur on either the nitrogen or oxygen atoms. Therefore, the nitrogen was protected by formation of the hydrochloride salt before reaction with acetic anhydride. The structure was verified by comparison of the NMR spectrum of the product (4(7')-acetoxymethylbenzimidazole (69a)) with the spectra of the doubly acylated compound (73) and N-acetylbenzimidazole (74) (Table 16). In general, acylation on nitrogen for all these imidazole compounds results in a signal due to the N-acetyl methyl between δ 2.6 and δ 3.0. Acylation on nitrogen also disperses the signals in the aromatic region.

Both 4(7')-thioacetoxybenzimidazole (65) and 1-methyl-4-thioacetoxybenzimidazole (27) were prepared by displacement of the halogen from the corresponding chlorides (21) and (24) using

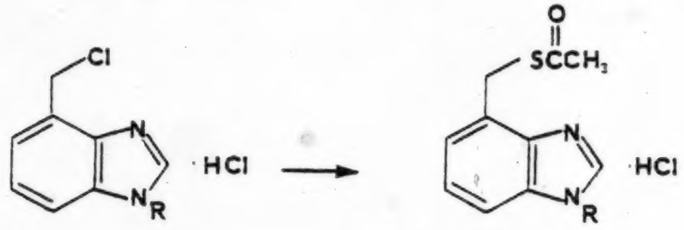

(21) R=H
(24) R=CH₃

(65) R=H
(27) R=CH₃

potassium thioacetate in room temperature THF. If this displacement was carried out in refluxing THF or ethanol large quantities of the thionester were produced. The thionester is easily identified by its characteristic bright red colour. In principle it is possible that once the thioacetates had been formed the acetyl group was immediately transferred to the nitrogen in the reaction mixture. On the basis of the earlier discussion (p 114-115) we had anticipated that this would occur but it was possible to show that in this experiment it had in fact not taken place. The products from the displacement reactions were titrated with I_2. No free thiol was found and therefore the acetyl group must be on sulphur.

Table 16

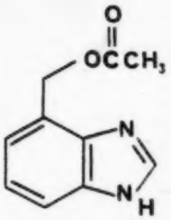

2.07	OAc
5.36	CH_2
7.14—7.20	ArH
7.46—7.60	ArH
8.22	N=C(H)-N

(69a)

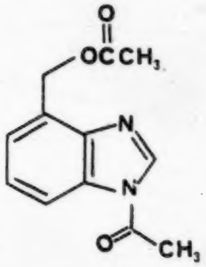

2.07	OAc
2.77	NAc
5.46	CH_2
7.3—7.4	ArH
8.05—8.2	ArH
9.0	N=C(H)-N

(73)

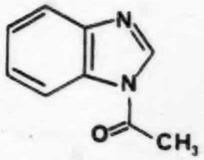

2.78	NAc
7.38—8.26	ArH
9.0	N=C(H)-N

(74)

Catalytic Studies

The measurements monitoring the decomposition of benzyl thioacetate (70) were followed spectrophotometrically at 251 nm. The reaction was checked for buffer catalysis by using 0.31 M, 0.21 M, 0.16 M and 0.02 M buffers which were obtained by dilution of the original 0.3 M buffers with H_2O. The final rate constants, therefore, were obtained by extrapolaton to [buffer] = 0 . Data were fit to a non-linear least squares program (Appendix II) and each rate constant was average of at least three reproducible experiments at each [buffer]. It was found that the total difference between the UV-VIS spectra of the thioacetate and product became smaller and smaller as one descended in pH. This was probably due to the decreasing amounts of thiolate anion present. Therefore, below pH 10 the decomposition rates could not be followed by this method. Attempts were made to titrate the liberated acid at lower pH's with 0.1000 N NaOH but due to the quantities of benzyl thioacetate (70) required and its low solubility in the aqueous ethanol mixture this could not be done. The results are given in Table 17 (Figure 17). The products were analyzed using the NMR techniques described earlier for the acylation studies. The peaks due to the methylene group (δ 4.04) and the S-acetyl methyl group (δ 2.26) of (70) slowly diminished as the singlet due to the methylene group (δ 3.66) of benzyl mercaptan (6) and the singlets representing ethyl acetate (δ 2.03) and the acetate anion (δ 1.88) appeared. The final spectrum was identical to that obtained by dissolving (6) in the same solvent system except for the peak at δ 1.88 due to the acetate anion. In the case of benzyl acetate (71) there was no difference between the

TABLE 17

PSEUDO-FIRST ORDER AND SECOND ORDER RATE CONSTANTS FOR THE DECOMPOSITION OF BENZYL THIOACETATE[a]

pH±0.02	$k_{obs.}$ min.$^{-1}$	k_{OH^-} M.$^{-1}$ min.$^{-1}$	[OH$^-$]
10.8	$7 \pm 1.5 \times 10^{-3}$	12	5.62×10^{-4}
10.6	$4 \pm 1 \times 10^{-3}$	11	3.55×10^{-4}
10.4	$1 \pm 2.4 \times 10^{-3}$	11	2.24×10^{-4}
		Av. = 11.3 ± 0.7	

a. Determined in 31.6% EtOH/H_2O (v/v). [Buffer] = 0.21, 0.16, 0.13 and 0.02 M.

b. $k_{OH^-} = k_{obs.}/[OH^-]$.

Figure 17: Plot of k_{obs} vs pH for the decomposition of benzyl thioacetate (70), benzyl acetate (71), 4(7')-acetoxymethylbenzimidazole (69a), 1-methyl-4-acetoxymethylbenzimidazole (69b), 4(7')-thioacetoxymethylbenzimidazole (65) and 1-methyl-4-thioacetoxymethylbenzimidazole (27).

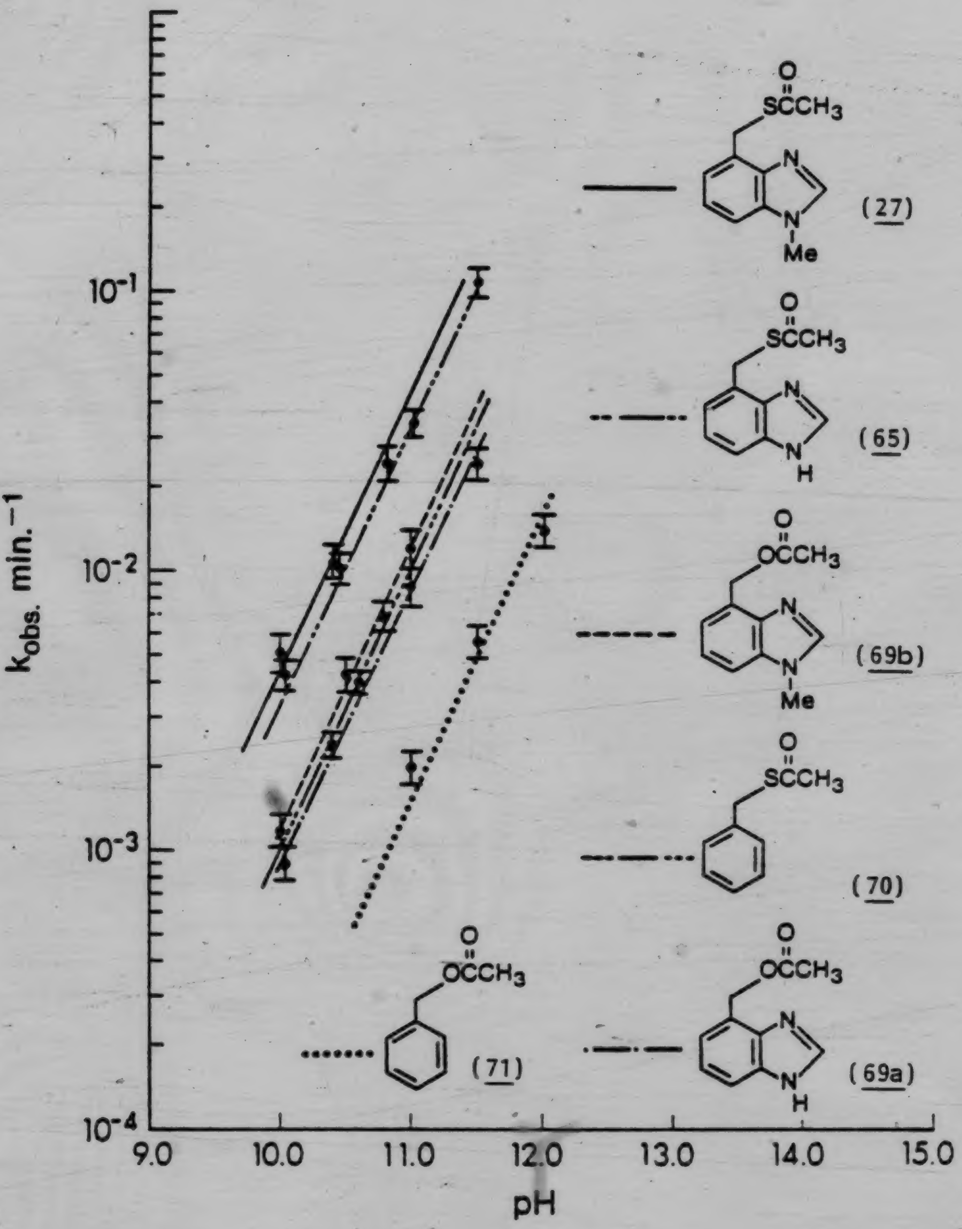

k obs. min.⁻¹
10⁻¹
10⁻²
10⁻³
10⁻⁴
9.0
10.0
11.0
12.0
13.0
14.0
15.0
pH
SCCH3
(27)
(65)
OCCH3
(69b)
(70)
(71)
(69a)
N
Me
H
O

UV-VIS spectrum of the acetate and the product. This meant that all kinetics had to be done using "pH stat" techniques (titrating the liberated acid with 0.1000 N NaOH). The hydrolysis was followed to completion and the data fit to a non-linear least squares program to determine the rate constant (Appendix 2). Plots of $\ln(C_\infty - C_t)$ were made to insure the reaction was following first order kinetics. For each pH the rate constants shown in Table 18 are the result of at least three reproducible runs (Figure 17). Again below pH 10 the low solubility in the aqueous ethanol solvent prevented the acquisition of the kinetic data. NMR product analysis showed the disappearance of the singlets at δ 5.06 (CH_2) and δ 2.02 (OAc) and the growth of singlets at δ 4.59 (CH_2OH) and δ 1.90 (OAc^-). The final spectrum was identical to that obtained from benzyl alcohol (72) in the same solvent system with the exception of the singlet due to acetate anion.

Plots of $k_{obs}/[OH^-]$ vs pH for both benzyl thioacetate (70) and benzyl acetate (71) give straight lines of zero slope indicating that in this pH region it is hydroxide ion which is the active species in catalysis. Tarbell[74] examined the hydrolysis rates of a series of thiol esters and their corresponding oxygen esters at elevated temperatures in order to accelerate their slow decomposition rates. From his results, in combination with the ones given in Tables 17 and 18 it can be assumed that the decomposition of (70) and (71) will continue to have a first order dependence in base until neutral pH's are reached.

The decomposition of 4(7')-thioacetoxymethylbenzimidazole(65) and 1-methyl-4-thioacetoxymethylbenzimidazole (27) could be monitored

TABLE 18

PSEUDO-FIRST ORDER AND SECOND ORDER RATE CONSTANTS FOR THE DECOMPOSITION OF BENZYL ACETATE.[a]

pH±0.02	$k_{obs.}$ min.$^{-1}$	k_{OH^-} M.$^{-1}$ min.$^{-1}$	$[OH^-]^b$
12.0	$1.4 \pm 0.3 \times 10^{-2}$	2.6	5.37×10^{-3}
11.5	$5.5 \pm 0.2 \times 10^{-3}$	2.4	2.24×10^{-3}
11.0	$2.0 \pm 0.3 \times 10^{-3}$	2.5	7.94×10^{-4}
		Av. = 2.5 ± 0.1	

---

[a] Generally 10 mg of benzyl acetate were dissolved in 1 ml of ethanol and then added to a cell thermostatted at 25 ± 0.1°C along with 3.0 ml of 0.5 N KCl. An additional 1 ml of ethanol was added so that experimental conditions approximated those used for the spectrophotometric measurements as closely as possible.

[b] $k_{OH^-} = k_{obs.}/[OH^-]$.

spectrophotometrically at 250 nm and at 273 nm respectively in the high pH range. Data were analyzed as described for (70). To check that the results we were obtaining spectrophotometrically were agreeing with those obtained by "pH stat" measurements, we also followed the decomposition of (65) by titrating the liberated acid at pH's 11.5, 11.0 and 10.4. The value obtained at pH 10.4 by both methods was identical within the experimental error and a plot of k_{obs} vs pH with values obtained from both methods gave a straight line which showed a first order dependence on $[OH^-]$ (Table 19, Figure 17). The results for (27) are shown in Table 20. Again for both compounds the total difference in the UV-VIS spectra of the thioacetate and the resulting thiols decreased with descending pH. Therefore, in an attempt to obtain rate constants in the pH 7-8 region large amounts of these compounds were titrated with NaOH as the acid produced from hydrolysis was released. It was hoped that if the reaction could be followed even to 15-20% completion the rate constants could be obtained from plots of $\ln(C_\infty - C_t)$ vs time where C_t is the $[OH^-]$ added at time t and C_∞ is the calculated amount of OH^- needed to completely hydrolyze the thioacetate plus the amount needed to appropriately ionize the resulting thiol. The extent of the latter's ionization was calculated from its known pKa. However, the reaction at these pH's (at 25°C) was so slow that accurate results for the rate constants could not be obtained and therefore the numbers were rejected.

An exactly analogous situation existed for 4(7')-acetoxymethylbenzimidazole (69a) and 1-methyl-4-acetoxymethylbenzimidazole (69b). Both of these compounds showed no change in their UV-VIS spectrum

TABLE 19

PSEUDO-FIRST ORDER AND SECOND ORDER RATE CONSTANTS FOR THE DECOMPOSITION OF 4(7')-THIOACETOXYMETHYLBENZIMIDAZOLE.

pH±0.02	$k_{obs.}$ min.$^{-1}$	k_{OH^-} M.$^{-1}$ min.$^{-1}$[c]	[OH$^-$]
11.5[a]	$1.1 \pm 0.1 \times 10^{-1}$	49	2.24×10^{-3}
11.0[a]	$3.5 \pm 0.2 \times 10^{-2}$	45	7.94×10^{-4}
10.0[b]	$4.6 \pm 0.3 \times 10^{-3}$	46	1×10^{-4}
		$\bar{Av}$. = 46.7 ± 2.3	

[a] Generally 15 mg of 4(7')-thioacetoxymethylbenzimidazole were dissolved in 1 ml of ethanol and then added to a cell thermostatted at 25 ± 0.1°C along with 3.0 ml of 0.5 N KCl. An additional 1 ml of ethanol was added so that experimental conditions approximated those used for the spectrophotometric measurements as closely as possible.

[b] Determined in 31.6% EtOH/H_2O (v/v). [Buffer] = 0.21, 0.16, 0.13 and 0.02 M.

[c] $k_{OH^-} = k_{obs.}/[OH^-]$.

TABLE 20

PSEUDO-FIRST ORDER AND SECOND ORDER RATE CONSTANTS FOR THE DECOMPOSITION OF 1-METHYL-4-THIOACETOXYMETHYLBENZIMIDAZOLE.[a]

pH±0.02	$k_{obs.}$ min.$^{-1}$	k_{OH^-} M.$^{-1}$ min.$^{-1}$ [b]	$[OH^-]$
10.8	$2.7 \pm 0.1 \times 10^{-2}$	48	5.62×10^{-4}
10.4	$1.1 \pm 0.2 \times 10^{-2}$	49	2.23×10^{-4}
10.0	$5.2 \pm 0.2 \times 10^{-3}$	52	1×10^{-4}
		A$\bar{\text{v}}$. = 49.7 ± 2.3	

[a] Determined in 31.6% EtOH/H_2O (v/v). [Buffer] = 0.21, 0.16, 0.13 and 0.02 M.

[b] $k_{OH^-} = k_{obs.}/[OH^-]$.

when hydrolyzed but rate constants could be obtained at high pH's by titrating the liberated acid as described earlier and the data were analyzed as described for (71) (Tables 21, 22, Figure 17). A plot of $k_{obs}/[OH^-]$ vs pH gives a straight line of zero slope indicating that it is OH^- which is the active species. Again, when attempts were made to obtain rate constants in the pH 7-8 region, the rates were found to be so slow that accurate rate constants could not be obtained.

Hydrolysis rates for 4(7)'-acetoxymethyltetrahydrobenzimidazole (75) have also been measured[47] and found to be 3×10^{-3} min^{-1} (50°C) at pH 10. Therefore, increasing the basicity of the imidazole by formally saturating the benzene ring system does not appear to have significantly increased the hydrolysis rate.

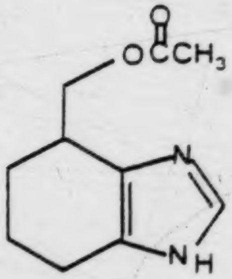

(75)

In summary for the compounds we have studied (27, 65, 69, 70 and 71), there does not appear to be any significant difference in the hydrolysis rates between compounds with adjacent imidazoles and those without. This means that either there is no significant rate enhancement due to the proximally positioned imidazole at the pH's studied or that the acetyl group has indeed transferred to the nitrogen and the decomposition of the resulting N-acetyl compound is very slow and is fortuitously comparable to the hydrolysis rates of

TABLE 21

PSEUDO-FIRST ORDER AND SECOND ORDER RATE CONSTANTS FOR THE DECOMPOSITION OF 4(7')-ACETOXYMETHYLBENZIMIDAZOLE.[a]

pH±0.02	$k_{obs.}$ min.$^{-1}$	k_{OH^-} M.$^{-1}$ min.$^{-1}$[b]	[OH$^-$]
11.5	$2.5 \pm 0.1 \times 10^{-2}$	11	2.24×10^{-3}
11.0	$9.4 \pm 0.2 \times 10^{-3}$	11.8	7.94×10^{-4}
10.0	$9.0 \pm 0.3 \times 10^{-4}$	9	1×10^{-4}

[a] Generally 15 mg of 4(7')-acetoxymethylbenzimidazole were dissolved in 1 ml of ethanol and then added to a cell thermostatted at 25 ± 0.1°C along with 3.0 ml of 0.5 N KCl. An additional 1 ml of ethanol was added so that experimental conditions approximated those used for the spectrophotometric measurements as closely as possible.

[b] $k_{OH^-} = k_{obs.}/H_2O$.

TABLE 22

PSEUDO-FIRST ORDER AND SECOND ORDER RATE CONSTANTS FOR THE DECOMPOSITION OF 1-METHYL-4-ACETOXYMETHYLBENZIMIDAZOLE.[a]

pH±0.02	$k_{obs.}$ min.$^{-1}$	k_{OH^-} M.$^{-1}$ min.$^{-1}$[b]	[OH$^-$]
11.0	$1.2 \pm 0.1 \times 10^{-2}$	15	7.94×10^{-4}
10.5	$4.3 \pm 0.2 \times 10^{-3}$	15	2.81×10^{-4}
10.0	$1.2 \pm 0.2 \times 10^{-3}$	12	1×10^{-4}

[a] Generally 15 mg of 1-methyl-acetoxymethylbenzimidazole were dissolved in 1 ml ethanol and then added to a cell thermostatted at 25 ± 0.1°C along with 3.0 ml of 0.5 N KCl. An additional 1 ml of ethanol was added so that experimental conditions approximated those used for the spectrophotometric measurements as closely as possible.

[b] $k_{OH^-} = k_{obs.}/[OH^-]$.

ordinary sulphur and oxygen acetates. In the studies of Jencks et al.[38a,b,c] on the decomposition of N-acetylimidazole (66) and N-acetyl-N'-methylimidazolium chloride (67) the released imidazoles have a pKa of approximately 7.5. In our systems the pKa of the imidazole ring after hydrolysis are at least two units smaller. Therefore, if the rates of hydrolysis are related to the inherent basicity of the imidazole rings our systems could be hydrolyzing at substantially different rates than those systems studied by Jencks et al.[38a,b,c] In fact Staab reported in 1957[75] that N-acetylbenzimidazole (74) had a half life of 21 hours in water at room temperature. In order to investigate the effect of basicity on the hydrolysis of N-acetylimidazole compounds, N-acetylbenzimidazole (74), 1-acetyl-3-methylbenzimidazolium acetate (76) and 1-acetyl-3-methyltetrahydrobenzimidazolium acetate (77) were synthesized. Compound (74) was synthesized from the reaction of acetyl chloride with benzimidazole (10a) while both (76) and (77) were made by reacting the corresponding N-methyl compounds with acetic anhydride (Scheme 26).

The hydrolysis of (74) and (76) was followed spectrophotometrically at 290 nm while the decomposition of (77) was monitored at 265 nm. The measurements were done at 0.2 M, 0.13 M and 0.02 M [buffer] and the final rate constants obtained by extrapolation to [buffer] = 0. Data were analyzed as described for the acylation studies. Product analysis for the decomposition of these N-acetyl compounds was followed spectrophotometrically by continuous scans in the UV-VIS and the product identified by comparison of the final spectrum to that of the corresponding authentically made non-acylated compound in the same medium. In all three cases, as

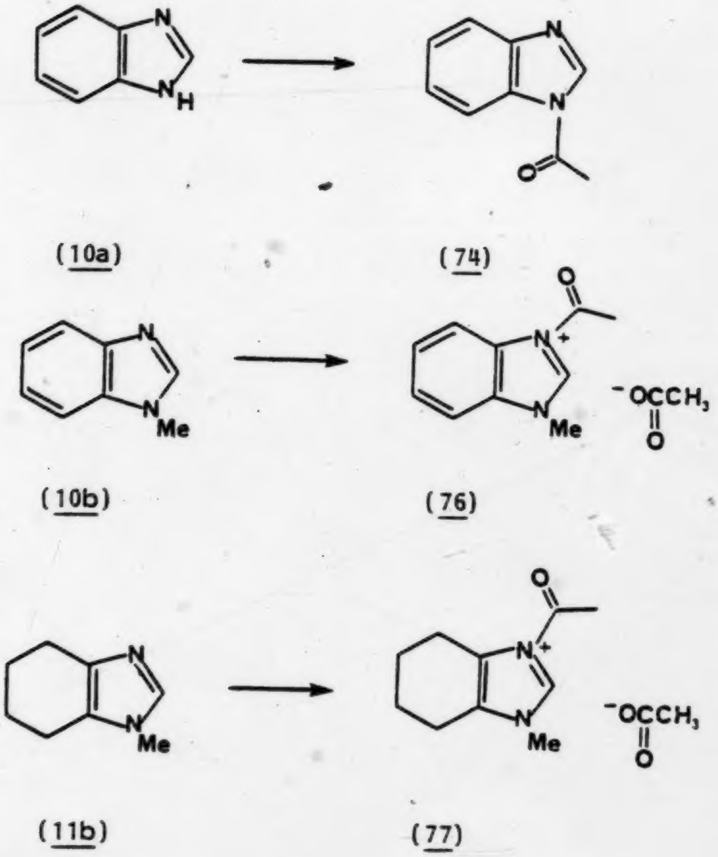
N
N
H
N
N
N
N
Me
N
N
Me
$^{-}$OCCH$_3$
O
N
N
Me
N
N
Me
$^{-}$OCCH$_3$
O
O
O
O

(10a) (74)

(10b) (76)

(11b) (77)

Scheme 26

depicted for the decomposition of (74) in Figure 18, the final spectra were identical to those of the corresponding non-acylated compounds. Also by adding D_2O to an NMR tube containing the N-acetyl compound in DMSO-d_6 the NMR spectrum of the N-acetyl compound

Figure 18: A plot of the continuous scans of the UV-VIS spectrum of N-acetylbenzimidazole (74) as it is hydrolyzed to benzimidazole (10a) in formic acid/sodium formate buffer at 25°C.

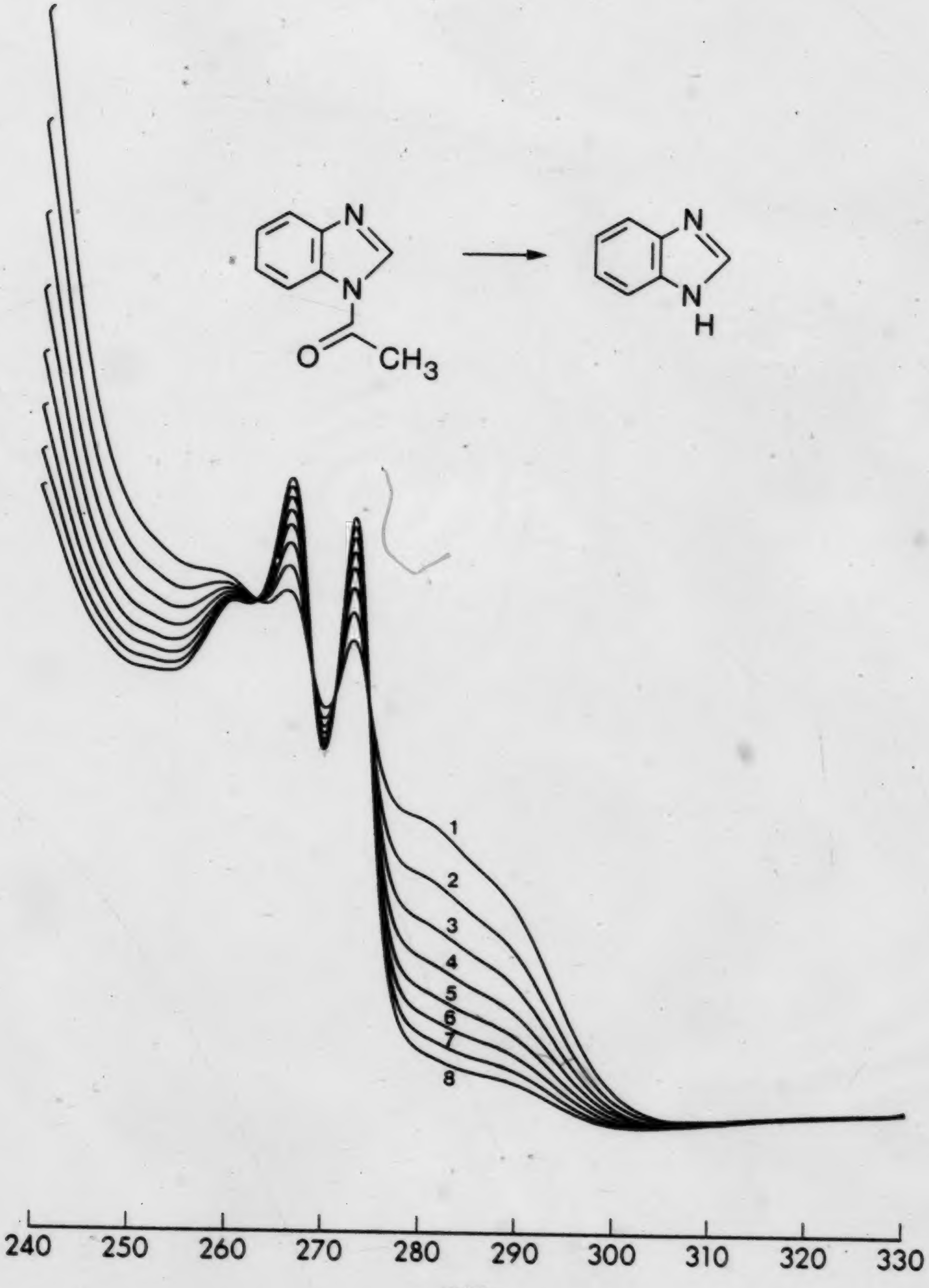
N
N
O
CH3
N
N
H
1
2
3
4
5
6
7
8
240
250
260
270
280
290
300
310
320
330
nm

collapsed to that of the corresponding "NH" or "NMe" compound. The results of the hydrolysis studies carried out on N-acetylbenzimidazole (74) are shown in Table 23 (Figure 19). As Jencks'[38a] found for N-acetylimidazole (66) (Figure 19), the rate of hydrolysis of (74) increases sharply above and below neutrality. The only difference between acetylimidazole (66) and (74) lies in the fact that for the former, below pH 4, the rate approaches a plateau and remains constant up to a hydrochloric acid concentration of 1 M. In this pH range compound (66) becomes completely converted to its conjugate acid so that a further increase in acid concentration does not increase the concentration of the reactive acetyl imidazolium cation. From these data the pKa of acetyl imidazole was estimated by Jencks to be 3.6 and the rate law for acetyl imidazole hydrolysis formulated as:

43. $v = 2.8[\mathrm{AcIm}^+] + 0.005\ [\mathrm{AcIm}] + 19000[\mathrm{AcIm}][\mathrm{OH}^-]$

For (74) this plateau region has not been reached at pH 2.8 indicating a lower pKa for this compound. The rate law for this compound can be formulated as:

44. $v = 53[\mathrm{H}^+][\mathrm{AcIm}] + 0.00037[\mathrm{AcIm}] + 28000[\mathrm{AcIm}][\mathrm{OH}^-]$

The rates of hydrolysis of 1-acetyl-3-methylimidazolium chloride (67), 1-acetyl-3-methylbenzimidazolium acetate (76) and 1-acetyl-3-methyltetrahydrobenzimidazolium acetate (77) all remain constant from pH 1 to pH 6 and increase as neutrality is approached (Tables 24 and 25). In Figure 19 the observed pH-rate profiles for these compounds are plotted. The increase in the rates near neutrality is proportional to [OH⁻]. The rate laws for compounds (67), (76) and (77) respectively are:

TABLE 23

PSEUDO-FIRST ORDER AND SECOND ORDER RATE CONSTANTS FOR THE DECOMPOSITION OF 1-ACETYLBENZIMIDAZOLE[a].

pH±0.02	$k_{obs.}$ min.$^{-1}$	k_{OH^-}[b] M^{-1} min.$^{-1}$	k_{H^+}[c] M^{-1} min.$^{-1}$	k_{H_2O}[d] min.$^{-1}$
8.8	$2.0 \pm 0.3 \times 10^{-1}$	3.2×10^{4}		
8.4	$5.5 \pm 0.2 \times 10^{-2}$	2.2×10^{4}		
8.0	$2.5 \pm 0.3 \times 10^{-2}$	2.5×10^{4}		
7.6	$1.1 \pm 0.2 \times 10^{-2}$	2.8×10^{4}		
6.8	$2.0 \pm 0.3 \times 10^{-3}$	3.2×10^{4}		
		$\bar{Av}. = 2.8 \times 10^{4}$		
6.4	$6.6 \pm 0.3 \times 10^{-4}$			3.2×10^{-4}
5.6	$5.9 \pm 0.2 \times 10^{-4}$			5.1×10^{-4}
4.8	$1.1 \pm 0.2 \times 10^{-3}$			2.9×10^{-4}
				$\bar{Av}. = 3.7 \times 10^{-4}$
4.0	$5.0 \pm 0.1 \times 10^{-2}$		5.0×10^{1}	
3.6	$1.5 \pm 0.2 \times 10^{-2}$		6.0×10^{1}	
2.8	$7.5 \pm 0.3 \times 10^{-2}$		4.8×10^{1}	
			$\bar{Av}. = 5.3 \times 10^{1}$	

Table 23 (continued)

a. Determined in 31.6% $EtOH/H_2O$ (v/v). [Buffer] = 0.21, 0.13 and 0.02 M.

b. $k_{OH^-} = k_{obs.}/[OH^-]$

c. $k_{H^+} = k_{obs.}/[H^+]$.

d. $k_{H_2O} = k_{obs.} - k_{OH^-}[OH^-] - k_{H^+}[H^+]$

Figure 19: A plot of k_{obs} vs pH for N-acetylimidazole (66), 1-acetyl-3-methylimidazolium chloride (67), N-acetylbenzimidazole (74), 1-acetyl-3-methylbenzimidazolium acetate (76) and 1-acetyl-3-methyltetrahydrobenzimidazolium acetate (77). The plots for (66) and (74) are reproduced from reference 38.

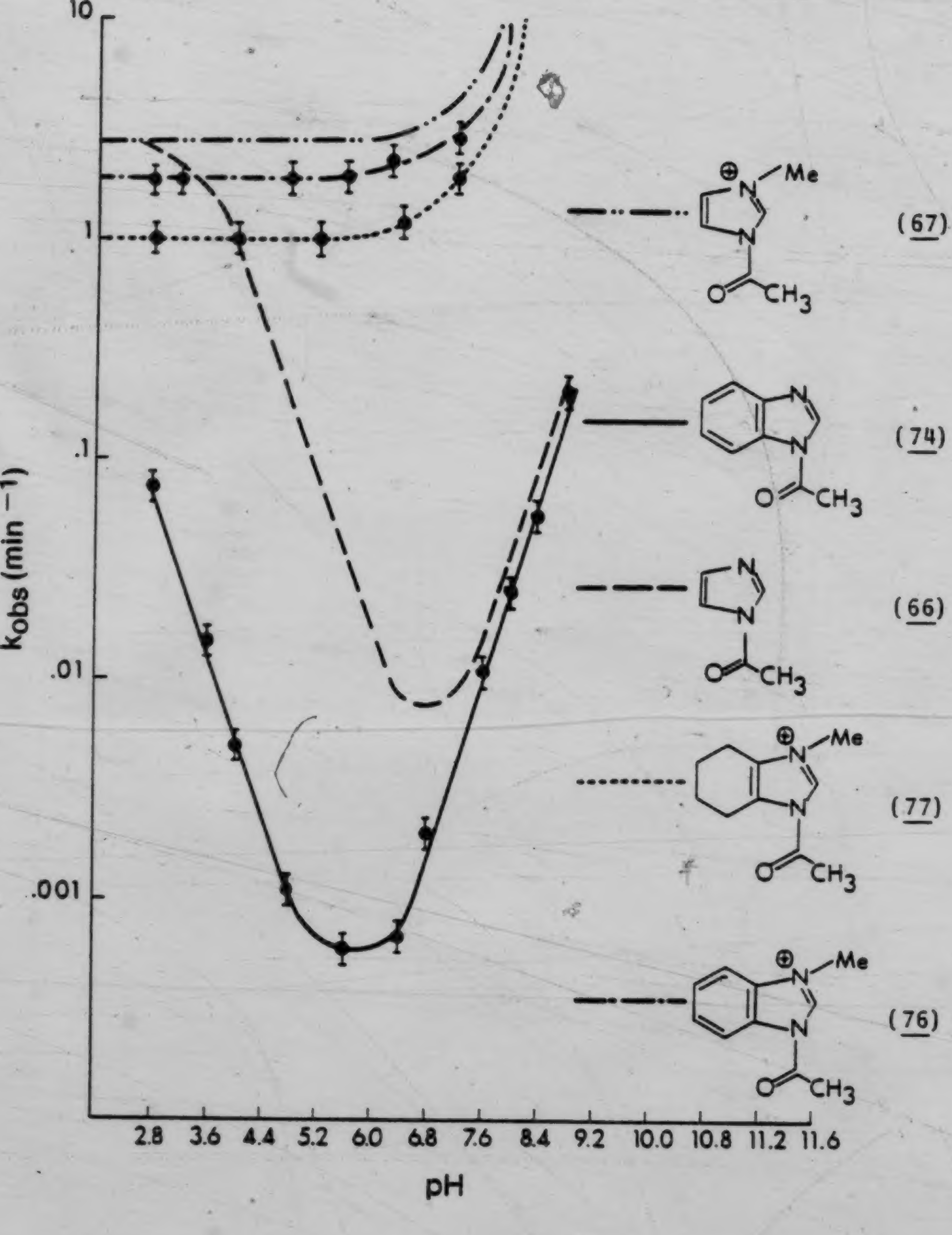
10
1
.1
.01
.001
kobs (min −1)
2.8
3.6
4.4
5.2
6.0
6.8
7.6
8.4
9.2
10.0
10.8
11.2
11.6
pH
Me
N
O
CH3
(67)
(74)
(66)
(77)
(76)

Table 24

PSEUDO-FIRST ORDER AND SECOND ORDER RATE CONSTANTS FOR THE DECOMPOSITION OF 1-ACETYL-3-METHYLBENZIMIDAZOLIUM ACETATE.[a]

pH±0.02	$k_{obs.}$ min.$^{-1}$	k_{OH^-} M.$^{-1}$ min.$^{-1}$[b]
2.8	1.8 ± 0.1	
3.2	1.9 ± 0.1	
4.8	1.9 ± 0.1	
5.6	1.9 ± 0.1	
6.4	2.2 ± 0.1	1.2×10^7

[a] Determined in 31.6% EtOH/H_2O (v/v). [Buffer] = 0.21, 0.13, and 0.02 M.

[b] $k_{OH^-} = (k_{obs} - k_{H_2O})/[OH^-]$

TABLE 25

PSEUDO-FIRST ORDER AND SECOND ORDER RATE CONSTANTS FOR THE HYDROLYSIS OF 1-ACETYL-3-METHYLTETRAHYDROBENZIMIDAZOLIUM ACETATE.[a]

pH±0.02	$k_{obs.}$ min.$^{-1}$	k_{OH^-} M.$^{-1}$ min.$^{-1}$[b]
2.8	1.0 ± 0.1	
4.0	1.0 ± 0.1	
5.2	1.0 ± 0.1	
6.4	1.15 ± 0.2	6×10^6
7.2	1.9 ± 0.2	6×10^6
8.0	6.6 ± 0.2	6×10^6

[a] Determined in 31.6% EtOH/H_2O (v/v). [Buffer] = 0.21, 0.31 and 0.02 M.

[b] $k_{OH^-} = (k_{obs} - k_{H_2O})/[OH^-]$

45. $v = 2.8[\text{AcMeIm}^+] + 9.0 \times 10^6[\text{AcMeIm}^+][\text{OH}^-]$

46. $v = 1.9[\text{AcMeIm}^+] + 1.2 \times 10^7[\text{AcMeIm}^+][\text{OH}^-]$

47. $v = 1.0[\text{AcMeIm}^+] + 6 \times 10^6\,[\text{AcMeIm}^+][\text{OH}^-]$

In summary it appears that changing the pKa of the imidazole changes the position of the bottom of the well for the N-acetyl compounds and has little effect on the N-acetyl-N'-methyl compounds. In any case if the corresponding N-acetyl compounds were being formed from our O or S-acetylimidazoles (ie (27), (65) and (69)) we would expect their decomposition to be extremely fast at the pH's studied.

NMR studies confirmed that there was indeed no build up of N-acetyl compounds. Product analysis for 4(7')-thioacetoxymethylbenzimidazole (65) showed the diminuation of singlets at δ4.48 (CH_2) and δ2.36 (S-Ac) and the growth of singlets at δ3.96 (CH_2SH) and δ1.88 (OAc^-), the latter being identical to those obtained for 4(7')-thiomethylbenzimidazole (8a) and the acetate anion. Similarly, singlets at δ4.00 (CH_2SH), δ3.80 (N-Me) and δ1.88 (OAc^-) due to 1-methyl-4-thiomethylbenzimidazole (8b) and the acetate anion appeared at the expense of the peaks due to compound (27) at δ4.46 (CH_2), δ3.96 (N-Me) and δ2.32 (SAc). For the oxygen compounds the spectra for the hydrolysis of 4(7')-acetoxymethylbenzimidazole (69a) showed the disappearance of the singlets due to the methylene hydrogens (δ5.51) and the O-acetyl methyl group (δ2.12) of compound (69a) and the appearance of singlets at δ4.02, δ2.02 and δ1.88 due to the methylene group of (12a), ethyl acetate and the acetate anion, respectively. Similarly for (69b) peaks at δ5.48 (CH_2), δ3.88 (N-Me) and δ2.08 (OAc) diminished and peaks at δ5.04

(CH_2OH), δ3.86 (N-Me), δ2.02 (EtOAc) and δ1.88 (OAc^-) due to the the formation of the corresponding alcohol appear.

We know that if the corresponding N-acetyl compounds were being formed from compounds (27), (65) and (69) that their hydrolysis would be fast at the pH's studied (as described on p 142) but the observed hydrolysis rates are slow. This permits certain possibilities. The acetyl group may not be transferring and hydrolysis may be taking place strictly by attack of hydroxide ion. Our observed rates are in fact comparable to those observed for esters lacking an imidazole unit. However, we know nitrogen to be a powerful nucleophile and molecular models show it to be suitably oriented to attack the carbonyl in compounds (27), (65) and (69). It may actually be attacking the carbonyl but in a manner which is nonproductive: (a) the tetrahedral intermediate (78) could be formed, and if so, it would have to exist in equilibrium with S-acyl starting material rather than collapse to the N-acetyl compound (Scheme 27).

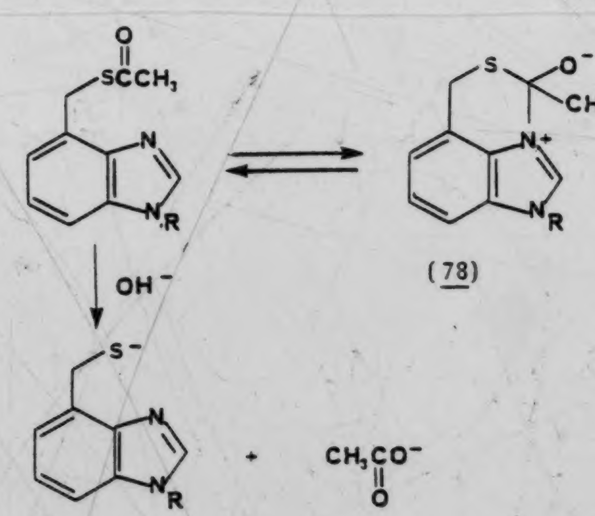

Scheme 27

(b) the acetyl could be transferring to the nitrogen but the adjacent oxygen or sulphur competes favourably with external nucleophile so that the equilibrium lies largely on the side of the S-acyl starting material (Scheme 28).

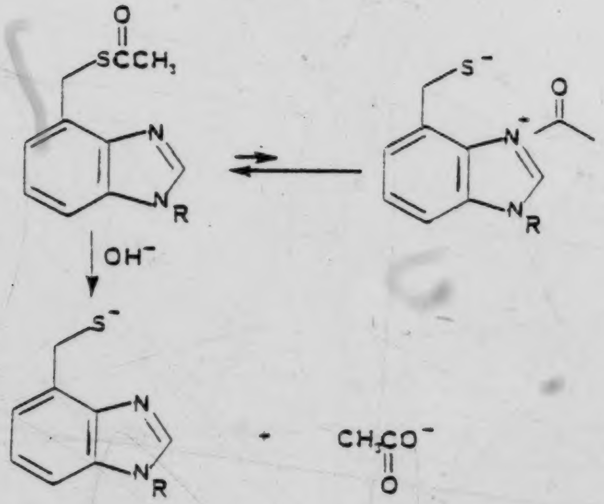

Scheme 28

Intramolecular attack by a nucleophile can be much faster (up to 10^7 - 10^8 times[1]) than intermolecular nucleophilic attack by the same nucleophile.

A fast reverse reaction would also explain the difference between our models and those studied by Bruice[15] and Fife[70] in which the thiol portion was expelled into solution after hydrolysis effectively cutting off the reverse reaction.

Although our system appears to have failed to transfer the acyl group from sulphur to nitrogen we know that Bruice[15] and Fife[70] were able to do this (Schemes 21 and 22). They, however, did not investigate whether this transfer would occur if the imidazole was methylated to give the corresponding charged imidazolium intermediate whose decomposition, according to our studies on compounds (67), (76) and (77), should occur rapidly. Future studies could be directed to the study of the hydrolysis of compound (79)

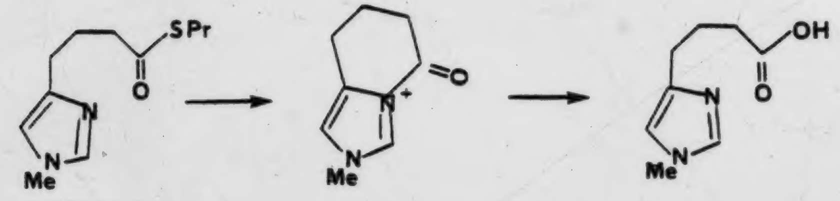

(79)

or (80). If the intermediate N-acetylimidazolium compound was formed

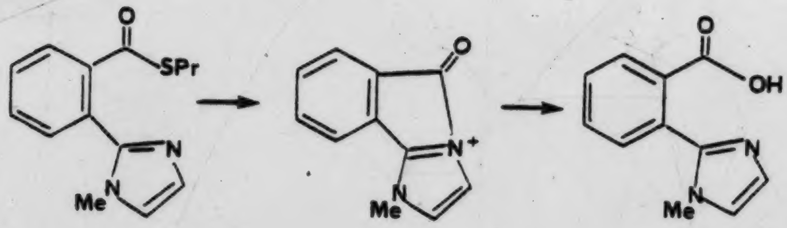

(80)

and found to decompose rapidly, this route would be a viable alternative to the well-accepted but unproven proposal of a general-base assisted hydrolysis of the S-acyl intermediate in the enzyme.

Experimental

All infrared spectra were run on a 7199 Nicolet FT IR interferometer. Mass spectra were taken on a AEI MS-50 spectrometer (E.V. 70). All NMR spectra are designated as to whether they were run on 90, 100 200 or 400 MHz instruments which were: a Perkin Elmer R-32 spectrometer; a Varian HA-100-15 spectrometer with Fourier transform modifications provided by a Digilab FTS NMR-3 System; a Bruker WH 200 DS; and a Bruker WH 400, respectively. All Raman spectra were measured on a Beckman 700 spectrophotometer.

2-Acetamido-3-nitrotoluene (15).

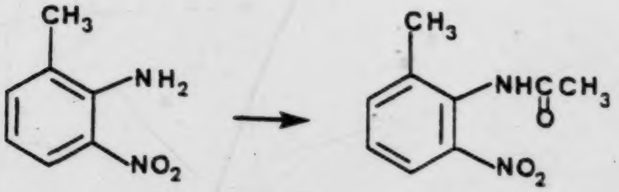

(14) (15)

2-Acetamido-3-nitrotoluene (15) was prepared according to the method of James et al.[40] 2-Methyl-6-nitroaniline (14) (50 g, 0.33 mol) was dissolved in acetic anhydride (65 g) and conc H_2SO_4 (5 g). The solution was stirred and the temperature increased rapidly to 70° C. Immediately afterwards crystals began to form. When crystallization was complete the mixture was diluted with H_2O and filtered. Recrystallization from 20% (v/v) aqueous acetic acid gave 49.3 g (0.25 mol, 76% yield) of 2-acetamido-3-nitrotoluene: mp 163-165°C (lit.[39] mp 160-161°C).

IR (KBr) 3310, 1666, 1534, 1360 cm^{-1}.

NMR (DMSO-d_6,100 MHz) δ 2.03(3H,s,CH_3), 2.16(3H,s,$CH_3C=O$), 7.5(3H, m,ArH) and 9.81(1H,br s,NH).

Mass spectrum m/e (rel intensity) 194(M^+,12.2), 152(100), 134(22.5).

Exact mass 194.0699 (calcd for $C_9H_{10}N_2O_3$, 194.0692).

2-Acetamido-3-nitrobenzoic acid (16).

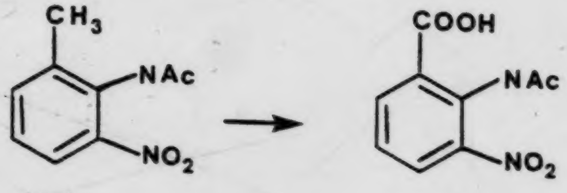

(15) (16)

2-Acetamido-3-nitrobenzoic acid (16) was prepared according to the method of James et al.[40] $KMnO_4$ (44 g), $MgSO_4$ (32 g) and 2-acetamido-3-nitrotoluene (15) (20 g, 0.10 mol) were dissolved in H_2O (1 L) and heated at 100°C until no purple colour remained. The hot solution was then filtered through a sintered glass funnel containing a layer of celite. The pKa of the solution was adjusted to 1 with conc HCl whereupon 21.9 g (0.098 mol, 98% yield) of 2-acetamido-3-nitrobenzoic acid precipitated. The crude product (5 g, 0.022 mol) was recrystallized from 95% ethanol to give 4.2 g (0.019 mol, 82% yield overall) of yellow crystals: mp 259-261°C (lit.[39] mp 254-255°C).

IR (KBr) 3440, 1695, 1533, 1355 cm^{-1}.

NMR (DMSO-d_6,100MHz) δ2.06(s,3H,CH_3), 4.10(br s,1H,NH), 7.32(t,1H, J=7Hz), 7.93(d of d,1H,J=7Hz,J=1Hz) and 8.19(d of d,1H,J=7Hz,J=1Hz).

Mass spectrum m/e (rel intensity) 206(8), 182(100), 164(69).

Exact Mass 206.03278 (calcd for $C_9H_8N_2O_5-H_2O$, 206.0332).

2-Amino-3-nitrobenzoic acid (17).

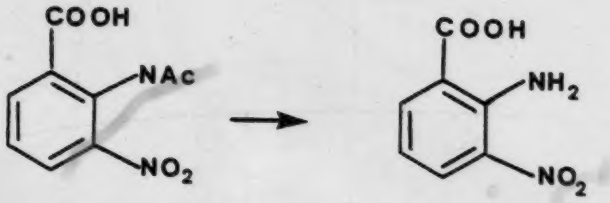

(16) (17)

2-Amino-3-nitrobenzoic acid (17) was prepared according to the procedure published by James et al.[40] 2-Acetamido-3-nitrobenzoic acid (16) (51.8 g, 0.23 mol) was added to 10% (v/v) aqueous HCl (400 mL) and refluxed for 3 h to give 38 g (0.21 mol, 91% crude yield) of 2-amino-3-nitrobenzoic acid. The crude product (5 g, 0.027 mol) was recrystallized from H_2O to give 4.7 g (0.026 mol, 85.5% yield) of orange needles: mp 212-215°C (lit.[40] mp 208.5-209°C).

IR (KBr) 3456, 3346, 1678, 1251 cm^{-1}.

NMR (DMSO-d_6,100 MHz) δ 6.72(t,1H), 8.29(m,2H), 8.52(br s,2H) and 11.26(br s,1H).

Mass spectrum m/e (rel intensity) 182(M^+,100), 164(73), 134(14).

Exact mass 182.0328 (calcd for $C_7H_6N_2O_4$, 182.03278).

2,3-Diaminobenzoic acid (18).

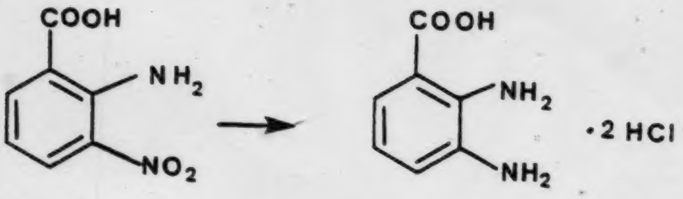

(17) (18)

2,3-Diaminobenzoic acid (18) was prepared according to the procedure published by Jones and Taylor.[39] 2-Amino-3-nitrobenzoic acid (17) (10 g, 0.055 mol), $SnCl_2.2H_2O$ (38 g) and conc HCl (62.5 mL) were mixed together in a 1 L Erlenmeyer flask and heated to 50°C on a steam bath to initiate the reaction. The flask was placed in an ice bath to maintain the exothermic reaction at 100°C. When the exothermic reaction was complete the mixture was heated on a steam bath for an additional 15 min, cooled, and poured into a solution of NaOH (46.25 g) in H_2O (150 mL). The mixture obtained (pH 7) was filtered and the pH of the filtrate adjusted to 1 with conc HCl. The 2,3-diaminobenzoic acid·2HCl was filtered and sublimed at 135° C/0.7 torr to give 11.1 g (0.049 mol, 90% yield) of purified acid: mp 196-197°C (lit.[39] mp 196-198°C).

IR (KBr) 3420, 2880, 2585, 1675, 1631, 1465, 1220 cm^{-1}.

NMR (DMSO-d_6,100MHz) δ 6.68(t,1H,J=3.5Hz), 7.67(d of ABq,2H, J=3.5Hz,1Hz) and 9.15(br s,NH,OH).

Mass spectrum m/e (rel intensity) 152(M^+,85), 135(25), 134(78), 106(100).

Exact Mass 152.05864 (calcd for $C_7H_8N_2O_2$, 152.05864).

Benzimidazole-4(7')-carboxylic acid . HCl (19).

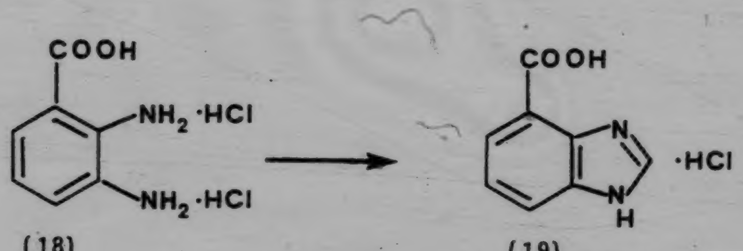

(18)   (19)

The hydrochloride salt of benzimidazole-4(7')-carboxylic acid (19) was prepared by the method of Jones and Taylor.[39] Freshly sublimed 2,3-diaminobenzoic acid (18) (7.8 g, 0.035 mol), formic acid (6.25 mL) and 4 N HCl (100 mL) were heated at reflux for 1 h under N_2. The mixture was cooled and the hydrochloride salt of benzimidazole-4(7')-carboxylic acid was filtered and recrystallized from 0.5 N aqueous HCl to give 5.4 g (0.027 mol, 78% yield) of white crystals: mp > 300°C (lit.[39] mp > 360°C).

IR (KBr) 3320, 3090, 1711, 1691, 1630, 1620, 1530, 1475, 1430, 1345, 1230, 1210, 1160, 1145, 1120, 760 cm^{-1}.

NMR (DMSO-d_6,100MHz) δ 7.71(t,1H,J=3.5Hz), 8.18(m,2H) and 9.68(s, 1H,N=C(H)-N).

Mass spectrum m/e (rel intensity) 162(M^+,99.5), 144(100), 116(86).

Exact mass 162.04298 (calcd for $C_8H_6N_2O_2$, 162.0425).

Benzimidazole-4(7')-carboxylic acid was obtained by adding enough saturated aqueous Na_2CO_3 to adjust the pH to 7-8 at which point 4.29 g (0.026 mol, 98% yield) of benzimidazole-4(7')-carboxylic acid precipitated: mp > 300°C.

IR (KBr) 3380, 3220, 3150, 1688, 1624, 1600, 1535, 1492, 1390, 1365, 1345, 1255, 1222, 1155, 1110, 772 cm^{-1}.

NMR ($DMSO-d_6$,100MHz) δ 7.30(t,1H,J=3.5Hz), 7.92(m,2H) and 8.30(s, 1H,N=C(H)-N).

Mass spectrum m/e (rel intensity) 162(M+,98.5), 144(100), 116(78).

Exact mass 162.04298 (calcd for $C_8H_6N_2O_2$, 162.046).

Methyl benzimidazole-4(7')-carboxylate (20).

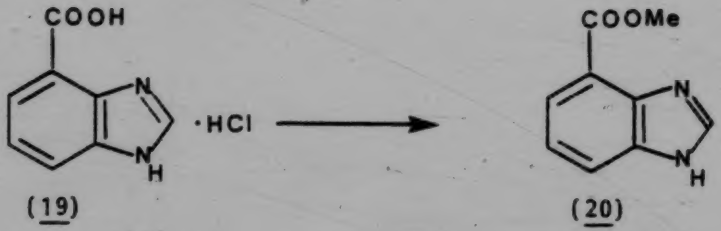

Methyl benzimidazole-4(7')-carboxylate (20) was prepared by Fischer esterification[41] of 4(7')-benzimidazole carboxylic acid (19). The hydrochloride salt of the acid (11.3 g, 0.057 mol) was dissolved in freshly distilled dry methanol (400 mL). Hydrogen chloride was bubbled through the solution for 2 h with vigorous stirring and at a rate which kept methanol below its boiling point. The solution was stirred at room temperature overnight. The methanol was removed under reduced pressure to yield the hydrochloride salt of methyl benzimidazole-4(7')-carboxylate. The hydrochloride salt was dissolved in H_2O (50 mL) and the pH was adjusted to 9-10 with saturated aqueous potassium carbonate at which point methyl benzimidazole-4(7')-carboxylate precipitated. The product was recrystallized from THF to give 9.5 g (0.054 mol, 94.5% yield) of white crystals: mp 219-220°C (lit.[39] 214-215°C).

IR (KBr) 3440, 1713, 1703, 1273, 735 cm^{-1}.

NMR (DMSO-d_6,100MHz) δ 3.94(s,3H,CH_3), 7.30(t,1H,J=3.5Hz), 7.86(d of d,1H,J=3.5Hz,J=1Hz), 7.97(d of d,1H,J=3.5Hz,J=1Hz) and 8.34(s,1H, N=C(H)-N).

Mass spectrum m/e (rel intensity) 176(M^+,100), 145(57.5), 144(70), 117(47).

Exact mass 176.0583 (calcd for $C_9H_8N_2O_2$, 176.05864).

Anal. Calcd for $C_9H_8N_2O_2$: C,61.36; H,4.58; N,15.90. Found: C,61.06; H,4.66; N,15.72.

4(7')-Hydroxymethylbenzimidazole (12a).

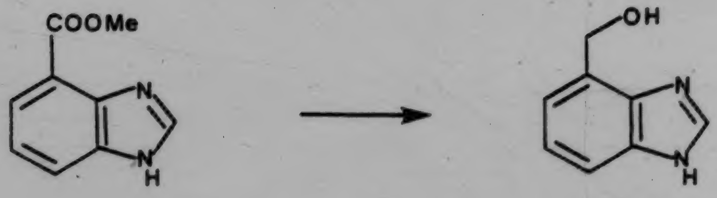

(20) (12a)

4(7')-Hydroxymethylbenzimidazole (12a) was prepared by the reduction of methyl benzimidazole-4(7')-carboxylate (20). Methyl benzimidazole-4(7')-carboxylate (20) (2 g, 0.011 mol) was dissolved in refluxing THF (150-200 mL) and added dropwise to a stirred suspension of $LiAlH_4$ (0.44 g) in THF (20 mL) under N_2. Once the addition had been completed the reaction mixture was heated at reflux for 30 min. After cooling the excess $LiAlH_4$ was decomposed with a minimum amount of H_2O (~0.5 mL). The solution was filtered, dried with $MgSO_4$ and the THF removed under reduced pressure to give (12a). The product was recrystallized by dissolving it in THF (5 mL) at room temperature and adding pentane until the first signs of cloudiness appeared. This afforded 1.27 g (0.0086 mol, 78% yield) of the final product: mp 166-167°C.

IR (nujol) 3100, 1010, 743 cm^{-1}.

NMR ($DMSO-d_6$,100MHz) δ 3.88(br s,1H,OH), 4.88(s,2H,CH_2), 7.1-7.6 (m,3H) and 8.20(s,1H,N=C(H)-N).

Mass spectrum m/e (rel intensity) 148(M^+,80), 147(54), 131(25), 119(100).

Exact mass 148.0635 (calcd for $C_8H_8N_2O$, 148.06374).

Anal. Calcd for $C_8H_8N_2O$: C,64.85; H,5.44; N,18.91. Found: C,64.49; H,5.37; N,18.99.

4(7')-Chloromethylbenzimidazole•HCl (21).

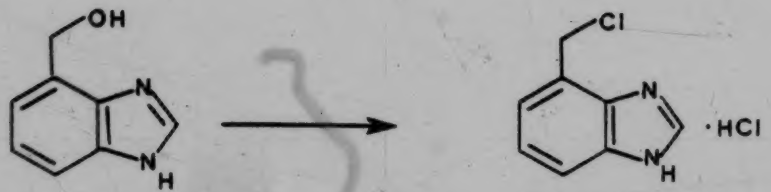

(12a) (21)

4(7')-Hydroxymethylbenzimidazole (12a) (2 g, 0.0135 mol) was dissolved in dry THF (100 mL) and added very slowly (over ~3 h) to thionyl chloride (10 equiv.) in THF (50 mL) with stirring. Once addition was complete the reaction mixture was stirred overnight. The hydrochloride salt of 4(7')-chloromethylbenzimidazole, which precipitated out of solution, was filtered and washed with THF to give 1.73 g (0.0085 mol, 63% yield) of microanalytically pure product: mp 247-249°C. When the addition was not done slowly, a mixture of the hydrochloride salts of 4(7')-hydroxymethylbenzimidazole and 4(7')-chloromethylbenzimidazole was obtained.

IR (nujol): 2800, 1450, 1430, 1235, 1180, 1030 cm^{-1}.

NMR (DMSO-d_6,100MHz) δ 5.22(s,2H,CH_2), 7.46-7.90(m,3H) and 9.06(s, 1H,N=C(H)-N).

Mass spectrum m/e (rel intensity) 166(M^+,40), 131(100), 77(14).

Exact mass 166.0297 (calcd for $C_8H_7ClN_2$, 166.02991).

Anal. Calcd for $C_8H_7ClN_2$.HCl: C,47.32; H,3.97; N,13.79; Cl,34.92.

Found: C,47.29; H,4.09; N,13.76; Cl,35.09.

Ethyl-S-4(7')-benzimidazolmethyl xanthate (22).

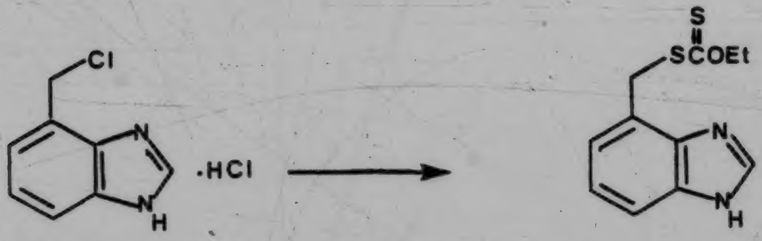

(21) .(22)

The hydrochloride salt of 4(7')-chloromethylbenzimidazole (0.8

g, 0.004 mol) and potassium ethyl xanthate (4 equiv.) were placed in a round-bottomed flask (500 mL) containing 300 mL of dried, freshly distilled THF and stirred overnight at room temperature. The THF was removed under reduced pressure and the solid residue was washed several times with ether. The ether was removed under reduced pressure leaving 0.8 g (0.0032 mol, 79.4% crude yield) of ethyl-S-4(7')-benzimidazolmethyl xanthate. The crude product, a greenish oil, was crystallized from ether by adding an excess (20 mL) and allowing the resultant solution to stand in the atmosphere for 6-7 h. This afforded 0.66 g (0.026 mol, 66% yield) of white crystals: mp 132-133°C.

IR ($CHCl_3$ cast) 1230, 1020, 775 cm^{-1}.

NMR (DMSO-d_6,100 MHz) δ 1.33(t,3H,CH_3,J=4Hz), 4.42(q,2H,CH_2,J=4Hz), 4.5(s,2H,CH_2), 7.04-7.6(m,3H), 8.22(s,1H,N=C(H)-N) and 12.55(brs,1H, NH).

Mass spectrum m/e (rel intensity) 252(M$^+$,12), 163(17), 131(100).

Exact mass 252.0397 (calcd for $C_{11}H_{12}N_2OS_2$, 252.03926).

Anal. Calcd for $C_{11}H_{12}N_2OS$: C,52.36; H,4.79; S,25.41; O,6.34; N,11.10. Found: C,52.17; H,4.93; S,25.61; O,6.22; N,11.18.

4(7')-Thiomethylbenzimidazole•HCl (8a).

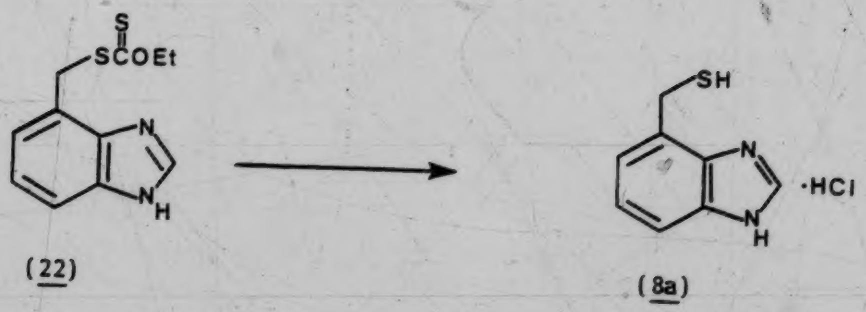

Ethyl-S-4(7')-benzimidazolmethyl xanthate (0.8 g, 0.0032 mol) was dissolved in dry THF (10 mL) and added dropwise to a stirred suspension of $LiAlH_4$ (0.15 g) in THF (30 mL) under a nitrogen atmosphere. Once the addition had been completed the reaction mixture was heated at reflux for 15-20 min. After cooling, the excess $LiAlH_4$ was decomposed with a minimum amount of H_2O (~0.5 mL) and the solution filtered. The residue was washed several times with THF and the combined filtrates dried with $MgSO_4$. The THF was removed under reduced pressure and the solid residue was dissolved immediately in H_2O (5 mL) containing HCl (1 equiv. based on the number of moles of xanthate used). This solution was evaporated to dryness under high vacuum to give 0.50 g (0.0025 mol, 78% yield) of microanalytically pure product: mp 216-218°C. The free thiol was found to be oxidized rapidly in solutions above pH 7 or in organic solvents which had not been degassed. The percentage of free thiol was determined by titration with iodine in ethanolic solution as described by Harnish and Tarbell.[44] Freshly made solutions were found to have 100% free thiol which would oxidize completely to the disulfide in a day.

IR $C_8H_8N_2$.HCl (MeOH cast) 1495, 1435, 794, 740 cm^{-1}.

NMR $C_8H_8N_2S$•HCl (DMSO-d_6, 100 MHz) δ 3.39(t,5H,J=8Hz), 4.15(d,CH_2, J=8Hz), 7.48-7.78(m,ArH) and 9.64(s,1H,N=C(H)-N).

NMR $C_8H_8N_2S$ (DMSO-d_6,100MHz) δ 2.84(t,5H,J=8Hz), 4.05(d,CH_2,J=8Hz), 7.0-7.3(m,ArH) and 8.20(s,1H,N=C(H)-N).

Mass spectrum m/e (rel intensity) 164(M^+,57), 131(100), 119(27).

Anal. Calcd for $C_8H_8N_2$.HCl: C,47.88; H,4.49; N,13.96: Cl,17.67; S,15.98. Found:C,47.83; H,4.42; H,13.94; Cl,17.79; S,15.81.

Raman (solid): 2600, 2580 (SH) cm^{-1}.

NMR ($C_8H_7N_2S_2$ (DMSO-d_6,100MHz) δ 4.12(s,CH_2), 6.9-7.2, 7.4-7.5(m ArH) and 8.24(s,1H,N=C(H)-N).

1-Methyl-4-carboxymethylbenzimidazole (23).

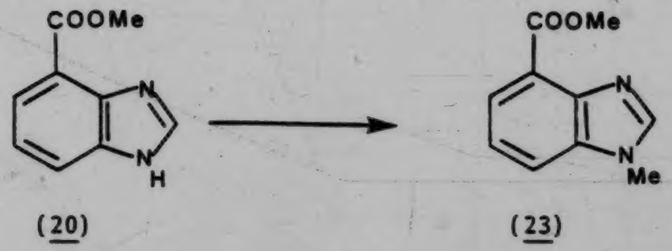

4(7')-Carboxymethylbenzimidazole (20) (2 g, 0.011 mol), dry THF (300 mL), NaH (1.1 equiv.) and MeI (1.1 equiv.) were placed in a round-bottomed flask (500 mL) and stirred for 6-7 h at room temperature. After filtration, the THF was removed under reduced pressure and the residue dissolved in 5% aqueous sodium thiosulfate (40 mL) and extracted three times with $CHCl_3$. The combined $CHCl_3$ extracts were dried with $MgSO_4$ and the solvent was removed under reduced pressure. The residue was recrystallized from $CHCl_3$/ hexane to give 1.57 g (0.008 mol, 75.2% yield) of product: mp 118-120°C.

IR ($CHCl_3$ cast) 1720, 1700, 1265, 1120, 770 cm^{-1}.

NMR (Acetone-d_6, 100MHz) δ 3.92(s,3H,NCH_3), 3.94(s,3H,OCH_3), 7.33 (t,1H,J=8Hz), 7.74(d of d,J=8Hz,J=1Hz), 7.84(d of d, J=8Hz,J=1Hz) and 8.14(s,1H,N=C(H)-N).

Mass spectrum m/e (rel intensity) 190(M^+,81.5), 176(27), 159(94), 132(100).

Exact mass 190.0744 (calcd for $C_{10}H_{10}H_2O_2$, 190.0743).

NMR ($CDCl_3$,400MHz) δ 3.90(s,3H,NCH_3), 4.08(s,3H,OCH_3), 7.36(t,1H, J=8Hz), 7.57(d of d,J=8Hz,J=1Hz), 8.0(d of d,1H,j=8Hz,J=1Hz) and 8.0(s,1H,N=C(H)-N).

NOE of NMe led to enhancement of d of d centered at 7.57 δ (6%) and the singlet at 8.0 δ (5%).

NOE of OMe led to no enhancement of any of the signals.

4-Hydroxymethyl-1-methylbenzimidazole (12b).

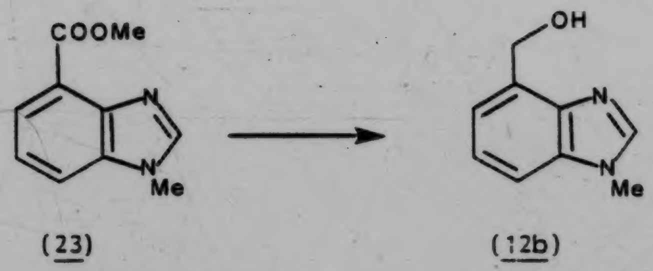

The N-methyl derivative of 4(7')-carbomethoxybenzimidazole (23) (0.9 g, 0.0042 mol) was dissolved in dry THF (50 mL) and added dropwise to a suspension of $LiAlH_4$ (0.15 g) in THF (10 mL). Once the addition had been completed the reaction mixture was stirred for and additional half hour and then the excess $LiAlH_4$ was decomposed with H_2O (0.5 mL). The solution was filtered and the solid residue washed several times with THF. The combined filtrate and washings were dried ($MgSO_4$) and the THF removed under reduced pressure. The residue was recrystallized from ether to give 0.48 g (0.003 mol, 70% yield) of 4-hydroxymethyl-1-methylbenzimidazole: mp 90-100°C. After removal of the THF the hydrochloride salt of the alcohol can be made directly by dissolving the residue in dry ether and bubbling HCl gas through the rapidly stirred solution to give 0.49 g (0.0025 mol, 60% yield) of the hydrochloride salt imidazole: mp 241-243°C.

IR ($CHCl_3$ cast): 3230, 1500, 1270, 1070, 1045, 750 cm^{-1}.

NMR $C_9H_{10}N_2O$ ($CDCl_3$,100MHz) δ 3.30(br s,1H,OH), 3.84(s,3H,NMe),5.14 (s,2H,CH_2), 7.17-7.24(m,3H) and 7.84(s,1H,N=C(H)-N).

NMR $C_9H_{10}N_2O$•HCl (DMSO-d_6,100MHz) δ 4.06(s,3H,NMe). 4.90(s,2H,CH_6), 7.52-7.90(m,3H) and 9.63(s,1H).

Mass spectrum m/e (rel intensity) 162(M^+,82), 161(100), 133(87).

Exact mass 162.0781 (calcd for $C_9H_{10}N_2O$, 162.0794).

Anal. Calcd for $C_9H_{10}N_2O$.HCl: C,54.42; H,5.58; N,14.10; Cl,17.85.

Found: C,54.07; H,5.51; N,14.01; Cl,17.47.

4-Chloro-1-methylbenzimidazole•HCl (24).

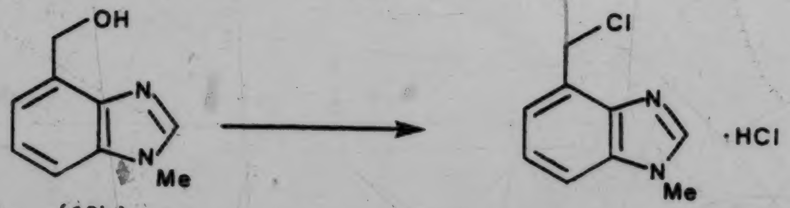

(12b)

(24)

The N-methyl derivative of 4(7')-hydroxymethylbenzimidazole

(12b) (0.8 g, 0.005 mol) was dissolved in THF (50 mL) and added dropwise to 10 equivalents of thionyl chloride in THF (20 mL). Once the addition had been completed the reaction mixture was allowed to stir overnight and 0.99 g (0.0045 mol, 90% yield) of the hydrochloride salt of the chloride precipitated out of solution as the microanalytically pure product: mp 262°C (decomp).

IR (KBr disc): 3000, 1562, 1440, 1145, 990, 760 cm^{-1}.

NMR (DMSO-d_6,100MHz) δ 4.06(s,3H,NCH_3), 4.20(br s,NH), 5.21(s,2H), 7.52-7.72(m,2H), 7.89-8.0(m,1H) and 9.57(s,1H).

Mass spectrum m/e (rel intensity 182, 180(M^+, 13,43),145(100).

Exact mass 180.0451, 182.0425 (calcd for $C_9H_9ClN_2$, 180.0456, 182.0426).

Anal. Calcd for $C_9H_9ClN_2$.HCl: C,49.79; H, 4.64; N,12.90; Cl, 32.66. Found: C,49.92; H,4.65; N,12.61; Cl,32.51.

Potassium Ethyl Xanthate (81).

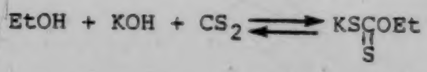

$$\mathrm{EtOH + KOH + CS_2 \rightleftharpoons KS\underset{\underset{S}{\|}}{C}OEt}$$

Potassium ethyl xanthate (81) was made according to the method of Vogel[41] in a 60% yield: mp 225-226°C.

IR (MeOH cast): 1150, 1120, 1100, 1050 cm^{-1}.

NMR (DMSO-d_6,100MHz) δ 1.17(t,CH_3,J=7Hz), 4.22(q,CH_2,J=7Hz).

Mass spectrum m/e (rel intensity) 89(M^+ -KS,5).

1-Methyl-ethyl-S-4-benzimidazolmethyl Xanthate (25).

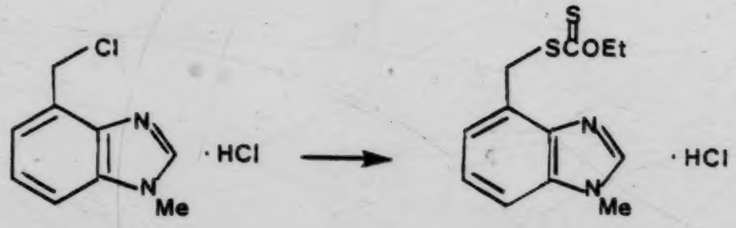

(24) (25)

The hydrochloride salt of the chloride (0.8 g, 0.0037 mol) and a three fold excess of potassium ethyl xanthate were placed in 300 mL dry THF and stirred overnight at room temperature. The THF was removed under reduced pressure and the solid residue washed several times with ether. Dry HCl gas was bubbled through the ethereal solution and 0.6 g (0.002 mol, 54% yield) of the hydrochloride salt of the xanthate precipitated out of solution. The yellow powder was recrystallized from methanol/ether to give 0.4 g (0.0013 mol, 66% yield) of pale yellow crystals: mp 129-130°C.

IR (MeOH cast): 2980, 2940, 1500, 1440, 1420, 1335, 1270, 1220, 1150, 1110, 1050, 750 cm^{-1}.

NMR ($CDCl_3$,100MHz): δ 141(t,CH_3,J=7Hz), 3.82(s,NCH_3), 4.66(q,CH_2, J=7Hz), 4.84(s,CH_2), 7.24-7.34(m,3H) and 7.86(s,1H).

Mass spectrum m/e (rel intensity) 266(M+,28), 178(14), 177(87), 146(24), 145(100).

Exact mass 266.0550 (calcd for $C_{12}H_{14}N_2OS$, 266.0549).

Anal. Calcd for $C_{12}H_{14}N_2OS.HCl$: C,47.59; H,4.99; N,9.24.

Found: C,47.46; H,5.05; N,9.13.

1-Methyl-4-thiomethylbenzimidazole (8b).

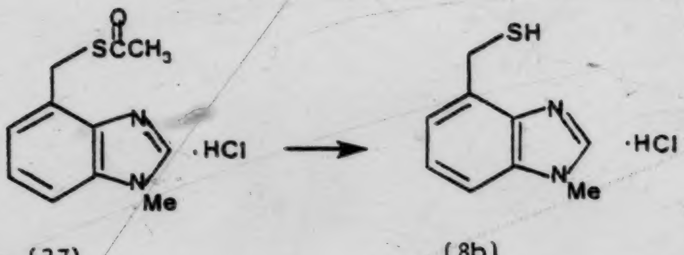

(27) (8b)

The hydrochloride salt of 1-methyl-4-thioacetoxymethylbenzimidazole (27) (1 g, 0.0039 mol) was dissolved in 1 N NaOH (~5 mL) and shaken for approximately 5 min. The solution was adjusted to pH 7 as quickly as possible with dilute HCl and extracted several times with chloroform. The combined chloroform extracts were dried and the chloroform removed under pressure. The residue was dissolved in dry ether and HCl gas was bubbled through the solution to precipitate 0.5 g (0.0023 mol, 59.0% yield) of the hydrochloride salt of 1-methyl-4-thiomethylbenzimidazole. The slightly yellow powder was recrystallized from methanol/ether to give 0.3 g (0.0014 mol, 61% yield) of white crystals: mp 225-226°C.

IR (powder): 1625, 1560, 1490, 1440, 1145, 860, 750 cm^{-1}.

NMR $C_9H_{10}N_2S \cdot HCl$ (90MHz, DMSO-d_6) δ 3.5(t,1H,J=8Hz), 4.15 (s,NCH_3), 4.4(d,CH_2,J=8Hz), 7.5-8.0(m,3H), 9.61(s,1H).

Mass spectrum m/e (rel intensity) 178(M,66), 177(25), 145(100).

Exact mass 178.0562 (calcd for $C_9H_{10}N_2S$, 178.0566).

Anal. Calcd for $C_9H_{10}N_2S$: C,60.64; H,5.65; N,15.72. Found: C, 60.24; H,5.68; N,15.81.

Benzimidazole (10a).

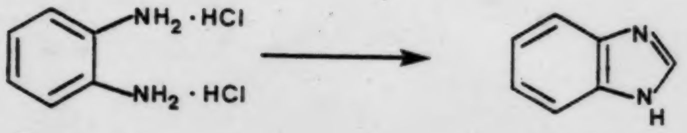

(28) (10a)

The hydrochloride salt of phenylenediamine (5.25 g, 0.029 mol), 4 N HCl (25 mL) and formic acid (3.6 mL) were combined under a N_2 atmosphere and heated at reflux for 1 h. The aqueous solution was adjusted to pH 9 with saturated aqueous potassium carbonate and crystals precipitated which were filtered and recrystallized from ether to give 3.28 g (0.028 mol, 96% yield) of benzimidazole: mp 176-177 °C (lit.[42] mp 170-172°C).

IR (KBr): 3500, 1478, 1459, 1409, 1245, 748 cm^{-1}.

NMR (DMSO-D_6,100MHz) δ 7.1-7.3(m,2H), 7.5-7.7(m,2H), 8.2(s,1H) and 9.3(br s,NH).

Mass spectrum m/e (rel intensity) 118(M^+,100), 91(67), 90(36).

Exact mass 118.0526 (calcd for $C_7H_6N_2$, 118.0532).

1-Methylbenzimidazole (10b).

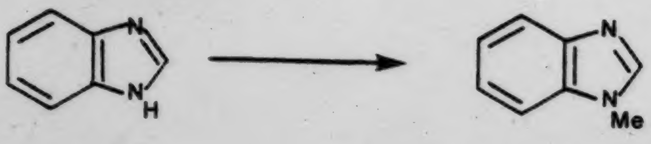

(10a) (10b)

Benzimidazole (2 g, 0.017 mol) was dissolved in dry THF (100 mL) and 1.1 equivalents of NaH followed by 1.1 equivalents of MeI were added. The reaction mixture was stirred for 7-8 h at room temperature, filtered and the THF removed under reduced pressure.

The residue was dissolved in 5% aqueous sodium thiosulfate (40 mL) and extracted three times with chloroform. The chloroform was washed twice with 10% HCl (10 mL) and the aqueous layer was evaporated to dryness under high vacuum. The solid residue was washed several times with boiling THF to yield 1.3 g (0.0098 mol, 58% yield) of the hydrochloride salt of N-methyl benzimidazole: mp 2240-225°C (lit.[74] mp 225-226°C).

IR $C_8H_8N_2 \cdot HCl$ (MeOH cast) 3120, 3010, 2600, 1460, 1445, 750 cm^{-1}.

NMR $C_8H_8N_2 \cdot HCl$ (DMSO-d_6,100MHz) δ 4.06(s,3H,NCH_3), 7.56-7.70(m,2H), 7.8-8.02(m,2H) and 9.64(s,1H).

NMR ($CDCl_3$,100MHz) δ 3.70(s,3H,NCH_3), 7.18-7.34(m,3H) and 7.68-7.84 (m,2H).

Mass spectrum m/e (rel intensity) 132(M^+,100), 131(47), 104(16), 77(11).

Exact mass 132.0687 (calcd for $C_8H_8N_2$, 132.0688).

Tetrahydrobenzimidazole (11a).

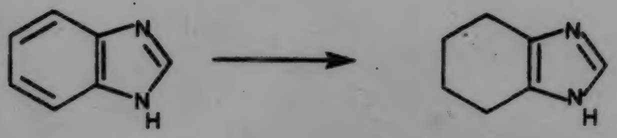

(10a) (11a)

Tetrahydrobenzimidazole (11a) was prepared by the method of Butula.[43] Benzimidazole (10a) (1 g, 0.0085 mol), 5% palladium on charcoal (1 g), perchloric acid (0.7 mL of 70%) and glacial acetic acid (20 mL) were combined in a hydrogenation bomb and heated at

120°C under 900 psi H_2 pressure overnight. After cooling, the reaction mixture was filtered and the glacial acetic acid removed under reduced pressure (rotoevaporator at 60°C). The residue was dissolved in H_2O and adjusted to pH 9-10 with aqueous potassium carbonate. The aqueous layer was extracted several times with chloroform. The combined chloroform extracts were dried with $MgSO_4$ and the solvent removed under reduced pressure. The residue was recrystallized from THF/pentane to give 0.63 g (0.0052 mol, 61% yield) of tetrahydrobenzimidazole: mp 138.5-139°C (lit.[43] mp 150°C). IR ($CHCl_3$ cast) 3200, 3020, 2930, 2850, 1610, 1490, 1460, 960 cm^{-1}. NMR ($CDCl_3$,100MHz) δ 1.7-2.0(m,4H), 2.4-2.8(m,4H) and 7.46(s,1H). Mass spectrum m/e (rel intensity) 122(M^+,50), 94(100). Exact mass 122.0845 (calcd for $C_7H_{10}N_2$, 122.0845).

1-Methyltetrahydrobenzimidazole (11b).

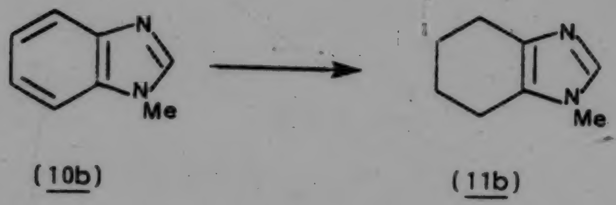

1-Methylbenzimidazole (10b) (1 g, 0.0076 mol), 5% rhodium on carbon (1 g), glacial acetic acid (20 mL) and 1.1 equivalents of conc HCl were placed in a hydrogenation bomb and heated overnight at 120°C under 1000 psi hydrogen pressure.[43] After cooling, the reaction mixture was filtered off and the acetic acid removed under reduced pressure (rotoevaporator at 60°C). The residue was dissolved in H_2O (20 mL) and adjusted to pH 9-10 with saturated aqueous potassium carbonate and the aqueous layer extracted several times with chloroform. The combined chloroform extracts were dried with $MgSO_4$ and the solvent removed under reduced pressure. The gummy residue was dissolved in dry Et_2O (200 mL) and dry HCl gas was bubbled through the solution. A white powder precipitated which was recrystallized from 98% EtOH/ether to give 0.5 g (0.0029 mol, 38% yield) of 1-methyltetrahydrobenzimidazole: mp 194-195°C.

IR ($CHCl_3$ cast) 1670, 1500, 1450, 800 cm^{-1}.

NMR $C_8H_{12}N_2$($CDCl_3$,90MHz) δ 1-1.9(m,4H), 2.35-2.7(m,4H), 3.44(s,3H, NCH_3) and 7.24(s,1H).

NMR $C_8H_{12}N_2 \cdot HCl$(DMSO-d_6,100MHz) δ 1.68-1.84(m,4H), 2.48-2.64(m,4H), 3.70(s,3H,NCH_3) and 8.90(s,1H).

Mass spectrum m/e (rel intensity) 136(M^+,96), 135(80), 108(100).

Exact mass 136.0998 (calcd for $C_8H_{12}N_2$, 136.1000).

Anal. Calcd for $C_8H_{12}N_2 \cdot HCl$: C,55.65; H,7.59; N,16.22. Found: C,55.38; H,7.49; N,16.28.

Cyclohexylmethyltosylate (30).

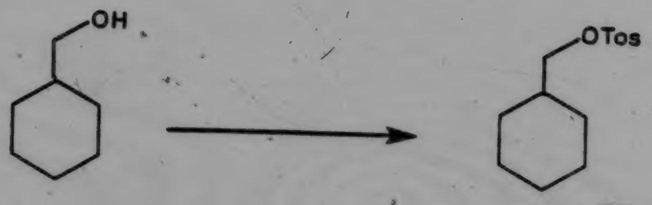

(29) (30)

The tosylate of cyclohexylmethanol (30) was prepared according to a general procedure of Fieser and Fieser.[45] Cyclohexylmethanol (29) (25 g, 0.22 mol) was dissolved in methylene chloride (100 mL) and slightly more than 1 equivalent of pyridine was added. The reaction mixture was cooled in an ice bath and 1.1 equivalents of TsCl was added. The solution was stirred for 2 h in the ice bath and pyridine•HCl precipitated out of solution. The mixture was dissolved in H_2O, acidified and extracted with ether. The ether extracts were dried with $MgSO_4$ and the ether removed under reduced pressure. The crude product was recrystallized from Skelly B (250 mL) at -78°C to give 52.5 g (0.019 mol, 89% yield) of the tosylate of cyclohexylmethanol: mp 25°C.

IR (liquid film) 1360, 1195, 1190, 980, 956, 840, 820, 670, 560 cm^{-1}.

NMR ($CDCl_3$,100MHz) δ 0.62-1.80(m,11H), 2.23(s,3H,CH_3), 3.81(d,2H, J=3Hz) and 7.32, 7.72(ABq,4H,J=4Hz).

Mass spectrum m/e (rel intensity) 268(M^+,10.5), 96(100).

Exact mass 268.1133 (calcd for $C_{14}H_{20}O_3S$, 268.1134).

Anal. Calcd for $C_{14}H_{20}O_3S$: C,62.65; H,7.51; S,11.95. Found: C,62.43; H,7.41; S,11.82.

Cyclohexylmethyliodide (31).

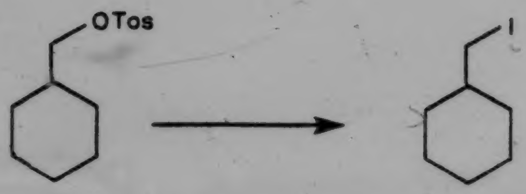

(30) (31)

Cyclohexylmethyliodide (31) was prepared by the method of Finklestein.[46] The tosylate of cyclohexylmethanol (30) (10 g, 0.037 mol) and a four-fold excess of sodium iodide were dissolved in acetone and held at reflux for three days. The white solid was filtered and the acetone removed in vacuo. The residue was dissolved in $CHCl_3$ (30 mL) and extracted with H_2O (20 mL), 5% sodium thiosulfate (20 mL) and saturated NaCl (20 mL). The chloroform was dried and removed in vacuo. The residue was distilled (bp 90°C/14 torr) to give 4.1 g (0.0185 mol, 50% yield) of cyclohexylmethyl iodide.

IR (liquid film) 2950, 1714, 1449 cm^{-1}.

NMR ($CDCl_3$,100MHz) δ 0.72-2.02(m,11H) and 3.10(d,2H,J=3Hz).

Mass spectrum m/e (rel intensity) 96(100), 81(66).

Exact mass 96.0939 (calcd for $C_7H_{13}I$-HI, 96.09396).

Anal. Calcd for $C_7H_{13}I$: C,37.5; H,5.80. Found: C,37.50; H,5.72.

Ethyl-S-cyclohexylmethyl xanthate (32).

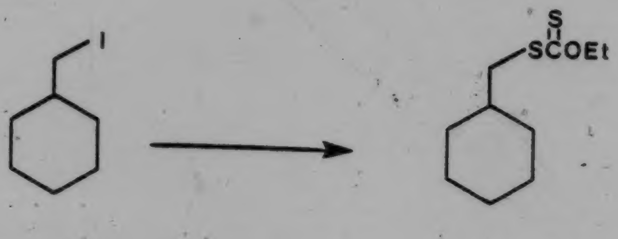

(31) (32)

Cyclohexylmethyliodide (31) (7 g, 0.031 mol) was dissolved in dry THF (75 mL) and 1.2 equivalents of potassium ethyl xanthate were added. The reaction mixture was held at reflux for 3 h, cooled and the THF removed under reduced pressure. The semi-solid residue was washed several times with diethyl ether which dissolved the product but not the remaining unreacted potassium ethyl xanthate. The ether extracts were dried with $MgSO_4$ and the ether removed under reduced pressure. The residue was distilled (80°C/0.05 torr) to give 5.3 g (0.024 mol, 78% yield) of the ethyl xanthate of cyclohexylmethanol.

IR ($CHCl_3$ cast) 1448, 1215, 1110, 1050 cm^{-1}.

NMR ($CDCl_3$,100MHz) δ 0.8-2.0(m,11H), 2.98(d,CH_2,J=6Hz), 2.58(q,CH_2, J=7Hz).

Mass spectrum m/e (rel intensity) 218(M^+,62) 97(100), 96(62).

Exact mass 218.0796 (calcd for $C_{10}H_{18}OS_2$, 218.0800).

Cyclohexylmethylthiol (7).

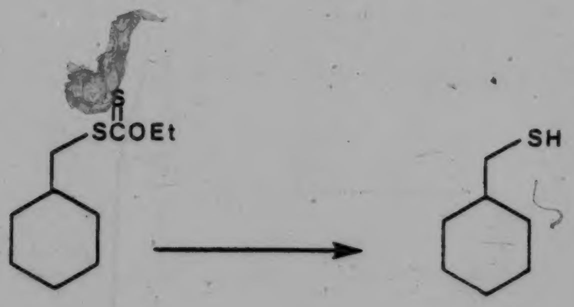

(32) (7)

The xanthate (32) (1.0 g, 0.0046 mol) was dissolved in dry THF (10 mL) and added dropwise to a stirred suspension of $LiAlH_4$ (0.2 g) in dry THF (10 mL) under a static nitrogen atmosphere. Once the addition had been completed the reaction mixture was heated at reflux for 15 min. After cooling, the excess $LiAlH_4$ was decomposed with H_2O (~0.5 mL) and the solution filtered. The resulting solid was washed several times with THF and the combined filtrates dried with $MgSO_4$. The THF was removed under reduced pressure and the product (0.42 g 0.0032 mol, 70% yield) was found to be analytically pure. Distillation can lead to the formation of the disulfide.

IR ($CHCl_3$ cast) 2920, 2850, 1448 cm^{-1}.

NMR ($CDCl_3$,100MHz) δ 0.6-2.0(m,11H), 1.24(t,5H,J=8Hz) and 2.38(d of d,CH_2,J=8Hz,J=8Hz).

Mass spectrum m/e (rel intensity) 130(M^+,6), 95(100).

Exact mass 130.0815 (calcd for $C_7H_{14}S$, 130.0817).

Anal. Calcd for $C_7H_{14}S$: C,64.55; H,10.83; S,24.62. Found: C,64.30; H,10.66; S,24.65.

Dimethyl pimelate (34).

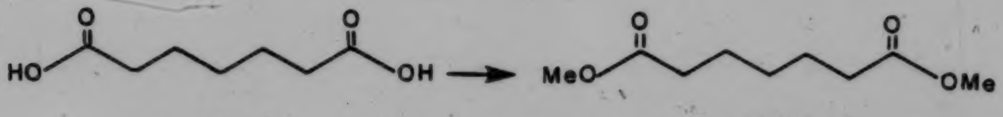

(33) (34)

Pimelic acid (25 g, 0.16mol) was dissolved in dry MeOH (300 mL) and cooled in an ice-water bath. Gaseous HCl was passed through the stirred solution for ~3 h. The reaction mixture was stirred overnight and the methanol removed under reduced pressure. The residue was distilled (bp 82°C/0.05 torr) lit.[77] bp 120°C/10 torr) to give 24.4 g (0.13 mol, 82% yield) of the dimethylester.

IR ($CHCl_3$ cast) 1738, 1438, 1200, 1170 cm^{-1}.

NMR ($CDCL_3$,100MHz) δ 1.2-1.9(m,6H), 1.2-1.4(m,4H) and 3.7(s,3H, OCH_3).

Mass spectrum m/e (rel intensity) 157(M^+-OCH_3,50) 115(100).

Exact mass 157.0857 (calcd for $C_9H_{16}O_4$-OCH_3, 157.086).

2-Carbomethoxycyclohexanone (36a).

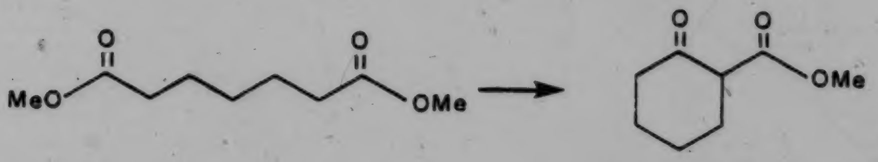

(34) (36a)

2-Carbomethoxycyclohexanone (36a) was prepared in 55% yield by a Dieckmann condensation of dimethyl pimelate as described by Pinkney[48] (bp 72°C/0.5 torr) (lit.[49] bp 68°C/0.8 torr).

IR (liquid film) 1747, 1716, 1650, 1635, 1480, 1360, 1300, 1260, 1220, 1080 cm^{-1}.

NMR ($CDCl_3$,100 MHZ) δ 1.50-1.80(m), 2.14-2.36(m) and 3.74(s,3H).

Mass spectrum m/e (rel intensity) 156(M^+,38), 124(55), 111(40), 55(100).

Exact mass 156.0778 (calcd for $C_8H_{12}O_3$, 156.07866).

2-Carbethoxycyclohexanone (36b).

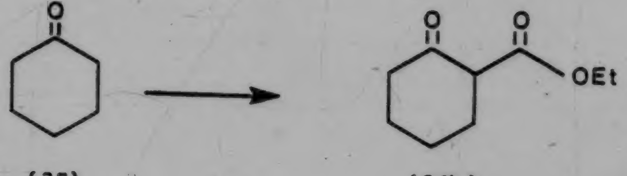

(35) (36b)

2-Carbethoxycyclohexanone (36b) was prepared according to the procedure of Deslongchamps et al.[49] Dry diethylcarbonate (23.65 g, 0.20 mol), sodium hydride (0.25 mol) and anhydrous THF (50 mL) were placed in a 500 mL, 3-necked round-bottomed flask equipped with a mechanical stirrer, condenser, dry nitrogen inlet tube and a pressure-equalizing dropping funnel. The stirred suspension was heated to reflux and freshly distilled cyclohexanone (7.8 g, 0.08 mol) in dry THF (20 mL) was added dropwise. After 2 min of addition, 306 mg (0.0076 mol) of potassium hydride was added to initiate the reaction. The addition of the cyclohexanone was continued over a period of 1 h and the mixture refluxed and stirred for an additional 1 h after the complete addition of the cyclohexanone. The reaction mixture was cooled in an ice bath and the mixture hydrolyzed by the slow addition of 3 M acetic acid until all the solid disappeared. The mixture was poured into a NaCl solution (100 mL) and extracted with $CHCl_3$. The organic layer was dried with $MgSO_4$ and the chloroform removed. The residual liquid was distilled (bp 75°C/1 torr) (lit.[48] bp 75°C/1 torr) to give 6.7 g (0.04 mol, 50% yield) of 2-carbethoxycyclohexanone.

IR (thin film) 1700, 1630, 1600, 1280, 1240, 1195 cm^{-1}.

NMR ($CDCl_3$,60MHz) δ 1.37(t,3H,J=7Hz), 1.62(m), 2.23(m) and 4.2(q, 2H,J=7Hz).

Mass spectrum m/e (rel intensity) 170(M^+,51), 124(100), 114(19).
Exact mass 170.0942 (calcd for $C_9H_{14}O_3$, 170.09432).

6-Bromo-2-ethoxycarbonylcyclohexanone (37b).

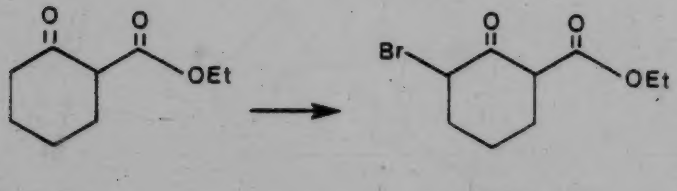

(36b) (37b)

6-Bromo-2-ethoxycarbonylcyclohexanone (37b) was prepared according to the method of Usaka, Koyama and Takeda.[47] Bromine (54.5 g, 0.34 mol) was added dropwise to 2-ethoxycarbonylcyclohexanone (36b) (41.4 g, 0.25 mol) with stirring at 0°C. After the addition was complete, the mixture was stirred for a further 1 h in the ice bath. The mixture was dissolved in ether and washed twice with water, several times with saturated aqueous sodium carbonate and again with water. All traces of HBr must be removed or the distillation does not proceed well. The ether was dried over a mixture of $MgSO_4$ and Na_2CO_3. The solution was removed and the residue distilled under reduced pressure to give a slightly yellow oil. A second distillation afforded 34.8 g (0.14 mol, 56.5% yield) of a colorless oil: bp 92°C/0.1 torr (lit.[47] bp 80-92°C/0.09 torr).
IR (thin film) 1735, 1710, 1650, 1610 cm^{-1}.
NMR ($CDCl_3$,60MHz) δ 1.3(t,CH_3,J=7Hz), 1.6-2.5(m),
4.23(q,CH_2,J=7Hz), 4.68(m), 12.05(s) and 12.5(s, enol OH).
Mass spectrum m/e (rel intensity) 248, 250(M^+,13,13), 123(100).

Exact mass 248.0042, 250.0025 (calcd for $C_9H_{13}BrO_3$, 248.00479, 250.00279).

4,5[1'(4')-Ethoxycarbonyltetramethylene]imidazole (38b).

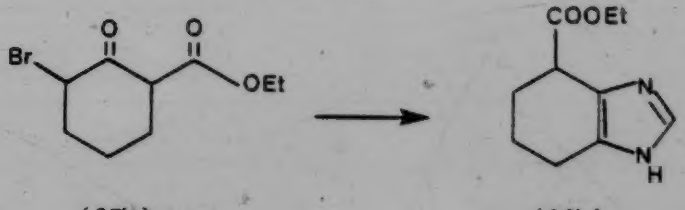

(37b) (38b)

Method I

4,5[1'(4')-Ethoxycarbonyltetramethylene]imidazole (38b) was prepared according to the method of Utaka, Koyama and Takeda.[47] 6-Bromo-2-ethoxycarbonylcyclohexanone (37b) (15.0 g, 0.06 mol) and freshly distilled formamide (38 g, 0.78 mol) were placed in a 3-necked round-bottomed flask equipped with a condenser and a nitrogen inlet tube. The solution was heated at 150-160°C for 1.5 h with stirring. The excess formamide was removed by distillation at reduced pressure (bp 50-60°C/0.2 torr). The residue was dissolved in H_2O and washed several times with ether. The pH of the aqueous layer was adjusted to 8-9 with saturated sodium carbonate and the solution was then extracted several times with chloroform. After drying with $MgSO_4$ the chloroform was removed under reduced pressure to yield a glassy yellow solid. This was purified by column chromatography employing a jacketed column (1 1/2" x 30") and Grade 3 alumina. The column was packed with a hexane suspension of alumina. Elution was initiated with $CHCl_3$:hexane (1:1). After each litre of eluate had been collected the $CHCl_3$ content of the solvent was increased by 10% until 100% $CHCl_3$ was used. The desired compound (0.35 g, 0.0018 mol) was removed from the column after 3 days in 3% yield. The product was recrystallized from THF/pentane to give 0.30 g (0.015 mol, 2.6% yield) of a white solid: mp 102-103°C (lit.[47] 101.5-102.6° C).

IR (KBr) 3600-2200, 1715, 1445, 1270, 1205, 1165, 1138 cm^{-1}.

NMR ($CDCl_3$,60 MHz) δ 1.23(t,3H,J=6.5Hz), 2.02(m,4H,CH_2), 2.61(m,2H,=C-CH_2), 3.75(m,1H,CHC=O) and 4.13(q,2H,J=6.5Hz).

Mass spectrum m/e (rel intensity) 194(M^+,20), 121(100).

Exact mass 194.1051 (calcd for $C_9H_{14}N_2O_2$, 194.10562).

Anal. Calcd for $C_9H_{14}N_2O_2$: C,61.84; H, 7.43; N,14.42; O,16.47.

Found: C,61.85; H,7.21; N,14.43; O,16.40.

Method II

4,5[1'(4')-Ethoxycarbonyltetramethylene]imidazole (38b) was also prepared by the method of Tanaka, Shimodaura and Fuga.[50] 6-Bromo-2-ethoxycarbonylcyclohexanone (25.4 g, 0.10 mol) and formamidine acetate (20.8 g, 0.2 mol) were dissolved in formic acid (30 mL) and heated to 120°C for 6 h. The solution was dissolved in H_2O and the pH adjusted to 9-10 with aqueous sodium carbonate. The aqueous layer was extracted with $CHCl_3$, dried with $MgSO_4$ and the solvent removed under reduced pressure. The residue was purified by chromatography as in Method I. The product from the column was recrystallized from THF/pentane to give 1.21 g (0.006 mol, 6% yield) of 4,5[1'(4')-ethoxycarbonyltetramethylene]imidazole: mp 102-103°C (lit.[47] 101.5-102.6°C).

4,5[1'(4')-Methoxycarbonyltetramethylene]imidazole (38a) can be made using the same procedures but starting with 6-bromo-2-methoxycarbonylcyclohexanone.

IR ($CHCl_3$ cast) 2900, 2853, 1738, 1458, 1263, 1225, 1198, 1170 cm^{-1}.

NMR ($CDCl_3$,100MHz) δ 1.60-2.18(m,4H), 2.44-2.68(m,2H), 3.63(s,3H,OCH_3), 3.66(m,1H) and 7.45(s,1H).

Mass spectrum m/e (rel intensity) 180(M^+,74), 121(100), 94(56).

Exact mass 180.0896 (calcd for $C_9H_{12}N_2O_2$, 180.08996).

Formamidine Acetate (82).

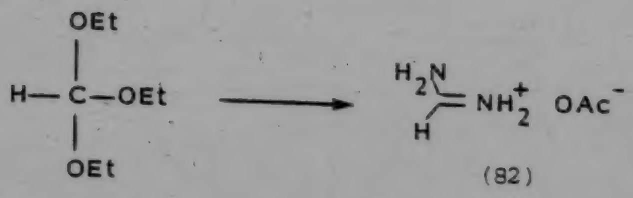

Formamidine acetate (82) was made according to the method of Taylor, Ehrhart and Kawanisi[51] in 60% yield: mp 163-165°C (lit.[51] mp 162-164°C).

4,5[1'(4')-Hydroxymethyltetramethylene]imidazole (13a).

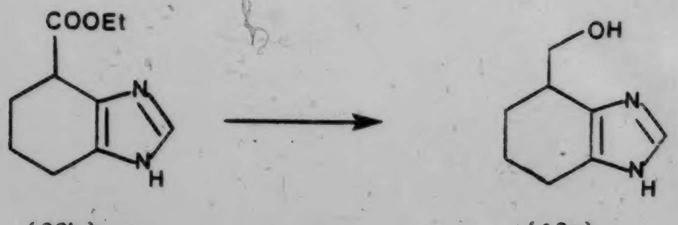

(38b) (13a)

4,5-[1'(4')-Hydroxymethyltetramethylene]imidazole was prepared according to the procedure of Utaka, Koyama and Takeda.[47] 4,5-[1'(4')-Ethoxycarbonyltetramethylene]imidazole (38b) (0.87 g, 0.0046 mol) in THF (5 mL) was added dropwise to a suspension of $LiAlH_4$ (0.4 g) in THF (10 mL) under nitrogen. After the addition was completed the reaction mixture was stirred for 30 min and the excess hydride was destroyed by addition of the minimum amount of 15% (v/v) NaOH (~0.5 mL) and then H_2O (~0.5 mL). The mixture was adjusted to pH 9-10 with 1 M HCl and filtered. The white precipitate was washed repeatedly with THF and, after drying , the combined filtrate and washings were evaporated under reduced pressure. The crude product was recrystallized from THF/pentane to give 0.42 g (0.0028 mol, 60% yield) of 4,5-[1'(4')-hydroxymethyltetramethylene]imidazole: mp 145-146°C (lit.[47] mp 145-147°C).

IR (KBr) 3150, 2910, 2820, 1595, 1450, 1020 cm^{-1}.

NMR (Me_2CO-d_6,100MHz) δ 1.84(m,4H,CH_2CH_2), 2.54(m,2H,$=CCH_2$), 2.80(m,1H,=CH-C(H)), 3.60 (ABq,2H,OCH_2), 3.90(br s,OH,NH) and 7.42(s,1H,N-CH=N).

Mass spectrum m/e (rel intensity) 152(M^+,18), 121(100).

Exact mass 152.0950 (calcd for $C_8H_{12}N_2O$, 152.09506).

Anal. Calcd for $C_8H_{12}N_2O$: C,63.13; H,7.95; N,18.41.

Found: C,63.37; H,8.04; N,18.05.

1-Methyl-4-carboxymethyl-4,7-dihydrobenzimidazole (43).

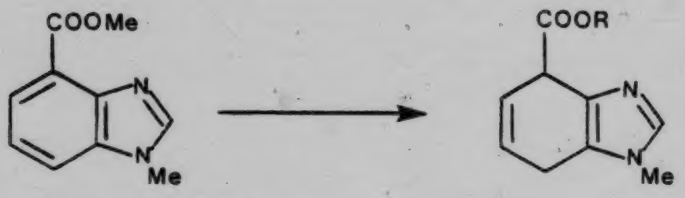

(23) (43)

1-Methyl-4-carboxymethylbenzimidazole (1 g, 0.0053 mol) and isopropanol (0.18 mL, 0.01 mol) were dissolved in dry THF (75 mL) and added to a 3-necked round-bottomed flask (250 mL) equipped with a mechanical stirrer, dry-ice condenser and nitrogen inlet tube. The reaction vessel was cooled to -78°C with a dry ice/acetone bath and ~100 mL of liquid ammonia were distilled in. Sodium (0.5 g, 0.02 mol) was added in small quantities with rapid stirring at -78°C. After the addition had been completed the reaction mixture was stirred for an additional 20 min and ammonium chloride (~1.0 g) was added until the deep blue colour disappeared. After warming to room temperature the solution was filtered and the THF removed under reduced pressure. This yielded 0.7 g of a yellow oil which was a mixture of the isopropyl and methyl esters of 1-methyl-4,7-dihydrobenzimidazole-4-carboxylic acid. Due to the ease with which this was air oxidized back to starting material, the compound was used without further purification in the next step.

IR ($CHCl_3$ cast): 1717, 1500, 1265, 1105 cm^{-1}.

NMR (partial,$CDCl_3$,100MHz) δ 3.2-3.32(m,CH_2), 3.54(s,NMe), 3.72(s, OMe), 5.84-6.0(m,2H,C(H)=C(H)) and 7.4(s,N=C(H)-N).

Mass spectrum m/e (rel intensity) 220(M^+,7), 192(M^+,8), 133(100).

Exact mass 220.1208, 192.0894 (calcd for $C_{12}H_{16}N_2O_2$, 220.1212; $C_{10}H_{12}N_2O_2$, 192.0899.

1-Methyl-4-methoxycarbonyltetrahydrobenzimidazole (44).

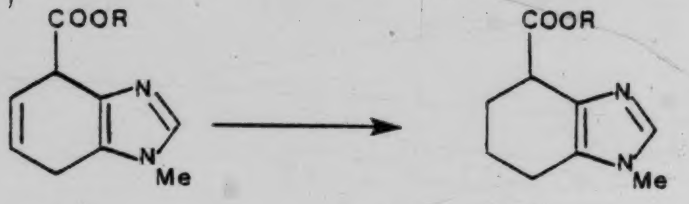

(43) (44)

A mixture of 1-methyl-4-carboxymethyl-4,7-dihydrobenzimidazole and 1-methyl-4-carboxyisopropyl-4,7-dihydrobenzimidazole (0.7 g) was dissolved in methanol (50 mL) and a catalytic amount of PtO_2 was added. The flask was shaken overnight under 40 psi H_2 pressure. Decolourizing carbon was added, the reaction mixture filtered through a layer of celite in an E frit sintered glass funnel and the methanol removed under reduced pressure. The residue was dissolved in ether and any insoluble material filtered off. Dry HCl gas was bubbled through the ethereal solution and a gummy residue formed which could be triturated in THF to give 0.5 g of a mixture of the methyl and isopropyl esters of 1-methyltetrahydrobenzimidazole-4-carboxylic acid as a white solid.

IR ($CHCl_3$ cast): 1730, 1200, 1105 cm^{-1}.

NMR $C_{10}H_{14}N_2O_2$.HCl and $C_{12}H_{18}N_2O_2$.HCl ($CDCl_3$,100MHz): δ 1.21(d,CH_3, J=6Hz), 1.7-2.10(m), 2.5-2.7(m), 3.34-3.46(m), 3.68(s,OMe), 3.74(s, NMe), 4.94(septet,1H,J=6Hz) and 9.0(s,N=C(H)-N).

Mass spectrum m/e (rel intensity) 222(M^+,54), 194(M^+,28), 135(100).

Exact mass 222.1369, 194.1052 (calcd for $C_{12}H_{18}N_2O_2$, 222.1369; $C_{10}H_{14}N_2O_2$ 194.1055).

1-Methyl-4-hydroxymethyltetrahydrobenzimidazole (13b).

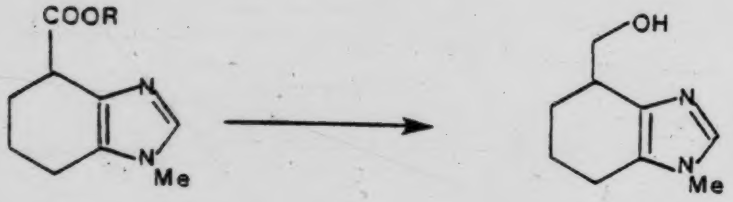

(44)

(13b)

A mixture of the methyl and isopropyl esters of 1-methyltetrahydrobenzimidazole-4-carboxylic acid (0.5 g) was dissolved in THF (20 mL) and added dropwise to a suspension of $LiAlH_4$ (0.2 g) in THF under a static nitrogen atmosphere. After the addition had been completed the reaction mixture was heated at reflux for 20 min. After cooling, the excess $LiAlH_4$ was decomposed with H_2O (~0.5 mL) and the solution filtered. The THF was removed under reduced pressure and the residue recrystallized from $CHCl_3$/ether to give 0.25 g (0.0015 mol) of 1-methyl-4-hydroxymethyltetrahydrobenzimidazole: mp 141-142°C.

IR (MeOH cast): 3300, 1545, 1265, 1105 cm^{-1}.

NMR ($CDCl_3$,200MHz): δ 1.6-2.1(m,4H), 2.44-2.56(m,2H), 2.84-3.0(m, 1H), 3.53(s,3H,NCH_3), 3.53-3.86(m,2H,CH_2) and 7.34(s,1H,N=C(H)-N).

Mass spectrum m/e (rel intensity) 166(M^+,12), 135(100).

Exact mass 166.1106 (calcd for $C_9H_{13}N_2O$, 166.1098).

1-Methyl-4-chloromethyltetrahydrobenzimidazole (45).

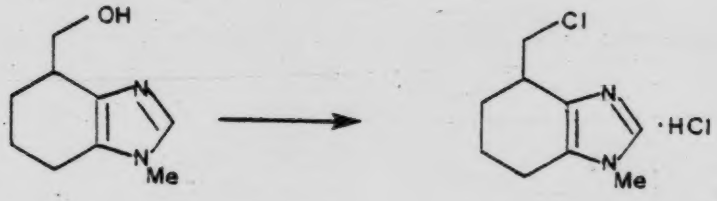

(13b)

(45)

1-Methyl-4-hydroxymethyltetrahydrobenzimidazole (13b) (0.3 g, 0.0018 mol) was dissolved in dry THF (20 mL) and added dropwise to a ten fold excess of thionyl chloride in THF (20 mL) and stirred overnight. The THF and excess thionyl chloride were removed under reduced pressure and the residue dissolved in H_2O, basified with saturated potassium carbonate and extracted with chloroform.

The chloroform was removed under reduced pressure and the residue dissolved in dry ether. Dry HCl gas was bubbled through the solution and 0.3 g (0.0013 mol, 75% yield) of 1-methyl-4-chloromethyltetrahydrobenzimidazole hydrochloride precipitated out of solution: mp 170-171°C.

IR (KBr) 1640, 1550, 1305, 860 cm^{-1}.

NMR $C_9H_{13}N_2Cl.HCl$ (DMSO-d_6,100MHz) δ 1.60-2.10(m,4H), 2.50-2.70 (m,2H), 3.2-3.3(m,1H), 3.5-4.1(m,2H), 3.71(s,3H,NMe), and 9.02(s,1H, N=C(H)-N).

NMR $C_9H_{13}N_2Cl$ ($CDCl_3$,100MHz): δ 1.60-2.10(m,4H), 2.40-2.60(m,2H), 3.0-3.2(m,1H), 3.55-4.15(m,2H), 3.70(s,3H,NMe) and 7.32(s,1H, N=C(H)-N).

Mass spectrum m/e (rel intensity) 186,184(M^+,6,19), 135(100).

Exact mass 186.0737, 184.0763 (calcd for $C_9H_{13}N_2Cl$, 186.0738, 184.0768).

Anal. Calcd for $C_9H_{13}N_2Cl.HCl$: C,48.89; H,6.38; N,12.64. Found: C,48.78; H,6.22, N,12.61.

Benzyl acetate (71).[78]

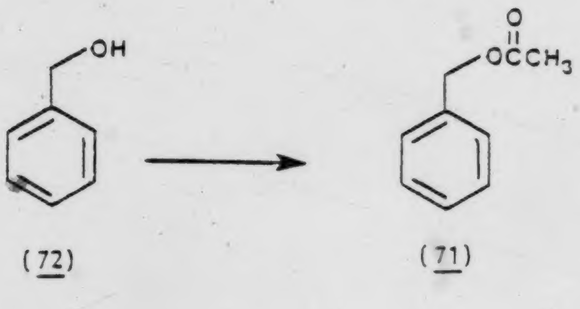

Benzyl alcohol (72) (10 g, 0.093 mol) and 3 equiv. of acetic anhydride were combined in an Erlenmeyer flask and a drop of conc H_2SO_4 was added. The reaction was stirred at room temperature for 2 h and H_2O (40 mL) was added and the reaction mixture stirred for another 15 min. The aqueous layer was extracted three times with ether. The combined ether extracts were dried with $MgSO_4$ and the ether removed under reduced pressure. The residue was distilled (bp 40-42°C/0.1 torr) (lit. bp 93-94°C/10 torr)[78] under high vacuum to give 12.3 g (0.082 mol, 88% yield) of the final product.

IR (thin film) 1742, 1230, 1028, 750, 698 cm^{-1}.

NMR ($CDCl_3$,100MHz) δ 2.08(s,CH_3), 5.09(s,CH_2), 7.32(s,ArH).

Mass spectrum m/e (rel intensity) 150(M^+,69), 108(100).

Exact mass 150.0678 (calcd for $C_9H_{10}O_2$, 150.0681).

Anal. Calcd for $C_9H_{10}O_2$: C,71.98; H,6.71; O,21.31. Found: C,72.02; H,6.73; O,21.06.

Benzylthioacetate (70).[79]

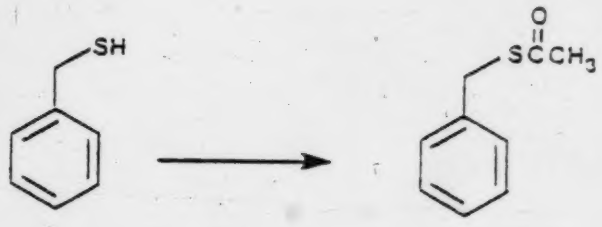

(6) (70)

Benzyl mercaptan (6) (10 g, 0.081 mol) and a three-fold excess of acetic anhydride were combined in an Erlenmeyer flask and a drop of conc H_2SO_4 was added. The reaction mixture was stirred for 3-4 h at room temperature and the solution was dissolved in H_2O and extracted several times with ether. The ether was dried with $MgSO_4$ and removed under reduced pressure. The residue was distilled (bp 55-57°C/0.1 torr) to give 11.7 g (0.07 mol, 87% yield) of the final product.

IR (thin film) 1691, 1552, 1495, 1132, 955, 700, 625 cm^{-1}.

NMR ($CDCl_3$,100MHz) δ 2.34(s,CH_3), 4.12(s,CH_2) and 7.27(s,5H).

Mass spectrum m/e (rel intensity) 166(M^+,62), 123(35), 122(32), 91(100).

Exact mass 166.0450 (calcd for $C_9H_{10}OS$, 166.0453).

Anal. Calcd for $C_9H_{10}OS$: C,64.90; H,6.07; O,9.92; S,19.30.

Found: C,65.03; H,6.06; O,9.62; S,19.29.

4(7')-Acetoxymethylbenzimidazole (69a).

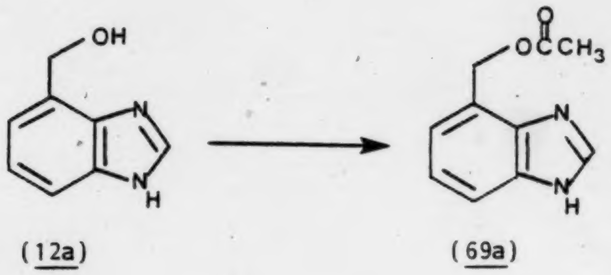

4(7')-Hydroxymethylbenzimidazole (12a) (1 g, 0.0067 mol) was dissolved in H_2O (5 mL) containing 1.1 equivalents of conc HCl. The solution was evaporated to dryness under high vacuum. The hydrochloride salt of the alcohol, acetic anhydride (10 mL) and 2 drops of conc H_2SO_4 were heated at reflux until all the alcohol went into solution. The reaction mixture was cooled and an equal volume of H_2O added. The aqueous layer was adjusted to pH 9-10 with saturated aqueous potassium carbonate and extracted three times with chloroform. The combined chloroform extracts were dried with $MgSO_4$ and the chloroform removed under reduced pressure. The residue was recrystallized from THF/pentane to give 0.78 g (0.0041 mol, 61% yield) of the acetate of 4(7')-hydroxymethylbenzimidazole: mp 168-169°C.

IR (MeOH cast): 1720, 1240 cm^{-1}.

NMR ($DMSO-d_6$,100MHz) δ 2.07(s,2H,CH_3), 5.38(s,2H,CH_2), 7.15-7.20(m, 2H), 7.48-7.60(m,1H) and 8.22(s,1H).

Mass spectrum m/e (rel intensity) 190(M^+,90), 148(100), 130(91).

Exact mass 190.0740 (calcd for $C_{10}H_{10}N_2O_2$, 190.0743).

Anal. Calcd for $C_{10}H_{10}N_2O_2$: C,63.15; H,5.30; N,14.60; O,16.82.

Found: C,63.14; H,5.30; N,14.60; O,16.53.

4-Acetoxymethyl-1-methylbenzimidazole (69b).

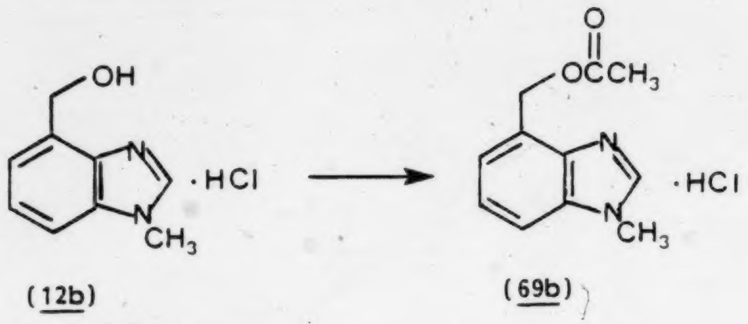

The hydrochloride salt of 4-hydroxy-1-methylbenzimidazole (12b) (1 g, 0.005 mol), 10 equiv. of acetic anhydride and a few drops of conc H_2SO_4 were combined and stirred at room temperature for 2 h. The reaction mixture was dissolved in H_2O and adjusted to pH 9-10 with saturated potassium carbonate and extracted three times with chloroform. The combined chloroform extracts were dried with $MgSO_4$

and the chloroform removed under reduced pressure. The residue was dissolved in H_2O (10 mL) containing 1.1 equivalents of HCl and evaporated to dryness under high vacuum to give 0.6 g (0.0029 mol, 58.8% yield) of the hydrochloride salt of 4-acetoxy-methyl-1-methylbenzimidazole which was recrystallized from methanol/ ether: mp 204-207°C.

IR (MeOH cast) 1725, 1240, 1020 cm^{-1}.

NMR $C_{11}H_{12}N_2O_2$ ($CDCl_3$,100MHz) δ 2.10(s,3H,CH_3), 3.81(s,3H,NCH_3), 5.59(s,2H,CH_2), 7.2-7.4(m,3H) and 7.88(s,1H).

NMR $C_{11}H_{12}N_2O_2 \cdot HCl$ (DMSO-d_6,100MHz) δ 2.08(s,3H,CH_3), 4.06(s,3H, NCH_3), 5.43(s,2H,CH_2), 7.56-7.64(m,2H), 7.87-7.98(m,1H) and 9.66(s,1H).

Mass spectrum m/e (rel intensity) 204(M^+,27), 161(100), 145(32).

Exact mass 204.0899 (calcd for $C_{11}H_{12}N_2O_2$, 204.0890).

Anal. Calcd for $C_{11}H_{12}N_2O_2$: C,54.89; H,5.44; Cl,14.73; N,11.64

Found: C,54.49; H,5.53; Cl,14.83; N,11.84.

4(7')-Thioacetoxymethylbenzimidazole (65).

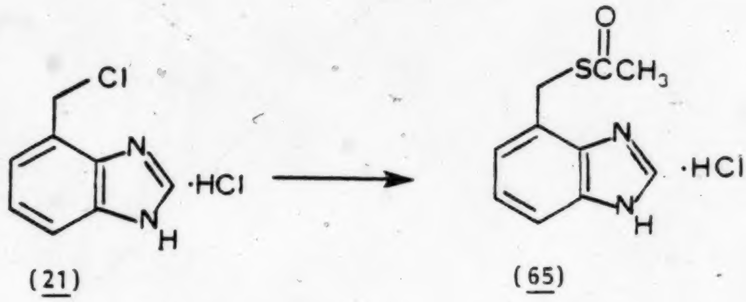

The hydrochloride salt of 4(7')-chloromethylbenzimidazole (21) (1 g, 0.0048 mol) and 3 equivalents of potassium thioacetate were placed in dry THF (100 mL) and stirred at room temperature for 6-7 h. The THF was removed under reduced pressure and the residue washed several times with ether. Dry HCl gas was bubbled through the rapidly stirred combined ether washings and the hydrochloride salt of the thioacetate precipitated out of solution. This was recrystallized from methanol/ether to give 0.6 g (0.0029 mol, 61% yield) of the final product: mp 223-225°C.

IR (KBr) 1690, 1140, 740 cm^{-1}.

NMR $C_{10}H_{10}N_2OS$ (DMSO-d_6,200MHz) δ 2.14(s,3H,CH_3), 3.96(s,2H,CH_2), 7.32(t,1H), 7.86(d of d,1H,J=2Hz,J=8Hz), 7.97(d of d,1H,J=2Hz, J=8Hz), and 8.34(s,1H).

NMR $C_{10}H_{10}N_2OS.HCl$ (DMSO-d_6,100MHz) δ 2.36(s,3H,CH_3), 4.32(s,1H, CH_2), 6.46-6.80(m,3H), and 9.62(s,1H).

Mass spectrum m/e (rel intensity) 206(M^+,37), 164(13), 132(11), 131(100).

Exact mass 206.0513 (calcd for $C_{10}H_{10}N_2OS$, 206.0512).

Anal. Calcd for $C_{10}H_{10}N_2OS\cdot HCl$: C,49.48; H,4.57; N,11.54. Found: C,49.59; H,4.49; N,11.66.

Potassium thioacetate (83).

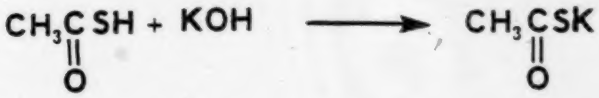

$$CH_3\underset{\displaystyle O}{\underset{\|}{C}}SH + KOH \longrightarrow CH_3\underset{\displaystyle O}{\underset{\|}{C}}SK$$

(83)

Thioacetic acid (6.8 g, 0.089 mol) was added to a solution of KOH (5 g) in H_2O (50 mL) and stirred at room temperature for 2 h.

The aqueous layer was extracted with ether to remove any unreacted thioacetic acid. The water was removed under reduced pressure (rotoevaporation at 70°C) and the crystals washed with 98% ethanol to give 4.1 g (0.036 mol, 40.4% yield) of white needles: mp 248-250°C.

IR (KBr) 1532, 1140 cm^{-1}.

NMR ($DMSO-d_6$, 100MHz) δ 2.10 (s, CH_3).

1-Methyl-4-thioacetoxymethylbenzimidazole (27).

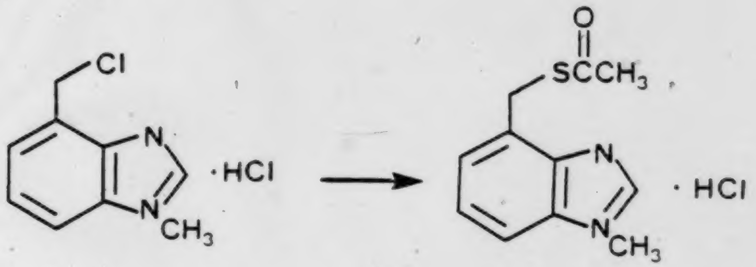

(24) (27)

The hydrochloride salt of 4-chloromethyl-1-methylbenzimidazole (24) (0.6 g, 0.0028 mol) and 3 equivalents of potassium thioacetate were placed in THF (100 mL) and stirred at room temperature for 7 h. The THF was removed under reduced pressure and the residue washed several times with ether. Dry HCl was bubbled through the ethereal solution and the hydrochloride salt of 1-methyl-4-thioacetoxymethylbenzimidazole precipitated out of solution. This was recrystallized from methanol/ether to yield 0.4 g (.00155 mol, 56% yield) of product: mp 214-215°C.

IR ($CHCl_3$ cast) 1690, 1500, 1135, 755, 630 cm^{-1}.

NMR $C_{11}H_{12}N_2OS$ ($CDCl_3$,100MHz) δ 2.32(s,3H,CH_3), 3.80(s,3H,NCH_3),4.57 (s,2H,CH_2), 7.22-7.30(m,3H) and 7.86(s,1H).

NMR $C_{11}H_{12}N_2OS$.HCl (DMSO-d_6,100MHz) δ 2.34(s,3H,CH_3), 4.02(s,3H, NCH_3), 4.50(s,2H,CH_2), 7.48-7.88(m,3H) and 9.47(s,1H).

Mass spectrum m/e (rel intensity) 220(M^+,13), 177(100), 145(71).

Exact mass 220.0668 (calcd for $C_{11}H_{12}N_2OS$, 220.0672).

Anal. Calcd for $C_{11}H_{12}N_2OS \cdot HCl$: C,51.46; H,5.10; N,10.91; Cl,13.81; S,12.49.

Found: C,51.40; H,5.38; N,11.13; Cl,14.09; S,12.57.

1-Acetylbenzimidazole (74).

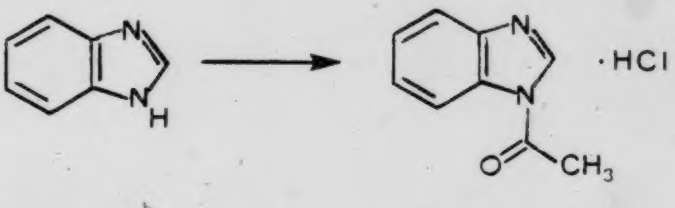

(10a) (74)

Benzimidazole (10a) (1 g, 0.0085 mol) and 1.1 equivalents of acetyl chloride were combined in dry THF (100 mL) and stirred for 1 h. The hydrochloride salt of benzimidazole precipitated and was filtered off. The THF was removed and the residue washed with ether. Any precipitate which formed was filtered off and the ether removed under reduced pressure. The product was recrystallized from benzene/pentane: mp 112-114°C (lit.[76] 113°C). The hydrochloride salt of 1-acetyl-benzimidazole could be made directly by bubbling dry HCl gas through the ethereal solution to precipitate 0.3 g (0.0015 mol, 18% yield) of product: mp 195-196°C.

IR (KBr) 1760, 1545, 1490, 1315, 1245, 1215, 1170, 760 cm^{-1}.

NMR $C_9H_8N_2O \cdot HCl$ (DMSO-d_6,100MHz) δ 2.78(s,3H,CH_3), 7.38-8.26(m,4H) and 9.00(s,1H).

Mass spectrum m/e (rel intensity) 160(M^+,77), 118(100).

Exact mass 160.0635 (calcd for $C_9H_8N_2O$, 160.0632).

1-Acetyl-3-methylbenzimidazolium acetate (76).

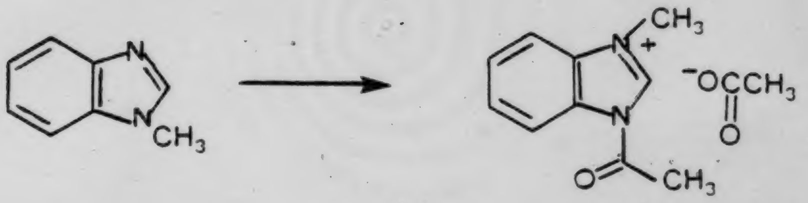

(10b) (76)

The hydrochloride salt of 1-methylbenzimidazole (10b) (1 g, 0.0059 mol) was added to acetic anhydride (10 mL) and stirred at room temperature until all of the solid had dissolved. Dry ether was added until the solution became cloudy and 0.7 g of a mixture of the chloride and acetate salts of 1-acetyl-3-methylbenzimidazole and 1-methylbenzimidazole precipitated.

Due to the extremely labile nature of this salt, separation from the unreacted starting material could not be effected. The mixture was used in the pseudo-first order decomposition kinetic studies. Spectral analyses of the kinetic mixtures after reaction were identical with those made up from N-methylbenzimidazole in the same buffer.

IR (KBr) 1765, 1752, 1570, 1460, 1375, 1330, 1230, 1130, 770 cm^{-1}.

NMR (DMSO-d_6,100MHz) δ 1.92(s,3H,OAc), 2.92(s,3H,NAc), 4.22(s,3H, NMe), 7.70-8.44(m,4H) and 9.68(s,1H).

D_2O hydrolysis yielded 1-methylbenzimidazole.

Mass spectrum m/e (rel intensity) 160(M^+-Me,1.85), 133(23), 131(100).

Exact mass 160.0639 (calcd for $C_{10}H_{11}N_2O$-Me, 160.0637).

1-Acetyl-3-methyltetrahydrobenzimidazolium acetate (77).

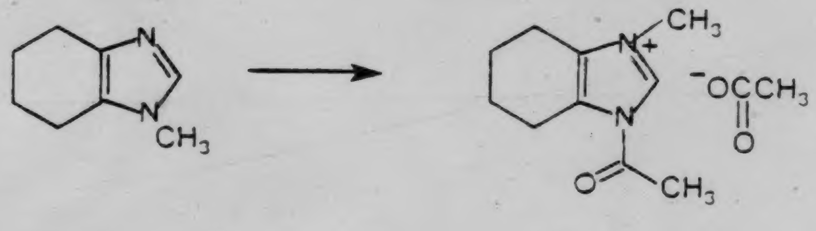

(11b) (77)

The hydrochloride salt of 1-methyltetrahydrobenzimidazole (11b) (1 g, 0.0058 mol) was added to acetic anhydride (10 mL) and stirred at room temperature until all of the solid had dissolved. Dry ether was added until the solution became cloudy and 0.65 g of a mixture of the chloride and acetate salts of 1-acetyl-3-methyltetrahydrobenzimidazole and 1-methyltetrahydrobenzimidazole precipitated. Due to the extremely labile nature of this salt separation from the unreacted starting material could not be effected. The mixture was used for pseudo-first order decomposition kinetics. Spectral analysis of the kinetic mixtures after reaction were identical with those made up from N-methyltetra-hydrobenzimidazole in the same buffer.

IR (KBr) 1641, 1543, 1445, 740, 628 cm^{-1}.

NMR ($DMSO-d_6$,100MHz) δ 1.6-1.9(m,4H), 1.92(s,OAc^-), 1.4-2.0(m,4H), 2.74(s,NAc), 3.86(s,NMe), 8.94(s,1H). Addition of D_2O yields 1-methyltetrahydrobenzimidazole.

Mass spectrum m/e (rel intensity) 164(M^+-Me,0.1), 108(100).

Exact mass 164.0022 (calcd for $C_{10}H_{15}N_2O$-Me, 164.0095).

Kinetic Measurements

All kinetics which were followed spectrophotometrically were monitored using a Cary 210 UV-VIS spectrophotometer equipped with a cell programmer, wavelength programmer and timer accessory. A Rockwell Aim 65 microprocessor was interfaced to the Cary 210 to aid in data collection (Appendix 1). The cell compartments were thermostatted at 25±0.1°C by means of a Colora Ultra Thermostat constant temperature bath. All experiments were carried out using 1 cm path length, 3 mL capacity, matching quartz cuvettes.

Sodium formate/formic acid buffer was used from pH 2.8 to 4.0, sodium acetate/acetic acid from 4.4 to 5.2, MES (2[N-morpholino]ethane sulfonic acid) from 5.6 to 6.4, HEPES (N-2-hydroxyethylpiperazine-N'-2-ethanesulfonic acid) from 6.8 to 7.2, TRICINE (N-tris[hydroxymethyl]methylglycine) from 7.6 to 8.8, CHES (2-N-cyclohexylamino]ethanesulfonic acid) from pH 9.2 to 10.0 and CAPS (cyclohexylaminopropane sulphonic acid) from pH 10.4 to 10.8. Buffer reagents were used as supplied from Sigma.

Water was purified by distilling first from a solution of potassium permanganate followed by three further distillations. The ethanol (95%) was purified by distillation. The tetrahydrofuran (THF) was dried over sodium and distilled immediately before its use.

Unless otherwise stated, all reaction rates were monitored in 31.6% ethanol/H_2O (v/v) with an ionic strength equal to 0.345 M by addition of a calculated amount of KCl (after correction for the amount of ionized buffer) and a [buffer]=0.21 M, in large excess over [catalyst].

The pH of all reaction mixtures was recorded before and after every kinetic measurement using a Radiometer 6K2402B combined electrode in conjunction with a TTT2 titrator to ensure that the pH remained constant throughout the course of the reaction. The electrode was standardized and checked for linearity by using Canlab 4.0 (Potassium Acid Phthalate 10.21 g/l), 7.0 (Sodium Phosphate, dibasic 5.77 g/l, Potassium Phosphate, monobasic 3.54 g/l) and 10.0 (Borate) buffers.

All reactions were checked by repetitive scanning in the ultraviolet/visible and were found to show tight isosbestic points.

All experiments were followed to completion and the pseudo-first order rate constants were obtained from a non-linear least squares analysis of the data (Appendix II). In order to determine that the reactions were indeed first order, plots of $\ln(A_\infty - A_t)$ vs time were checked for linearity over at least three half lives.

Acylation rates were followed under pseudo-first order conditions where [catalyst]=10,20,30 [PNPA] by monitoring the appearance of p-nitrophenoxide at 400 nm. Stock solutions of PNPA as synthesized by the method of Chattaway[80] (mp 79-80°C, lit.[80] 79.5-80° C) were made every few days in 95% ethanol ($1\text{-}2 \times 10^{-4}$ M). All rate constants were determined from at least three reproducible results for each of three different catalyst to PNPA concentrations.

The measurements involving the acylation of cyclohexylmethylthiol (7) with PNPA were monitored in H_2O/EtOH (95%)/THF (64.4/29/6.6) (v/v) with an ionic strength of 0.32 M and a [buffer] = 0.19 M due to the insolubility of cyclohexylmethylthiol in the aqueous ethanol mixture. Otherwise the measurements were executed in the same manner as discussed above.

The kinetic measurements for the acylation of 4(7')-thiomethylbenzimidazole (8a) and 1-methyl-4-thiomethylbenzimidazole (8b) with PNPA were monitored in a similar manner except that all solutions were degassed by bubbling argon through the stock solutions for 30 min before the kinetic run was executed. This was done to prevent air oxidation of the thiol to the corresponding disulfide. Even with this precaution consistent experimental values for k_{obs} at pH > 9.2 were impossible to obtain. From pH 9.6 to 10.8 the curve was extrapolated from the known pKa of the compound (Table 2) as shown in Figure 6. The results from the kinetic experiments for the acylation of PNPA are shown in Tables 3 to 8, 11 and 12. Acylation rates with 4(7')-hydroxymethylbenzimidazole (12a), 1-methylbenzimidazole (11b) and 4-hydroxymethyl-1-methylbenzimid-azole (12b) showed no enhancement over the buffer and hydroxide terms. The k_{obs} vs pH values for all the acylation studies are given in Appendix III.

The measurements monitoring the decomposition of 4(7')-acetoxymethylbenzimidazole (69a), 4-acetoxymethyl-1-methylbenzimid-azole (69b) and benzyl acetate (71) were followed by titrating the liberated acid with a titration assembly consisting of a Radiometer TTT2 titrator and PHA943B titration module in conjunction with a Radiometer 6K2402B combined electrode and recorded as a function of added 0.1000 N NaOH (delivered by a Radiometer ABU12 autoburette) on a Radiometer SBR3 titrigraph. In a typical run 10 mg of 4(7')-acetoxymethylbenzimidazole (69a) were dissolved in 1 mL of ethanol and added to a cell thermostatted at 25°C±0.1 along with 3.0 mL of 0.5 N

KCl. An additional 1 mL of ethanol was added so that the experimental conditions approximated those used for the spectrophotometric measurements as closely as possible. A slow stream of nitrogen was bubbled through the stirred solution as the 0.1000 N NaOH was added. The reactions were followed to completion and the rate constant was obtained from a plot of $\ln(C_{\infty} - C_t)$ vs time where C_{∞} is the total amount of OH^- which had to be added to completely hydrolyze (69a) and C_t is the [OH] added at time t. All rate constants were derived from at least 3 reproducible runs.

The decomposition of benzylthioacetate (70) and 1-methyl-4-thioacetoxymethylbenzimidazole (27) were followed spectrophotometrically at 251 nm and 273 nm respectively. The reactions were checked for buffer catalysis by using 0.21 M, 0.16M, 0.13M and 0.02M buffers which were obtained by dilution of the original 0.3 M buffers with water. The final rate constants, therefore, were obtained by extrapolation of k_{obs} to zero [buffer]. Data were fit to a non-linear least squares program (Appendix 2) and each rate constant was the result of at least three reproducible results.

The decomposition of 4(7')-thioacetoxymethylbenzimidazole (65) was followed titrimetrically at pH's 11.5 and 11.0 as per the method used for compounds (69) and (71) and spectrophotometrically at 250 nm for pH's 10.4 and 10.0 as per the method used for compounds (27) and (70).

The decomposition of 1-acetyl-3-methylbenzimidazolium acetate (76) and 1-acetylbenzimidazole (74) was monitored at 290 nm in buffered solutions. The reaction was checked for buffer catalysis by using 0.21 M and 0.02 M buffers and the final rate constants obtained as per the method used for benzyl thioacetate (70). The rate constants for the decomposition of 1-acetyl-3-methyltetrahydrobenzimidazolium acetate (77) were obtained in an analogous manner by monitoring the reaction at 265 nm.

Product analysis for the kinetic experiments was done either by NMR studies (Varian HA-100-15 spectometer with Fourier Transform modifications provided by a Digilab FTS NMR-3 System) or analysis of UV-VIS spectra (Cary 210 spectrometer). For the second order reactions the catalyst and p-nitrophenylacetate were dissolved in ethanol-d_6 and D_2O/NaOD was added to initiate the reaction. Spectra were taken intermittantly to monitor the changes occurring.

The decomposition of the O and S-acetates were done in the same way without PNPA. The decomposition of the imidazole N-acetyl compounds was followed spectrophotometrically by continuous scans in the UV-VIS and the product analyzed by comparison of the final spectrum with the UV-VIS spectrum of the corresponding NH compound (Figure 18) in the same medium.

pKa Determinations

The pKa determinations were performed in a jacketed cell kept at 25±0.1°C with a Colora Ultra Thermostat constant temperature bath. Carbon dioxide was excluded from the cell by passing a gentle stream of nitrogen through the cell. The pH was recorded as a function of added 0.1000 N NaOH by the method described earlier for 4(7')-acetoxymethylbenzimidazole (69a).

A typical run was performed by adding 3.0 mL of 0.5 N KCl, 1 mL 0.1051 N HNO_3, 1 mL 95% ethanol and 0.025 mmol of the substance to be titrated in 1 mL ethanol to the thermostatted cell (25°C) and titrating with 0.1000 N NaOH.

Each pKa was the average of at least three reproducible runs.

REFERENCES

1. Fife, T. H. Advances in Physical Organic Chemistry 1968, 6,1.

2a. Tsunada, J. N.; Yasunoba, K. T. J. Biol. Chem. 1966, 242, 4610.

b. Wong, R. C.; Liener, I. E. B. B. R. C. 1964, 17,470.

c. Husain, S. S.; Lowe, G. Chem. Commun. 1968, 1387.

d. Castaneda-Agulto, M.; Hernandez, A.; Loaeza, F.; Salazar, W. J. Biol. Chem. 1945, 159, 751.

e. Carpenter, D. C.; Lovelace, F. J. Am. Chem. Soc. 1943, 65, 2364.

f. Lennox, F. G.; Willis, W.J. Biochem. J. 1945, 39,465.

g. Fersht, A. "Enzyme Structure and Mechanism"; W. H. Freeman and Co.: San Francisco, 1977.

h. Mitchell, W. N.; Harrington, W. F. "The Enzymes"; P. D. Boyer, Academic Press: New York, 1971; pp 699-719.

i. Liu, T. Y.; Elliot, S. D. "The Enzymes" ; P. D. Boyer, Academic Press: New York, 1971; pp 609-649.

3. Hartley, B. S.; Massey, V. Ann. Rept. Progr. Chem. 1954, 51, 311.

4. Bender, M. L.; Turnquest, B. W. J. Am. Chem. Soc. 1957, 79, 1652,1656.

5a. Bruice, T. C.; Schmir, G. L. J. Am. Chem. Soc. 1957, 79, 1663.

b. Bruice, T. C.; Schmir, G. L. J. Am. Chem. Soc. 1958, 80, 148.

6. Jencks, W. P. Biochem. Biophys. Acta 1957, 24. 227.

7. Brecher, A. S.; Balls, A. K. J. Biol. Chem. 1957, 227, 845.

8. Brouwer, D. M.; van der Vlugt, M. J.; Havinga, *E. Proc. Koninkl. Ned. Akad. Wetenshep* **1957**, B60, 275.

9. Jencks, W. P.; Carriuolo, J. *J. Am. Chem. Soc.* **1961**, 83, 1743.

10. Bruice, T. C.; Schmir, G. L. *J. Am. Chem. Soc.* **1958**, 80,148.

11. Caplow, M.; Jencks W. P. *Biochem.* **1962**, 1, 883.

12. Kirsch, J. F.; Jencks, W. P. *J. Am. Chem. Soc.* **1964**, 86, 833.

13. Rogers, G. A.; Bruice, T. C. *J. Am. Chem. Soc.* **1974**, 96, 2463.

14. Bruice, T. C.; Sturtevant, J. M. *J. Am. Chem. Soc.* **1959**, 81, 2860.

15. Bruice, T. C. *J. Am. Chem. Soc.* **1959**, 81, 5444.

16. Fife, T. H.; Bamberg, R. J.; Demark, B. R. *J. Am. Chem. Soc.* **1978**, 100, 5500.

17a. Drenth, J.; Janosius, J. N.; Koekoeck, R.; Wolthers, B. "The Enzymes"; P. D. Boyer, Academic Press: New York, 1971, pp 485-499.

b. Drenth, J.; Janosius, J. N.; Wolthers, B. *J. Mol. Biol.* **1967**, 24, 449.

c. Drenth, J.; Janosius, J. N.; Koekoeck, R.; Swen, H. M.; Wolthers, B. *Nature* **1968**, 218, 929.

d. Baker, E.N., *J. Mol. Biol.* **1980**, 141, 441.

18a. Lowe, G. *Phil. Trans. Roy. Soc. London* **1970**, B257, 237.

b. Lowe, G. *Tetrahedron* **1976**, 32, 291.

19a. Brubacker, L. J.; Bender, M. L. J. Am. Chem. Soc. 1966, 88, 5781.

b. Brubacker, L. J.; Bender, M. L. J. Am. Chem. Soc. 1964, 86, 5333.

c. Lowe, G.; Williams, A. Proc. Chem. Soc. 1964, 140.

d. Lowe, G.; Williams, A. Biochem. J. 1965, 96, 189.

e. Storer, A. C.; Murphy, W. F.; Carey, P. R. J. Biol. Chem. 1979, 254, 3163.

20. Lowe, G.; Williams, A. Biochem. J. 1965, 96, 199.

21. Lowe, G.; Yuthavong, Y. Biochem. J. 1971, 124, 117.

22. O'Leary, M. H.; Urberg, M.; Young, A. P. Biochemistry 1974, 13, 2077.

23. Whitaker, J. R.; Bender, M. L. J. Am. Chem. Soc. 1965, 87, 2728.

24. Zannis, V. I.; Kirsch, J. F. Biochemistry 1978, 17, 2669.

25a. Schonbaum, G. R.; Bender, M. L. J. Am. Chem. Soc. 1960, 82, 1900.

b. Lindley, H. Biochem. J. 1960, 74, 577.

c. Olgilvie, J. W.; Tildon, J. T.; Strauch, B. S. Biochemistry, 1964, 3, 754.

d. Fersht, A. R. J. Am. Chem. Soc. 1971, 93, 3504.

e. Bennett, R. E.; Jencks, W. P. J. Am. Chem. Soc. 1969, 91, 2358.

f. Whitaker, J. R. J. Am. Chem. Soc. 1962, 84, 1900.

g. Jencks, W. P.; Carriuolo, J. J. Biol. Chem. 1959, 234, 1280.

h. Lienhard, G. E.; Jencks, W. P. *J. Am. Chem. Soc.* **1966**, 88, 3982.

i. Bennett, R. E.; Jencks, W. P. *J. Am. Chem. Soc.* **1967**, 89, 5963.

26. Sluyterman, L. A. AE.; Wijdenes, J. *Eur. J. Biochem.* **1976**, 71, 383.

27. Nicholson, E. M.; Shafer, J. A. *Arch. Biochem. Biophys.* **1980**, 200, 560.

28a. Polgar, L. *F. E. B. S. Letts.* **1974**, 47, 15.

b. Polgar, L. *Eur. J. Biochem.* **1973**, 33, 104.

c. Polgar, L. *Int. J. Biochem.* **1977**, 8, 171.

29. Lewis, S. D.; Johnson, F. A.; Shafer, J. A. *Biochemistry* **1976**, 15, 5009.

30. Lewis, S. D.; Johnson, F. A.; Shafer, J. A. *Biochemistry* **1981**, 20, 44.

31. Lewis, S. D.; Johnson, F. A.; Shafer, J. A. *Biochemistry* **1981**, 20, 48.

32. Lewis, S. D.; Johnson, F. A.; Shafer, J. A. *Biochemistry* **1981**, 20, 52.

33. Lewis, S. D.; Johnson, F. A.; Ohno, A. K.; Shafer, J. A. *J. Biol. Chem.* **1978**, 253, 5080.

34a. Fink, A. *Acc. of Chem. Res.* **1977**, 10, 233.

b. Angelides, K. J.; Fink, A. *Biochemistry* **1978**, 17, 2659.

c. Angelides, K. J.; Fink, A. *Biochemistry* **1979**, 18, 2355.

d. Angelides, K. J.; Fink, A. Biochemistry 1976, 15, 5287.
e. Gwyn, C.; Fink, A. Biochemistry 1974, 13, 1190.
f. Angelides, K. J.; Fink, A. Biochemistry 1979, 18, 2363.

35a. Anderson, B. M.; Cordes, E. H.; Jencks W. P. J. Biol. Chem. 1961, 236, 455.
b. Milstien, J. B.; Fife, T. H. J. Am. Chem. Soc. 1968, 90, 2164.

36a. Felton, S. M.; Bruice, T. C. Chem. Commun. 1968, 908.
b. Felton, S. M.; Bruice, T. C. J. Am. Chem. Soc. 1969, 91, 6721.

37. Fife, T. H.; M^{c}Mahon, D. M. J. Org. Chem. 1970, 35, 3699.

38a. Jencks, W. P.; Carriuolo, J. J. Biol. Chem. 1959, 234, 1272.
b. Wolfenden, R.; Jencks W. P. J. Am. Chem. Soc. 1961, 83, 4390.
c. Marburg, S. M.; Jencks W. P. J. Am. Chem. Soc. 1962, 84, 232.
d. Huskey, W. P.; Hogg, J. L. J. Org. Chem. 1981, 46, 53.

39. Jones, J. B.; Taylor, K. E. Canad. J. Chem. 1977, 55, 1653.

40. James, C. W.; Kenner, J.; Stubbings, W. V. J. Chem. Soc. 1920, 117, 775.

41. Vogel, A. I. "Practical Organic Chemistry"; Longman: London, 1974.

42. Phillips, M. A. J. Am. Chem. Soc. 1928, 49, 2393.

43. Butula, I. Croatica Chimica Acta 1973, 45, 297.

44. Harnish, D. P.; Tarbell, D. S. Analytical Chemistry 1949, 21, 968.

45. Fieser, L. F.; Fieser, M. "Reagents for Organic Synthesis", Vol. I; 1967, 1180.

46. Finklestein, *H. Ber.* **1910**, 43, 1528.

47. Utaka, M.; Koyama, J.; Takeda, A. *J. Am. Chem. Soc.* **1976**, 98, 984.

48. Pinkney, P. S. *Org. Syn. Coll. Vol. II* **1943**, 116.

49. Ruest, L.; Blouin, G.; Deslongchamps, P. *Synth. Comm.* **1976**, 6, 169.

50. Tanaka, M.; Shimodaura, T.; Fuga, N. *Chem. Abstr.* **1978**, 89, 163471.

51. Taylor, E. C., Ehrhart, W. A.; Kawanisi, M. *Org. Syn. Coll. Vol. V.* **1973**, 582.

52. Corey, E. J.; Gras, J. L.; Ulrich, P. *Tetrahedron Lett.* **1976**, 11, 809.

53. Grummitt, O.; Budewitz, E. P.; Chudd, C. C. *Org. Syn. Coll. Vol. IV.* **1963**, 748.

54. Curtis, N. J.; Brown, R. S. *J. Org. Chem.* **1980**, 45, 4038.

55. Breslow, R. Private communication.

56. Hammett, L. P. *Chem. Rev.* **1933**, 13, 61.

57. Harned, H. S.; Robinson, R. A. "Multicomponent Electrolyte Solutions"; Pergamon Press: New York, 1968.

58. Bates, R. G. "Determination of pH, Theory and Practice"; John Wiley and Sons: New York, 1965.

59. Lochon, P.; Schoenleber, J. *Tetrahedron* **1976**, 32, 2023.

60. Bender, M. L. "Mechanisms of Homogeneous Catalysis from Protons to Proteins"; Wiley Interscience: New York, 1971.

61. Jencks, W. P. "Catalysis in Chemistry and Enzymology"; McGraw-Hill Inc.: New York, 1969, pp 250.

62a. Schneider, V. F. *Z. Physiol. Chem.* **1967**, 348, 1034.
  b. Schneider, V. F.; Wenck, H. *Z. Physiol. Chem.* **1969**, 350, 1653.

63. Laitenen, H. A.; Harris, W. E. "Chemical Analysis"; McGraw-Hill Inc.: New York, 1975, pp 45-46.

64a. Rabenstein, D. L.; Sayer, T. L. *Analytical Chemistry* **1976**, 48, 1141.
  b. Rabenstein, D. L.; Sayer, T. L. *Canad. J. Chem.* **1976**, 54, 3392.
  c. Rabenstein, D. L.; Greenbur[illegible], M. S.; Evans, C. A. *Biochemistry* **1977**, 10, 977.
  d. Coates, E.; Marsden, C. G.; Rigg, B. *Trans. Faraday Soc.* **1969**, 65, 3032.
  e. Benesch, R. E.; Benesch, R. *J. Am. Chem. Soc.* **1955**, 77, 5877.
  f. Ryklan, R. L.; Schmidt, C. L. A. *Arch. Biochem.* **1944**, 5, 89.
  g. Wrathall, D. P.; Izatt, R. M.; Christensen, J. J. *J. Am. Chem. Soc.* **1964**, 86, 4779.

h. Wrathall, D. P.; Izatt, R. M.; Cristensen, J. *J. Am. Chem. Soc.* **1965**, 87, 5809.

i. Edsall, J. T.; Martin, R. B.; Hollingworth, B. R. *Proc. Natl. Acad. Sci. USA* **1958**, 44, 505.

65. Hershfeld, R.; Schmir, G. L. *J. Am. Chem. Soc.* **1973**, 95, 3994.

66. Fedor, L. R.; Schmir, G. L. *J. Am. Chem. Soc.* **1965**, 87, 4138.

67. Barnett, R.; Jencks, W. P. *J. Org. Chem.* **1969**, 34, 2777.

68. Patel, G.; Satchell, R. S. *J. Chem. Soc. Perken II* **1978**, 452.

69. Patterson, J. F.; Huskey, W. P.; Venkatasubban, K. S.; Hogg, J. C. *J. Org. Chem.* **1978**, 43, 4935.

70. Fife, T. H.; Demark, B. R. *J. Am. Chem. Soc.* **1979**, 101, 7381.

71. Noda, L. H.; Kuby, S. A.; Lardy, H. A. *J. Am. Chem. Soc.* **1953**, 75, 913.

72a. Schwyzer, R. *Helv. Chem. Acta* **1953**, 54, 414.

b. Hawkins, P. J.; Tarbell, D. S. *J. Am. Chem. Soc.,* **1953**, 75, 2982.

c. Wieland, T.; Lang, H. U.; Lieback, D. *Ann.* **1955**, 597, 227.

d. Bruice, T. C.; Fedor, L. R. *J. Am. Chem. Soc.* **1964**, 86, 4880.

e. Bruice, T. C.; Fedor, L. R. *J. Am. Chem. Soc.* **1964**, 86, 4117.

73. Bendall, M. R.; Lowe, G. *Eur. J. Biochem.* **1976**, 65, 481.

74a. Rylander, P. N.; Tarbell, D. S. *J. Am. Chem. Soc.* **1950**, 72, 3021.

b. Morse, B. K.; Tarbell, D. S. *J. Am. Chem. Soc.* **1952**, 74, 416.

75. Staab, H. A. *Ber.* **1957**, 90, 1320.

76. Hoffmann, K. " The Chemistry of Heterocyclic Compounds: Imidazole and its Derivatives "; Interscience Publishers: New York, 1953.

77. Handbook of Physics and Chemistry, Robert C. Weast, Ed., CRC Press, Inc. 1969-1970, C-322.

78. CRC Atlas of Spectral Data and Physical Constants, J.G. Graselli, W.M. Ritchey, Ed. CRC Press, Inc. 1975.

79. Zervas, L.; Photaki, I.; Ghelis, N. *J. Am. Chem. Soc.* **1963**, 85, 1337.

80. Chattaway, F.D. *J. Chem. Soc.* **1931**, 134, 2495.

APPENDIX I

Instrumentation

All the spectrophotometric kinetic measurements were run on a Varian Cary 210 spectrometer equipped with a cell programmer, wavelength programmer and timer accessory. The spectrophotometer was interfaced to a Rockwell Aim 65 microprocessor.

It was necessary to collect and store the numbers representing the absorbance of the molecule under study vs time. The Digital Interface Port of the Cary 210 spectrometer contains a 72-bit output register arranged in an 18-word deep, 4-bit wide shift register configuration. Upon command from the peripheral controller this data is clocked out of the shift register and into the D.I.P. output buffers in 18 serial words composed of 4 parallel bits or nybbles. The 4-bit word or "nybble" is then available on lines "BCD1" through "BCD8". All numeric data is in binary coded decimal (BCD) format.

Only the nybbles which contained the cell-programmer sample position, the sign and position of the decimal place and the digits of the absorbance were of interest.

The D.I.P. operates in a handshake mode in which the D.I.P. is the slave and the data stream is under the control of the peripheral controller.

The interfacing was done in the following manner. The chopper within the spectrometer produces a "SYNCH" pulse every 61 ms which is 5 ms in duration. The data must be collected before another "SYNCH" pulse causes a "RESET" which starts the collection over again with the first 4-bit word. Therefore, the handshake operation for a particular transfer of information began with a search for the "SYNCH" pulse.

The other status and input/output lines included:

1) PRINT: "PRINT" comes from the timer accessory after every record interval and synchronizes the taking of data with the pen drop on the strip chart recorder.

2) CNTL: A transition from high to low starts an input/output data transfer.

3) FLAG: A transition from high to low tells the peripheral controller that the D.I.P. has completed its half of the input/output transfer that was started by "CNTL" becoming active. "FLAG" changes state from low to high to signify that the D.I.P. is ready for another I/O cycle.

4) FIRST: When "FIRST" goes low the first 4-bit word of the 18-word block is being transferred from the D.I.P. on lines "BCD1" through "BCD8" during this particular I/O cycle.

5) I/O: When "I/O" is low the data is being inputted into the peripheral controller.

The timing diagram is illustrated in Figure 20.

Electronically, all input lines were passed through a TTL 7404 inverter equipped with a 5 volt resistor. The output lines "I/O" and "CNTL" were buffered through 7404 inverters.

Port B on the 6522 I/O chip was used as control and Port A as the data collector. In Port B bits 0 and 1 were used as output for "CNTL" and "I/O" respectively and bits 4-7 were used as input for "SYNCH", "PRINT", "FIRST" and "FLAG". "BCD1" through "BCD8" were hooked up to PA0 to PA3.

Figure 20

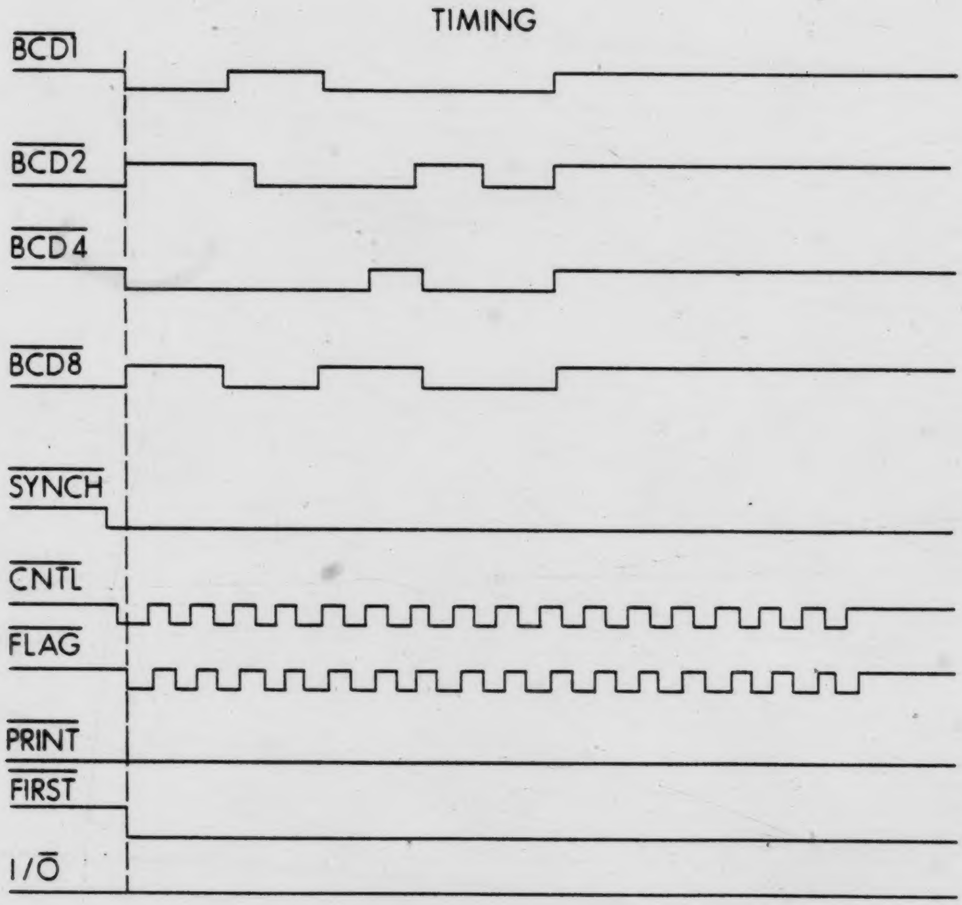
TIMING
$\overline{BCD1}$
$\overline{BCD2}$
$\overline{BCD4}$
$\overline{BCD8}$
$\overline{SYNCH}$
$\overline{CNTL}$
$\overline{FLAG}$
$\overline{PRINT}$
$\overline{FIRST}$
$I/\overline{O}$

The data collection sequence was controlled by the machine language program. Step 1 checked for a "PRINT" pulse which coordinated the collection of our data with the pen drop on the strip chart recorder. Step 2 checked for the transition of a "SYNCH" pulse from high to low which meant we were at the beginning of a 61 ms period in which the data was valid. Step 3 checked for "FIRST" to tell us when the first 4-bit word was on line. Step 4 pushes "CNTL" low and waits for "FLAG" to go low. Once "FLAG" is low the data was collected. Step 5 pushes "CNTL" high and waits for "FLAG" to go high which signifies that the D.I.P. is ready to undergo another I/O cycle. The "I/O" line is kept low as the D.I.P. was used only to input into the peripheral device. This cycle is repeated until all 18 4-bit words have been collected. The machine language program discards any of the nybbles which are unwanted and transfers control to BASIC where the mathematical manipulations are performed.

KINETIC DATA ACQUISITION

```
BASIC                               COMMENTS

5 DIM M(250)
6 DIM S(5)
7 DIM H(150)
10 DIM B(5)
20 PRINT"INPUT # RUNS"
30 INPUT R
31 W=R
40 PRINT"INPUT # CELLS"
50 INPUT C
60 POKE 8961,R                      Number of runs in $2301
70 POKE 8962,C                      Number of cells in $2302
80 PRINT"INPUT CONC OF CELLS"
90 FOR N=1 TO C
100 INPUT B(N)
110 NEXT
120 PRINT"INPUT SCAN TIME IN MINUTES"
130 INPUT D1
140 POKE 8963,D1                    Scan time in $2303
150 PRINT"INPUT SAMPLING INTERVAL"
160 INPUT D2
170 POKE 8964,D2                    Sampling interval in $2304
180 D3=D1*D2
190 POKE 8965,D3
200 PRINT"NUMBER OF RUNS =";R
210 PRINT"NUMBER OF CELLS =";C
220 FOR N=1 TO C
221 PRINT"CELL";N;"CONC";B(N)
222 NEXT
223 PRINT"INTERVAL BETWEEN POINTS IS ";D3
224 PRINT"ENTER 1 FOR MISTAKE ELSE 9"
225 INPUT M
226 IF M=1 THEN 20
227 POKE 04,00                      Lower byte of memory location of
                                    machine language program
228 POKE 05,32                      Upper byte of memory location of
                                    machine language program
229 X=USR(1)                        Jumps to machine language program
230 IF R<51 THEN D5=1
231 IF R>50 THEN D5=R/50
232 Q=PEEK(8417)*256                High byte of last memory location
                                    used (20E1)
233 B=PEEK(8979)                    Low byte of last memory location
                                    (2313)
234 J=1
235 U=1
240 FOR E=1 TO (C*8) STEP 8
241 K=Q+B+E-1
251 G=K+7
252 S(U)=PEEK(G)
255 U=U+1
260 L=K+6
270 FOR N=K TO 24575 STEP (C*8*D5);24575 = 5FFF
280 X=PEEK(N)
290 X=X+PEEK(N+1)*10
300 X=X+PEEK(N+2)*100               Combines digits of absorbance
310 X=X+PEEK(N+3)*1000
320 X=X+PEEK(N+4)*10000
```

```
    BASIC                                    COMMENTS

330 Y=PEEK(L)
340 IF Y=1 THEN X=X/100000
350 IF Y=2 THEN X=X/10000
360 IF Y=3 THEN X=X/1000                Places decimal point in correct
370 IF Y=4 THEN X=X/100                 place
380 IF Y=5 THEN X=X/10
390 M(J)=X
410 L=L+(C*8*D5)
420 J=J+1

430 NEXT N
440 NEXT E
470 FOR F=1 TO W STEP D5
480 H(F)=D3*F                           Time is claculated
490 NEXT
501 K=W
510 T=(W/D5)+1
530 FOR X=1 TO (C-1)
540 O=1
550 FOR JJ=1 TO K/D5
560 RR=M(O+(W/D5))-M(JJ)                The baseline is subtracted from the
                                        cell absorbance
570 M(T)=RR
590 T=T+1
600 O=O+1
610 NEXT
620 W=W+R
630 NEXT
631 PRINT" "
632 PRINT" "
640 AA=1+(R/D5)
650 FOR U=2 TO C
660 PRINT"CELL#";S(U)
670 PRINT"ABS.     ";"TIME(MINS.)"
680 FOR F=R TO 1 STEP -D5               Data is printed out
690 PRINT M(AA),H(F)
700 AA=AA+1
710 NEXT
711 PRINT" "
720 NEXT
730 PRINT "ENTER 1 FOR PP ELSE 9"
740 INPUT H1
750 IF H1=9 THEN 800
760 AA=1+(R/D5):FOR U=2 TO C
770 FOR F=R TO 1 STEP -D5
780 PRINT M(AA),H(F)
790 AA=AA+1:NEXT:NEXT
800 END
```

ASSEMBLER LANGUAGE PROGRAM

```
*=$2000
LDA #$00
STA $2314                 Sets up space for the run counter
LDA #$00
STA $2319                 Sets up space for the run counter
LDY #00
LDA #00
STA $A003                 Sets up Port A for all input
LDA #03
STA $A002                 Sets up Port A so that Bits 0, 1 are output
LDA #$01
STA $A000                 Sets up I/O low and CNTL high
JSR PRINT
F10 LDA $2304             2304 contains the sampling interval
STA $2310
F9 DEC $2310
BEQ Z1
LDA $2302                 2302 contains the number of cells
STA $2308
K6 JSR SETP
JSR SYNCH
JSR FIRST
JSR SSTOR
DEC $2308
BNE K6
JMP F9
Z1 LDA $2302
STA $2308
JSR $E9F0                 Monitor subroutine which prints a black line
JSR NUM
C2 JSR SETP
JSR SYNCH
JSR FIRST
LDX #$FF
LDA $A001                 Loads data from Port A
STA $2900,X               Stores the first 4-bit word
DEX
LDA #$11
STA $2307
Z7 JSR SETUP
LDA $A001
STA $2900,X               Stores the next 17 4-bit words of data
DEX
JSR AGAIN
DEC $2307
BNE Z7
JSR TRANS
JSR CONV
JSR RUN
DEC $2308
BNE C2
DEC $2301                 2301 contains the number of runs to be
                          executed
BNE F10
STY $2313                 Contains last memory location where data is
                          stored
RTS
```

```
SYNCH LDA $A000               Subroutine Synch waits for a Synch pulse
AND #$10
BEQ SYNCH
QQ1 LDA $A000
AND #$10
BNE QQ1
RTS
SETUP LDA #00                 Pushes control low
STA $A000
Z8 LDA $A000                  Waits for flag to go low
BMI Z8
RTS
AGAIN LDA #01                 Pushes control high
STA $A000
Z9 LDA $A000                  Waits for flag to go high
BPL Z9
RTS
TRANS LDX #06                 Selects 4-bit words of the 18 we want
C1 LDA $29F6,X
STA $29A0,X
DEX
BNE C1
LDA $29FF
STA $29A8
LDA $29A6                     29A6 contains sign plus decimal place
STA $29A7
LDA $29A6
CLC
AND #$08
BEQ D1
LDA #$2B
STA $29A6                     Loads 29A6 with "+"
JMP EE1
D1 LDA #$2D
STA $29A6                     Loads 29A6 with "-"
EE1 LDA $29A7
AND #$07                      Clears bit 4 if set
STA $29A7
LDX #$08
F1 LDA $29A0,X
DEY
F2 STA $5F00,Y
BNE F3
DEC F2+2                      Changes page when Y=0
F3 DEX
BNE F1
RTS
CONV LDX #$05                 Converts 4-bit words to ASCII for printout
J1 LDA $29A0,X
CLC
AND #$0F
ADC #$30
STA $29A0,X
DEX
BNE J1
LDA $29A8,X
AND #$0F
ADC #$30
```

```
STA $29A8
RTS
PRINT LDA #$52                Prints "R"
JSR $E97A
LDA #$55                      Prints "U"
JSR $E97A
LDA #$4E                      Prints "N"
JSR $E97A
LDA #$23                      Prints "#"
JSR $E97A
LDA #$20
JSR $E97A
LDA #$20
JSR $E97A
LDA #$20
JSR $E97A
LDA #$20
JSR $E97A
LDA #$20
JSR $E97A
LDA #$20
JSR $E97A
LDA #$20
JSR $E97A
LDA #$20
JSR $E97A
LDA #$43                      Prints "C"
JSR $E97A
LDA #$45                      Prints "E"
JSR $E97A
LDA #$4C                      Prints "L"
JSR $E97A
LDA #$4C                      Prints "L"
JSR $E97A
LDA #$23                      Prints "#"
JSR $E97A
LDA #$20
JSR $E97A
LDA #$20
JSR $E97A
LDA #$20
JSR $E97A
LDA #$20
JSR $E97A
LDA #$20
JSR $E97A
LDA #$20
JSR $E97A
LDA #$20
JSR $E97A
LDA #$20
JSR $E97A
LDA #$41                      Prints "A"
JSR $E97A
LDA #$42                      Prints "B"
JSR $E97A
LDA #$53                      Prints "S"
```

```
JSR $E97A
LDA #$2E                  Prints "."
JSR $E97A
RTS
FIRST LDA $A000           Waits for "First" bit to be set
AND #$40
BEQ FIRST
RTS
SETP LDA $A000            Waits for "Print" bit to be set
AND #$20
BEQ SETP
RTS
SSTOR LDA #$11            Skips storing the data if interval >1
STA $2307
K4 JSR SETUP
LDA $A001
DEX
JSR AGAIN
DEC $2307
BNE K4
RTS
NUM SED                   Subroutine run counts the runs
LDA $2314                 Sets dec. counter and stores run # in 2314
CLC
ADC #01
STA $2314
CLD
LDA $2314
CMP #$00
BNE EE3
LDA #01                   If count >99 location 2319 is loaded with #01
STA $2319
EE3 RTS
RUN LDA $2319             Contents of 2319 are changed to ASCII
CLC
ADC #$30
JSR $E97A                 Prints ASCII number
LDA $2314                 Contents of 2314 are changed to 2 ASCII #'s.
CLC
AND #$F0
ROR A
ROR A
ROR A
ROR A
ADC #$30
JSR $E97A
LDA $2314
CLC
AND #$0F
ADC #$30
JSR $E97A
LDA #$20
JSR $E97A
LDA #$20
JSR $E97A
LDA #$20
JSR $E97A
```

```
LDA #$20
JSR $E97A
LDA #$20
JSR $E97A
LDA #$20
JSR $E97A
LDA #$20
JSR $E97A
LDA #$20
JSR $E97A
LDA #$20
JSR $E97A
LDA $29A8
JSR $E97A
LDA #$20
JSR $E97A
LDA #$20
JSR $E97A
LDA #$20
JSR $E97A
LDA #$20
JSR $E97A
LDA #$20
JSR $E97A
LDA #$20
JSR $E97A
LDA #$20
JSR $E97A
LDA #$20
JSR $E97A
LDA #$20
JSR $E97A
LDA #$20
JSR $E97A
LDA #$20
JSR $E97A
LDA #$20
JSR $E97A
LDA $29A6                      Prints the cell #
JSR $E97A
LDA $29A5                      Prints first digit of absorbance
JSR $E97A
LDA #$2E                       Prints decimal point
JSR $E97A
LDX #$04
L1 LDA $29A0,X                 Prints remaining digits of absorbance
JSR $E97A
DEX
BNE L1
JSR $E9F0
RTS
END
```

Appendix II

Non-Linear Least Squares Analysis

1). The numbers representing the absorbance vs time are read from the paper tapes generated by the Rockwell Aim 65 Microprocessor.

```
203          PNPA + 10 EQUIV. THEME 8.0
203.5         3 50 1 10 .001
204           .009 0 -1
205          1.355      200
206          1.3487     196
207          1.3399     192
208          1.3324     188
209          1.3227     184
210          1.3151     180
211          1.3059     176
212          1.2958     172
213          1.2871     168
214          1.2776     164
215          1.2669     160
216          1.2573     156
217          1.2461     152
218          1.2346     148
219          1.2242     144
220          1.2121     140
221          1.2        136
222          1.1868     132
223          1.1745     128
224          1.1609     124
225          1.1475     120
226          1.1328     116
227          1.1183     112
228          1.1032     108
229          1.0878     104
230          1.071      100
231          1.0543     96
232          1.0364     92
233          1.0183     88
234          1.0004     84
235          .9802      80
236          .9608      76
237          .9407      72
238          .9193      68
239          .8965      64
240          .8743      60
241          .8503      56
242          .8251      52
243          .8011      48
244          .774       44
245          .7472      40
246          .7197      36
247          .6918      32
248          .6615      28
249          .6299      24
250          .5976      20
251          .5643      16
252          .5286      12
253          .4899      8
254          .4468      4
```

2). A non-linear least squares fit is executed on the data to determine the rate constant.

```
1        $RUN *WATFIV SCARDS=LSQ3PAR(2,208)+MINUS8 8=PLOTIP(LAST+1) 6=*PRINT*
1.5      $SOURCE *MSOURCE*
2        /COMPILE NOWARN NOEXT
3        C
4        C PROGRAM FOR 3 PARAMETER MODEL ABS(T)=ABS(*)+(ABS(O)-ABS(*))*EXP(-K*T)
5              IMPLICIT REAL*8(A-H,O-Z)
6              REAL*8 BETA(10),C(10),D(10,10),DINV(10,10),DER(10),
7             1     Y(200),FSAVE(200),STDDEV(10),DEL(10),X(10,200)
8             2     ,YIN(200),TITLE(10)
9              LOGICAL DONE
9.2            WRITE(8,4222)
9.4       4222 FORMAT('5.0     5.0')
10          10 READ 2223, TITLE
11        2223 FORMAT(10A8)
12             READ,NPAR,NPTS,NVAR,NMAX,EPS
13             READ,(BETA(I),I=1,NPAR)
14             READ,(YIN(I),(X(J,I),J=1,NVAR),I=1,NPTS)
15             DO 5 I = 1 , NPTS
16           5 Y(I) = YIN(I)
17     C
18     C        A RUN-TIME FORMAT IS USED HERE TO OUTPUT THE TABLE OF
19     C        X, Y, YCALC, Y-YCALC  AT LINE 51
20     C
21             WRITE(6,1000)TITLE,NPAR,NPTS,NVAR,NMAX,EPS
22             WRITE(8,2224)NPTS,TITLE
22.5      2224 FORMAT(I3/10A8)
24             WRITE(6,1010)(BETA(K),K=1,NPAR)
25             WRITE(6,1015)
26             DO 15 I = 1 , NPTS
28          15 WRITE(6,2222) (X(J,I),J=1,NVAR),Y(I)
29        2222 FORMAT(F10.2,3F10.5)
30             ITER = 0
31     C
32     C        SET THE C-VECTOR AND THE D-MATRIX TO ZERO.
33     C
34          20 DO 30 K = 1 , NPAR
35             C(K) = 0.000
36             DO 30 IS = K , NPAR
37             D(IS,K) = 0.000
38          30 CONTINUE
39             DO 50 I = 1 , NPTS
40     C
41     C        GET VALUE OF FUNCTION AND DERIVATIVES AT THE I-TH POINT.
42     C
43             DI=Y(I)-FCALC(BETA,X(1,I),DER)
44     C
45     C        USE THESE VALUES TO COMPUTE APPROPRIATE TERMS IN SUMMATIONS
46     C        AND STORE THE RESULTS IN THE C-VECTOR AND THE LOWER HALF OF
47     C        THE D-MATRIX.
48     C
49             DO 40 K = 1 , NPAR
50             C(K) = C(K) + DI*DER(K)
51             DO 40 IS = K , NPAR
52          40 D(IS,K)=D(IS,K) + DER(IS)*DER(K)
53          50 CONTINUE
54     C
55     C        COPY LOWER OFF-DIAGONAL ELEMENTS ACCROSS TO UPPER OFF-DIAGONAL.
56     C
57             DO 60 K = 1 , NPAR
58             DO 60 IS=K,NPAR
```

```
   60 D(K,IS)=D(IS,K)
C
C      INVERT D.
C
      CALL GJINV(NPAR,10,D,DINV)
C
C      COMPUTE THE INCREMENTS TO THE PARAMETERS.
C
      DO 80 K = 1 , NPAR
      DI = 0.0D0
      DO 70 IS = 1 , NPAR
   70 DI = DI + DINV(K,IS)*C(IS)
   80 DEL(K)=DI
      ITER = ITER + 1
      WRITE(6,1020)ITER,(DEL(K),K=1,NPAR)
      DONE = .TRUE.
C
C      ADD INCREMENTS TO PARAMETERS AND TEST FOR CONVERGENCE.
C
      DO 90 K = 1 , NPAR
      BETA(K)=BETA(K)+DEL(K)
      IF(DABS(BETA(K)*EPS).LT.DABS(DEL(K))) DONE = .FALSE.
   90 CONTINUE
      WRITE(6,1030)(BETA(K),K=1,NPAR)
      IF((.NOT.DONE).AND.(ITER.LT.NMAX)) GO TO 20
      SIGY = 0.0D0
      WRITE(8,9999) BETA(2)
 9999 FORMAT(E16.8)
      DO 92 I=1,NPTS
   92 WRITE(8,2222) X(1,I),Y(I)
C
C      COMPUTE THE VARIANCE AND STANDARD DEVIATION IN Y.
C
      DO 95 I = 1 , NPTS
      FSAVE(I) = FCALC(BETA,X(1,I),DER)
   95 SIGY = SIGY + (Y(I) - FSAVE(I))**2
      SIGY = SIGY/DFLOAT(NPTS-NPAR)
C
C      COMPUTE STANDARD DEVIATIONS IN EACH OF THE PARAMETERS.
C
      DO 98 K = 1 , NPAR
   98 STDDEV(K) = DSQRT(SIGY*DINV(K,K))
      WRITE(6,1040)NPAR,NPTS,ITER
      WRITE(6,1050)(BETA(K),STDDEV(K),K=1,NPAR)
      WRITE(6,1060)
      WRITE(6,2222) ((X(J,I),J=1,NVAR),Y(I),FSAVE(I),Y(I)-FSAVE(I)
     1             ,I = 1 , NPTS)
      GO TO 10
 1000 FORMAT('1',10A8//
     A  ' NON-LINEAR LEAST SQUARES ANALYSIS USING A MODEL '
     1/'DABS(T)=ABS(*)+(ABS(0)-ABS(*))*EXP(-K*T)'/
     1     ,' WITH',I3,' PARAMETERS'//' THERE ARE',I4,' DATA POINTS'
     2     ,' AND',I3,' INDEPENDENT VARIABLES.'//' ITERATIONS ARE'
     3     ,' CONTINUED UNTIL',I3,' ITERATIONS HAVE BEEN PERFORMED'
     4/' OR THE RELATIVE CORRECTIONS TO THE PARAMETERS ',
     5     'FALL BELOW',1PD12.4)
 1010 FORMAT(///' THE INITIAL VALUES OF THE PARAMETERS ARE:'//
     1     (10(1PD12.4)))
 1015 FORMAT(///' DATA TO BE FIT TO THIS MODEL BY LEAST SQUARES ROUTINE',
     1/ ' LISTED BY COLUMNS IN THE ORDER T(I),ABS(I)')
 1020 FORMAT(//' ITERATION #',I2/' CORRECTIONS TO PARAMETERS:'
     1      (10(1PD12.4)))
 1030 FORMAT(12X,'NEW PARAMETERS:'(10(1PD12.4)))
 1040 FORMAT('1RESULTS OF NON-LINEAR LEAST-SQUARES ANALYSIS WITH',
     1      ' A MODEL CONTAINING',I3,' PARAMETERS ON A DATA SET OF'
     2      ,I3,' POINTS'//I5,' ITERATIONS PERFORMED')
 1050 FORMAT(///T18,'PARAMETER',T38,'STD. DEV.'//
     1' RATE CONSTANT',T15,1PD13.5,D20.5/
     2' A(*)              ',T15,D13.5,D20.5/
     3' A(0)-A(*)',T15,D13.5,D20.5)
 1060 FORMAT(///' TABLE OF OBSERVED AND CALCULATED Y-VALUES.'
     1//'  LISTED BY COLUMNS IN THE ORDER:  X(1,I), X(2,I),...'
     2,' X(NVAR,I), YOBS(I), YCALC(I), (YOBS(I)-YCALC(I)'/)
 1005 FORMAT(10A8)
      END
      SUBROUTINE GJINV(N,NDIM,A,B)
      IMPLICIT REAL*8(A-H,O-Z)
      DIMENSION A(NDIM,NDIM),B(NDIM,NDIM)
      DIMENSION IPVOT(100),INDEX(2,100)
      EQUIVALENCE (IROW,JROW),(ICOL,JCOL)
      DET=1.0D0
      DO 20 J= 1,N
      DO 10 I = 1 , N
   10 B(I,J) = A(I,J)
   20 IPVOT(J)=0
      DO 170 I=1,N
C     FOLLOWING 12 STATEMENTS FOR SEARCH FOR PIVOT ELEMENT
      PIVOT = 0.0D0
      DO 70 J=1,N
      IF(IPVOT(J).EQ.1) GO TO 70
   30 DO 60 K=1,N
      IF(IPVOT(K)-1) 40,60,170
   40 IF(DABS(PIVOT).GE.DABS(B(K,J))) GO TO 60
   50 IROW=J
      ICOL=K
      PIVOT = B(K,J)
   60 CONTINUE
   70 CONTINUE
      IPVOT(ICOL)=IPVOT(ICOL)+1
      IF(IPVOT(ICOL).LE.1)  GOTO 80
      WRITE(6,1000) N
 1000 FORMAT(16H MATRIX SINGULAR,10X,12HDIMENSION = ,I3)
      GOTO 200
C     FOLLOWING 15 STATEMENTS TO PUT PIVOT ELEMENT ON DIAGONAL
   80 IF(IROW.EQ.ICOL) GO TO 110
   90 DET=-DET
      DO 100 L=1,N
      T=B(L,IROW)
      B(L,IROW)=B(L,ICOL)
  100 B(L,ICOL)=T
  110 INDEX(1,I)=IROW
      INDEX(2,I)=ICOL
      DET=DET*PIVOT
C     FOLLOWING 6 STATEMENTS TO DIVIDE PIVOT ROW BY PIVOT ELEMENT
      B(ICOL,ICOL)=1.0D0
      DO 120 L=1,N
  120 B(L,ICOL)=B(L,ICOL)/PIVOT
C     FOLLOWING 10 STATEMENTS TO REDUCE NON-PIVOT ROWS
  130 DO 160 LI=1,N
      IF(LI.EQ.ICOL) GO TO 160
  140 T=B(ICOL,LI)
      B(ICOL,LI)=0.0D0
      DO 150 L=1,N
  150 B(L,LI)=B(L,LI)-B(L,ICOL)*T
  160 CONTINUE
  170 CONTINUE
C     THE FOLLOWING 11 STATEMENTS TO INTERCHANGE COLUMNS.
      DO 190 I=1,N
      L=N-I+1
      IF(INDEX(1,L).EQ.INDEX(2,L))  GOTO 190
      JROW = INDEX(1,L)
      JCOL= INDEX(2,L)
      DO 180 K=1,N
      T=B(JROW,K)
      B(JROW,K)=B(JCOL,K)
  180 B(JCOL,K)=T
  190 CONTINUE
  200 RETURN
      END
C
C FCALC=BETA(2)+BETA(3)*EXP(-BETA(1)*X)
C WHERE BETA(1)=RATE CONSTANT,BETA(2)=A(*) AND BETA(3)=A(0)-A(*)
C
C
      FUNCTION FCALC(BETA,X,DERIV)
      IMPLICIT REAL*8(A-H,O-Z)
      REAL*8 BETA(3),DERIV(3)
      DERIV(3) = DEXP(-BETA(1)*X)
      DERIV(2) = 1.0D0
      DERIV(1) = - BETA(3)*X*DERIV(3)
      FCALC = BETA(2) + BETA(3)*DERIV(3)
      RETURN
      END
/EXECUTE
```

```
      PNPA + 10 EQUIV. THEME 8.0

NON-LINEAR LEAST SQUARES ANALYSIS USING A MODEL

ABS(T)=ABS(*)+(ABS(0)-ABS(*))*EXP(-K*T)
WITH  3 PARAMETERS

THERE ARE  50 DATA POINTS AND  1 INDEPENDENT VARIABLES.

ITERATIONS ARE CONTINUED UNTIL 10 ITERATIONS HAVE BEEN PERFORMED
OR THE RELATIVE CORRECTIONS TO THE PARAMETERS FALL BELOW  1.00000-03


THE INITIAL VALUES OF THE PARAMETERS ARE:

 9.00000-03  0.00000-01 -1.00000 00


DATA TO BE FIT TO THIS MODEL BY LEAST SQUARES ROUTINE
LISTED BY COLUMNS IN THE ORDER T(I),ABS(I)
   200.00   1.35500
   196.00   1.34870
   192.00   1.33990
   188.00   1.33240
   184.00   1.32270
   180.00   1.31510
   176.00   1.30590
   172.00   1.29580
   168.00   1.28710
   164.00   1.27760
   160.00   1.26690
   156.00   1.25730
   152.00   1.24610
   148.00   1.23460
   144.00   1.22420
   140.00   1.21210
   136.00   1.20000
   132.00   1.18680
   128.00   1.17450
   124.00   1.16090
   120.00   1.14750
   116.00   1.13280
   112.00   1.11830
   108.00   1.10320
   104.00   1.08780
   100.00   1.07100
    96.00   1.05430
    92.00   1.03640
    88.00   1.01830
    84.00   1.00040
    80.00   0.98020
    76.00   0.96080
    72.00   0.94070
    68.00   0.91930
    64.00   0.89650
    60.00   0.87430
    56.00   0.85030
    52.00   0.82510
    48.00   0.80110
    44.00   0.77400
    40.00   0.74720
    36.00   0.71970
    32.00   0.69180
    28.00   0.66150
    24.00   0.62990
    20.00   0.59760
    16.00   0.56430
    12.00   0.52860
     8.00   0.48990
     4.00   0.44680


ITERATION # 1
CORRECTIONS TO PARAMETERS: -6.3090D-04  1.5633D 00 -1.4598D-01
           NEW PARAMETERS:  8.3691D-03  1.5633D 00 -1.1460D 00

ITERATION # 2
CORRECTIONS TO PARAMETERS:  6.8562D-05  2.2111D-03 -2.2415D-03
           NEW PARAMETERS:  8.4377D-03  1.5655D 00 -1.1482D 00

ITERATION # 3
CORRECTIONS TO PARAMETERS:  2.1206D-07  3.4879D-06 -1.4055D-05
           NEW PARAMETERS:  8.4379D-03  1.5655D 00 -1.1482D 00
```

```
RESULTS OF NON-LINEAR LEAST-SQUARES ANALYSIS WITH A MODEL CONTAINING  3 PARAMETERS ON A DATA SET OF 50 POINTS
   3 ITERATIONS PERFORMED


                     PARAMETER          STD. DEV.

RATE CONSTANT  8.437870-03          4.078850-05
A(*)            1.565510 00          2.588990-03
A(0)-A(*)      -1.148240 00          2.117290-03


TABLE OF OBSERVED AND CALCULATED Y-VALUES.

 LISTED BY COLUMNS IN THE ORDER:  X(1,I), X(2,I),... X(NVAR,I), YOBS(I), YCALC(I), (YOBS(I)-YCALC(I)

   200.00    1.35500   1.35312   0.00188
   196.00    1.34870   1.34583   0.00287
   192.00    1.33990   1.33829   0.00161
   188.00    1.33240   1.33049   0.00191
   184.00    1.32270   1.32243   0.00027
   180.00    1.31510   1.31408   0.00102
   176.00    1.30590   1.30545   0.00045
   172.00    1.29580   1.29652  -0.00072
   168.00    1.28710   1.28729  -0.00019
   164.00    1.27760   1.27774  -0.00014
   160.00    1.26690   1.26786  -0.00096
   156.00    1.25730   1.25764  -0.00034
   152.00    1.24610   1.24707  -0.00097
   148.00    1.23460   1.23614  -0.00154
   144.00    1.22420   1.22484  -0.00064
   140.00    1.21210   1.21314  -0.00104
   136.00    1.20000   1.20105  -0.00105
   132.00    1.18680   1.18853  -0.00173
   128.00    1.17450   1.17559  -0.00109
   124.00    1.16090   1.16221  -0.00131
   120.00    1.14750   1.14836  -0.00086
   116.00    1.13280   1.13404  -0.00124
   112.00    1.11830   1.11923  -0.00093
   108.00    1.10320   1.10391  -0.00071
   104.00    1.08780   1.08807  -0.00027
   100.00    1.07100   1.07168  -0.00068
    96.00    1.05430   1.05473  -0.00043
    92.00    1.03640   1.03719  -0.00079
    88.00    1.01830   1.01906  -0.00076
    84.00    1.00040   1.00030   0.00010
    80.00    0.98020   0.98090  -0.00070
    76.00    0.96080   0.96083  -0.00003
    72.00    0.94070   0.94007   0.00063
    68.00    0.91930   0.91860   0.00070
    64.00    0.89650   0.89639   0.00011
    60.00    0.87430   0.87343   0.00087
    56.00    0.85030   0.84967   0.00063
    52.00    0.82510   0.82509   0.00001
    48.00    0.80110   0.79968   0.00142
    44.00    0.77400   0.77339   0.00061
    40.00    0.74720   0.74620   0.00100
    36.00    0.71970   0.71807   0.00163
    32.00    0.69180   0.68898   0.00282
    28.00    0.66150   0.65889   0.00261
    24.00    0.62990   0.62777   0.00213
    20.00    0.59760   0.59558   0.00202
    16.00    0.56430   0.56229   0.00201
    12.00    0.52860   0.52785   0.00075
     8.00    0.48990   0.49223  -0.00233
     4.00    0.44680   0.45538  -0.00858
```

3). The data is stored for plotting. Plots were made to check the order of the reaction.

```
5.0    5.0
 50
        PNPA + 10 EQUIV. THEME 8.0
     0.15655108D 01
      200.00    1.35500
      196.00    1.34870
      192.00    1.33990
      188.00    1.33240
      184.00    1.32270
      180.00    1.31510
      176.00    1.30590
      172.00    1.29580
      168.00    1.28710
      164.00    1.27760
      160.00    1.26690
      156.00    1.25730
      152.00    1.24610
      148.00    1.23460
      144.00    1.22420
      140.00    1.21210
      136.00    1.20000
      132.00    1.18680
      128.00    1.17450
      124.00    1.16090
      120.00    1.14750
      116.00    1.13280
      112.00    1.11830
      108.00    1.10320
      104.00    1.08780
      100.00    1.07100
       96.00    1.05430
       92.00    1.03640
       88.00    1.01830
       84.00    1.00040
       80.00    0.98020
       76.00    0.96080
       72.00    0.94070
       68.00    0.91930
       64.00    0.89650
       60.00    0.87430
       56.00    0.85030
       52.00    0.82510
       48.00    0.80110
       44.00    0.77400
       40.00    0.74720
       36.00    0.71970
       32.00    0.69180
       28.00    0.66150
       24.00    0.62990
       20.00    0.59760
       16.00    0.56430
       12.00    0.52860
        8.00    0.48990
        4.00    0.44680
```

time	$\ln(A_\infty - A_t)$
0.200000E+03	-0.155822E+01
0.196000E+03	-0.152873E+01
0.192000E+03	-0.148894E+01
0.188000E+03	-0.145624E+01
0.184000E+03	-0.141547E+01
0.180000E+03	-0.138465E+01
0.176000E+03	-0.134857E+01
0.172000E+03	-0.131041E+01
0.168000E+03	-0.127866E+01
0.164000E+03	-0.124511E+01
0.160000E+03	-0.120861E+01
0.156000E+03	-0.117697E+01
0.152000E+03	-0.114128E+01
0.148000E+03	-0.110591E+01
0.144000E+03	-0.107496E+01
0.140000E+03	-0.104012E+01
0.136000E+03	-0.100646E+01
0.132000E+03	-0.970983E+00
0.128000E+03	-0.939021E+00
0.124000E+03	-0.904830E+00
0.120000E+03	-0.872248E+00
0.116000E+03	-0.837686E+00
0.112000E+03	-0.804726E+00
0.108000E+03	-0.771518E+00
0.104000E+03	-0.738750E+00
0.100000E+03	-0.704187E+00
0.960000E+02	-0.670974E+00
0.920000E+02	-0.636557E+00
0.880000E+02	-0.602921E+00
0.840000E+02	-0.570733E+00
0.800000E+02	-0.535612E+00
0.760000E+02	-0.503005E+00
0.720000E+02	-0.470306E+00
0.680000E+02	-0.436630E+00
0.640000E+02	-0.401955E+00
0.600000E+02	-0.369311E+00
0.560000E+02	-0.335178E+00
0.520000E+02	-0.300550E+00
0.480000E+02	-0.268650E+00
0.440000E+02	-0.233812E+00
0.400000E+02	-0.200513E+00
0.360000E+02	-0.167460E+00
0.320000E+02	-0.135006E+00
0.280000E+02	-0.100914E+00
0.240000E+02	-0.665557E-01
0.200000E+02	-0.326154E-01
0.160000E+02	0.120948E-02
0.120000E+02	0.362452E-01
0.800000E+01	0.728881E-01
0.400000E+01	0.112177E+00

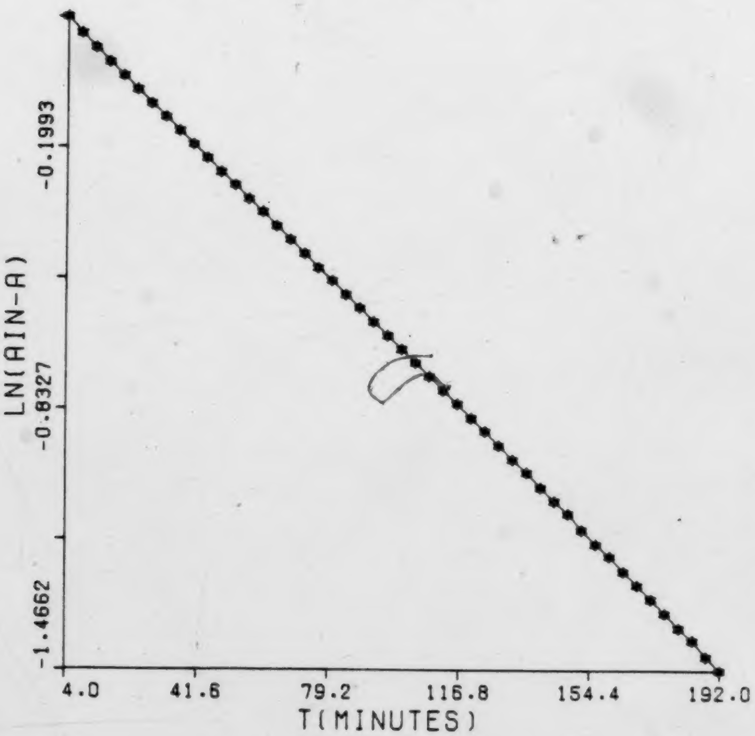
PNPA + 10 EQUIV. THBME 8.0

APPENDIX 3

TABLE 26

PSEUDO-FIRST ORDER RATE CONSTANTS FOR THE HYDROLYSIS OF *p*-NITROPHENYLACETATE WITH BENZYL MERCAPTAN[a].

pH ± 0.02	[RSH][b] 10^3 M	k_{obs}[c] min^{-1}
10.8	0	2.15 ± 0.02 x 10^{-1}
10.8	1.34	1.506 ± 0.035
10.8	2.68	2.975 ± 0.006
10.8	4.02	3.74 ± 0.02
10.4	0	1.43 ± 0.01 x 10^{-1}
10.4	1.34	1.13 ± 0.0055
10.4	2.68	2.110 ± 0.025
10.4	4.02	2.980 ± 0.075
10.0	0	5.16 ± 0.02 x 10^{-2}
10.0	.667	3.60 ± 0.1 x 10^{-1}
10.0	1.34	6.18 ± 0.06 x 10^{-1}
10.0	2.02	1.04 ± 0.03
10.0	1.26	6.16 ± 0.01 x 10^{-1}
9.6	0	2.91 ± 0.06 x 10^{-2}
9.6	.667	1.88 ± 0.2 x 10^{-1}
9.6	1.34	3.45 ± 0.05 x 10^{-1}
9.6	2.02	4.96 ± 0.07 x 10^{-1}
9.6	4.02	1.00 ± 0.025
9.6	2.52	6.54 ± 0.1 x 10^{-1}
9.6	1.26	3.19 ± 0.03 x 10^{-1}
9.6	3.78	9.42 ± 0.03 x 10^{-1}
9.2	0	1.21 ± 0.01 x 10^{-2}
9.2	2.26	2.52 ± 0.06 x 10^{-1}
9.2	3.39	3.96 ± 0.02 x 10^{-1}
9.2	1.34	1.68 ± 0.03 x 10^{-1}
9.2	1.34	1.62 ± 0.02 x 10^{-1}
9.2	1.26	1.75 ± 0.02 x 10^{-1}
8.8	0	1.06 ± 0.01 x 10^{-2}
8.8	1.13	8.24 ± 0.06 x 10^{-2}
8.8	2.26	1.45 ± 0.02 x 10^{-1}
8.8	3.39	2.09 ± 0.03 x 10^{-1}
8.8	1.26	7.84 ± 0.07 x 10^{-2}

Table 26 (continued)

8.4	0	7.32 ± 0.03 x 10^{-3}
8.4	1.13	3.26 ± 0.03 x 10^{-2}
8.4	2.26	5.92 ± 0.05 x 10^{-2}
8.4	3.39	9.42 ± 0.05 x 10^{-2}
8.0	0	3.99 ± 0.02 x 10^{-3}
8.0	1.13	1.65 ± 0.075 x 10^{-2}
8.0	2.26	2.85 ± 0.055 x 10^{-2}
8.0	3.39	4.04 ± 0.075 x 10^{-2}
7.6	0	1.97 ± 0.03 x 20^{-3}
7.6	1.13	6.85 ± 0.2 x 10^{-3}
7.6	2.26	1.17 ± 0.15 x 10^{-2}
7.6	3.39	1.34 ± 0.04 x 10^{-2}

a. Determined in H_2O/EtOH (95%) 30.9% ethanol. [Buffer] = 0.021 M. (pH 10.8, 10.4 (CAPS), pH 10.0, 9.6, 9.2 (CHES), pH 8.8, 8.4, 8.0, 7.6 (TRICINE). μ = 0.345 M, T = 25.0 ± 0.1°C. [PNPA] = 1.13 x 10^{-4} M.

b. [RSH] = total concentration of thiol added.

c. All values were determined as the average of at least three reproducible runs.

TABLE 27

PSEUDO-FIRST ORDER RATE CONSTANTS FOR THE HYDROLYSIS OF *p*-NITROPHENYLACETATE WITH CYCLOHEXYLMETHYLTHIOL[a].

pH ± 0.02	[RSH][b]	k_{obs}[c]
10.8	0	2.15 ± 0.02 x 10^{-1}
10.8	3.14	1.10 ± 0.003
10.8	4.04	1.37 ± 0.01
10.8	5.50	1.64 ± 0.10
10.4	0	1.43 ± 0.01 x 10^{-1}
10.4	3.14	6.75 ± 0.03 x 10^{-1}
10.4	3.59	7.02 ± 0.02 x 10^{-1}
10.4	3.19	6.66 ± 0.06 x 10^{-1}
10.0	0	5.16 ± 0.02 x 10^{-2}
10.0	3.19	2.40 ± 0.04 x 10^{-1}
10.0	4.40	3.06 ± 0.06 x 10^{-1}
10.0	5.50	4.00 ± 0.03 x 10^{-1}
9.6	0	2.91 ± 0.06 x 10^{-2}
9.6	3.19	1.30 ± 0.03 x 10^{-1}
9.6	4.40	1.60 ± 0.03 x 10^{-1}
9.6	4.40	1.51 ± 0.05 x 10^{-1}
9.2	0	1.21 ± 0.01 x 10^{-2}
9.2	3.19	5.31 ± 0.09 x 10^{-2}
9.2	3.63	5.39 ± 0.03 x 10^{-2}
9.2	3.62	4.72 ± 0.05 x 10^{-2}
8.8	0	1.06 ± 0.01 x 10^{-2}
8.8	3.19	2.60 ± 0.04 x 10^{-2}
8.8	3.63	2.93 ± 0.09 x 10^{-2}
8.8	3.62	2.35 ± 0.04 x 10^{-2}
8.4	0	7.32 ± 0.103 x 10^{-3}
8.4	3.63	1.45 ± 0.003 x 10^{-2}
8.4	3.19	1.454 ± 0.006 x 10^{-2}
8.4	2.86	1.38 ± 0.009 x 10^{-2}

Table 27 (continued)

a. Determined in H_2O/EtOH (95%)/THF (64.4/29/6.6) (v/v). [Buffer] = 0.19 M (pH 10.8, 10.4 (CAPS), pH 10.0, 9.6, 9.2 (CHES), pH 8.8, 8.4 (TRICINE). μ = 0.33 M. T = 25.0 ± 0.1°C. [PNPA] = 1.52 x 10^{-4} M.

b. [RSH] = total concentration of thiol added.

c. All values were determined as the average of at least three reproducible runs.

TABLE 28

PSEUDO-FIRST ORDER AND SECOND ORDER RATE CONSTANTS FOR THE HYDROLYSIS OF *p*-NITROPHENYLACETATE WITH BENZIMIDAZOLE[a].

pH ± 0.02	[RIm][b] 10^3 M	k_{obs}[c] min^{-1}
8.4	0	$7.32 \pm 0.03 \times 10^{-3}$
8.4	4.02	$9.2 \pm 0.4 \times 10^{-3}$
8.4	2.52	$8.37 \pm 0.15 \times 10^{-3}$
8.4	2.68	$8.03 \pm 0.02 \times 10^{-3}$
8.0	0	$3.99 \pm 0.02 \times 10^{-3}$
8.0	1.34	$4.53 \pm 0.1 \times 10^{-3}$
8.0	2.68	$4.89 \pm 0.07 \times 10^{-3}$
8.0	4.02	$5.5 \pm 0.1 \times 10^{-3}$
7.6	0	$1.97 \pm 0.03 \times 10^{-3}$
7.6	2.68	$3.20 \pm 0.06 \times 10^{-3}$
7.6	2.52	$2.80 \pm 0.08 \times 10^{-3}$
7.6	1.26	$2.54 \pm 0.06 \times 10^{-3}$

a. Determined in H_2O/EtOH (95%) 36.9% ethanol. [Buffer] = 0.21 M (TRICINE). $\mu = 0.345$ M. T = 25.0 ± 0.1°C. [PNPA] = 1.52×10^{-4} M.

b. [RIm]= total concentration of benzimidazole added.

c. All values were determined as the average of at least three reproducible runs.

TABLE 29

PSEUDO-FIRST ORDER RATE CONSTANTS FOR THE HYDROLYSIS OF *p*-NITROPHENYLACETATE WITH TETRAHYDROBENZIMIDAZOLE[a].

pH ± 0.02	$[RIm]_T$[b] 10^3 M	k_{obs}[c] min^{-1}
8.8	0	$1.06 \pm 0.01 \times 10^{-2}$
8.8	1.14	$2.56 \pm 0.01 \times 10^{-2}$
8.8	1.43	$2.98 \pm 0.04 \times 10^{-2}$
8.8	2.23	$4.05 \pm 0.05 \times 10^{-2}$
8.4	0	$7.32 \pm 0.03 \times 10^{-3}$
8.4	1.14	$1.91 \pm 0.01 \times 10^{-2}$
8.4	2.23	$3.00 \pm 0.06 \times 10^{-2}$
8.4	1.55	$2.33 \pm 0.02 \times 10^{-2}$
8.0	0	$3.99 \pm 0.02 \times 10^{-3}$
8.0	1.01	$1.030 \pm 0.004 \times 10^{-2}$
8.0	1.14	$1.140 \pm 0.001 \times 10^{-2}$
8.0	1.43	$1.370 \pm 0.001 \times 10^{-2}$
7.6	0	$1.97 \pm 0.03 \times 10^{-3}$
7.6	1.14	$6.41 \pm 0.01 \times 10^{-3}$
7.6	1.43	$7.59 \pm 0.04 \times 10^{-3}$
7.6	1.01	$5.73 \pm 0.06 \times 10^{-3}$
7.2	0	$2.95 \pm 0.04 \times 10^{-4}$
7.2	1.55	$3.45 \pm 0.65 \times 10^{-3}$
7.2	2.23	$4.90 \pm 0.02 \times 10^{-3}$
7.2	1.01	$2.34 \pm 0.04 \times 10^{-3}$

a. Determined in H_2O/EtOH (95%) 30.9% ethanol. [Buffer] = 0.21 M (pH 8.8, 8.4, 8.0, 7.6 (TRICINE), pH 7.2 (HEPES)). μ = 0.345 M, T = 25.0 ± 0.1°C. [PNPA] = 1.54×10^{-4} M.

b. $[RIm]_T$ = total concentration of tetrahydrobenzimidazole added.

c. All values were determined as the average of at least three reproducible runs.

TABLE 30

PSEUDO-FIRST ORDER RATE CONSTANTS FOR THE HYDROLYSIS OF p-NITROPHENYLACETATE WITH 1-METHYLTETRAHYDROBENZIMIDAZOLE[a].

pH ± 0.02	$[\mathrm{RIm}]_T$[b] 10^3 M	k_{obs}[c] min^{-1}
8.8	0	$1.06 \pm 0.01 \times 10^{-2}$
8.8	1.16	$1.12 \pm 0.05 \times 10^{-2}$
8.8	2.33	$3.53 \pm 0.05 \times 10^{-2}$
8.8	1.75	$2.86 \pm 0.03 \times 10^{-2}$
8.4	0	$7.32 \pm 0.03 \times 10^{-3}$
8.4	1.16	$1.55 \pm 0.01 \times 10^{-2}$
8.4	2.33	$2.48 \pm 0.06 \times 10^{-2}$
8.4	1.75	$2.11 \pm 0.04 \times 10^{-2}$
8.0	0	$3.99 \pm 0.02 \times 10^{-3}$
8.0	1.16	$8.41 \pm 0.06 \times 10^{-3}$
8.0	2.33	$1.25 \pm 0.01 \times 10^{-2}$
8.0	1.75	$1.13 \pm 0.01 \times 10^{-2}$
7.6	0	$1.97 \pm 0.03 \times 10^{-3}$
7.6	1.16	$5.01 \pm 0.04 \times 10^{-3}$
7.6	1.75	$6.18 \pm 0.05 \times 10^{-3}$
7.6	1.43	$5.39 \pm 0.06 \times 10^{-3}$

a. Determined in H_2O/EtOH (95%) 30.9% ethanol. [Buffer] = 0.21 M (TRICINE) μ = 0.345 M, T = 25.0 ± 0.1°C. [PNPA] = 1.17×10^{-4} M.

b. $[\mathrm{RIm}]_T$ = total concentration of 1-methyltetrahydrobenzimidazole added.

c. All values were determined as the average of at least three reproducible runs.

TABLE 31

PSEUDO-FIRST ORDER RATE CONSTANTS FOR THE HYDROLYSIS OF *p*-NITROPHENYLACETATE WITH 1-METHYL-4-HYDROXYMETHYLTETRAHYDROBENZIMIDAZOLE[a]

pH ± 0.02	$[RIm]_T$[b] 10^3 M	k_{obs}[c] min^{-1}
8.8	0	$1.06 \pm 0.01 \times 10^{-2}$
8.8	2.34	$1.34 \pm 0.01 \times 10^{-2}$
8.8	1.17	$1.20 \pm 0.01 \times 10^{-2}$
8.8	2.34	$1.35 \pm 0.01 \times 10^{-2}$
8.4	0	$7.32 \pm 0.03 \times 10^{-3}$
8.4	1.17	$8.3 \pm 0.1 \times 10^{-3}$
8.4	2.34	$9.3 \pm 0.1 \times 10^{-3}$
8.4	3.51	$1.04 \pm 0.01 \times 10^{-2}$
8.0	0	$3.99 \pm 0.02 \times 10^{-3}$
8.0	3.51	$6.2 \pm 0.1 \times 10^{-3}$
8.0	2.34	$5.5 \pm 0.1 \times 10^{-3}$
8.0	1.17	$4.78 \pm 0.02 \times 10^{-3}$

a. Determined in H_2O/EtOH (95%) 30.9% ethanol. [Buffer] = 0.21 M (TRICINE) $\mu = 0.345$ M, T = 25.0 ± 0.1°C. [PNPA] = 1.17×10^{-4} M.

b. $[RIm]_T$ = total concentration of 1-methyl-4,5-[4'-hydroxymethyltetramethylene]imidazole.

c. All values were determined as the average of at least three reproducible runs.

TABLE 32

PSEUDO-FIRST ORDER RATE CONSTANTS FOR THE HYDROLYSIS OF *p*-NITROPHENYLACETATE WITH 4(7')-THIOMETHYLBENZIMIDAZOLE[a].

pH ± 0.02	$[\mathrm{RImSH}]_T$[b] 10^3 M	k_{obs}[c] min^{-1}
9.2	0	$1.21 \pm 0.01 \times 10^{-2}$
9.2	0.52	$1.10 \pm 0.03 \times 10^{-1}$
9.2	0.45	$8.44 \pm 0.06 \times 10^{-2}$
9.2	1.90	$3.50 \pm 0.5 \times 10^{-1}$
8.8	0	$1.06 \pm 0.01 \times 10^{-2}$
8.8	1.26	$1.22 \pm 0.55 \times 10^{-1}$
8.8	1.26	$1.28 \pm 0.50 \times 10^{-1}$
8.8	0.94	$8.40 \pm 0.40 \times 10^{-1}$
8.4	0	$7.32 \pm 0.03 \times 10^{-3}$
8.4	0.63	$3.37 \pm 0.20 \times 10^{-2}$
8.4	1.26	$4.94 \pm 0.05 \times 10^{-2}$
8.4	0.94	$4.23 \pm 0.20 \times 10^{-2}$
8.0	0	$3.99 \pm 0.02 \times 10^{-3}$
8.0	1.23	$2.39 \pm 0.03 \times 10^{-2}$
8.0	1.40	$2.89 \pm 0.03 \times 10^{-2}$
8.0	0.57	$1.23 \pm 0.025 \times 10^{-2}$
7.6	0	$1.97 \pm 0.03 \times 10^{-3}$
7.6	1.25	$1.14 \pm 0.024 \times 10^{-2}$
7.6	1.81	$1.70 \pm 0.03 \times 10^{-2}$
7.6	1.25	$9.76 \pm 0.08 \times 10^{-3}$
7.2	0	$2.95 \pm 0.04 \times 10^{-4}$
7.2	0.73	$3.24 \pm 0.06 \times 10^{-3}$
7.2	0.56	$2.59 \pm 0.04 \times 10^{-3}$
7.2	0.59	$2.71 \pm 0.10 \times 10^{-3}$
6.8	0	$1.52 \pm 0.02 \times 10^{-4}$
6.8	0.56	$1.38 \pm 0.03 \times 10^{-3}$
6.8	0.59	$1.57 \pm 0.10 \times 10^{-3}$
6.8	0.78	$2.06 \pm 0.07 \times 10^{-3}$

Table 32 (continued)

a. Determined in H_2O/EtOH (95%) 30.9% ethanol. [Buffer] = 0.21 M (pH 9.2 (CHES), pH 8.8, 8.4, 8.0, 7.6 (TRICINE), pH 7.2, 6.8 (HEPES)). μ = 0.345 M, T = 25.0 ± 0.1°C. [PNPA] = 1.06 x 10^{-4} M.

b. $[RImSH]_T$ = total concentration of 4(7')-thiomethylbenzimidazole.

c. All values were determined as the average of at least three reproducible runs.

TABLE 33

PSEUDO-FIRST ORDER RATE CONSTANTS FOR THE HYDROLYSIS OF

p-NITROPHENYLACETATE WITH 1-METHYL-4-THIOMETHYLBENZIMIDAZOLE[a].

pH ± 0.02	$[\mathrm{RImSH}]_T$[b] 10^3M	k_{obs}[c] min^{-1}
9.2	0	$1.21 \pm 0.01 \times 10^{-2}$
9.2	1.87	$1.80 \pm 0.10 \times 10^{-1}$
9.2	1.25	$1.28 \pm 0.10 \times 10^{-1}$
9.2	1.25	$1.28 \pm 0.08 \times 10^{-1}$
8.4	0	$7.32 \pm 0.03 \times 10^{-3}$
8.4	1.25	$3.39 \pm 0.06 \times 10^{-2}$
8.4	1.25	$2.84 \pm 0.04 \times 10^{-2}$
8.4	1.87	$3.81 \pm 0.07 \times 10^{-2}$
8.0	0	$3.99 \pm 0.02 \times 10^{-3}$
8.0	1.87	$2.06 \pm 0.03 \times 10^{-2}$
8.0	1.11	$1.43 \pm 0.05 \times 10^{-2}$
8.0	1.97	$2.43 \pm 0.02 \times 10^{-2}$
7.6	0	$1.97 \pm 0.03 \times 10^{-3}$
7.6	1.25	$7.4 \pm 0.1 \times 10^{-3}$
7.6	1.87	$8.96 \pm 0.07 \times 10^{-3}$
7.6	1.25	$7.78 \pm 0.06 \times 10^{-3}$
6.8	0	$1.52 \pm 0.02 \times 10^{-4}$
6.8	.938	$1.33 \pm 0.07 \times 10^{-3}$
6.8	1.87	$2.95 \pm 0.10 \times 10^{-3}$
6.8	2.48	$3.33 \pm 0.10 \times 10^{-3}$

Table 33 (continued)

a. Determined in H_2O/EtOH (95%) 30.9% ethanol. [Buffer] = 0.21 M (pH 8.4, 8.0, 7.6 (TRICINE), pH 6.8 (HEPES)). μ = 0.345 M, T = 25.0 ± 0.1°C. [PNPA] = 1.26 x 10^{-4} M.

b. $[RImSH]_T$ = total concentration of 1-methyl-4-thiomethylbenzimidazole.

c. All values were determined as the average of at least three reproducible runs.

TABLE 34

PSEUDO-FIRST ORDER RATE CONSTANTS FOR THE HYDROLYSIS OF *p*-NITROPHENYLACETATE WITH 4(7')-HYDROXYMETHYLBENZIMIDAZOLE[a].

pH ± 0.02	$[\mathrm{RIm}]_T$[b] 10^3 M	k_{obs}[c] min^{-1}
8.4	0	$7.32 \pm 0.03 \times 10^{-3}$
8.4	1.77	$7.35 \pm 0.03 \times 10^{-3}$
8.4	2.02	$7.28 \pm 0.04 \times 10^{-3}$
8.4	3.54	$7.38 \pm 0.02 \times 10^{-3}$
8.0	0	$3.99 \pm 0.02 \times 10^{-3}$
8.0	1.77	$4.01 \pm 0.04 \times 10^{-3}$
8.0	2.02	$3.97 \pm 0.05 \times 10^{-3}$
8.0	3.54	$4.05 \pm 0.06 \times 10^{-3}$
6.8	0	$1.52 \pm 0.02 \times 10^{-4}$
6.8	1.77	$1.61 \pm 0.05 \times 10^{-4}$
6.8	2.02	$1.57 \pm 0.03 \times 10^{-4}$
6.8	3.54	$1.59 \pm 0.07 \times 10^{-4}$

a. Determined in H_2O/EtOH (95%) 30.9% ethanol. [Buffer] = 0.21 M (pH 8.4, 7.6 (TRICINE), pH 6.8 (HEPES)). $\mu = 0.345$ M, T = 25.0 ± 0.1°C. [PNPA] = 1.77×10^{-4} M.

b. $[\mathrm{RIm}]_T$ = total concentration of 4(7')-hydroxymethylbenzimidazole added.

c. All values were determined as the average of at least three reproducible runs.

TABLE 35

PSEUDO-FIRST ORDER RATE CONSTANTS FOR THE HYDROLYSIS OF *p*-NITROPHENYLACETATE WITH 1-METHYL-4-HYDROXYMETHYLBENZIMIDAZOLE[a].

pH ± 0.02	$[RIm]_T$[b] 10^3 M	k_{obs}[c] min^{-1}
8.4	0	$7.32 \pm 0.03 \times 10^{-3}$
8.4	1.46	$7.28 \pm 0.04 \times 10^{-3}$
8.4	2.92	$7.26 \pm 0.04 \times 10^{-3}$
8.4	3.08	$7.29 \pm 0.05 \times 10^{-3}$
7.6	0	$1.97 \pm 0.03 \times 10^{-3}$
7.6	1.46	$1.88 \pm 0.06 \times 10^{-3}$
7.6	2.92	$1.89 \pm 0.08 \times 10^{-3}$
7.6	3.08	$1.86 \pm 0.10 \times 10^{-3}$
6.8	0	$1.52 \pm 0.02 \times 10^{-4}$
6.8	1.46	$1.60 \pm 0.04 \times 10^{-4}$
6.8	2.92	$1.57 \pm 0.03 \times 10^{-4}$
6.8	3.08	$1.57 \pm 0.03 \times 10^{-4}$

a. Determined in H_2O/EtOH (95%) 30.9% ethanol. [Buffer] = 0.21 M (pH 8.4, 7.6 (TRICINE), pH 6.8 (HEPES)). $\mu = 0.345$ M, T = 25.0 ± 0.1°C. [PNPA] = 1.46×10^{-4} M.

b. $[RIm]_T$ = total concentration of 1-methyl-4-hydroxymethylbenzimidazole added.

c. All values were determined as the average of at least three reproducible runs.

TABLE 36

PSEUDO-FIRST ORDER RATE CONSTANTS FOR THE HYDROLYSIS OF p-NITROPHENYLACETATE WITH 1-METHYLBENZIMIDAZOLE[a].

pH ± 0.02	[RIm][b] 10^3 M	k_{obs}[c] min^{-1}
7.6	0	$1.97 \pm 0.03 \times 10^{-3}$
7.6	1.26	$1.89 \pm 0.07 \times 10^{-3}$
7.6	2.52	$1.90 \pm 0.06 \times 10^{-3}$
7.6	3.09	$1.94 \pm 0.08 \times 10^{-3}$
7.2	0	$2.95 \pm 0.04 \times 10^{-4}$
7.2	1.26	$3.01 \pm 0.06 \times 10^{-4}$
7.2	2.52	$3.03 \pm 0.06 \times 10^{-4}$
7.2	3.09	$3.02 \pm 0.05 \times 10^{-4}$
6.8	0	$1.52 \pm 0.02 \times 10^{-4}$
6.8	1.26	$1.63 \pm 0.08 \times 10^{-4}$
6.8	2.52	$1.65 \pm 0.10 \times 10^{-4}$
6.8	3.09	$1.59 \pm 0.09 \times 10^{-4}$

a. Determined in H_2O/EtOH (95%) 30.9% ethanol. [Buffer] = 0.21 M (pH 7.6 (TRICINE), pH 7.2, 6.8 (HEPES)). $\mu = 0.345$ M, T = 25.0 ± 0.1°C. [PNPA] = 1.26×10^{-4} M.

b. $[RIm]_T$ = total concentration of 1-methylbenzimidazole added.

c. All values were determined as the average of at least three reproducible runs.